Hybrid peripheral-spinal neuroprosthesis for refined motor execution after paralysis

THÈSE N^{O} 8245 (2018)

PRÉSENTÉE LE 26 JANVIER 2018
À LA FACULTÉ DES SCIENCES ET TECHNIQUES DE L'INGÉNIEUR
LABORATOIRE D'INGÉNIERIE NEURALE TRANSLATIONNELLE
PROGRAMME DOCTORAL EN NEUROSCIENCES

ÉCOLE POLYTECHNIQUE FÉDÉRALE DE LAUSANNE

POUR L'OBTENTION DU GRADE DE DOCTEUR ÈS SCIENCES

PAR

Sophie Marie Marthe WURTH

acceptée sur proposition du jury:

Prof. D. N. A. Van De Ville, président du jury
Prof. S. Micera, Prof. G. Courtine, directeurs de thèse
Prof. D. Weber, rapporteur
Prof. A. Jackson, rapporteur
Prof. K. Aminian, rapporteur

ÉCOLE POLYTECHNIQUE
FÉDÉRALE DE LAUSANNE

Suisse
2018

"We are at the very beginning of time for the human race. It is not unreasonable that we grapple with problems. There are tens of thousands of years in the future. Our responsibility is to do what we can, learn what we can, improve the solutions and pass them on. It is our responsibility to leave the men of the future a free hand. In the impetuous youth of humanity, we can make grave errors that can stunt our growth for a long time. This we will do if we say we have the answers now, so young and ignorant; if we suppress all discussion, all criticism, saying, 'This is it, boys, man is saved!' and thus doom man for a long time to the chains of authority, confined to the limits of our present imagination. It has been done so many times before. It is our responsibility as scientists, knowing the great progress and great value of a satisfactory philosophy of ignorance, the great progress that is the fruit of freedom of thought, to proclaim the value of this freedom, to teach how doubt is not to be feared but welcomed and discussed, and to demand this freedom as our duty to all coming generations."

— Richard Feynman, Public address to the National Academy of Science, 1955

Acknowledgements

First of all, I would like to wholeheartedly thank Silvestro to have taken me into his lab and given me the opportunity to carry out my PhD thesis, for his support and trust along the four years. I would like to equally thank Grégoire for his guidance and for permitting me to consider his lab my second workplace. Their passion for science was inspiring from the first day.
I would like to sincerely thank Marco and Stani for initiating me to my thesis project, for many inspiring discussions, and for constructive feedback in critical moments.

I had the chance to work in great teams and be surrounded by fantastic people. Among all the many persons that contributed to the accomplishment of this thesis, I would like to specially thank Jerome for the many hours of work spent together in the behavior rooms modulating and observing rat legs. I want to thank Quentin and Gabrielle for guiding me through histology and showing me its value and its beauty. I thank Annarita for providing me with the many SELINE electrodes and Romain to introduce me to the world of image processing. Thanks to Alessandra and the EPFL HistoCore facility for their precious advice regarding histological procedures. Thanks to Natasha and Polina for all the work relating to surgical procedures and for teaching me some of their surgical skills. I want to thank Nawal and Gabrielle, the most amazing students I could teach and follow. I want to thank Laetitia for her help and support with many issues that went far beyond animal experimentation. And Leo, thanks for all the moments we shared, for the discussions, support and invaluable friendship. Many thanks to the entire STIMO team for their help at the CHUV, to Edo for sharing his expertise with transcutaneous stimulation, and especially to Karen and Fabien for their valuable support in these experimental sessions. I would like to thank Prof. Eric Rouiller, Marco, and Silvestro for their support in making the NeuGrasp project become a reality and Mélanie and Marion for joining the team and giving it its core.
I thank Prof. Douglas Weber, Prof. Andrew Jackson, Prof. Kamiar Aminian, and Prof Dimitri Van de Ville, for reading and revising this work as members of my thesis examination committee. Emanuele, Karen, Fabien, Jerome, and Marco, thank you for your critical input on parts of the work.

I am very grateful to my parents for their unconditional support and trust, and for the values they taught me that guide me through life. And Javi, thank you for your genuine support throughout so much more than just those four thesis years, for being the backbone of my life, for being my person.

Lausanne, 25 Octobre 2017

Abstract

Spinal cord injury (SCI) disrupts the communication between the brain and the spinal circuits responsible for movement, thereby causing severe motor deficits. Current strategies to restore function to paralyzed limbs have separately investigated electrical stimulation of the spinal cord or of the peripheral neuromuscular system. Various neuromodulation strategies, for instance electrical epidural stimulation (EES) of the spinal cord, reactivate spinal circuits below the lesion and enable the generation of locomotor activity. EES targets muscle synergies rather than specific muscles or joints, and can therefore be limited by low selectivity. Accessing distal muscles individually is key to restore refined movement. Peripheral nerve stimulation (PNS) offers this possibility by selectively recruiting fibers innervating distinct muscles. Here, I developed a hybrid electrical stimulation paradigm, concomitantly targeting the spinal cord and the peripheral nerves for a global activation of coordinated multi-joint leg movements and a selective activation of distal muscles respectively. This approach combines two highly complementary stimulation paradigms into one refined neuroprosthetic system that could improve functional restoration after paralysis.

The first part of this work addressed the validation of intraneural electrodes for selective and stable PNS. Albeit highly promising, incomplete characterization of long-term usability and biocompatibility has so far restricted their widespread use. To bridge this gap, I conducted a longitudinal assessment and comprehensively characterized their functional properties in light of their bio-integration in rats. Results showed that i) stimulation thresholds increased moderately during one month after implantation and then stabilized, ii) these changes correlated with progressive implant encapsulation, and iii) selectivity in muscle recruitment was retained in spite of the encapsulation, permitting precise control over ankle kinematics in anesthetized experiments. Overall, these results demonstrated the potential for long-term usability of intraneural implants.

In the second part of this work, I developed and characterized a hybrid PNS-EES paradigm that concomitantly stimulated the spinal cord and the sciatic nerves in rat models of severe SCI, and validated it in a pilot study with a human SCI. I showed that i) muscle recruitment obtained by EES and PNS was highly complementary, ii) PNS enabled controllable adjustments in leg movements during locomotion, and iii) the hybrid PNS-EES paradigm permitted refined movements that increased functionality during locomotion in rats and a human pilot subject.

This thesis provides evidence about the long-term functionality of intraneural implants and demonstrates their potential for stable interfacing with peripheral nerves. The hybrid PNS-EES paradigm reveals how the complementarity of both strategies effectively improved functional outcomes for paralyzed lower limbs. These findings open promising perspectives for the development of hybrid neuroprosthetic systems to restore functional and refined movements to paralyzed limbs.

Key words: peripheral nerve stimulation, intraneural electrodes, bio-integration, epidural spinal cord stimulation, movement restoration after paralysis, personalized neuroprostheses

Résumé

Une lésion de la moelle épinière (LME) interrompt la communication entre le cerveau et les circuits spinaux responsables du mouvement, causant ainsi de graves déficits moteurs. Les stratégies actuelles pour restaurer la fonction des membres paralysés ont séparément étudié la stimulation électrique de la moelle épinière ou du système neuromusculaire périphérique. Par exemple, la stimulation épidurale électrique (EES) de la moelle épinière réactive les circuits spinaux au-dessous de la lésion et permet la génération de l'activité locomotrice. L'EES cible les synergies musculaires plutôt que les muscles ou articulations spécifiques, et peut donc être limité par une faible sélectivité. Un accès individuel aux muscles distaux est clé pour restaurer un mouvement raffiné. La stimulation du nerf périphérique (PNS) offre cette possibilité en recrutant sélectivement des fibres innervant des muscles distincts. Ici, j'ai développé un paradigme de stimulation électrique hybride, ciblant à la fois la moelle épinière et les nerfs périphériques pour une activation globale des mouvements locomoteurs et une activation sélective des muscles distaux respectivement. Cette approche combine deux paradigmes complémentaires en une neuroprothèse raffiné qui pourrait considérablement améliorer la restauration fonctionnelle.

La première partie de ce travail portait sur la validation des électrodes intraneurales pour une PNS sélective et stable. Jusqu'ici, une caractérisation incomplète de l'utilisation à long terme et de la biocompatibilité a limité leur usage. Pour combler cette lacune, j'ai effectué une évaluation longitudinale et caractérisé leurs propriétés fonctionnelles à la lumière de leur bio-intégration chez le rat. Les résultats ont montré que i) les seuils de stimulation augmentaient modérément après l'implantation et se stabilisaient après un mois, ii) ces changements étaient corrélés avec l'encapsulation progressive des implants, et iii) la sélectivité du recrutement musculaire était conservée malgré l'encapsulation, permettant un contrôle précis du mouvement de la cheville lors d'expériences anesthésiées. Dans l'ensemble, ces résultats ont démontré leur potentiel d'utilité à long terme.

Dans la seconde partie de ce travail, j'ai développé et caractérisé un paradigme hybride PNS-EES chez des rats atteints de LME, et l'ai validé dans une étude pilote avec un sujet humain atteint de LME. J'ai montré que i) le recrutement musculaire obtenu par EES et PNS était complémentaire, ii) PNS a permis des ajustements contrôlables dans les mouvements des jambes pendant la locomotion, et iii) le paradigme hybride PNS-EES a permis d'augmenter la fonctionnalité chez les rats et le sujet humain pilote. Cette thèse fournit un ensemble de preuves sur la fonctionnalité chronique des implants intraneuraux et démontre leur potentiel d'interface stable. Le paradigme hybride PNS-EES révèle comment la complémentarité des deux stratégies améliore efficacement les résultats fonctionnels pour les membres inférieurs paralysés. Les résultats ouvrent des perspectives prometteuses pour le développement de systèmes hybrides neurprosthétiques pour restaurer des mouvements fonctionnels et précis aux membres paralysés.

Mots clés : stimulation des nerfs périphériques, implant intraneural, bio-intégration, stimulation épidurale de la moelle épinière, recupération du movement après paralysie, neuroprothèses personnalisées

Contents

Acknowledgements **i**

Abstract (English/Français) **iii**

List of figures **xi**

List of tables **xiii**

1 Introduction **1**
- 1.1 Spinal cord injury 2
- 1.2 Restorative neurology for recovering lower limb motor control 2
  - 1.2.1 Electrical stimulation of the spinal cord 3
  - 1.2.2 Functional electrical stimulation of peripheral nerves and muscles 5
- 1.3 Interfaces with the Peripheral Nervous System 7
  - 1.3.1 Anatomical organization of the Somatic Peripheral Nervous System 7
  - 1.3.2 Mechanisms of excitation of peripheral nerves 8
  - 1.3.3 Trade-off between selectivity and invasiveness of nerve interfaces 10
- 1.4 Considerations for clinically accepted neuroprostheses 11
- 1.5 Thesis outline 12

2 Chronic assessment of functionality and bio-integration of intraneural electrodes **15**
- 2.1 Abstract 16
- 2.2 Introduction 17
- 2.3 Materials and methods 18
  - 2.3.1 Animals 18
  - 2.3.2 Chronic experimental model 19
  - 2.3.3 Chronic electrode characterization 20
  - 2.3.4 Modulation of movement amplitude 22
  - 2.3.5 Closed-loop control of movement-evoked traction force 22
  - 2.3.6 Impact assessment of implantation and implant removal 23
  - 2.3.7 Perfusion and tissue handling 24
  - 2.3.8 Histology and immunohistochemistry 24
  - 2.3.9 Image acquisition, selection, and processing 24
  - 2.3.10 Statistical analyses 25
  - 2.3.11 Supplementary methods for image processing 25
- 2.4 Results 30
  - 2.4.1 Stability and selectivity of polyimide-based intraneural implants 30
  - 2.4.2 Functionality of polyimide-based intraneural implants 32
  - 2.4.3 Assessment of the developing foreign body response 35

2.4.4 Impact of implantation and implant removal on fine motor control 43
2.5 Discussion 44
2.5.1 Stability and usability of polyimide-based intraneural implants 45
2.5.2 Immediate and chronic biological responses to the implant insertion 46
2.5.3 Potential for long-term clinical applications 47
2.6 Conclusion 48

3 Combining peripheral nerve and spinal cord stimulation in a hybrid neuroprosthesis 49
3.1 Abstract 50
3.2 Introduction 51
3.3 Materials and methods 52
3.3.1 Acute electrophysiology for functional mapping of PNS and EES 52
3.3.2 Chronic animal model and surgical procedures 53
3.3.3 Neurorehabilitation procedure after SCI 55
3.3.4 Multi-system recording platform 56
3.3.5 Control architecture for phasic PNS based on monitoring of gait kinematics 56
3.3.6 Characterization of hybrid PNS-EES neuromodulation paradigm during treadmill locomotion 58
3.3.7 Functional impact of hybrid PNS-EES neuromodulation during treadmill and over-ground locomotion 58
3.3.8 Tissue processing and histology procedures 59
3.3.9 Pilot study investigating hybrid PNS-EES neuromodulation in an individual with SCI 60
3.3.10 Statistical analysis 62
3.4 Results 63
3.4.1 PNS elicits selective sensory-motor responses 63
3.4.2 Complementary peripheral and spinal muscle recruitment 65
3.4.3 Characterization of hybrid PNS-EES neuromodulation paradigm 66
3.4.4 Refined locomotion during treadmill and over-ground stepping using the hybrid PNS-EES neuroprosthesis 69
3.4.5 Bio-integration of stimulating intraneural implants 72
3.4.6 Hybrid peripheral-spinal neuroprosthesis refines gait in individual with SCI 75
3.5 Discussion 79
3.5.1 Direct and reflex responses evoked by intraneural PNS 80
3.5.2 PNS permits selective and controllable activation of distal muscles during locomotion 80
3.5.3 Synergistic interactions between PNS and EES 81
3.5.4 Towards clinical applications 81

4 Perspectives on functional restoration for lower and upper limb movements 85
4.1 Opportunities for refinement of the lower limb hybrid PNS-EES neuroprosthesis 85
4.2 Hybrid PNS-EES neuroprosthesis for functional restoration of upper limb movements after paralysis 87

5 General conclusion 91

A Appendix 93
A.1 Kinematic and kinetic variables characterizing gait 93
A.2 Quantification of spared tissue in lesion epicenter after severe SC contusion 96
A.3 Effect of frequency modulation of enhanced extension in hybrid PNS-EES 97

Bibliography **117**

Curriculum Vitae **119**

List of Figures

1.1 Level of spinal cord injury determines extent of paralysis . . . 3
1.2 Electrochemical neuromodulation enabled locomotion after severe SCI in rats . . . 4
1.3 Example of FES to alleviate foot drop . . . 6
1.4 Anatomical organization of peripheral nervous system . . . 7
1.5 Trade-off between selectivity and invasiveness for choosing an interface with the peripheral nervous system . . . 10

2.1 Chronic experimental setup for the chronic assessment of functional polyimide-based intraneural implants. . . . 18
2.2 Implantation of the SELINE electrode in the rat sciatic nerve . . . 20
2.3 Assessment of muscle recruitment by intraneural stimulation . . . 21
2.4 Image processing for quantification of collagen deposition on SR stained sections. . . . 26
2.5 Image processing for quantification of cellularity on H&E stained sections. . . . 27
2.6 Image processing for quantification of inflammation . . . 28
2.7 Image processing for quantification of fiber density . . . 29
2.8 Channel longevity . . . 31
2.9 Selectivity of intraneural stimulation . . . 31
2.10 Stability of electrical properties over time . . . 32
2.11 Characterization of amplitude and frequency modulation of intraneural stimulation . . . 33
2.12 Characterization of PI-controller over step function . . . 34
2.13 High fidelity closed-loop control of traction force . . . 34
2.14 Macroscopic observations of implanted nerves at dissections . . . 35
2.15 Comparison of general nerve morphology for acute and chronic implants . . . 36
2.16 Highly cellular capsule progressively enlarges nerve . . . 37
2.17 Quantification of capsule components as function of duration of implantation . . . 37
2.18 Observation of inflammatory response to the implant . . . 38
2.19 Quantification of the inflammatory response . . . 39
2.20 Spatio-temporal dynamics of inflammatory response . . . 39
2.21 Observation of implant impact on axons and myelination during the first week of implantation 40
2.22 Observation of implant impact on axons and myelination after the first week of implantation 41
2.23 Quantification of implant impact on fiber density. . . . 42
2.24 Distance of closest 20 % of fibers from implant . . . 43
2.25 Impact of implantation and implant removal on leg motor control. . . . 43
2.26 Impact of implant removal on nerve tissue . . . 44
2.27 Schematic summary of observations . . . 45
2.28 Illustration of possible mechanisms contributing to the implant bio-integration . . . 46

3.1 Experimental time-line for the development and assessment of the hybrid peripheral-spinal neuromodulation paradigm in chronic rat models of SCI. 54
3.2 Bilateral implantation of intraneural electrodes in sciatic nerves 55
3.3 Experimental setup for the characterization of the hybrid PNS-EES paradigm 56
3.4 Gaussian Mixture Model (GMM) for the prediction of foot trajectories in real time 57
3.5 Experimental setup for hybrid PNS-EES paradigm in human SCI subject 61
3.6 CMAP obtained by PNS and EES exhibit different latencies 63
3.7 PNS evokes mixed sensory-motor responses 64
3.8 Range of motion obtained by direct and reflex responses 64
3.9 Peripheral, spinal and combined evoked CMAPs. 65
3.10 Characterization of hybrid PNS-EES paradigm with direct and reflex flexion responses 67
3.11 Hybrid PNS-EES paradigm gradually adjusts distal kinematics through enhanced flexion . . 68
3.12 Characterization of hybrid PNS-EES paradigm with extension responses 69
3.13 Hybrid PNS-EES paradigm modulates leg kinematics through enhanced extension. 69
3.14 Hybrid PNS-EES paradigm reduces foot dragging in real-time. 70
3.15 Hybrid PNS-EES paradigm enhances function over-ground. 71
3.16 Hybrid PNS-EES enhancing bilateral extension maintains locomotion performance and avoids collapsing. 72
3.17 Bio-integration of stimulating intraneural implants. 73
3.18 Inflammatory response to stimulating intraneural implants. 74
3.19 Snapshots extracted from video recordings showing a sequence of leg movements during (a) PNS only, (b) EES only, and (c) hybrid PNS-EES 75
3.20 Gait pattern of human subject under conditions PNS only, EES only, and hybrid PNS-EES during treadmill locomotion. 76
3.21 Hybrid PNS-EES refines locomotion in human SCI subject on the treadmill. 77
3.22 Gait pattern of human subject under conditions PNS only, EES only, and hybrid PNS-EES during over-ground locomotion. 78
3.23 Hybrid PNS-EES refines locomotion in human SCI subject on the treadmill. 79

4.1 Muscle recruitment obtained by median, ulnar, and radial intraneural stimulation 89

A.1 Lesion epicenter across contused animals 96
A.2 Enhanced extension affects different gait characteristics in different animals 97

List of Tables

1.1 ASIA Impairment scale of spinal cord injury severity 2
1.2 Types of sensory and motor fibers in the human peripheral nerve 8

2.1 Demographics of animals participating in the study 19

1 Introduction

In 2008, the "Global Burden of Disease" study, an initiative of the World Health Organization (WHO), the World Bank, and Harvard School of Public Health, has risen awareness about the global health impact of neurological disorders [1]. Paralysis as the result of neurological injury or disease is a major physical disability and psychological burden for the impaired person. The direct consequences range from impaired neural control of movement and sensation to severe deterioration of bladder, bowel, and sexual functions. As a result, the afflicted suffer from a dramatic decrease in mobility and independence, which coupled to the indirect consequences that accompany the disease, severely acts on their quality of life. The Christopher Reeve Foundation estimates that 5.5 million Americans are living with a form of paralysis, stroke (33.7%), spinal cord injury (SCI) (27.3%), and multiple sclerosis (18.6%) being among the main origins of this debilitating state [2].

The causes and the consequences of paralysis are numerous and diverse, and patients and their bodies are affected in different ways, depending greatly on the level and the extent of the injury. Consequently, approaches aiming at recovery from paralysis need to be tailored to patient-specific needs. Several studies have been conducted to understand the priorities of paralyzed people in the framework of improving their quality of life. Immediate and full functional recovery being far out of reach, incremental restoration of independence, with a particular emphasis on mobility was voiced as among the top priorities [3, 4].

Returning a certain amount of independence to paralyzed persons can be achieved through communication, assistance, and functional restoration. For instance, patients can be aided by helping them to regain an intuitive and fast way to communicate with others via email or on the phone. Alternatively, they could regain independence by using assistive devices, such as a wheelchair or an exoskeleton. In both cases, advanced machine learning algorithms transform the user input (for instance residual movements [5, 6] or brain signals [7]) into a control command for steering a wheelchair or moving a cursor on a screen [8]. While these approaches show the subtle advances in decoding and encoding biological and kinematic signals, at last they provide only a limited amount of functionality to the end users and may be demanding when physiologically unrelated to the natural movement.

Another strategy for recovering independence consists in restoring function to the paralyzed body itself, for instance by means of electrical stimulation. In fact, despite the great advances in human-machine interfaces with intuitive control paradigms of assistive technology, individuals affected by SCI prefer to restore function to their own limbs rather than augment function with external hardware [9].

The last decades have seen tremendous advances in developing and refining electrical stimulation systems and technologies that allow to restore movement after paralysis [10]. Neuromodulation of the peripheral or the central nervous system are being investigated as means of using the remaining capabilities of nerves, muscles, or spinal cord to generate multi-joint yet precise, powerful yet fatigue-resisting coordinated movements that allow useful mobility and restore independence. The opportunities are as numerous as the unmet clinical needs, and efforts need to be made in bridging gaps between technology and physiology, to promote translation beyond translational research and bring solutions, even if incremental, to the potential end-user.

1.1 Spinal cord injury

In the United States, more than five million people live with upper or lower limb paralysis, with spinal cord injury, only second to stroke, among the major causes [11]. The severity of spinal cord injuries can be defined by the "completeness" of the lesion. The American Spinal Cord Injury Association (ASIA) classifies the impairment resulting from spinal cord injury in five categories (Table 1.1).

Table 1.1 – ASIA Impairment scale of spinal cord injury severity, adapted from [12]

ASIA scale	Impairment	Definition
ASIA A	Complete	No sensory and motor function preserved
ASIA B	Incomplete	Sensory but no motor function preserved
ASIA C	Incomplete	Some sensory and motor function preserved, more than 50% of key muscles largely impaired
ASIA D	Incomplete	Useful motor function, at least 50% of key muscles largely unimpaired
ASIA E	Normal	No impairment

A spinal injury at one of the cervical levels results in tetraplegia (paralysis of arms, torso, and legs), while an injury at the thoracic level or lower causes paraplegia (paralysis of torso and legs). Which body parts are affected by the injury depends on the neurological level of the injury along the spinal cord (Fig. 1.1). In most cases of paralysis, the spinal cord below the lesion as well as the peripheral nerves and muscles remain intact. Due to the lesion however, the access to those structures is interrupted and consequently the individual has lost the direct control over his movement via normal activation pathways.

To this date, SCI is incurable. The costs associated with the care of SCI individuals are extremely high, and the personal expenses are immeasurable. Advances in understanding the pathophysiology of SCI and its impact on the body have progressively permitted to address the secondary complications arising from the trauma. Restoring useful function and mobility however remains an enormous challenge.

1.2 Restorative neurology for recovering lower limb motor control

Severe SCI interrupts the flow of information between supraspinal control centres and spinal circuits recruiting distal nerves and muscles, thereby causing paralysis of the affected body parts. Albeit cut-off from descending commands, these circuits and the distal neuromuscular system below the lesion remain largely intact [13]. The spinal circuits retain the ability to generate complex motor patterns when stimulated and the peripheral nerves remain capable of conducting action potentials and activating the musculature.

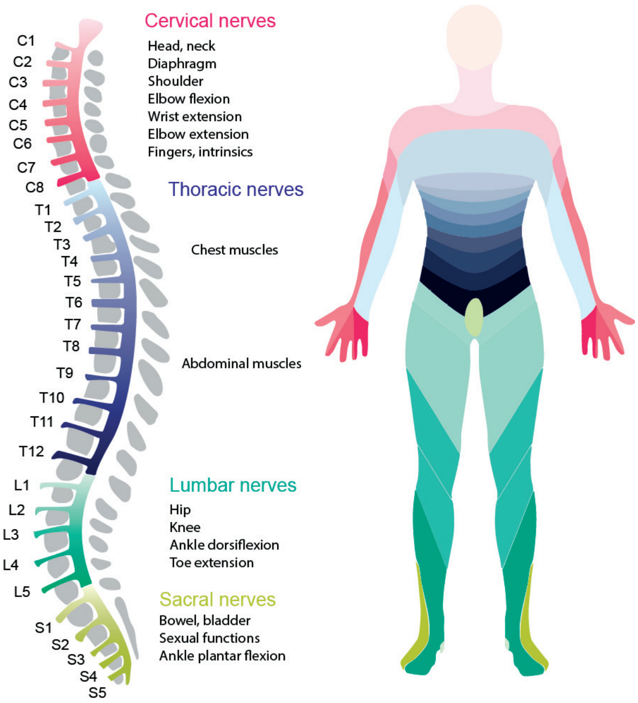
Cervical nerves
Head, neck
Diaphragm
Shoulder
Elbow flexion
Wrist extension
Elbow extension
Fingers, intrinsics
Thoracic nerves
Chest muscles
Abdominal muscles
Lumbar nerves
Hip
Knee
Ankle dorsiflexion
Toe extension
Sacral nerves
Bowel, bladder
Sexual functions
Ankle plantar flexion
C1
C2
C3
C4
C5
C6
C7
C8
T1
T2
T3
T4
T5
T6
T7
T8
T9
T10
T11
T12
L1
L2
L3
L4
L5
S1
S2
S3
S4
S5

Figure 1.1 – Level of spinal cord injury determines extent of paralysis

The voluntary control of movement however is lost, severely impeding on the mobility and independence of the afflicted. Restorative neurology and neuromodulation in particular, modulate the activity of the remaining intact neural system to enhance functional recovery and help regain independence [14].

1.2.1 Electrical stimulation of the spinal cord

Electrical stimulation of the spinal cord has been historically developed for the treatment of intractable pain in the late 1960s [15] but was found to be alleviating a variety of symptoms that appeared in movement disorders such as multiple sclerosis (MS) [16] but also SCI, cerebral palsy or stroke [17]. While these initial findings were rather coincidental, spinal cord physiology research carried out in parallel during the twentieth century demonstrated the existence of so-called pattern generators in the lumbar spinal segments of mammals that were capable of producing locomotor-like activity after complete interruption of brain input [18, 19, 20, 21].

These findings raised awareness in the community about the potential of exploiting these powerful and convenient properties for restoring function after paralysis. In parallel, increased understanding of the spinal networks involved in locomotion produced evidence about the role of afferent sensory feedback in the control of coordinated locomotor activity [22, 23, 20, 24, 25, 26, 27]. In this framework, computational [28, 29] and experimental [30, 31] studies have demonstrated that electrical epidural stimulation (EES) of the spinal cord primarily recruits large diameter afferent fibers carrying proprioceptive information and entering the spinal cord via the dorsal roots. During EES, the electrically activated spinal circuits filter the modulating effects of EES in accordance with the natural activity from muscle spindle feedback circuits engaged in locomotion to produce the appropriate motor output [32]. This has enabled adaptive and weight bearing locomotion in severely paralyzed rats [32, 33, 34, 35, 36] (Fig. 1.2).

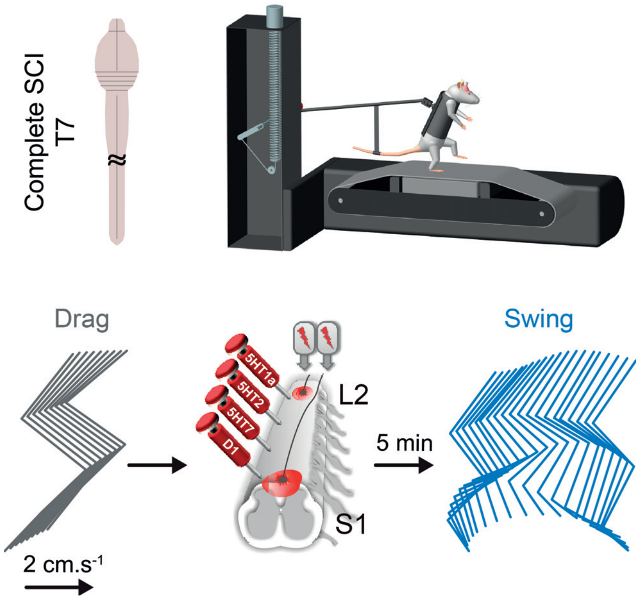

Figure 1.2 – Electrochemical neuromodulation enabled locomotion after severe SCI in rats, adapted from [33]

Increasing evidence from human studies shows that EES can similarly reactivate the lumbar motor circuits and enable locomotor-like activity after severe SCI [19, 37, 38]. For instance, EES promoted enhanced rhythmic muscle activity associated with locomotion when applied during passive, body-weight supported, manually assisted treadmill locomotion in individuals with motor complete spinal cord injury [37]. Those studies suggest that after paralysis in humans and animals alike, epidural spinal cord stimulation provides the missing neural drive to change the state of the dormant spinal circuitry into a functional one, capable of integrating sensory feedback from standing and stepping movements into the control and execution of those same tasks. Harkema and colleagues provided the first evidence that the results obtained from studies in animal models could be translated to a human being with motor complete SCI (ASIA B) [39]. More specifically, EES applied over the lumbosacral spinal segments of this individual provided bilateral load-bearing proprioceptive input and enabled full weight-bearing standing with assistance only for balance. In addition, the patient was able to voluntary control joint-specific muscle activation in the supine position when EES was delivered. Later, Angeli and colleagues showed how EES permitted individuals with chronic complete motor paralysis (ASIA A or B) to voluntarily generate graded muscle contractions and induce movements in their legs [40]. EES applied during manually assisted treadmill locomotion enabled volitional enhancement of cyclic leg muscle activity.

Non-withstanding those encouraging results, it was not possible to generate actual stepping, highlighting the leap that is yet to take for bridging animal experimentation and clinical application. It is indeed not anticipated that the experimental findings from rodent models will translate directly to human patients and restore adaptive and skilled weight-bearing stepping after severe SCI [41, 42, 43]. A variety of reasons may account for this. First, the control of human locomotion is more elaborate than the one of rodents and the human body's anatomical configuration requires interventions beyond whole leg flexion and extension to be functional. To complement multi-joint movements, local control such as foot rotation or ankle flexion are key to a functional gait. Data from human studies seem to suggest that such specificity, for instance through selective recruitment of the tibilais anterior muscle, may hardly be achieved with epidural spinal cord stimulation in human patients [40, 44, 38], among others because distal agonist and antagonist muscles seem to be partially innervated by the same spinal segments [45]. Second, anatomical and neurophysiological differences between rodents and humans will weigh on the translatability of EES paradigms [41, 46]. For instance, the natural firing rate of rodent afferent fibers is about four to five times higher than the one of humans ([47, 48, 49] and [50, 51, 52] respectively). This difference could heavily impact the interaction between EES and the naturally evoked muscle spindle feedback circuits during locomotion. Similarly, the anatomical location, organization, and to some extent the function of spinal fiber tracts differs between humans and rats [53, 54], which needs to be considered when experimental spinal cord lesions and electrical stimulation protocols are designed. Additionally, the scale difference between rodent and human spinal cords have to be taken into account. For instance, the lumbosacral enlargement extends from L2 to L6 in rodents and from L2 to S2 in humans [54]. Third, in the referred animal studies, the spinal cord was electrochemically enhanced with serotonin agonists, which is known to enhance the responsiveness to spinal stimulation. In humans however, such neuromodulation is currently not permitted, which may in part explain a lower responsiveness to the applied electrical stimulation when comparing with the studies in rodents.

1.2.2 Functional electrical stimulation of peripheral nerves and muscles

A more direct approach to restoring movement after paralysis consists in the clinically widely accepted functional electrical stimulation (FES) of the distal neuromuscular system. FES uses the persisting capacity of the peripheral nerves to conduct electricity and takes advantage of the persisting contractile properties of the muscles to produce artificial muscle contractions by means of electrical stimulation and return function to limbs whose motor control was impaired by upper motor neuron disorder. FES induces muscle contractions with timed sequences of bursts of electrical pulses in either of two ways:

- Direct muscle activation: localized muscle recruitment via stimulation of i) efferent fibers in the nerve terminals on the motor endplate of the target muscle (transcutaneous or epimysial) or ii) the muscle directly (intramuscular electrodes) [55]
- Indirect muscle activation: spinal reflex response via stimulation of afferent fibers in the peripheral nerve [56, 57]

In restorative neurology for the recovery of lower limb motor control, FES is employed for two applications: to alleviate foot drop by facilitating ankle dorsiflexion in people affected by hemiplegia (Fig. 1.3) or to generate standing and enable ambulation in SCI individuals. An example of an FDA-approved and commercially available FES system using transcutaneous stimulation for alleviating foot drop is the WalkAid System (Innovative Neurotronics, Inc., Austin, TX [58]). An implanted FES system targeting the same symptom but with increased functionality (dorsi- and plantar-flexion of the ankle as well as foot eversion and inversion) is the ActiGait system (Neurodan A/S, Alborg, Denmark [59]). The ActiGait system is currently in phase II clinical trial and improves walking speed and distance walked during 4 minutes walking tests [60]. Generally, these systems are used to facilitate the swing phase during locomotion in incomplete SCI individuals [61].

Unfortunately, patients suffering from severe SCI lack sufficient trunk stability and knee and hip extension to benefit from such a local intervention. To re-establish functional walking in these patients using FES, multi-site systems need to target agonist and antagonist muscles at multiple joints and provide sufficient contraction strengths to produce whole-leg movements. To date, rather simple bi- or tri-site FES systems have been developed, targeting quadriceps and gluteal muscles additionally to the peroneal nerve to generate limb extension during stance phase while triggering foot clearance at swing onset [62, 63, 64].

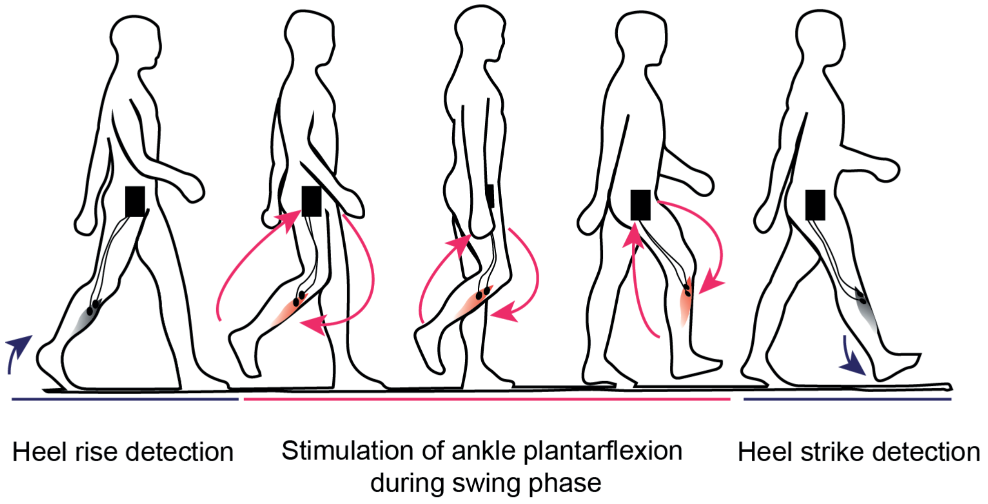
Heel rise detection
Stimulation of ankle plantarflexion during swing phase
Heel strike detection

Figure 1.3 – Example of FES to alleviate foot drop. In this example, ankle plantar-flexion is triggered upon detection of heel rise (for instance using tilt sensors or pressure sensors in the shoe). Stimulation is stopped when the foot touches the ground to permit the execution of the stance phase.

To provide additional functionality, more elaborate, implantable FES systems have been developed, for instance with 14 epimysial and 2 intramuscular electrodes targeting 8 muscles [65, 66]. Either system can generate standing and short-distance ambulation although under high energy expenditure and mostly with the aid of external hardware for the initiation of forward movement and additional stability.

A variety of issues have hindered the translation of multi-site FES systems into a clinically accepted and useful motor neuroprosthesis. For instance, epimysial or surface electrodes require very high currents to electrically excite muscles, which can produce discomfort [67]. Surface electrodes may cause skin irritations or even localized burns [68]. Neither surface, epimysial, and intramuscular electrodes are capable of selectively activating different motor units distributed within in the same muscle, thereby limiting the use due to fast generation of fatigue [69]. Other physiological (insufficient muscle quality, poor proprioception, lack of balance, high energy expenditure, and slow, unnatural ambulation) and practical (cumbersome hardware, high power demands imposing heavy batteries, reproducibility issues with electrode placement) reasons have limited their use to the clinical environment for exercising, where they provide a variety of secondary benefits other than mobility [70, 71, 72].

To address some of those issues, targeting the peripheral nerves instead of the distal muscles has been proposed as alternative. The currents needed are at least an order of magnitude smaller than those needed to activate motor units. Motor neuroprostheses based on peripheral nerve cuff electrodes have been developed. The cuffs wrap around the nerve and bring the electrodes on their inner surface in close contact with the nerve outer surface [73, 74, 75]. Those systems offer a solution to the drawbacks of surface stimulation in terms of electrode placement, skin irritation or discomforting sensation and enable a more efficient recruitment of motor units. However, the selectivity in recruiting distinct populations of fibers residing deeply inside the nerve or within the same fascicle is relatively low, due to stimulation from the surface. Nevertheless, such epineural electrodes have been used clinically to generate movement in the upper [76, 77] and lower limbs [60, 58]. Yet none of those systems are widely used today. None are able to return sustained, functional, and weight-bearing movements to paralyzed persons.

The development of a successful and widely accepted FES-based motor neuroprosthesis for paralyzed individuals has been hampered by difficulties to simultaneously but selectively generate and control graded activation of several muscles. FES suffers mainly from two main shortcomings. First, current FES applications to generate standing and walking are technically complicated and cumbersome to set up. They display limited functional benefits with respect to the i) effort that is needed to put them in place, and ii) the relatively low efficiency in permitting functional walking. The generation of coordinated multi-joint movements required for functional and weight-bearing locomotion would involve the simultaneous and graded control of FES of a very large number of muscles, which seems extremely challenging if not unrealistic. Second, FES induces fast muscle-fatigue, which reduces considerably its usability if the entire movement depends on it.

It will thus be of crucial importance to i) simplify the current way of interfacing multiple muscles and ii) to increase the efficiency of FES-based motor neuroprostheses. In spite of those challenges, targeting the distal neuromuscular system for selectively controlling distal muscle activation should not be underestimated for restoring controllable and precise movements.

1.3 Interfaces with the Peripheral Nervous System

An alternative to targeting the musculature consists in activating the peripheral nerves, which in turn conduct the stimuli to the distal muscles. Electrical interfaces with the peripheral nervous system allow for electrical communication between biological (neural tissue) and engineered (electrical conductor) systems.

1.3.1 Anatomical organization of the Somatic Peripheral Nervous System

The somatic peripheral nervous system relates to voluntary motor control and conscious sensation and contains afferent (sensory) and efferent (motor) fibers for the transfer of information from or to the periphery (Fig. 1.4 (a)). In the somatic peripheral nervous system, axons travel directly between the spinal cord and the target organ. The cell body of motor neurons is located within the spinal cord ventral horn along a well-organized somatotopy. Similarly, sensory neurons have their cell bodies residing in the dorsal root ganglia that are distributed along the spinal rostro-caudal axis. The axons of both types of neurons are bundled together into fascicles (separated or mixed) within the peripheral nerves (Fig. 1.4 (b)).

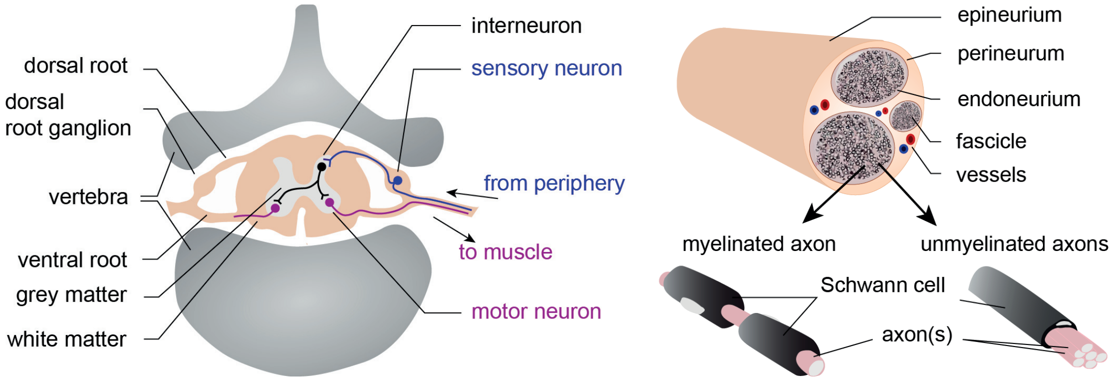

(a) Schematic cross-section of the spinal cord

(b) Structure of the peripheral nerve

Figure 1.4 – Anatomical organization of peripheral nervous system

The larger fibers in the somatic peripheral nervous system are myelinated by Schwann cells. The myelin sheath consists in a multi-layered, insulating membrane that permits high action potential conduction speed through regeneration of the action potential at the gaps in the myelin sheath between two Schwann cells (nodes of Ranvier, approximatively every 1 mm [78]). The nodes of Ranvier are highly enriched in voltage-gated sodium and potassium channels, permitting the increased exchange of ions required to regenerate the action potential, propagating it thus rapidly from node to node (saltatory). Unmyelinated axons are found alone or grouped and can be enclosed by non-myelinating Schwann cells and conduct action potentials by passive propagation (as opposed to saltatory conduction in myelinated fibers).

The types of sensory and motor fibers can be differentiated with respect to their diameter, function, and conduction velocities (Table 1.2).

Table 1.2 – Types of sensory and motor fibers in the human peripheral nerve [79]

Group	Myelin	Diameter (μm)	Conduction velocity (m/s)	Fiber types
Aα	Yes	12 - 20	70 - 120	*Sensory*: Group Ia and Ib afferents (proprioception), *Motor*: α motor neurons
Aβ	Yes	5 - 10	30 - 70	*Sensory*: Group II afferents (touch, pressure)
Aγ	Yes	3 - 6	15 - 30	*Motor* (to muscle spindle): γ motor neurons
Aδ	Thinly	< 3	12 - 30	*Sensory*: Group III afferents (fast pain, cold, touch, pressure)
C	No	0.1 - 2	0.5 - 4	*Sensory*: Group IV afferents (C fibers) (slow pain, temperature)

Peripheral nerves are composed of three main tissues that confer both structure and flexibility [80]. Each fascicle is enclosed by the *perineurium*, a strong collagenous membrane conferring mechanical stability. The space within the fascicles is called the *endoneurium* and contains myelinated and unmyelinated axons, Schwann cells, blood vessels, fibroblasts, collagen fibrils, and some resident macrophages [81]. Fascicles are enveloped by the *epineurium*, a thick and elastic structure made of collagen fibrils and adipose tissue [80] to form the peripheral nerve trunk (Fig. 1.4 (b)).

Interfaces with the peripheral nervous system interact with axons only. The selectivity of the intervention depends strongly on the location of the electrode within or around the nerve as the mechanism of excitation of fibers is dependent on the proximity between the source of excitation and the target fiber.

1.3.2 Mechanisms of excitation of peripheral nerves

The nature of the excitation of the nerves and enclosed fibers using extracellular stimulating electrodes has been described using axon cable models that model the axon as a segmented cylinder with capacitances (lipid bilayer in the axonal membrane) and resistances (axoplasm) combined in parallel [82]. The activation of axons depends on their distance from the current source and on their diameter as well as on the resistivity of the various tissues between the target axons and the current source [82, 83].

Influence of distance between current source and target axons Changes in the transmembrane potential due to electrical excitation are greatest in fibers that are closest to the source because the induced extracellular potential V_e decreases in amplitude with the distance r from the source (for a monopolar spherical electrode in an isotropic medium):

$$V_e = \frac{\rho_e I}{4\pi r},$$

where, ρ_e is the resistivity of the external medium and I is the current flowing from the electrode [82]. The recruitment of potential target fibers can be qualitatively described using the activating function, which is proportional to the second spatial derivative of the extracellular potential V_e along the axon nodes [83]. The activating function is inversely proportional to the distance between the electrode and the target axon. Consequently, axons closest to the electrode require the least current to get activated.

Influence of axon diameter If the target population of axons is far from the electrode, greater currents are required for their activation, but can result in the co-activation of other, unwanted axons. An important concept to consider here is fiber diameter selectivity. Fibers with larger diameters have larger inter-nodal distances and experience thus greater changes in transmembrane potential due to electrical excitation [82, 83]. At a certain distance from the current source the recruitment of axons is thus biased towards the activation of large diameter fibers [84]. This is the inverse of the physiological order of fiber recruitment, and in the case of motor nerves responsible for the early signs of muscle fatigue in applications using surface FES, since activating large motor fibers innervating fast-fatiguing motor units first.

While this holds for electrical stimulation applied outside of a nerve (transcutaneous or extraneural), Gaunt and colleagues found that microstimulation of the dorsal root ganglia (DRG) at spinal level L7 using penetrating microelectrode arrays allowed to selectively recruit smaller diameter fibers at low stimulation thresholds without activating the larger diameter fibers [85, 86]. He and others showed experimentally [87, 88] and computationally [89, 90] that the impact of the distance between the current source and the axons becomes negligible when stimulating intraneurally at low amplitudes and that the order of recruitment of axons was not biased towards large diameter fibers in this case. Similar results were obtained with thin-film intrafascicular electrodes [91]. Taken together, these results suggest that a neutralization of the recruitment order is possible when the distance between the stimulating source and the target fibers is small. The probabilities of recruiting fibers with different diameters are further influenced by the number of fibers of a given size that are likely to be present in the volume of tissue reached by the induced extracellular potential and by the likelihood of a fiber having a node of Ranvier in that volume. Indeed, the internodal distance in myelinated axons is proportional to their diameter [92], suggesting that large fibers are less likely to have a node of Ranvier in the volume of tissue that would be activated by a current source.

Influence of tissue resisitivity Peripheral nerves are mainly composed by the three main tissues endoneurium, perineurium, and epineurium that envelop the axons in several organized layers. The endoneurium is anisotropic, with a transversal and longitudinal conductivity of 0.0826 S/m and 0.571 S/m respectively [93]. The perineurium has a relatively low conductivity (0.0021 S/m, [94]). The conductivity of the endoneurium has not been experimentally determined but is often approximated to the transverse conductivity of the endoneurium for their high similarity in structure [95]. These tissues considerably influence the distribution of current flow inside the nerve. For instance, the perineurium largely attenuates current flow and makes its distribution more homogeneous inside a fascicle, thus increasing the difficulty of recruiting a small sub-population of fibers selectively using extraneural electrodes. In contrast, intra-fascicular electrodes could be capable of selectively activating small axon populations within the fascicle in specific conditions.

1.3.3 Trade-off between selectivity and invasiveness of nerve interfaces

The excitation of axons in peripheral nerves crucially depends on the chosen interface. While the considerations on selectivity in recruiting a given population of axons (for instance to avoid the perpetual recruitment of large diameter motor fibers causing rapid muscle fatigue) are crucial, the choice of neural interface also depends on the invasive nature of the device. In fact, the invasiveness and associated risks weigh heavily on user acceptance rate and the demonstration of safety, stability and good bio-integration is thus key for a successful interface with the peripheral nervous system.

Typically, a given neural interface is chosen based on a trade-off between invasiveness, selectivity, and reliability [96, 97]. Extraneural electrodes, for instance CUFF electrodes (Fig. 1.5 left), are placed around the nerve and stimulate the axons extraneurally [73]. The are relatively safe and have been successfully used in numerous clinical applications in humans, for instance to treat incontinence [98, 99]. While this type of interface is suitable when a relatively simple control of function is required, more advanced functional restoration has to target specific fiber bundles within the nerve in order to modulate their recruitment selectively in real-time using application-specific control strategies. Durand and colleagues have developed a modified version of the CUFF electrode that reshapes the nerve and flattens it for gaining access to the deeper fascicles within the nerve [75]. The large-to-small recruitment order may remain a concern with this extraneural stimulation strategy.

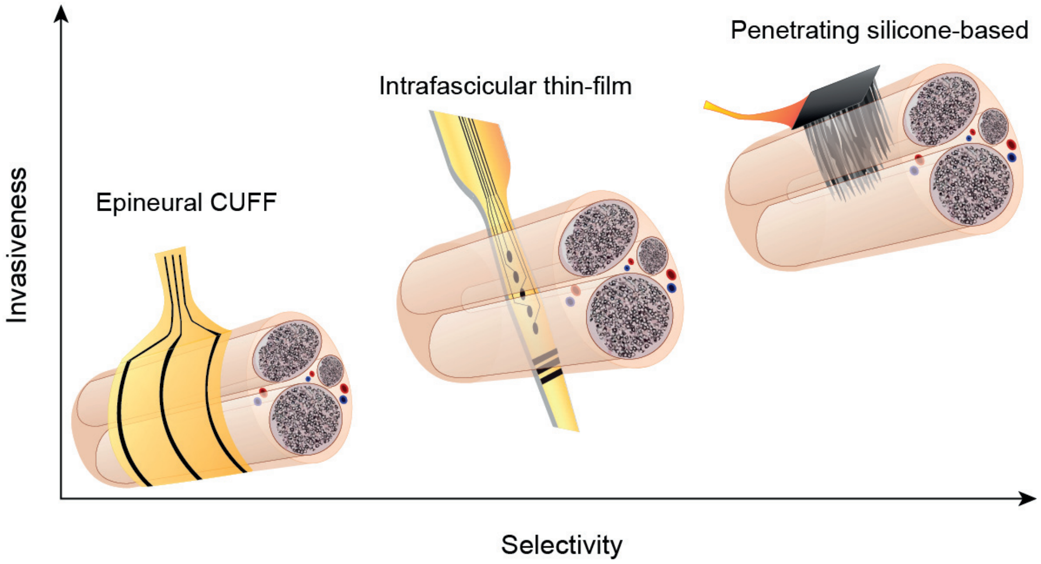

Figure 1.5 – Trade-off between selectivity and invasiveness for choosing an interface with the peripheral nervous system. From least invasive and least selective (left) to most invasive and most selective (right). Tripolar cuff electrode made of polyimide with three contacts surrounding the nerve, for instance [100, 74], transversally inserted intrafascicular multi-contact electrode with one or more contacts per fascicle ([101], and silicone-based penetrating multielectrode arrays [102] with tens of tips inserted per fascicle.

On the other side, silicone-based penetrating slanted multi-electrode arrays (Fig. 1.5 right) permit very high selectivity through a three-dimensional configuration of hundreds of stimulating tips within the nerve [102, 103, 104, 105]. Chronic and acute studies in animal models have shown the possibility of selectively stimulating efferent and afferent fibers within the peripheral nerves. Their impact on nerve conduction was assessed in acute preparations [106] and suggested limited acute damage by comparing recorded compound action potentials before and after insertion. Histology revealed however a compression zone of axons up to hundred micrometer below the electrode tips. Chronic implantation of functional or passive devices with different containment systems revealed an accumulation of connective tissue below the base of the array that pushed the tips out of the fascicles in many cases [103]. In some animals, the implant impeded the walking ability of the animals although in other animals little or no deficits in walking were observed. In the long term, the tips of the array were encapsulated by a connective tissue layer of about thirty micrometers. Stimulation capability was conserved at the chronic stage. A third study specifically and comprehensively assessed the foreign body reaction to slanted electrode arrays encapsulated in a silicone cuff implanted in cat sciatic nerves [107]. No functional impairment was observed but all arrays displayed accumulation of connective tissue beneath the array and signs of ongoing neuroinflammation inside the fascicles. Stimulation or recording capabilities were not assessed. Taken together, the results suggest that penetrating multi-electrode arrays have a relatively strong impact on the nerve. They are markedly more invasive than epineural electrodes. The substrate and the shafts are rigid and impose a strenuous mechanical stress on the nerve in a chronic, tethered implantation.

Poylimide-based intraneural multichannel electrodes (Fig. 1.5 middle) offer a great trade-off between selectivity and invasiveness as they penetrate the fascicles, thereby permitting high selectivity, while imposing a limited amount of stress to the nerve through thin-film technology and flexible substrates [101, 108, 109]. In addition, intrafascicular active sites are in close proximity with the axons, thereby neutralizing the recruitment order, which is of cardinal importance to potential applications in restorative neurology. Several limiting factors have so far prevented the deployment of intraneural implants in clinical applications. For instance, the reaction of the nerve to i) the immediate penetration and ii) long term implantation has been solely characterized on passive implants without cabled connections [110, 109]. On the other hand, while selective recruitment properties have been demonstrated in acute animal preparations, little is known about the stability of the selectivity of intra-neural implants to enable functional applications over extended time.

Given these considerations, I argue that thin-film intra-fascicular multichannel implants would be excellent candidates for peripheral nerve stimulation in the framework of restorative neurology. They provide a very acceptable trade-off between selectivity and invasiveness. A longitudinal study assessing the relationship between electrode functionality and bio-integration over time is however necessary to promote this peripheral interface to clinical applications.

1.4 Considerations for clinically accepted neuroprostheses

Over the last decades, implantable technologies have emerged as treatment method to restore function to a disabled person. A neuroprosthesis is defined as a system that delivers electrical current to the neuromuscular system and/or records electrical signals from the neuromuscular system with the purpose of restoring or replacing lost function due to trauma or disease [76]. Among the most successful and clinically accepted neuroprostheses are the cochlear implant or the cardiac pacemaker, which are both routinely implanted in millions of patients worldwide.

Nonetheless, the idea of implanting multiple electrodes within the body is greeted with reticence among the target population and despite incredible technological developments, the fear of additional injury, loss, or complications is often bigger than the anticipated benefits. These are key considerations for the usefulness and applicability of neuroprosthetic technology. The success of a neuroprosthesis does not solely depend on the technological development that engendered it. Safety, stability, bio-integration, customization to individual users, and related to all of these - user acceptance - are cornerstones for the success of the devices we are developing.

For potential end-users, areas of high concern regarding neuroprostheses are reversibility of interventions and cosmetics of the devices [111]. While implantable technology would favor the idea of "invisibility" of the neuroprosthesis, it is in my opinion of utmost importance to understand the impact of an implantation and also the removal of the implant from the body. In addition, improved surgical techniques and miniaturization of both the implantable technology and surgical tools will hopefully drive acceptance of neuroprostheses beyond the areas in which they are seen as a last resort. It seems likely that as neuroprosthetic interventions become more accepted as a form of medical treatment, they will be used to treat “simpler” conditions in addition to the more complex and involved interventions they are frequently targeted for today.

1.5 Thesis outline

This introduction provides a general overview on electrical stimulation paradigms in the context of restorative neurology for the recovery of lower limb motor function after paralysis and establishes the conceptual and methodological framework for the work I carried out during my thesis.

Spinal cord stimulation, and more precisely epidural electrical stimulation (**EES**) of the spinal cord, provides a way to exploit the spinal networks to accomplish simultaneous and coordinated activation of multiple muscles and permits to leverage the capacity of the spinal circuits to integrate and process sensory feedback, resulting in the restoration of coordinated and stereotyped movement patterns. EES enabled weight-bearing locomotion in animal models and also promoted locomotor-like activity in severely paralyzed human subjects, permitting a return of volitional control over the activation of otherwise paralyzed muscles. In spite of these encouraging results, it was not possible to actually generate stepping, indicating a translational gap between rodent experimentation and clinical studies. Major anatomical and neurophysiological differences between the two species account for this discrepancy. In addition, the human locomotor apparatus is characterized by high dexterity and functionality when compared to rodents, and requires thus interventions beyond leg flexion and extension to recover usable movements after paralysis. It is not clear to what extent EES will enable to selectively activate the distal neuromuscular system, crucial though for refining movement execution and permitting functional recovery.

FES systems provide an immediate functional benefit during stimulation, even though their usability depends on the user’s muscle quality. Direct muscle stimulation may cause rapid fatigue while reflex responses can quickly destabilize the ambulating individual. Especially in severe SCI individuals, the sole use of FES, be it multi-site, will hardly increase mobility and independence to a satisfactory level. Current strategies prevent access to deep muscles and have an overall limited selectivity. The complex and cumbersome set-ups are likely unrealistic for clinical applications because of the complexity that is involved in providing closed-loop control strategies for the simultaneous and smooth modulation of numerous muscle activation. Intraneural peripheral nerve stimulation (**PNS**) could address a number of these issues by i) neutralizing the physiological recruitment order, thereby potentially reducing fast fatigue, ii) allowing to selectively target multiple and deep muscles at once, and iii) avoiding cumbersome and non-reproducible donning and doffing. However, PNS does not alleviate the complexity of controlling the precisely-timed, coordinated, and graded activation of multiple muscles in real time and would hardly be able to generate functional and weight-bearing movements over time.

In this thesis, I argue that PNS and EES are complementary and that a hybrid neuromodulation paradigm targeting both the peripheral nerves and the spinal cord can provide a novel and highly promising opportunity to recover a high degree of functionality after paralysis. EES promotes the generation of multi-joint movements, providing the basic building block for locomotion. Precisely-timed and spatially selective PNS permits local interventions to refine movement execution and restore precise, local, and cardinal functions for locomotion. In *chapter 2*, I demonstrate the potential of intraneural, thin-film, multi-channel electrodes to interface the peripheral nerves in a sustainable, highly functional, and stable way. In *chapter 3*, I exploit these properties by developing a hybrid neuromodulation paradigm, concomitantly engaging the spinal cord and the peripheral nerves in severely paralyzed rats. I demonstrate that hybrid PNS-EES neuromodulation permits selective and graded control over the distal musculature during locomotion, which refined movement execution and increased functionality in rats and also in a human individual affected by a spinal cord injury.

These developments might have important implications in addressing functional restoration after neuromotor disorder and could represent a paradigm-shift towards personalizing neuroprosthetics. The hybrid peripheral-spinal approach provides an unprecedented comprehensiveness in neuromodulation by exploiting the complementary properties of the peripheral and the central nervous systems. These properties could significantly impact movement restoration after paralysis of lower and also of upper limbs. In this framework, and stemming from the developments of this thesis work, we are now investigating the feasibility of generating controllable and selective muscle activation in the arm and hand via intraneural stimulation of the upper limb peripheral nerves.

2 Chronic assessment of functionality and bio-integration of intraneural electrodes

Intraneural implants have the capacity to selectively activate a number of different muscles and integrate well within the nerve as passive implants. To anticipate clinical acceptance and permit successful translation, I believe that it is crucial to demonstrate safety and stability within the tissue alongside functionality in actively used implants. In this work, I assessed the long-term bio-integration of polyimide-based intraneural stimulating electrodes in light of their functionality. I show that the implant electrical properties evolve with the developing implant encapsulation during the first month post-implantation, after which both stabilize. The selectivity is conserved, permitting to achieve graded control over ankle movements months after implantation. With this work, I provide a large body of evidence highlighting the potential of intraneural, thin-film, multi-channel electrodes to interface the peripheral nerves in a sustainable, highly functional, and stable way.

The content of this chapter is adapted from the manuscript **Wurth** et al., "Long-term functionality and bio-integration of polyimide-based intraneural stimulating electrodes" published in the journal Biomaterials, Volume 122, April 2017, Pages 114 - 129.

Personal contributions: Responsible for the project. Conceived the study and designed the experiments, performed animal-related procedures and experiments, acquired and analyzed the electrophysiology data, processed tissue, performed stainings, acquired and analyzed the images obtained from histology, prepared the figures, wrote the manuscript.

Long term functionality and bio-integration of polyimide-based intraneural stimulating electrodes

S Wurth[1,2], M Capogrosso[1,3], S Raspopovic[1,3], J Gandar[2], G Federici[1], N Kinany[1], A Cutrone[3], A Piersigilli[4], N Pavlova[2,5], R Guiet[6], G Taverni[3], J Rigosa[1,7], P Shkorbatova[2], X Navarro[8], Q Barraud[2], G Courtine[2*], S Micera[1,3*]

[1] Bertarelli Foundation Chair in Translational Neuroengineering, Center for Neuroprosthetics and Institute of Bioengineering, École Polytechnique Fédérale de Lausanne (EPFL), Lausanne, Switzerland

[2] International Paraplegic Foundation Chair in Spinal Cord Repair, Center for Neuroprosthetics and Brain Mind Institute, École Polytechnique Fédérale de Lausanne (EPFL), Lausanne, Switzerland

[3] The Biorobotics Institute, Scuola Superiore Sant'Anna, Pisa, Italy

[4] Laboratory Animals Pathology Unit, Institute of Animal Pathology, University of Bern, Bern, Switzerland

[5] Pavlov Institute of Physiology, St Petersbourg, Russia

[6] Bioimaging and Optics Platform, Faculty of Life Sciences, École Polytechnique Fédérale de Lausanne (EPFL), Lausanne, Switzerland

[7] SAMBA lab, International School for Advanced Studies, Trieste, Italy

[8] Institute of Neurosciences, Department of Cell Biology, Physiology, and Immunology, Universitat Autònoma de Barcelona, and CIBERNED, Bellaterra, Spain

[*] Equal contribution as senior authors

2.1 Abstract

Stimulation of peripheral nerves has transiently restored lost sensation and has the potential to alleviate motor deficits. However, incomplete characterization of the long-term usability and bio-integration of intraneural implants has restricted their use for clinical applications. Here, we conducted a longitudinal assessment of the selectivity, stability, functionality, and biocompatibility of polyimide-based intraneural implants that were inserted in the sciatic nerve of twenty-eight healthy adult rats for up to six months. We found that the stimulation threshold and impedance of the electrodes increased moderately during the first four weeks after implantation, and then remained stable over the following five months. The time course of these adaptations correlated with the progressive development of a fibrotic capsule around the implants. The selectivity of the electrodes enabled the preferential recruitment of extensor and flexor muscles of the ankle. Despite the foreign body reaction, this selectivity remained stable over time. These functional properties supported the development of control algorithms that modulated the forces produced by ankle extensor and flexor muscles with high precision. The comprehensive characterization of the implant encapsulation revealed hyper-cellularity, increased microvascular density, Wallerian degeneration, and infiltration of macrophages within the endoneurial space early after implantation. Over time, the amount of macrophages markedly decreased, and a layer of multinucleated giant cells surrounded by a capsule of fibrotic tissue developed around the implant, causing an enlargement of the diameter of the nerve. However, the density of nerve fibers above and below the inserted implant remained unaffected. Upon removal of the implant, we did not detect alteration of skilled leg movements and only observed mild tissue reaction. Our study characterized the interplay between the development of foreign body responses and changes in the electrical properties of actively used intraneural electrodes, highlighting functional stability of polyimide-based implants over more than six months. These results are essential for refining and validating these implants and open a realistic pathway for long-term clinical applications in humans.

2.2 Introduction

The ability to communicate bi-directionally with the peripheral nervous system has opened promising perspectives to control neuroprostheses, restore lost sensation, and alleviate motor deficits resulting from neurological disorders [96, 112]. For example, peripheral nerve stimulation has been successfully used in humans to alleviate foot drop after neuromotor disorders [113, 114, 115, 116, 117], to treat bladder dysfunction [98, 99], and to reanimate paralyzed muscles after spinal cord injury [118, 119, 77, 120].

In all these applications, the stimulation was applied using an epineural cuff electrode [100]. While this type of interface is suitable when a simple and non-selective control of the stimulation is required, more advanced neuroprostheses rely on the ability to target specific fiber bundles within the nerve in order to modulate their recruitment in real-time using application-specific control strategies. In general, for a desired outcome, the type of neural interface is chosen based on the trade-off between invasiveness, selectivity, and reliability [96, 97]. To this respect, intraneural electrodes are the most appropriate implants since they provide superior selectivity of recording and stimulation, increased signal-to-noise ratio of recordings, and lower threshold of activation than extra-neural implants [121, 122]. For instance, intraneural stimulation of the median and ulnar nerves re-established graded sensory feedback that improved the control of a hand prosthesis after amputation in humans [123, 105]. Despite this success, clinical studies using intraneural implants have remained investigational and restricted to short-term implantation periods.

Several limiting factors have prevented the deployment of intraneural implants for extended durations in human patients. First, these implants are markedly more invasive compared to epineural cuffs [74, 124, 75, 73]. Second, the anatomical and functional consequences of the immediate penetration into and long term implantation within the host tissue have been solely characterized on passive implants without cabled connections [110, 109]. Third, little is known about the stability and selectivity of intraneural implants to enable functional applications over extended time.

To remedy these limitations, we evaluated the selectivity, stability, functionality, and biocompatibility of a polyimide-based intraneural implant over a period of 6 months. Polyimide is a common material used in thin film technology for in vivo applications that allows versatile micro-fabrication of electrode implants with varying shape and geometry [25-27]. Polyimide-based intraneural implants have emerged as a viable alternative to rigid silicon-based penetrating microelectrode arrays [105, 125, 126, 102] for clinical applications.

Previous studies in acute animal preparations showed that polyimide-based intraneural implants enable the preferential activation of specific groups of muscles that are innervated by different branches of the same stimulated nerve [122, 109, 101, 127]. However, the long-term stability of this selectivity has not been investigated. Independently, the foreign body response to polyimide-based intraneural implants has been evaluated using passive, untethered implants over periods of up to 3 months [110, 109, 108, 128]. Taken together, these studies described the formation of a mild fibrotic encapsulation around the implant that developed in parallel to inflammatory responses, but had no sustained impact on the density of nerve fibers, axonal conduction velocity, or locomotor capacities of the implanted animals.

While these studies have provided critical information that supported preliminary clinical applications, the results have all been obtained in different groups of animals, focusing on specific modalities, and at discrete time-points. Therefore, the interactions and inter-dependencies between foreign body reactions and electrical properties over time have not been studied systematically and conjointly in longitudinal studies. To date, no chronic and realistic studies on intraneural thin-film electrodes have been carried out that would allow to understand the impact of cabled implants and regular stimulation on electrode function and implant bio-integration.

Here, we studied the selectivity, stability, functionality, and biocompatibility of the SELINE polyimide-based intraneural implant [129, 109] that was inserted into the sciatic nerve of 28 healthy rats for durations of up to 6 months. After a period of adaptation that approximatively lasted one-month, the electrodes exhibited stable and selective responses to charge delivery that persisted over the remaining duration of the experiments. This selectivity supported the development of real-time stimulation paradigms that precisely controlled the forces produced at the ankle. In the same rats, we characterized the development of foreign body reaction over time, and showed that they tightly correlated with concomitant changes in the electrical properties of the electrodes. The removal of the implant did not cause detectable motor impairments and did not further harm the tissue. These results uncover relationships between actively used implants and neural tissue responses in rats and demonstrate the stability of intraneural electrodes for reliable long-term interfacing with the peripheral nervous system. Our study assessed for the first time intraneural thin-film electrode performance and in vivo biocompatibility in a chronic rat model. These unprecedented findings obtained in ecological settings provide a framework for the safe and long-term implantation of polyimide-based intraneural electrodes in clinical applications.

2.3 Materials and methods

2.3.1 Animals

All animal procedures and experiments were approved by the Veterinarian Offices of the Cantons of Vaud and Geneva, Switzerland. A total of 28 adult female Lewis rats (LEW-ORlj, Charles River Laboratories, France) with initial weight of ~200 g were implanted with a SELINE electrode [109] into their left sciatic nerve (Fig. 2.1), with different indwelling times ranging from 0 days to up to 6 months (Table 2.1).

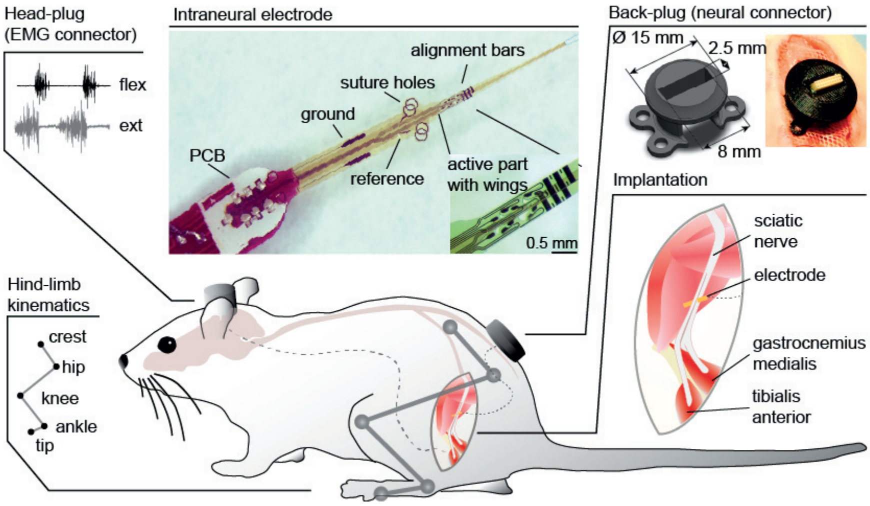
Head-plug
(EMG connector)
flex
ext
Intraneural electrode
alignment bars
suture holes
ground
PCB
reference
active part
with wings
0.5 mm
Back-plug (neural connector)
Ø 15 mm
2.5 mm
8 mm
Implantation
sciatic
nerve
electrode
gastrocnemius
medialis
tibialis
anterior
Hind-limb
kinematics
crest
hip
knee
ankle
tip

Figure 2.1 – Chronic experimental setup for the chronic assessment of functional polyimide-based intraneural implants.

The self-opening intraneural polyimide-based multi-channel electrodes were implanted into the rat sciatic nerve proximal to the separation of the different fascicles. The connector of the implant was embedded in a percutaneous 3D-printed pedestal (back-plug) that was sutured to the muscles on the back at the sacral spinal cord level (Fig. 2.1. EMG activity of ankle muscles (via percutaneous connector mounted on the head (head-plug)) and kinematics of hind-limb movements (via a motion capture system with reflective markers) were recorded during different experimental protocols. Three groups of animals were implanted during 28 days: we differentiated i) active from ii) passive implants to investigate the impact of electrical stimulation on the foreign body reaction and iii) removed the implanted in the third group to assess the impact of explantation on nerve function and morphology. All animals were housed three by three on a 12-hour light-dark cycle with food and water ad libitum and were given social time three times a week.

Table 2.1 – Demographics of animals participating in the study

Group	n	Implant duration (days)	Stimulation protocol	Additional experiment
1 - Acute	3	0	In surgery	no
2 - Sub-acute	3	1.5	In surgery	no
3 - Early	3	7	In surgery, weekly	no
4 - Mid	3	17	In surgery, weekly	no
5 - Late	3	28	In surgery, weekly	Locomotor task
6 - Late	3	28	never (passive)	Locomotor task
7 - Late	5	30	never (passive)	Locomotor task, implant removal at 30 days
8 - Chronic	5	165	In surgery, weekly	Force control task

2.3.2 Chronic experimental model

The experimental model is graphically summarized in Fig. 2.1. All surgical interventions were performed under aseptic conditions and full anaesthesia with isoflurane in oxygen enriched air (1 - 2 %). Animals were placed on a heating pad to prevent hypothermia during surgery. Analgesic medication (Buprenorphine (Temgesic), ESSEX Chemie AG, 0.01-0.05 mg per kg, subcutaneous) and antibiotics (Amoxicillin (Clamoxyl), Pfizer AG, 0.5 ml/kg, subcutaneous) were administered during 5 days post-surgery.

Intraneural electrode implantation with connector on backstage

The detailed implantation procedure for the SELINE electrode has been described previously [109]. Briefly, two longitudinal skin incisions of about 2 cm were made over the lower lumbar spine for the fixation of the backstage and at the level of the mid-thigh for access to the sciatic nerve. The sciatic nerve was carefully exposed and freed from surrounding tissues. Then, the 3D printed pedestal was sutured via its five suture-holes to the fascia of the back-muscles (multifidus muscle and gluteus superficialis) through a 2x2 cm piece of surgical mesh (Mersilene mesh, Ethicon Inc., NJ) to favour the stabilization by fibrotic healing. The wires (CZ1187, Cooner Wire Corp. CA), leading from the nano-strip connector (NPD-18-DD-GS, Omnetics Connector Corp, MN) incorporated in the pedestal to the printed circuit board (PBC), were passed subcutaneously and under the gluteus maximus muscle with a plastic tunnel guide until the opening leading to the sciatic nerve. From here, the needle was obliquely inserted into the sciatic nerve about 0.5 cm above bifurcation of tibial and peroneal branches (fig. 2.2). The wires were subcutaneously placed in a stress-release loop to allow for leg movements without pulling on the implant via the cables.

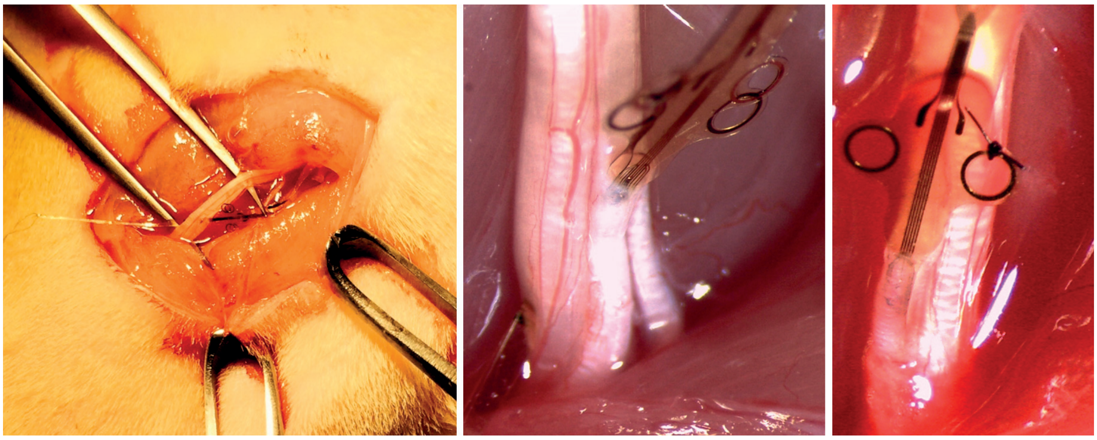

Figure 2.2 – Implantation of the SELINE electrode in the rat sciatic nerve

Intramuscular electrodes implantation with connector on head-stage

To record electromyography (EMG) activity, bipolar electrodes were implanted into the following four muscles of the left hindlimb: tibialis anterior (TA), soleus (SOL), gastrocnemius medialis (GM), plantaris (PL). Recording electrodes were fabricated by exposing a 0.5 mm notch in the insulation of the implanted Teflon-coated stainless steel wires (AS632, Cooner Wire Corp., CA). A common ground electrode was created by removing 1 cm of insulation at the distal extremity of one wire, which was then subcutaneously placed over the left shoulder. All wires were subcutaneously tunnelled to a single percutaneous amphenol connector (Omnetics Connector Corp., MN) that was fixated with dental cement to the skull of the rat.

Surgical interventions were identical for all animals, except for the acute group, which did not receive intramuscular electrodes and whose animals were euthanized immediately after testing the stimulation performance of the electrodes. After surgery, all rats were placed in an incubator until full recovery from anaesthesia. An additional recovery period of minimum five days was given before the start of the experiments. From there, both percutaneous interfaces at the back and at the head were cleaned regularly with saline or antiseptic spray (Bepanthen Plus, Bayer, Germany) as preventive treatment for infections.

2.3.3 Chronic electrode characterization

Weekly muscle recruitment curves were performed by injecting increasing amounts of charge into each of the channels of the intraneural implants while recording the obtained compound muscle action potential (CMAP) from each of the implanted muscles (Fig. 2.3 (a)). The schematic in Fig. 2.3 (a) shows the electrode insertion in tibial and peroneal fascicles of the rat sciatic nerve and how selective muscle recruitment of tibialis anterior (TA), gastrocnemius medialis (GM), soleus (SOL), or plantaris (PL) could be achieved. Two representative examples of compound muscle action potentials (CMAPs) recorded from TA and SOL muscles of the same rat upon stimulation of the nerve with two different channels are also shown in Fig. 2.3 (a).

A custom-made stimulation protocol (Matlab, The MathWorks Inc, MA) prompted a stimulator unit (IZ2H, Tucker Davis Technologies, FL) to deliver biphasic cathodic-first current pulses (1 Hz) of 40 to 80 µs duration and increasing current intensities ranging from sub-threshold to a saturation value of the recorded CMAPs for the channel being tested. The EMG activity was amplified (1000x, Differential AC amplifier, AM systems, WA), filtered (10 - 2000 Hz bandpass) and acquired into the TDT RZ2 system (Tucker

Davis Technologies, FL) at 25 kHz for offline analysis.

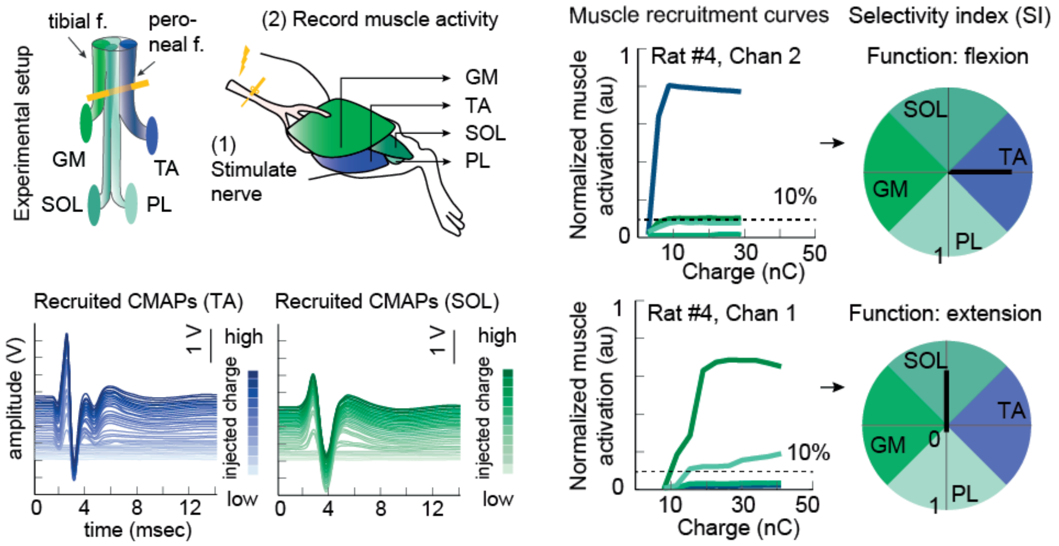

(a) Schematic of experiment and examples of recorded CMAPs

(b) Examples of muscle recruitment curves and channel selectivity

Figure 2.3 – Assessment of muscle recruitment by intraneural stimulation. (a) Top: Schematic of muscle recruitment and implanted muscles. Bottom: Examples of CMAPs recorded from tibialis anterior (TA) and soleus (SOL) muscles. (b) Examples of muscle recruitment curves and channel selectivity for two different channels in the same rat.

For every channel, three repetitions of each current step were performed and the average peak-to-peak amplitude of the evoked CMAP of each muscle was used to analyse the relationship between stimulation-evoked muscle activity and stimulation intensity via the computation of muscle recruitment curves (Fig. 2.3 (b)). In this animal, one channel (chan 2) elicited selective flexion (specific activation of TA vs. other muscles), while the other channel (chan 1) elicited selective extension (specific activation of SOL, and marginally PL, both ankle extensor muscles). At the end of the experiment, the recorded CMAPs were normalized to their maximal amplitude obtained throughout the duration of the experiment (up to 6 months). These data were then used to assess the stability of the selectivity in muscle recruitment for every channel, as well as the stability of the electrical properties of the implants over time.

Selectivity for every muscle was assessed by calculating a selectivity index (SI) as the ratio between the normalized CMAP of a target muscle i, and the sum of the normalized CMAPs elicited in all muscles recorded [122, 130]:

$$SI_i = \frac{CMAP_i}{\sum_{j=i}^{n} CMAP_j},$$

For a given channel, the SI for muscle i was comprised between 0 and 1, with 0 indicating absence of selectivity and 1 demonstrating exclusive activation of muscle i without activating other muscles. A channel was considered selective for one of the tested muscles when the SI for this muscle was higher than 0.6. In the rat sciatic nerve, SOL, GM, and PL muscles are innervated by the tibial fascicle, while the TA muscle is innervated by the peroneal fascicle (Fig. 2.3 (a)). As such, inter-fascicular selectivity (tibial vs. peroneal nerve stimulation) and intra-fascicular selectivity (SOL vs. PL vs. GM activation) could be assessed in this experimental setup.

To assess the stability of the implant in terms of electrical properties, for each channel, the threshold charge, defined as the amount of charge necessary to elicit 10% of a maximal muscle activation, was used to assess changes in stimulation efficiency from week to week. Further, impedance between each channel (intraneural) and the implant's ground (extra-neural) was measured at 1 kHz in vivo on a weekly basis. The stability over time in both metrics was assessed via pair-wise comparisons between all weeks (Kruskal-Wallis test) and further underlined by fitting an exponential decay function to the median time derivatives of each metric. Finally, we counted the number of functional channels per implant according whether muscle activity was elicited within the charge injection limits defined by cyclic voltammetry [101, 131].

2.3.4 Modulation of movement amplitude

We assessed the possibility of functionally exploiting the obtained selectivity and performed amplitude and frequency modulations of the stimulation for selective channels. Rats were lightly sedated with Dormitor (Dorbene, Graeub, DE, 0.0025 - 0.005 ml/kg) to isolate the effect of the stimulation protocol from possible movements artifacts, and were then placed at the edge of a small table with the legs hanging. The tail was pulled up with a string and fixated to an artificial ceiling in order to maintain the lower trunk straight and to ensure that legs were free from movement constraints. Joint kinematics of the left hind-limb were recorded using the high speed motion capture system Vicon (Vicon Motion Systems Ltd., UK) combining 12 infrared cameras (200Hz). Small reflective markers were positioned on the left hind-limb joints iliac (crest), greater trochanter (hip), lateral condyle (knee), lateral malleolus (ankle), and the distal end of the fifth metatarsal (MTP). The kinematic data (200 Hz) and EMG signals (2 kHz) were recorded simultaneously during stimulation protocols of either increasing amplitude (pulse width at 40 µs and frequency at 1Hz) or increasing frequency (pulse width at 40 µs and amplitude at value with highest SI obtained). For each step during either modulation, we computed the ankle joint angle using the cosinus law

$$\Theta = \cos^{-1} \frac{\mathbf{A \bullet B}}{\|A\| \times \|B\|} \times \frac{180}{\Pi},$$

where A and B are equal to the length of the segment between the knee and ankle markers and the ankle and foot markers respectively.

2.3.5 Closed-loop control of movement-evoked traction force

To assess the controllability of the observed modulation of movement amplitude with stimulation frequency, we built a proportional-integral controller (PI) that adjusted the stimulation frequency in closed loop based on real-time recordings of the traction force that was produced by the ankle movement upon stimulation through one channel (Fig. 2.12 (a)). The real time control platform was implemented in a multi-threaded C++ code (Visual Studio 2012, Microsoft, WA) as an adaptation from a real-time control structure previously developed [132].

Electrical stimulation was delivered with an IZ2H stimulator (Tucker Davis Technologies, FL) and real-time readouts of the evoked traction force were recorded through the Vicon system via a force plate (2 kHz, HE6X6, AMTI, MA). The data flow was imported into the C++ environment via Ethernet using the DataStream SDK software. The recorded force signal was filtered online using least mean squares adaptive filters and compared to a defined target force (either constant step function, for the characterization of the controller, or a sinusoidal function to assess controllability). The rat foot tip was attached with a string to the three-dimensional force plate while verifying no initial pulling was exerted from the leg hanging position over the string to the force plate. The controller adjusted the frequency of stimulation based on the error between the evoked traction force and the target force as follows:

$$f_{t+1} = f_t + k_p e_t + k_i \int_{t-20}^{t} e_t dt,$$

where f_t is the frequency of stimulation at frame t, k_p and k_i the coefficients for the proportional and integral parts respectively of the controller, and e_t the error between the produced force and the target force at frame t.

Characterization

We characterized the controller in a series of experiments, during which we put step functions of height 0.2 N and width 3.5 s as target force and varied the coefficients for the proportional and integral parts of the controller. The nerve was stimulated through an active site and consequent muscle recruitment produced a movement that was translated into force due to the attached string on the rat foot tip (Fig. 2.12 (a)). The produced force was then compared to a target force (step function). Metrics such as initial overshoot (% of target force), rise time (s), and sum of squared error (SSE) between target force and evoked traction force were assessed for each couple of proportional and integral coefficients to adapt the controller output (Fig. 2.12 (b)).

Control of stimulation frequency

We performed an additional set of experiments, to demonstrate the controllability of the produced muscle activations in real time. In each trial, the stimulation frequency was updated continuously based on the difference between recorded and target force, which in this case was a sinus function (wavelength 3 seconds, evaluated on 3 repetitions). Values for the proportional (k_p) and the integral (k_i) corrections of the controller were obtained from the characterization experiment, and were kept constant during each trial. To measure performance, we assessed correlation between the evoked and the target force throughout the three repetitions. We further computed the sum of squared errors between evoked and target signal and analysed the distributions of frequencies used to reproduce the target force during each repetition of the sinus function.

2.3.6 Impact assessment of implantation and implant removal

Previously obtained electrophysiological and walking track data has shown that the implantation of polyimide based implants does not alter nerve conduction velocities or stepping patterns [109, 108]. To complement this data, 5 rats were trained daily during two weeks to perform a skilled locomotor task, consisting in walking over a horizontal ladder with irregularly spaced rungs. Rats were tested prior to surgery, and every five days post-surgery during one month.

After this period, we explanted the implant from the nerve and tested leg motor control capacities of these rats on the ladder task during an additional month. Each session consisted in high-resolution kinematic recording (Vicon system) of five trials (runs). Performance per animal was computed as the percentage of missed steps across these five runs. A Kruskal-Wallis test was used to assess differences in performance between the different evaluations time-points before and after the implantation. One month after the removal, all rats were euthanized, perfused and their sciatic nerves were dissected for histological analyses to further assess the impact of the explant surgery on the nerves.

2.3.7 Perfusion and tissue handling

At the end of each experimental procedure, rats were terminally anaesthetized with an overdose of pentobarbital and trans-cardially perfused with Ringer' s solution containing 100000 IU/L heparin and 0.25 % $NaNO_2$ followed by 4% phosphate buffered paraformaldehyde (pH 7.3) containing 5% sucrose. The implanted sciatic nerve was harvested alongside with the contralateral control nerve and fixed overnight in the same fixative solution.

The nerves were washed in PBS 0.1M, routinely processed, embedded in paraffin blocks, and each sample was entirely sectioned (transversal cross sections) on a microtome (Hyrax M25, Microm, DE) at 4 μm thickness. Three tissue sections in a ribbon of ten were selected and mounted 3 by 3 onto coated glass slides (Superfrost Ultra Plus, Thermo Fisher Scientific, MA), yielding tissue slices of approximatively every 40 μm between glass slides. Mounted tissue samples were dried overnight at 37°C and then stored at +4°C until use.

Unless otherwise stated, the tissue reaction to the implants was assessed at the level of the implant (due to the oblique insertion, we selected slices with the implant visible in the tibial fascicle to ensure comparability between animals) and compared to tissue samples proximal and distal to the implant (approximatively 0.75 mm above and below entry/exit of electrode into the nerve) as well as to control tissue (intact contralateral nerve). The tissue at implant level of two animals (one in group P0 and one in group P165) could not be used for histology or immunohistochemistry as cutting on microtome resulted in torn tissue slices that were improper for analysis.

2.3.8 Histology and immunohistochemistry

Hematoxylin and Eosin (H&E) and Sirius red (SR) staining were performed with the automatic Tissue-Tek Prisma & Coverslipper HQplus machine (Sakura, NE). For immunohistochemistry, slides were dewaxed and placed 20 minutes in a citrate buffer bath (pH 6) at 95°C for antigen retrieval, followed by 1h blocking of non specific sites in bovine serum albumin (BSA 1% diluted in PBS 0.1M). Selected sections were then processed for immunohistochemical labelling against myelin (myelin basic protein MBP, 1:200, Abcam), axons (anti-beta III tubuline TUJ1, 1:200 Abcam), macrophages (anti protein CD68 1:400 Serotec), DNA/RNA of cells (4', 6-diamino-2-phenylindole DAPI, 1.5 μg/mL, Vector), and fibroblasts (fibroblast specific protein FSP1/S100A4, 1:200, MerckMillipore). The following secondary antibodies were used: goat anti-rabbit IgG Alexa488, goat anti-rat IgG Alexa555, goat anti-mouse IgG Alexa555 (ThermoFisher Scientific). Briefly, after blocking, sections were incubated overnight in a primary antibody solution at 4°C, followed by rinses in PBS 0.1M. Sections were then incubated once more for 1h in a solution of appropriate secondary antibody (Life Technologies) diluted 1:400 in PBS 0.1M and BSA 1%, followed by additional rinses. Slides for fluorescence microscopy were mounted with a DAPI-containing medium (Vectashield, Vector Laboratories). All stained slides were cover-slipped for microscopy.

2.3.9 Image acquisition, selection, and processing

Images of slices stained with H&E and SR were acquired with an optical microscope at 20x magnification (Olympus slide scanner VS120-L100, Olympus Corp., EU) while immunohistochemically stained tissue was imaged with a fluorescence microscope at 40x magnification (Leica TCS SPE, Leica Microsystems, DE). Determination of cross sectional area of i) nerve fascicles, ii) capsule, and iii) the foreign body giant cells layer carried manually out on H&E or SR sections using open source software Fiji for the area measurements (ImageJ, NIH, MD). Blood vessels were also counted manually on H&E sections in the entire tibial fascicle. All manual quantifications were performed twice to ensure robustness.

Collagen deposition was quantified on SR stained sections (see section 2.3.11) and the number of cell nuclei in the nerve fascicles was determined on H&E sections (see section 2.3.11), both with custom-written routines in Fiji-ImageJ, detailed in the supplementary material.

3D reconstructions of fascicles, capsule, and the implant were performed by manually contouring the different components on the images obtained from H&E stained serial sections (400 µm between sections) and subsequently aligning them in Neurolucida software (MBF Bioscience, Williston, VT, USA) for 3D reconstruction.

Macrophage presence in the different compartments of the nerve cross-section (extra-fascicular space, local endoneurial environment, and distant endoneurial environment) as well as the fiber density and their distance to the implant were quantified with two other custom written routines in Fiji (see section 2.3.11).

For the quantification of any metric in images obtained from immunohistochemistry, 3 consecutive sections per animal were analysed. Due to the oblique insertion, at the implant level, we selected slices with the implant visible in the tibial fascicle to ensure comparability between animals. This fascicle was then referred to as local endoneurial environment, as opposed to distant endoneurial environment for fascicles in which the implant was not present in the cross-section being analysed.

2.3.10 Statistical analyses

To determine time-dependent impact of the implant on the host tissue, we conducted Spearman's correlation analysis between all the metrics that were quantified across groups.

2.3.11 Supplementary methods for image processing

Quantification of collagen deposition around implant

Collagen deposition around the implant was quantified using a custom Fiji-ImageJ process chain. First, ImageJ built-in colour deconvolution plugin was applied on the original image (Fig. 2.4A) using the color vector FastRed-FastBlue-DAB to keep only the coral colour (stained collagen Fig. 2.4B a)). In parallel, a copy of the original image was transformed from RGB components to Hue-Saturation-Brightness (HSB) components (ImageJ built-in function HSB stack) and the saturation component was extracted to allow differentiation of stained tissue from non-stained tissue (Fig. 2.4C a)). The transformed images were then thresholded using ImageJ built in thresholding algorithm Yen (Fig. 2.4B b)), and Huang (Fig. 2.4C b)) and corresponding areas were measured in previously drawn regions of interest. For visual inspection, a merged image with both components was saved (Fig. 2.4D). Final quantification in manually drawn regions of interest (for instance the local endoneurial environment) was expressed as ratio of collagen-stained tissue over all the tissue in each region.

Quantification of cellularity

The level of cellularity within the nerve fascicle was determined on H&E stained sections (Fig. 2.5A). For this, the ImageJ in-built function color deconvolution was applied using the H&E color vector, to select the dark blue staining (Fig. 2.5B). This transformed image was then thresholded using ImageJ built in

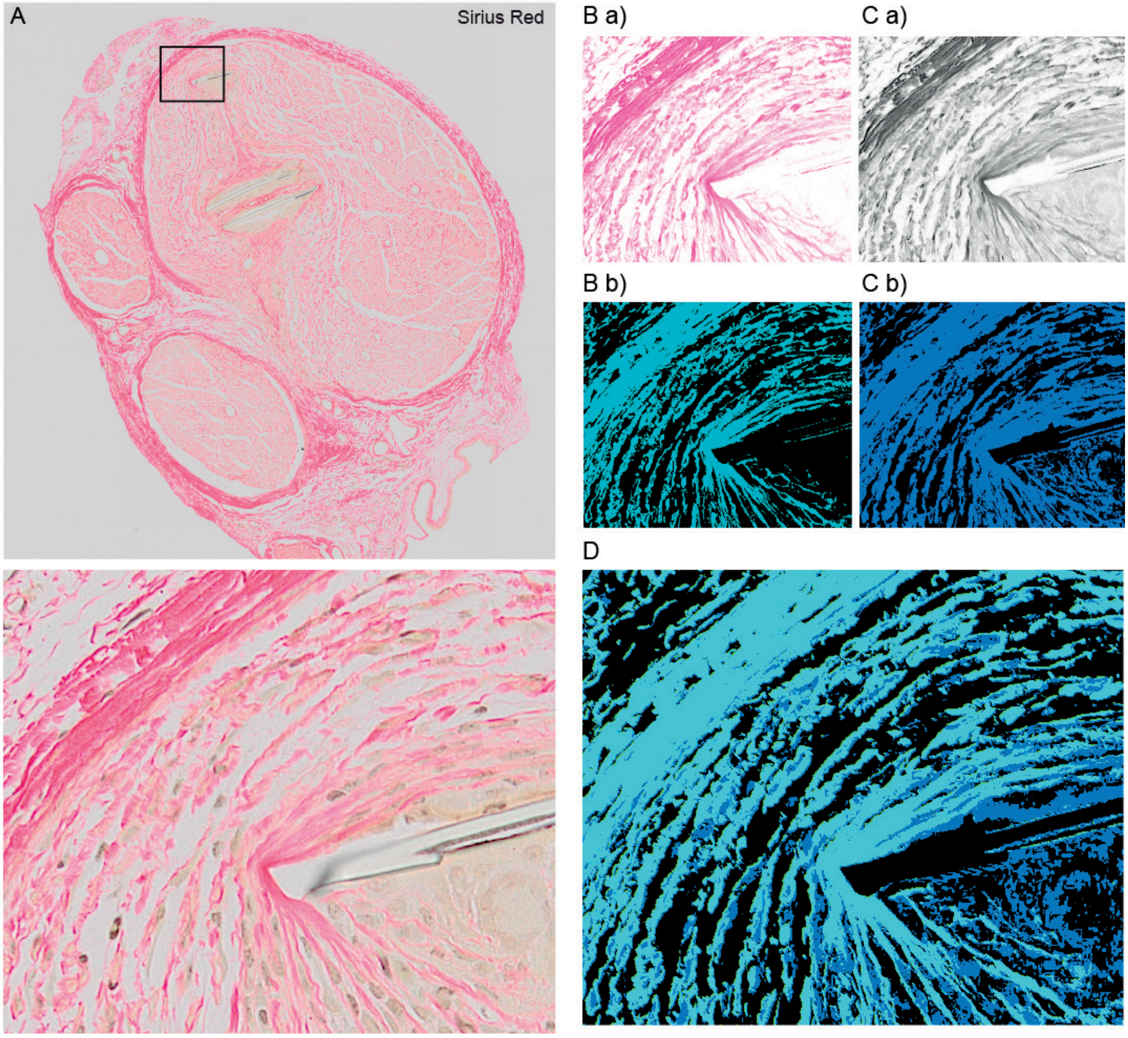

Figure 2.4 – Image processing for quantification of collagen deposition on SR stained sections. A) Original image and inset. B a) Coral color component of A (collagen), b) thresholded version of a). C a) Saturation component of A (other tissue), b) thresholded version of a). D) Merge of B b) and C b) for visual inspection.

thresholding algorithm Yen (Fig. 2.5C). Final quantification was computed in manually drawn regions of interest (for instance the local endoneurial environment (green)) and expressed as ratio of the area of the hematoxylin-stained tissue over the area of the region of interest (excluding the area of the electrodes) (Fig. 2.5D).

Quantification of inflammation

The spatio-temporal dynamics of the inflammatory response were quantified on images obtained from immunohistochemistry against macrophage marker CD68. For this, we first delimited each cross-section into three areas of interest extra-fascicular space (e) in light grey, local endoneurial environment (le) in middle grey, and distant endoneurial environment (de) in dark grey (Fig. 2.6B). Then, we created a distance map from the electrodes regions of interest (manually drawn), using ImageJ built-in plugin geometry to distance map (Fig. 2.6C). On the channel representing the staining against CD68 (Fig. 2.6D b)), ImageJ

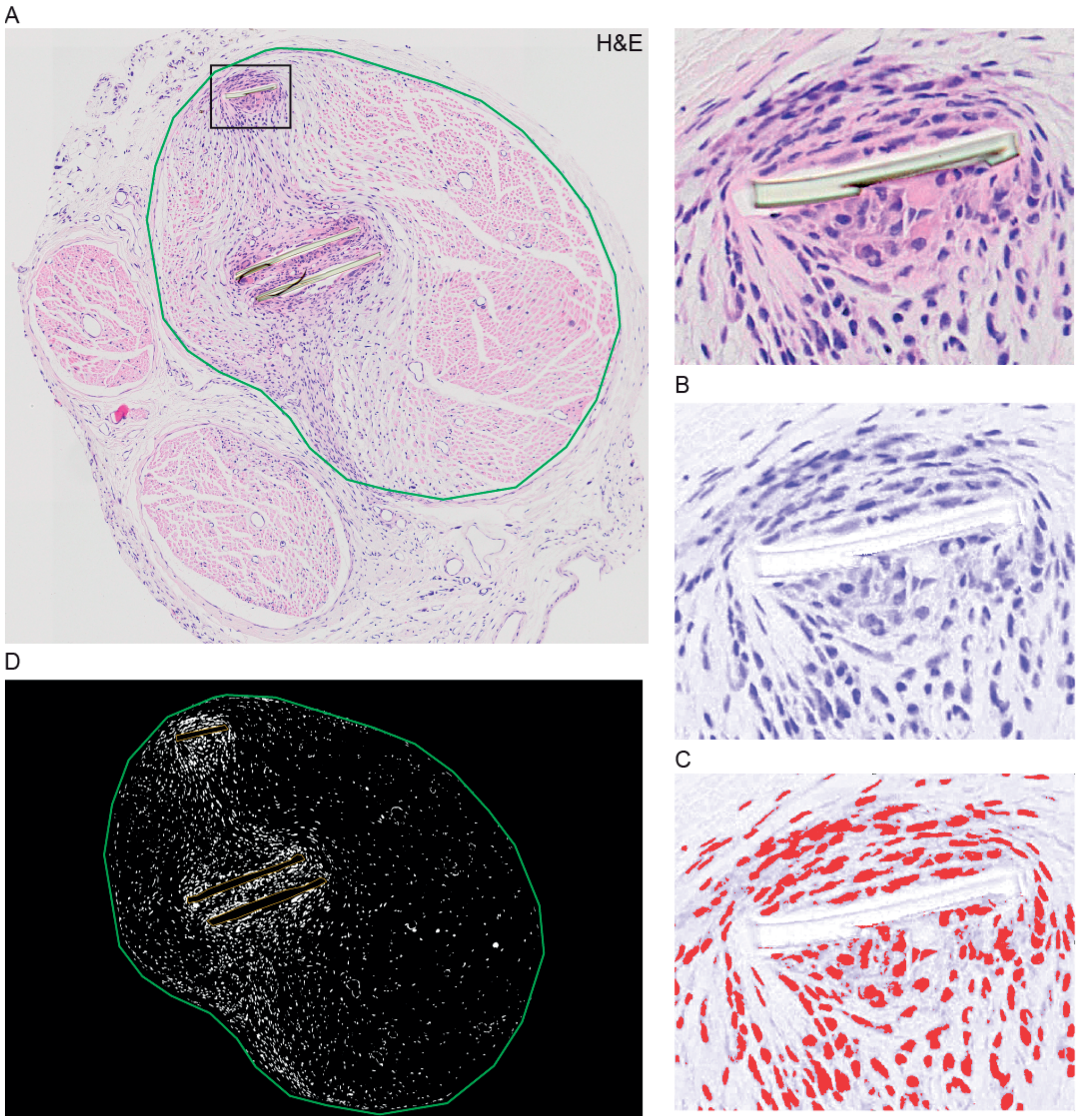

Figure 2.5 – Image processing for quantification of cellularity on H&E stained sections. A) Original image with drawn region of interest (green) and inset. B) Blue color component of A. C) Thresholded version of B. D) Measurement of thresholded area in drawn region of interest.

built-in threshold function Triangle was applied and yielded particles of different sizes and forms as function of the staining (Fig. 2.6E). For each particle, area and distance to the electrode from the distance map was measured. Presence of macrophages was computed as total area of fluorescence over area in the compartment of interest to avoid counting bias.

Quantification of fiber density

In order to quantify the number of axons in the fascicles manually drawn on images of stained nerve cross sections (Fig. 2.7A), an automated work-flow was used on image channel containing the staining against

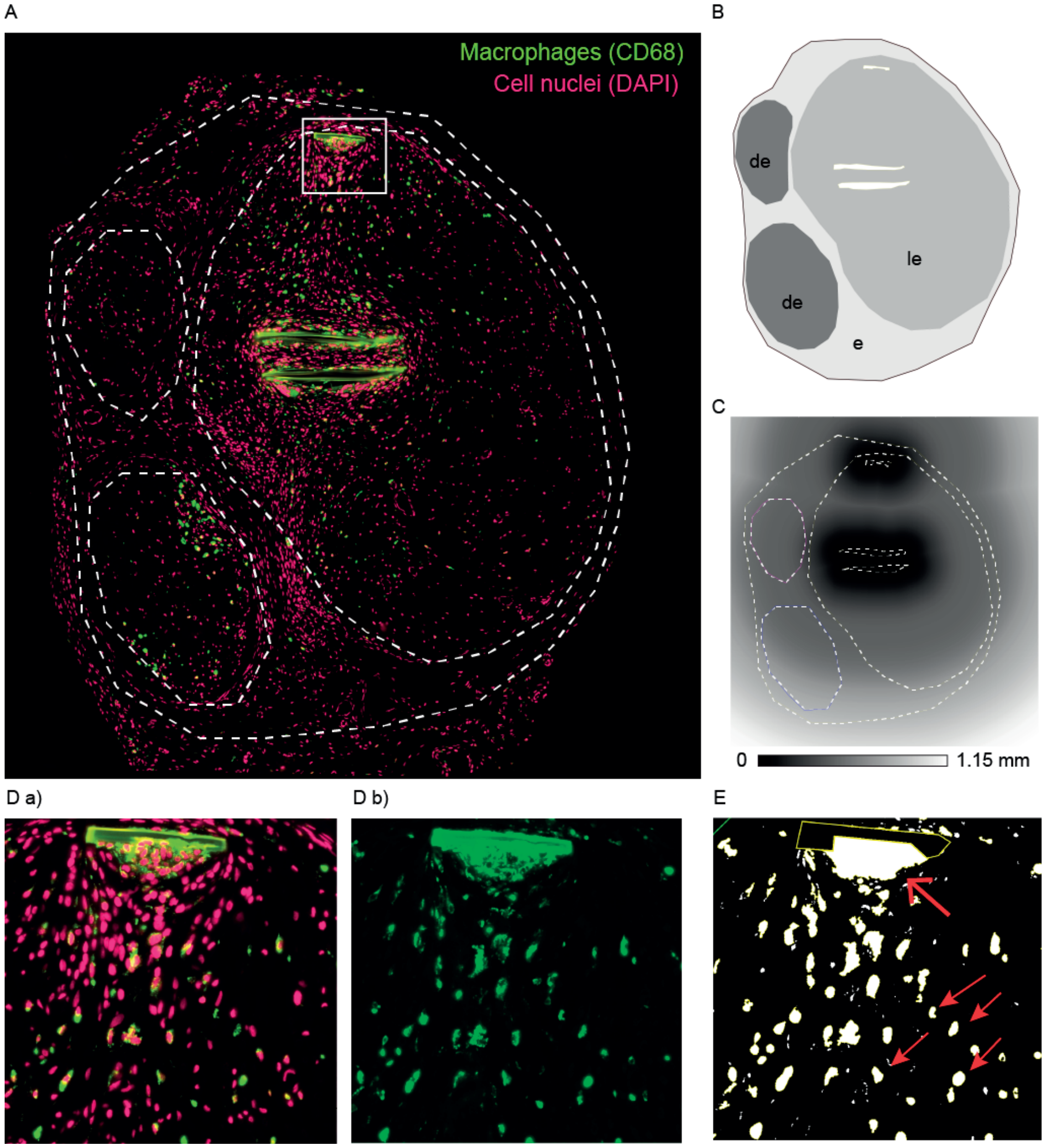

Figure 2.6 – Image processing for quantification of inflammation on sections immunohistochemically labeled against CD68. a) Original image with drawn regions of interest (white dashed lines). B) Extraction of regions of interest. C) Distance map from electrodes. D a) Inset of original image. D b) Select channel containing staining for CD68. E) Thresholded version of D b).

axons (Tuj1). The work-flow included the following steps: i) a whole image background measurement (Fig. 2.7B b)), ii) the detection of the local maxima on a multi-Difference of Gaussian (multi-DoG) image (Fig. 2.7C), iii) an intensity measurement of the local maxima (Fig. 2.7B a)) before their comparison to a cutoff value, and iv) the measurement of their distance from the electrode (Fig. 2.7B c)). Each of these steps is detailed below:

With this work-flow, we estimated the quantity of axons in the entire nerve cross section based on the

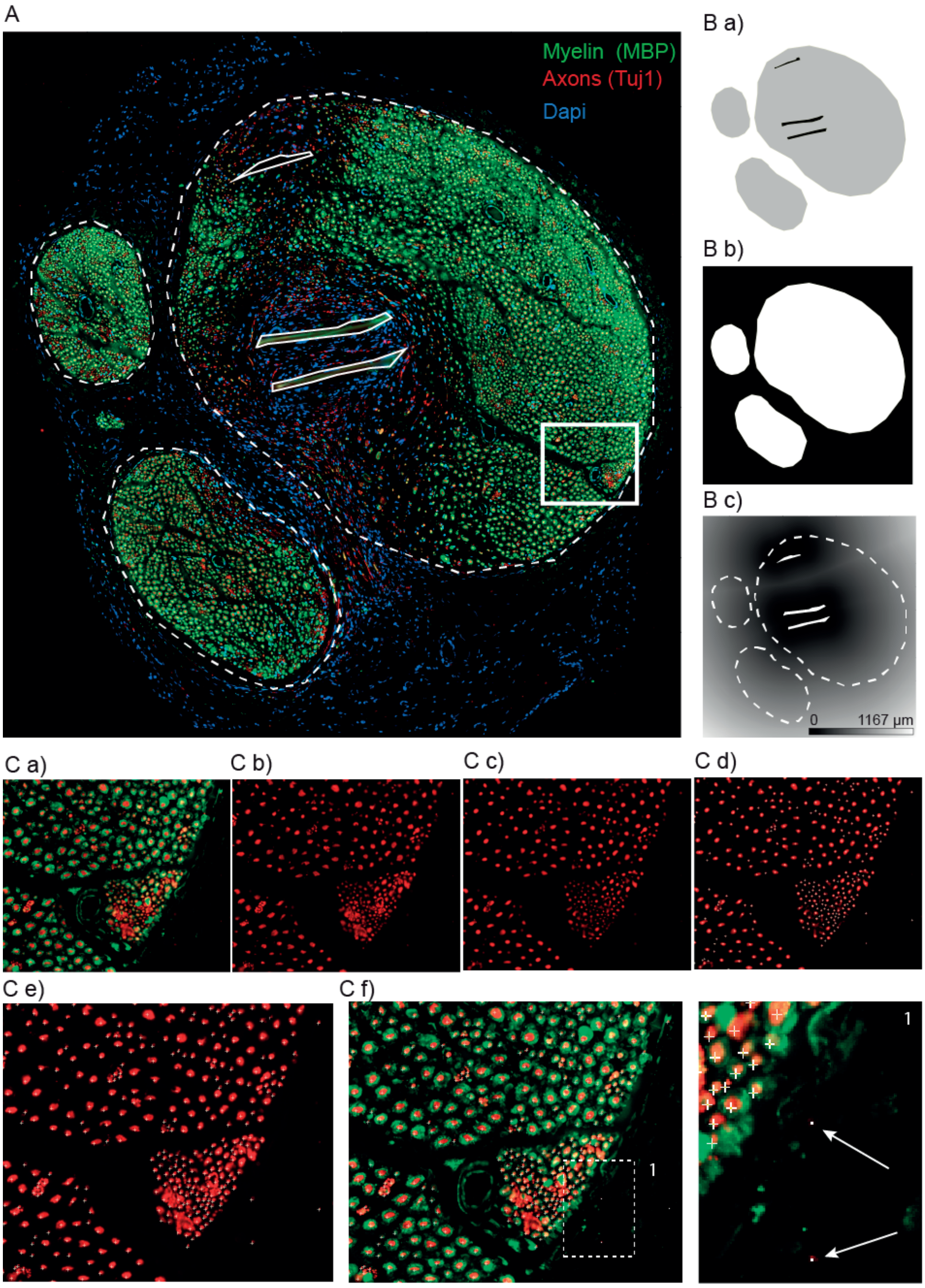

Figure 2.7 – Image processing for quantification of fiber density. A) Original image. B a)) Delimitation into regions “endoneurial space” (grey) and “electrode” (black). B b)) Inverse of “endoneurial space” region. B c)) Distance map from “electrodes region”. C a)) Inset from A. C b)) Channel 2 of the composite image (Tuj1 staining). C c)) Multiple Difference of Gaussians (DoG) of the previous image. (C d)) Detection of local maxima in the multi-DoG image. C e)) Projection of local maxima on original channel. C f)) Comparison with background noise (real axons (crosses) vs. staining artifacts/maxima out of the drawn regions (dots, evidenced with the arrows in the inset)).

immunohistochemical labeling against Tuj1. The original image was obtained from staining against Myelin (MBP), axons (Tuj1), and Dapi and acquired with a fluorescence microscope (Leica) at 40x (Fig. 2.7 A). On every image, we manually drew contours of fascicles and electrodes. The tiled image of the stained nerve section contained between 15000 and 20000 axons per image (Fig. 2.7 A, magnified in C a)), distributed in different Regions Of Interest (ROIs) (i.e. “endoneurial space” in grey and “electrode” in black) to define the area in which axons will be counted (Fig. 2.7 B a)).

The “endoneurial space” regions were inverted to create a background region (black) and measure the average intensity of the staining in the background (Fig. 2.7 B b)). This value was multiplied by a factor 3 and served as cutoff in the automated work-flow for deciding whether a local maximum was an axon or background noise).

From the “electrode” regions, a binary image was created and a distance map was computed (ImageJ Fiji Geometry to distance map) to later measure the distance of a detected axon from the electrode (Fig. 2.7 B c)).

To accurately detect the many local maxima, we generated a multiple difference of Gaussians (multi-DoG) image and detected on the result the local maxima in the staining with the “find maxima” function of ImageJ using a noise tolerance of 20. The size and density of the axons could vary a lot and this method appeared to be much more efficient than using a single Gaussian blur or a classic DoG as processing step before identifying the local maxima. The DoG image was generated by subtracting an image that was convoluted with a Gaussian of variance σ_2 to an image that was convoluted with a Gaussian of narrower variance (i.e. $\sigma_2 > \sigma_1$, here $\sigma_2 = 1.6 \text{ x } \sigma_1$ [133]). The multi-DoG image was obtained by creating a series of classic DoG images starting with $\sigma_1 = 1$, incremental step of 0.5, 10 iterations and each obtained DoG image was normalized by their standard deviation [134].

The resulting multi-DoG image was then obtained by stacking the image series and projecting minimum (light blobs on dark background). For each identified point, a circle with 2 pixels radius was used to measure intensity and the point was counted as an axon if the value was above the cutoff found from the background measurement. Finally, for axons, the same circle was used to measure the value on the distance map. Individual measurements and a summary per fascicles were generated.

2.4 Results

A SELINE implant was inserted into the sciatic nerve of five rats for a duration of six months. We performed weekly measurements and functional experiments in order to assess the functional stability of the implants for chronic applications and to determine their bio-integration within the implanted nerve. In addition, six groups of rats (n = 3 rats per group) underwent the same surgical procedures, but were sacrificed at earlier time-points in order to evaluate the relationships between the developing foreign body reaction and the electrical properties of the electrodes during the first month after implantation (Fig. 2.1 and Table 2.1). One of those groups of rats (Group 6 - 28 days of implantation, passive implants) was not stimulated, while the other groups received the same stimulation protocols as the rats implanted for 6 months. In one additional group of rats (Group 7, n=5 - 30 days of implantation, passive implants), we explanted the electrodes after 28 days to assess the impact of implant removal on leg motor control and on the tissue.

2.4.1 Stability and selectivity of polyimide-based intraneural implants

Post-mortem dissection revealed that all the implants had remained secured within the sciatic nerve over the entire duration of the experiment. None of the rats had to be terminated prematurely. During intra-operative testing, all the channels of all implants elicited movement. Weekly evaluations showed that 60% of channels were functional at 3-month post-implantation, and that 25 out of 100 channels were functional at 6-month post-implantation (Fig. 2.8), corresponding to about 12 years in humans [135]. A channel was considered "lost" when a maximum charge injection of 100 nC did not elicit a threshold response response (visual muscle twitch or evoked CMAP in EMG signal).

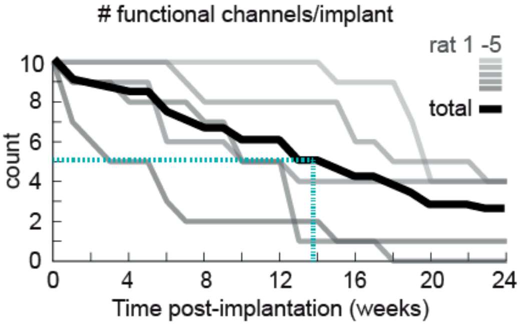

Figure 2.8 – Channel longevity. Grey lines refer to individual animals, black line represents sum of all channels. Turquoise line shows that 50 % of the channels remained at 14 weeks post implantation.

To characterize the selectivity of implants, we conducted weekly measurements of the relationships between the amount of injected charge in each channel of the implant and the amplitude of compound muscle action potentials (CMAPs) elicited into flexor and extensor muscles of the ankle (Fig. 2.3 (a)). We thus obtained recruitment curves, which are illustrated for two representative channels in Fig. 2.3 (b). To quantify the selectivity of muscle activation, we calculated a selectivity index (SI), which expressed the relative activation of a given muscle compared to all the recorded muscles. Immediately post-implantation, approximately 80% of all channels exhibited a selectivity index above 0.6 (Fig. 2.9 (a)). 20% were not selective after implantation (located between fascicles for instance). Channels classified as non-selective ($SI < 0.6$) were likely located between fascicles in the extra-fascicular space. About 30% of the selective channels activated a single extensor muscle, thus displaying intra-fascicular selectivity. The selectivity index of channels engaging extensor versus flexor muscles remained stable over time, even at 6-month post-implantation (Fig. 2.9 (b)).

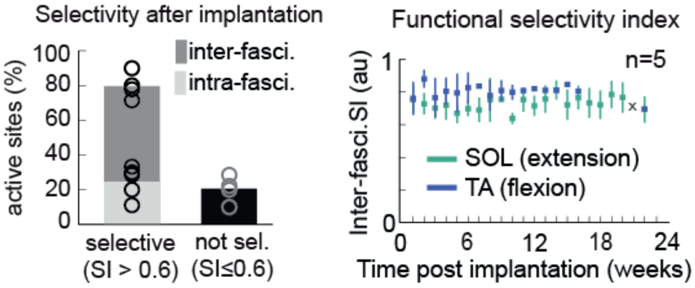

(a) Selectivity index of channels post implantation

(b) Stability of selectivity for flexion and extension

Figure 2.9 – Selectivity of intraneural stimulation

To evaluate the stability of electrical properties, we measured the stimulation threshold charge and impedance of all channels over the entire course of the experiment. We found that both electrical properties progressively increased during the first month post-implantation and then remained stable over the subsequent months.(Fig. 2.10). More precisely, threshold charge stabilized around 20nC after 4 weeks of moderate increase (green line) and a similar trend was observed for impedance measurements (stabilizing around 200 kΩ). No statistically significant differences between values from week to week were observed after this time in both metrics (Kruskal Wallis, $p<0.05$). Stability over time in both metrics was further underlined by fitting an exponential decay function (f(x) in green) to the median time derivatives of threshold charge (ΔQ, Fig. 2.10 (a)) and impedance (ΔZ, Fig. 2.10 (b)).

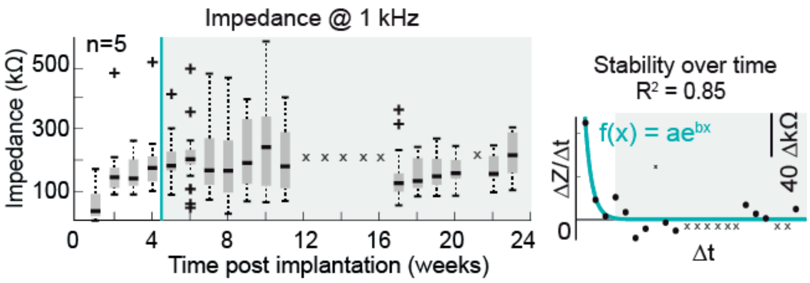

(a) Evolution of impedance over time

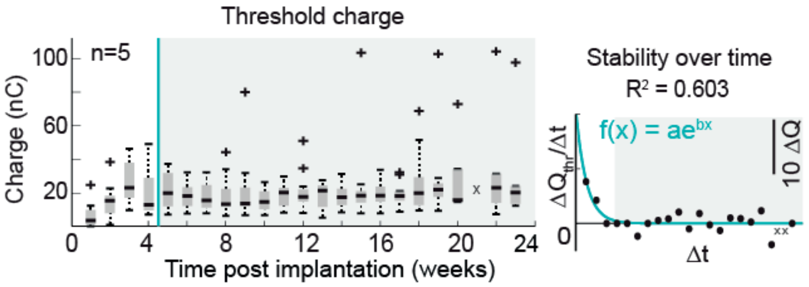

(b) Evolution of threshold charge over time

Figure 2.10 – Stability of electrical properties is achieved around four weeks post-implantation. (a) Impedance. (b) Threshold charge.

2.4.2 Functionality of polyimide-based intraneural implants

Amplitude and frequency modulation of intraneural stimulation

We then exploited the selective channels to evaluate the usability of the implant for functional applications. Rats were lightly sedated and then positioned with the legs in the air (Fig. 2.11 (a)). We measured the changes in leg kinematics and muscle activity when applying stimulation of increasing amplitude or frequency through the channels (Fig. 2.11 (b) and (c)).

Stimulation at low amplitude elicited a dorsiflexion or a plantarflexion of the ankle, depending on the selectivity of the selected channel. Increase in stimulation amplitude resulted in co-contraction of ankle flexors and extensors, which blocked the foot in a fixed position and would prevented the modulation of ankle joint movement (Fig. 2.11 (b)). On the contrary, we found a robust linear relationship between the stimulation frequency and the movement of the ankle in dorsiflexion and plantarflexion (Fig. 2.11 (c)). This result suggested that the stimulation frequency but not stimulation amplitude could be exploited to control the movement of the ankle.

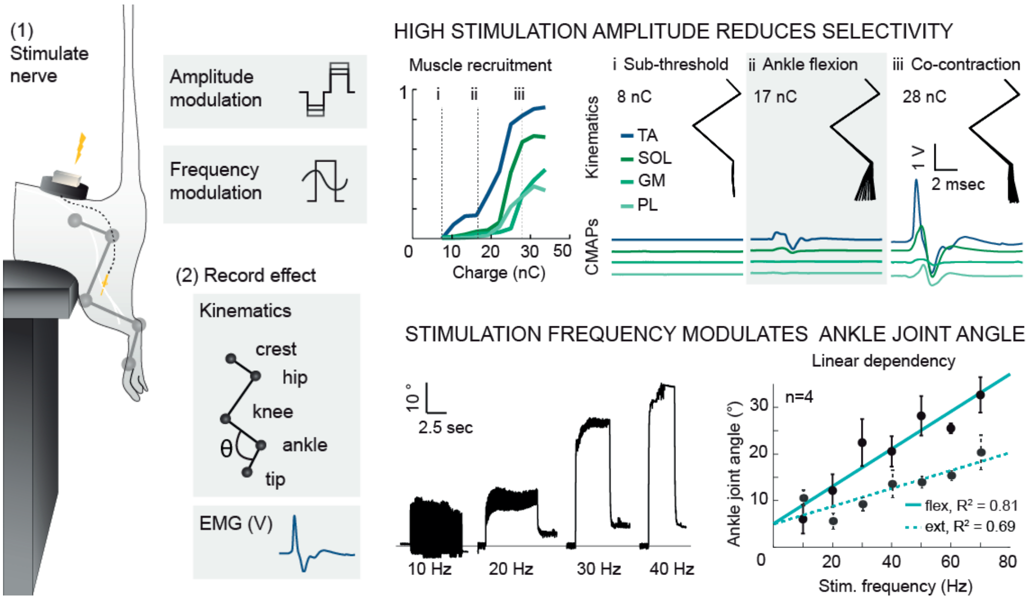

(a) Schematic of experimental setup

(b) Effect of amplitude (top) and frequency (bottom) modulation on kinematics

Figure 2.11 – Characterization of amplitude and frequency modulation of intraneural stimulation. (a) Experimental setup for intraneural stimulation with varying amplitudes or frequencies. Hind-limb kinematics and EMG signals were recorded. (b) Top: modulation of stimulation amplitude. Bottom; modulation of stimulation frequency.

Characterization of PI control of stimulation frequency

To test this possibility, we built a proportional-integral (PI) controller that adjusted the stimulation frequency in order to minimize the discrepancy between the traction force produced by the movements of the foot and a desired force (Fig. 2.12).

Rats were lightly sedated and then positioned on the edge of a table, with the leg to be stimulated attached to one side of a string, while the other side of the string was attached to a tri-axial force plate that measured the traction force in real time (Fig. 2.12 (a)).

We used a step function (3.5 sec, 0.2 N) to calibrate the proportional and integral coefficients of the controller (k_p and k_i respectively) for the control loop feedback mechanism. Example responses produced by purely proportional controller ($k_p = 1$, $k_i = 0$), enhanced proportional ($k_p = 10$, $k_i = 0$) and proportional-integral controller show overdamped, underdamped and optimal responses (Fig. 2.12 (b)). A Kruskal-Wallis test was used to assess differences between the variants across rats and channels. We found significant differences between the diverse couples, and found one consistent compromise of low error, fast response, and acceptable overshoot across animals that was used for the closed-loop control task ($k_p = 10$, $k_i = 25$) (Fig. 2.12 (c)).

High-precision control of movement-evoked traction force

We then used these coefficients to adjust the stimulation frequency in closed-loop in order to control the traction force produced by intraneural stimulation in real-time. The controller was able to reproduce a sinusoidal force with high fidelity (Fig. 2.13 (a) top, $R^2 = 0.85$, n = 4 rats with 2 or 3 channels tested per rat). We binned the frequencies used during the first, second, and third sinus (example from one animal in Fig.

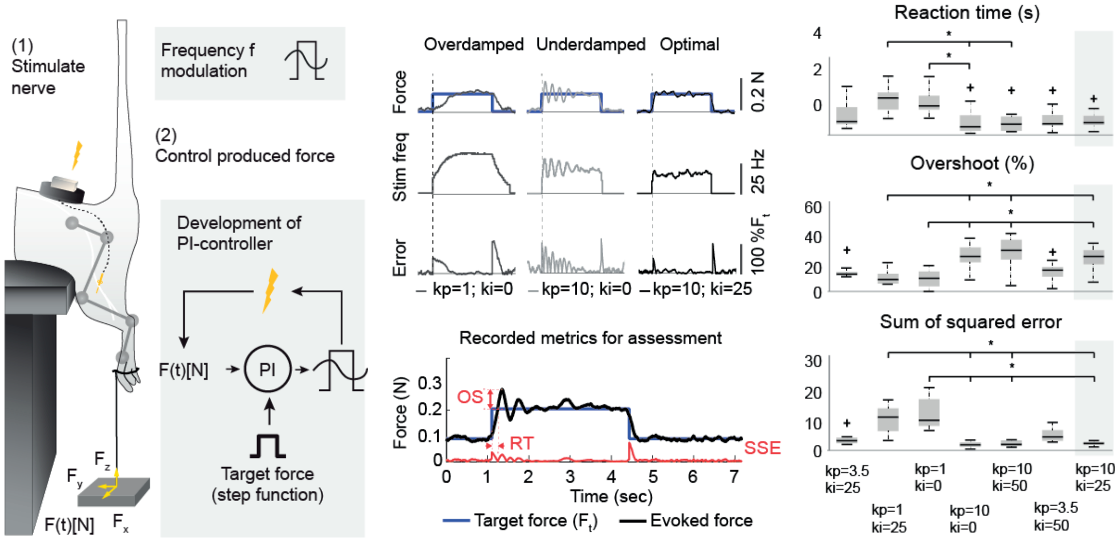

(a) Experimental setup for the characterization of the PI control

(b) Example responses for different controller coefficients

(c) Reaction time, overshoot, and error obtained for different couples of PI coefficients

Figure 2.12 – Characterization of PI-controller over step function. (a) Experimental setup. (b) Example responses. (c) Quantification of performance with different controller coefficients.

2.13 (a) bottom). To maintain a minimal error between the desired and recorded traction forces, the PI controller gradually increased the range of stimulation frequencies (Fig. 2.13 (b)).

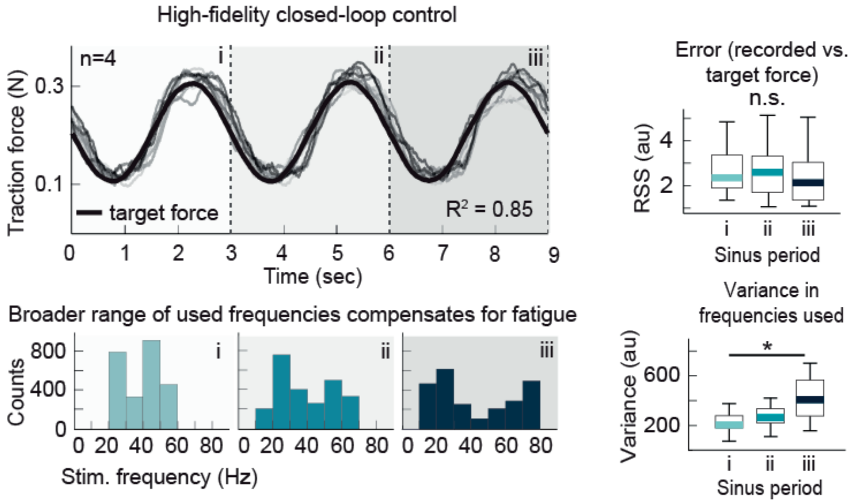

(a) Closed-loop control of stimulation frequency to match sinusoidal target force

(b) Constant performance through increased range of frequencies used

Figure 2.13 – High fidelity closed-loop control of traction force. (a) Produced force matched target force with high precision. (b) Error remains low while range of frequencies increases with duration of trial. (n=4)

2.4.3 Assessment of the developing foreign body response

We conducted a series of macroscopic and microscopic evaluations on the explanted nerves in order to assess the physical and biological consequences of the implant on the sciatic nerve.

Macroscopic observations

Dissection of the implanted nerves revealed the presence of extra-neural hemorrhages in the acute group, which were due to the interruption of superficial blood vessels on the nerve surface during implantation (Fig. 2.14).

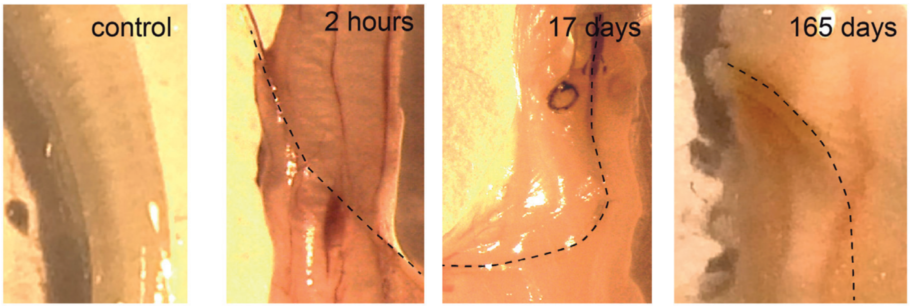

Figure 2.14 – Macroscopic observations of implanted nerves at dissections for different time-points. Dashed line shows the path of the implant.

With the exception of the acute and short term groups (up to 7 days post-implantation), all the explanted nerves displayed an excess of connective tissue at the entry and exit sites of the implant in the nerve. The overall shape of the nerves remained preserved, although chronically implanted nerves (6 months) displayed an enlargement around the site of implantation.

Encapsulation of polyimide-based intraneural implants

We stained serial cross-sections of the implanted nerves with H&E in order to assess the general morphology of the nerve. Comparison of acutely (Fig. 2.15 (a)) and chronically (Fig. 2.15 (b)) implanted nerves revealed that the size of the nerve increased in the region surrounding the implant (note the same scale bar between (a) and (b) in Fig. 2.15).

No hemorrhage was found inside the nerve of the acutely implanted animals, suggesting that during insertion, the fibers bend around the entering implant. The local enlargement derived from a highly cellularized capsule (Fig. 2.16 (a)) that enveloped the implant and was consistently observed across animals in the chronic group. Many of these cells were identified as fibroblasts (DAB revealed FSP1 positive nuclei), macrophages (Fast-blue revealed CD68 positive) or myofibroblasts (DAB revealed αSMA(Fig. 2.16 (a)).

To quantify the observed enlargement, we measured the diameter of the nerve along its length, the cross-sectional area of each fascicle, and the area of the capsule surrounding the implant in each group of animals. We found that the local enlargement of the nerve was primarily due to the progressive growth of this capsule around the implant (Spearman's R = 1, $p<0.0001$, Fig. 2.16 (b)). The capsule developed during the first 3 to 4 weeks after implantation, and then remained stable during the subsequent months

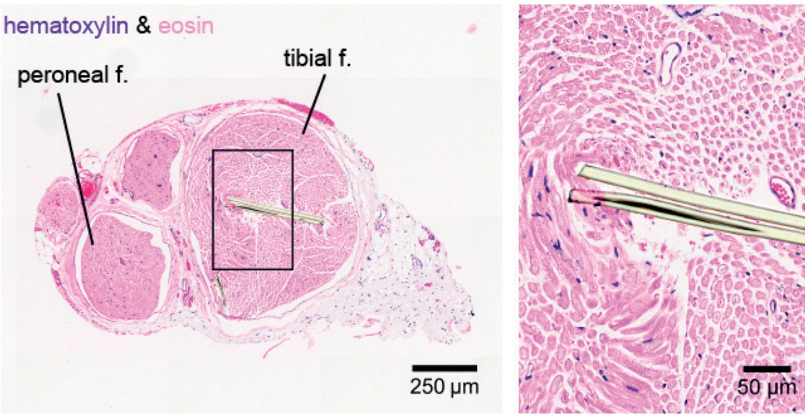

(a) Acute implant (0 days)

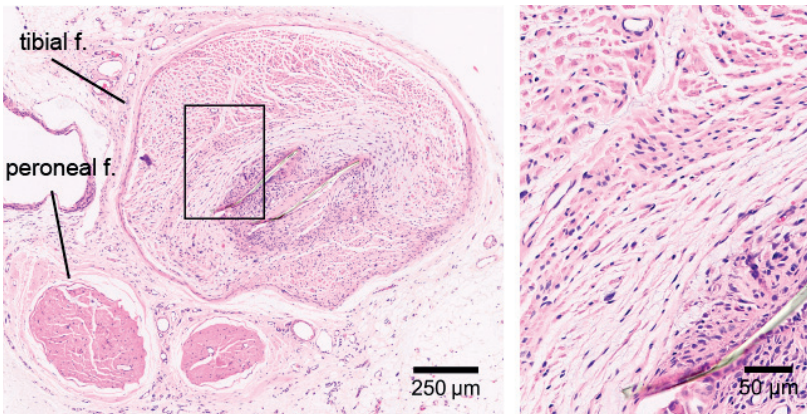

(b) Chronic implant (165 days)

Figure 2.15 – Comparison of general nerve morphology for (a) acute and (b) chronic implants on H&E stained sections.

post-implantation. 3D reconstructions of the fascicles, the implant and the surrounding capsule illustrated the important contribution of the fibrotic capsule to the enlargement of the nerve in one representative animal (Fig. 2.16) (c)).

We then quantified the components of the capsule and of the local endoneurial environment. For this, we stained nerve cross-section with Sirius Red in order to measure the area of the tight encapsulating layer of multi-nucleated giant cells around the implants, and the density of collagen in the local endoneurial environment. Insets of Sirius Red stained sections for different time-points show the appearance of an epithelioid layer of foreign body giant cells tightly around the implant that was quantified across animals (Fig. 2.17 (a)). We found aggregates of multi-nucleated giant cells around and in direct contact with the surface of the implant as early as seven days post-implantation. This layer increased gradually during the first four weeks post-implantation. At the chronic time-point, the size of this layer was considerably reduced.

Quantification of different components in the local endoneurial environment revealed increased collagen deposition at the chronic stage, a substantial increase in cellularity, and a gradual densification of microvasculature over the first four weeks post-implantation (Fig. 2.17 (b)). The amount of collagen relative to the cross-sectional area of the local endoneurial environment did not increase during the first four weeks post-implantation. While the size of neither nerve nor capsule changed between 4 weeks and 6

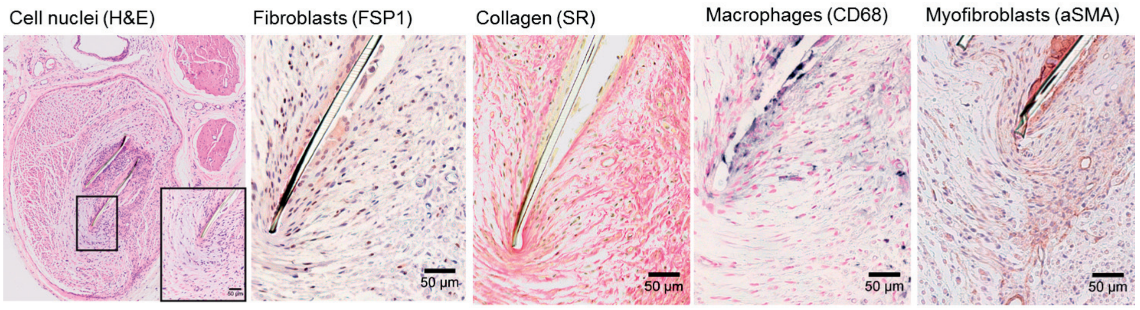
Cell nuclei (H&E)
Fibroblasts (FSP1)
Collagen (SR)
Macrophages (CD68)
Myofibroblasts (aSMA)
50 µm
50 µm
50 µm
50 µm
50 µm

(a) Identified cell types inside capsule at 165 days post-implantation.

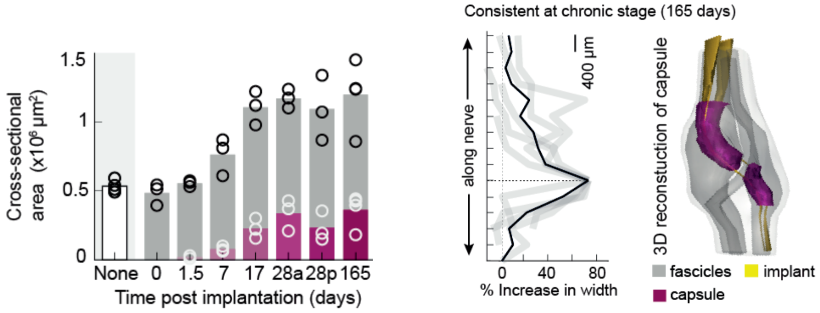

(b) Relationship between nerve enlargement and capsule development

(c) 3D reconstructions of fascicles, implant, and surrounding capsule

Figure 2.16 – Highly cellular capsule progressively enlarges nerve. (a) At the chronic stage, fibroblasts, myofibroblasts, and macrophages can be found within the capsule. (b) The capsule developped mainly during the first month, causing an enlargement of the nerve. (c) This enlargement was consistently observed at the implant location in the chronic group.

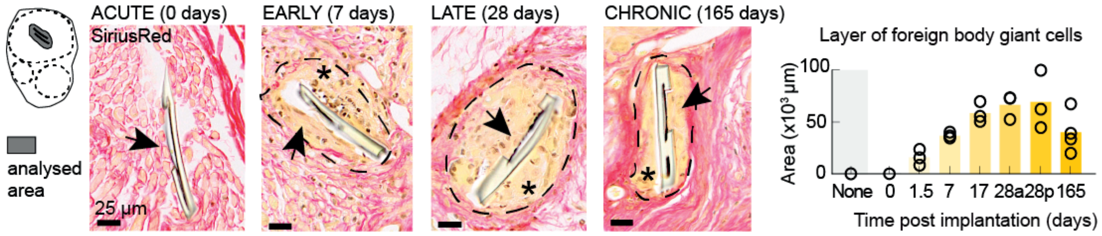
analysed area
ACUTE (0 days)
SiriusRed
25 µm
EARLY (7 days)
LATE (28 days)
CHRONIC (165 days)
*
*
*
Layer of foreign body giant cells
Area (x10³ µm)
100
50
0
None
0
1.5
7
17
28a
28p
165
Time post implantation (days)

(a) Epithelioid layer of foreign body giant cells. Dashed line: delimitates layer, *: multi-nucleate giant cells, full arrow: implant active site.

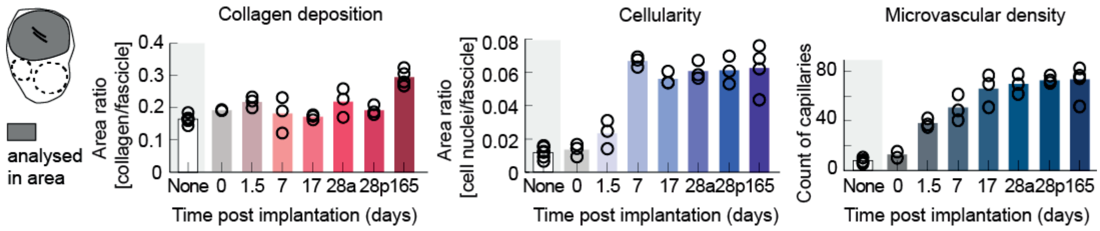

(b) Collagen, cellularity, and microvascular density

Figure 2.17 – Quantification of capsule components as function of duration of implantation.

months post- implantation, the density of collagen was increased at the chronic stage. The cellularity in the local endoneurial environment increased considerably, starting at 7 days post implantation. In turn, the endoneurial microvascular density increased as early as 1.5 days post-implantation. Both cellularity and microvascular density remained elevated at the chronic stage. Spearman's correlation analysis revealed that the growth of the capsule was significantly correlated with the amounts of vasculature (R = 1, p<0.0001), collagen (R = 0.997, p<0.0001), and cellularity (R = 0.78, p<0.0001) measured over time.

Inflammatory response to polyimide-based intraneural implants

The insertion of the implant into the nerve triggered an inflammatory response that aimed to eliminate the debris caused by the penetration and to engage repair mechanisms. To visualize the spatiotemporal dynamics of this inflammation, we stained nerve cross-sections against the monocyte/macrophage marker CD68 and quantified the staining in the different nerve compartments at all time-points (Fig. 2.18). Macrophages migrated from the vascular system, and infiltrated the extra-fascicular space early after implantation (Fig. 2.18 (a)). Evaluations at 17 days post implantation showed that both the local and the distant endoneurial environments were densely populated with macrophages (Fig. 2.18 (b)), indicating

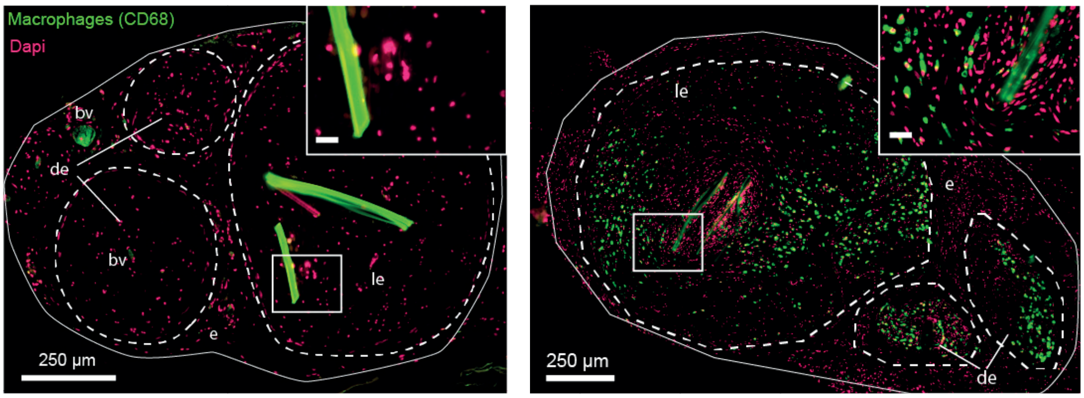

(a) Acute (0 days)

(b) Mid-term (17 days)

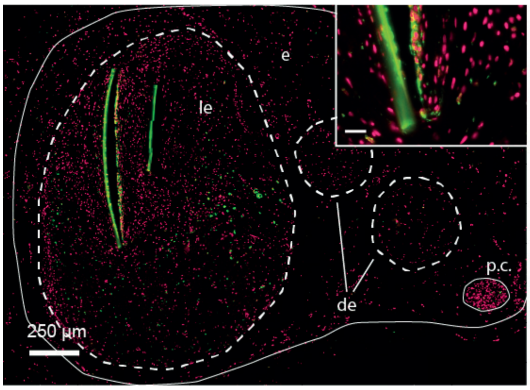

(c) Chronic (165 days)

Figure 2.18 – Observation of inflammatory response to the implant by immuno-histochemical labelling against macrophage marker CD68. (a) Acute (2 hours), (b) mid (17 days), and (c) chronic (165 days) stage of implantation. Scale bar on insets is 25 µm. Legend: le - local endoneurial environment, de – distant endoneurial environment, e - extra-fascicular space, bv - blood vessel, p.c. - posterior cutaneous branch.

a multifocal infiltration throughout the endoneurial environment. While inflammatory cells were still present in the chronic stage, their distribution was restricted to the local endoneurial environment (Fig. 2.18 (c)). To measure these inflammatory responses, we quantified CD68+ objects in the different nerve compartments by objectively expressing its presence as area of fluorescence normalized to the analysed area of the respective nerve compartment.

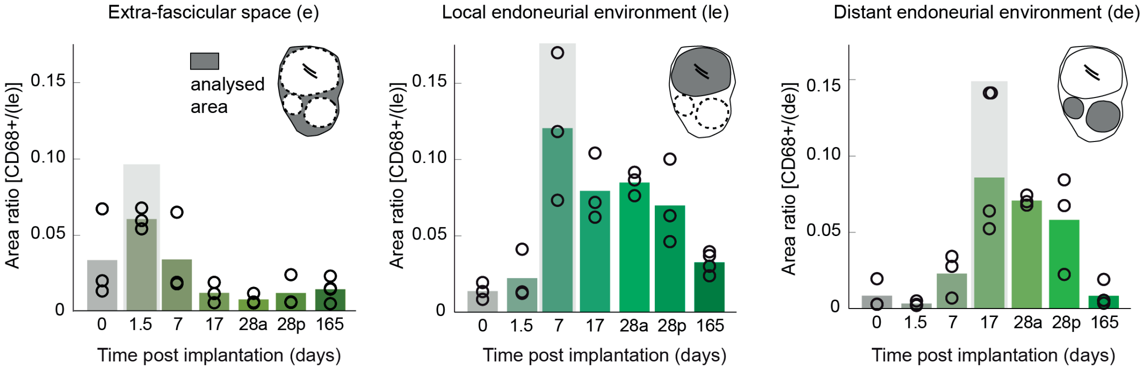

Figure 2.19 – Quantification of the inflammatory response in the extrafascicular space (left), the local endoneurial environment (middle), and the distant endoneurial environment (right).

We quantitatively confirmed that the infiltration of macrophages started from the extra-fascicular space and residing blood vessels (Fig. 2.19 (left)) as soon as 36h post implantation. The macrophages were then first recruited to the site of injury in the local endoneurial environment (Fig. 2.19 (middle)), before generalizing their presence throughout the fascicles (Fig. 2.19 (right)). In the chronic stage, their presence was restricted to the local endoneurial environment. To visualize this spatio-temporal pattern in the local endoneurial environment, we analyzed the area of each detected fluorescent particle as a function of its distance from the implant (Fig. 2.20). This analysis revealed a progressive accumulation of small particles into large clusters in the early phase of inflammation. Although macrophages persisted at the chronic stage, they were less distributed and did not appear as big clusters.

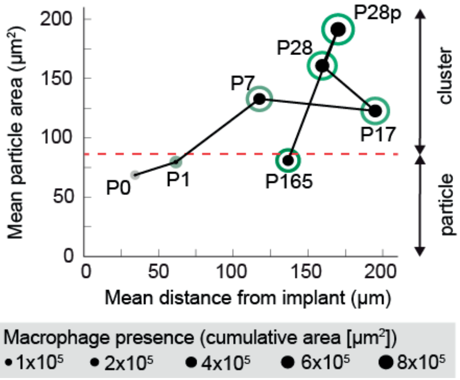

Figure 2.20 – Spatio-temporal dynamics of inflammatory response. The red line differentiates qualitatively particles from clusters based on the average surface area of detected macrophages (+- 80 µm).

Impact of the implant on fiber density

We assessed the impact of the implant on fiber density and organization around the implant. For this, we stained nerve cross-sections with antibodies against axons (TUJ1) and myelin (MBP) (Figs. 2.21 and 2.22).

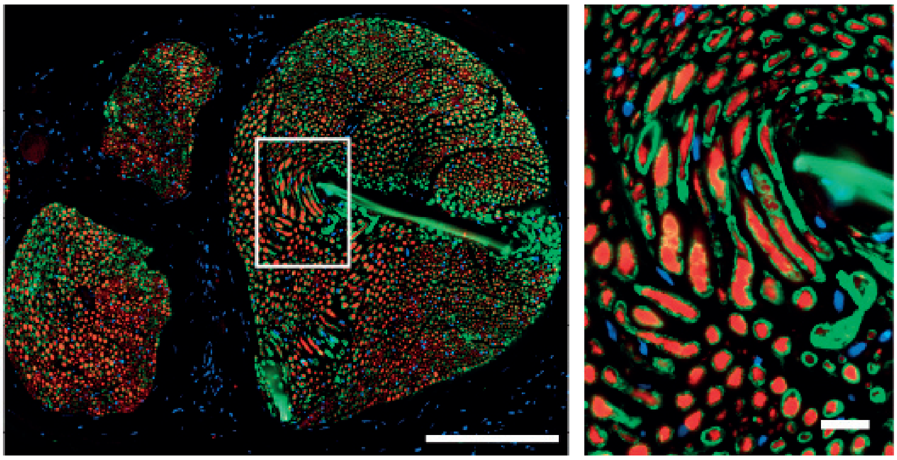

(a) Acute (2h post implantation)

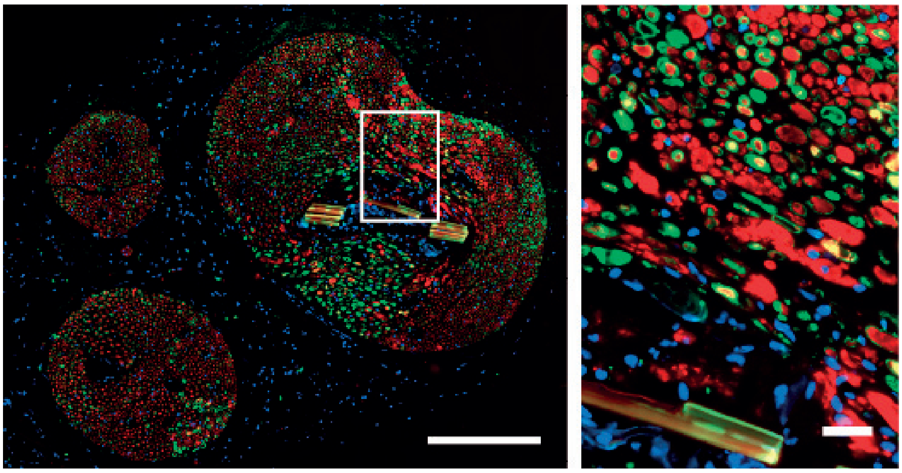

(b) Sub-acute (36 hours post implantation)

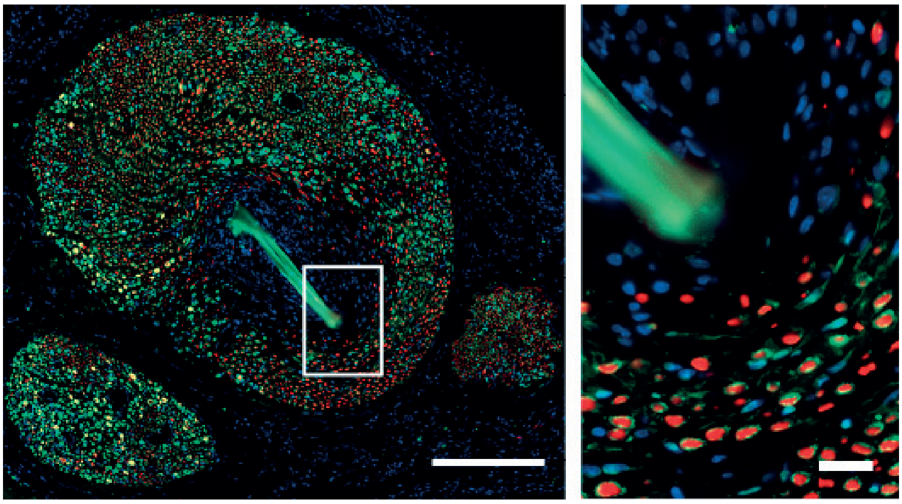

(c) Early (7 days post implantation)

Figure 2.21 – Observation of implant impact on axons and myelination during the first week of implantation. Large scale bar: 250 µm, small scale bar: 25 µm. Staining against axons (Tuj1, red), myelin basic protein (MBP, green), cell nuclei (dapi, blue).

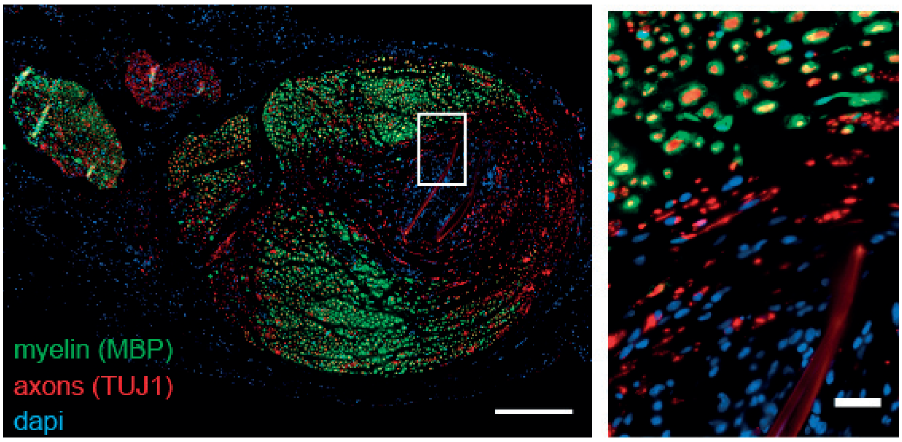

(a) Mid (17 days post implantation)

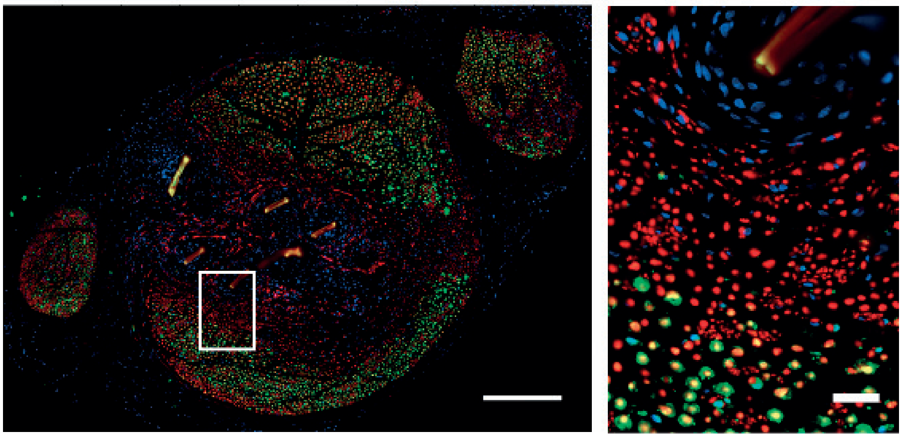

(b) Long (28 days post implantation)

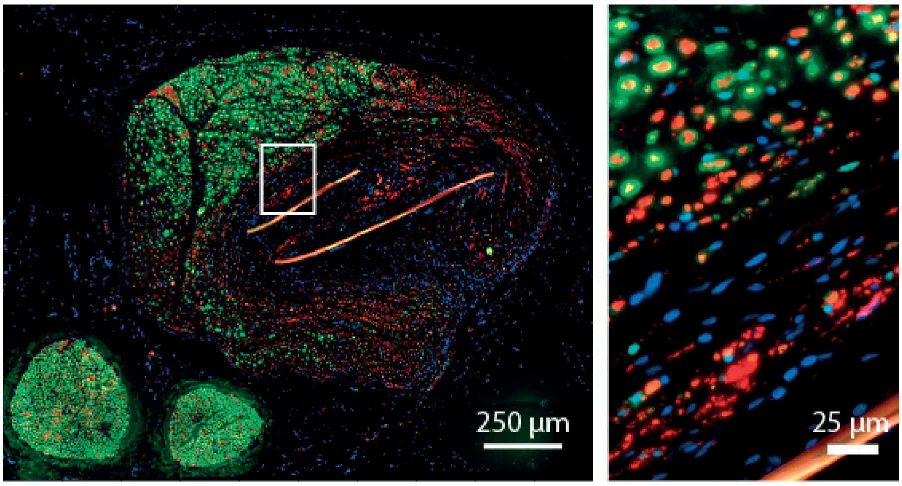

(c) Chronic (165 days post implantation)

Figure 2.22 – Observation of implant impact on axons and myelination after the first week of implantation. Large scale bar: 250 µm, small scale bar: 25 µm. Staining against axons (Tuj1, red), myelin basic protein (MBP, green), cell nuclei (dapi, blue).

The penetration of the implant induced an immediate change in the morphology of the fibers (Fig. 2.21). Close inspection showed that the axons adopted a bended shape indicating that the fibers had moved aside from the implant during the insertion. Indeed, we did not detect intraneural hemorrhage, suggesting that the fibers were not severed during implantation (Fig. 2.21 (a)). In the sub-acute stage, the nerve cross-sections exhibited swollen axons and spheroid formation in close vicinity of the implant (Fig. 2.21 (b)), indicating a breakdown of axons as consequence of the insertion. At one week post-implantation, a zone void of axons appeared around the electrode, which corresponded to the ongoing formation of a capsule (Fig. 2.21 (c)).

From this time point to the chronic stage, this zone progressively expanded (Fig. 2.22 (d) - (f)). During this process, mainly unmyelinated axons started to populate the capsule. In the chronic stage, some of these axons appeared to carry some myelin, although thin when compared to myelinated axons further away from the electrode. Some axons were as close as 30 to 50 µm from the implant.

We developed a semi-automatic algorithm to estimate the density of myelinated fibers in the entire nerve cross-section both proximal and distal to the implant (Section 2.3.11), and normalized the measured density also to contralateral control counts obtained from non-implanted nerves (Fig. 2.23 (a)). At each time point examined, the ratios of proximal to distal measurements as well as distal to control measurements were close to one, suggesting that no substantial change in number of myelinated fibers had occurred after implantation. Despite the development of the capsule, we consistently observed an increase in detected axons at the implant level that was highest at 4 weeks post implantation, and had remained substantially increased in the chronic stage (Fig. 2.23 (b)).

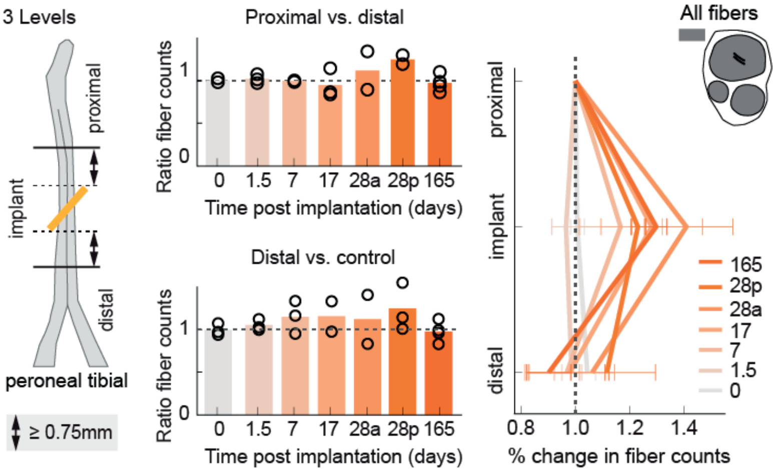

(a) Proximal-distal and distal-control ratios in fiber density

(b) Increased fiber counts around the implant

Figure 2.23 – Quantification of implant impact on fiber density. Dotted line indicates reference lines (in (a) and (b) a ratio of 1, in (c) the values from the control group (0 days post implantation).

We further measured the distance between the implant and the closest 20% of axons and myelin (Fig. 2.24). Both axons and myelin moved away from the implant during the first month post-implantation. Albeit in the chronic group the mean distance of the closest 20% of fibers resembled the distance from the implant in the acute group, the myelin had not moved closer, suggesting that most of the regenerating axons did not bear myelin.

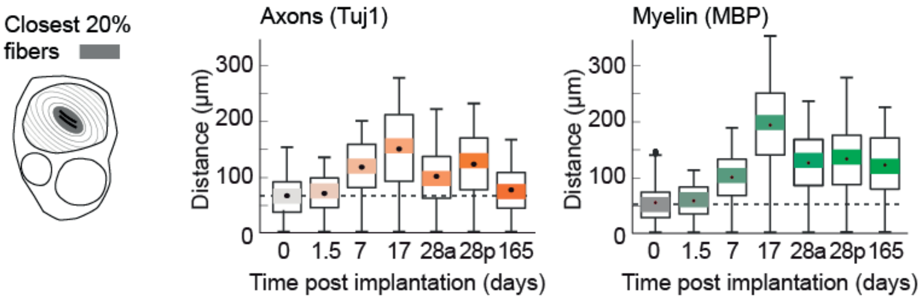

Figure 2.24 – Distance of closest 20 % of fibers from implant.

.

Electrical stimulating does not exacerbate the foreign body reaction

Previous studies have been looking at passive and untethered intraneural electrodes to assess the induced foreign body reaction of such implants. To evaluate the potential impact of providing stimulation to the nerve, we had created an additional control group that was implanted with a tethered implant and EMG electrodes but through which no stimulation was provided. Even though the number of animals per group did not allow us to statistically assess whether such differences were present, we obtained very similar results in all metrics examined for the animals in the groups 28a (active) and 28p (passive).

2.4.4 Impact of implantation and implant removal on fine motor control

We assessed the impact of the implant insertion and also implant removal on leg motor control capacities. For this, we conducted kinematic analyses during locomotion along the irregularly spaced rungs of a horizontal ladder in 5 animals (Fig. 2.25 (a)). We calculated the percent of missed steps of the leg with the implant during evaluations conducted before implantation, at regular intervals after implantation, and during one month after the removal of the implant.

We did not detect significant alteration of locomotor performance (measured by the percent of missed steps during five consecutive trials) after insertion or removal of the intraneural implant at any of the test time-points ($p>0.05$, Kruskal-Wallis test) (Fig. 2.25 (b)).

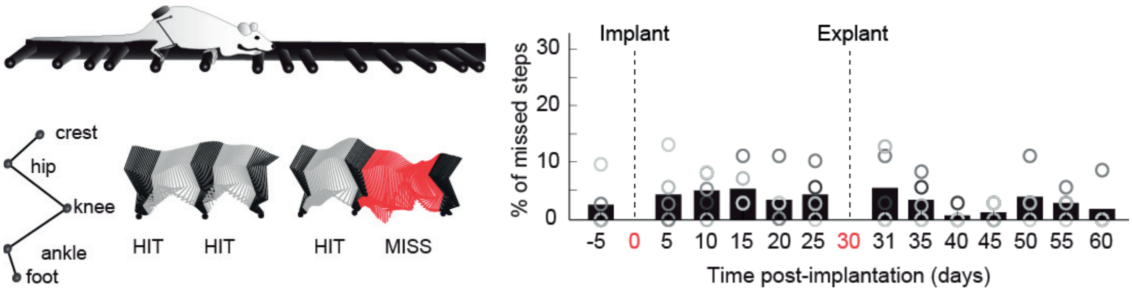

(a) Ladder task to assess leg motor control

(b) Quantification of missed steps

Figure 2.25 – Impact of implantation and implant removal on leg motor control. (a) Experimental setup. (b) Performance was measured before and after implantation and after explantation as the percent of missed steps during trials of quadrupedal locomotion along a ladder with unequally spaced rugs.

Evaluation of the nerve tissue one month after removal showed expected signs of scarring, mainly reflected by enhanced collagen deposition and increased cellularity at the passage site of the implant (Fig. 2.26 (a)). This was found consistently across animals. Immunohistochemical labelling against macrophage/monocyte marker CD68 revealed the presence of macrophages along the passage site of the implant (Fig. 2.26 (b)). No significant CD68 positive staining was found in the extrafascicular space. The observed signs of inflammation were extremely weak when comparing with the presence of inflammatory cells in the nerves that were implanted during one month and in which the implant was not removed (groups 28a and 28p).

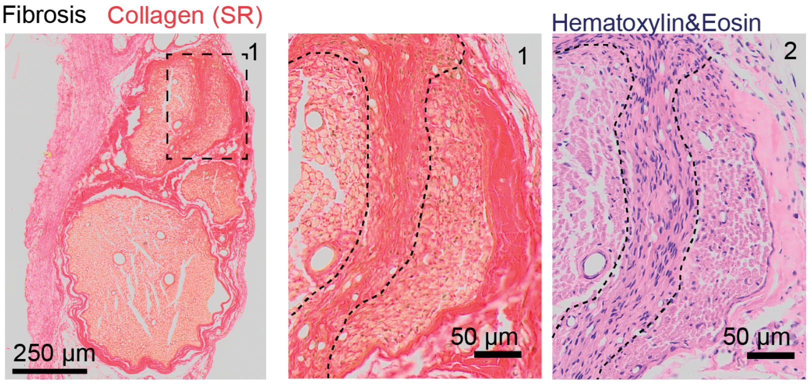

(a) Tissue reaction to implant removal

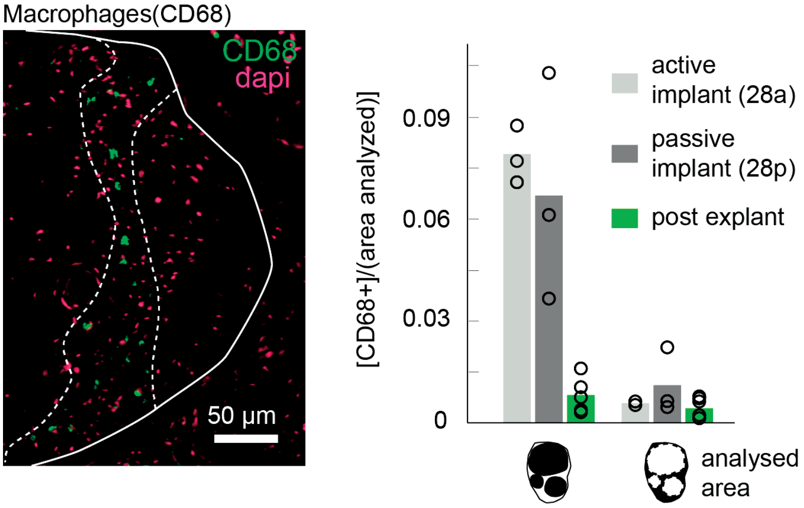

(b) Inflammation quantification after implant removal

Figure 2.26 – Impact of implant removal on nerve tissue

2.5 Discussion

We studied the selectivity, stability, functionality and biocompatibility of polyimide-based intraneural implants that were inserted into the sciatic nerve of rats for extensive durations. We found that after a period of approximatively one month during which a foreign body reaction developed around the implant, the electrodes maintained stable and selective responses to charge delivery that enabled the precise control of ankle movements in anesthetized rats. We discuss these results with a particular emphasis on the stability and usability of polyimide-based intraneural implants, the implication of the acute and chronic biological responses to the implant insertion, and the potential of this technology for long-term clinical applications.

2.5.1 Stability and usability of polyimide-based intraneural implants

We found that the SELINE electrodes exhibit remarkably stable responses to charge delivery that supported robust stimulation selectivity over extended periods of time notwithstanding the development of an encapsulating layer around the implant, in particular during the first month after insertion. Encapsulation of intra-cortical implants has been linked to the decline of recording electrode functionality [136, 137, 138]. Likewise, experimental and modelling studies showed that the accumulation of multi-nucleated giant cells around the implant alter the path of current flow [139, 140]. We confirmed these findings in the context of peripheral nerve stimulation. We found a tight relationship between the thickness of the encapsulating layer around the implant and the graded increases in stimulation thresholds and electrode impedance (Fig. 2.27). Spearman's correlation analysis revealed that the growth of the capsule was significantly correlated with the amounts of vasculature ($R = 1$, $p<0.0001$), collagen ($R = 0.997$, $p< 0.0001$), and cellularity ($R = 0.78$, $p<0.0001$) measured over time. Both changes from week to week in impedance and threshold charge were highly anti-correlated to fascicle size ($R = -1$), capsule size ($R = -1$), microvascular density ($R = -0.997$), and cellularity ($R = -0.78$) ($p > 0.0001$).

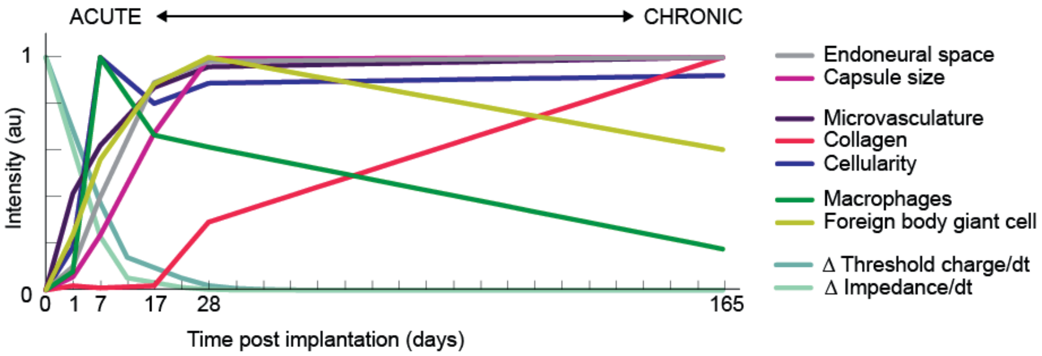

Figure 2.27 – Schematic summary of observations

The biological response to the insertion of the implant was particularly pronounced during the first month after implantation. During this period, the electrodes displayed a logical increase in impedance, which led to an augmentation of stimulation thresholds for the majority of the electrodes, stabilizing around 20nC. Such thresholds have been hown to be extremely usable in human applications [123] and are about one magnitude lower than epineural electrodes in similar applications [141]. Further, we were able to exploit the implants for long-term functional applications. Two factors contributed to maintaining implant functionality. First, inter-fascicular selectivity was preserved under a certain range of stimulation currents. Second, we were able to leverage this selectivity through the modulation of stimulation frequency. Indeed, we found a linear relationship between the stimulation frequency and hind-limb kinematics, which we used to control a range of forces with high precision in anesthetized rats. Previous studies similarly showed that the stimulation frequency was the most reliable control parameter to modulate limb kinematics or sensory information using intraneural or epidural spinal cord stimulation protocols [123, 142, 143, 144, 35]. This high degree of controllability over extended durations opens a realistic pathway to utilize intraneural implants to alleviate motor deficits and restore graded sensation for a range of clinical applications.

2.5.2 Immediate and chronic biological responses to the implant insertion

The characterization of the immediate mechanical consequence and long-term biological response to implant insertions plays an important role in optimizing implant design and validating their usability for clinical applications [145]. Here, we conducted comprehensive anatomical evaluations to characterize the mechanical impact, inflammation and foreign body reaction following insertion of the SELINE implant, and propose methods to mitigate these detrimental responses.

We observed a succession of inter-connected changes over the course of the implantation. During the first hours after insertion, the nerve fibers displayed minimal mechanical displacements in the immediate vicinity of the implant, but without noticeable signs of damage. As early as one day after the insertion, axonal swelling and myelin breakdown became apparent. Previous studies linked these changes to Wallerian degeneration [146, 147]. We found that during the first week after implantation, the macrophages emerging from the extra-fascicular space had migrated into the endoneurial space. The role of these macrophages is to scavenge and remove myelin and axonal debris [146, 147, 148, 149]. During the same period, a capsule developed around the implant, forming an approximately 100 µm broad zone of enhanced cellularity, mainly composed of monocytes and fibroblasts. This capsule increased in size until one month post-implantation, consistent with the one-month period of adjustments in the electrical properties of the implants (Fig. 2.27). Threshold charge increased at the capsule progressively increased the distance between axons and the implant active sites. Similarly, impedance, measured between each active site and the extra-neural reference site, increased as the capsule developed. At extended time-points post-implantation, the capsule combined two adherent layers. The first layer consisted of an accumulation of densely packed multinucleated giant cells in close vicinity of the implant (approximatively 25 µm thickness). The second layer (about 100-150 µm thickness) was composed of a fibrotic network surrounding the multinucleated giant cells (Fig. 2.28).

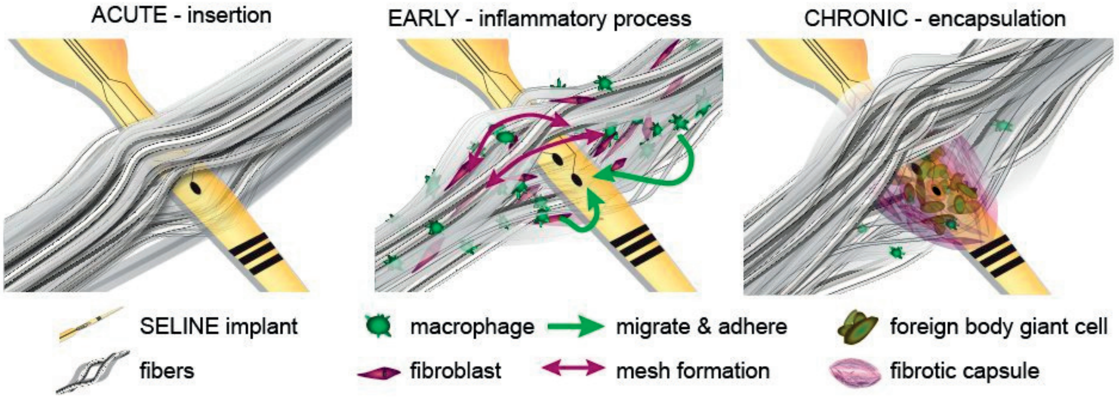

Figure 2.28 – Illustration of possible mechanisms contributing to the implant bio-integration

The size and structure of this capsule was comparable to the capsule that forms around implants inserted into the cerebral cortex [138]. Despite the persistence of inflammatory signs in the chronic stage, the amount of macrophages was substantially reduced compared to early time-points, and remained confined to the proximity of the implant. The evolution of this inflammatory process replicates Wallerian degeneration associated responses that have been described previously [150, 149, 151, 152, 153, 154].

The astroglial foreign body reaction that spontaneously forms around the tip of electrodes inserted in the brain repels nerve fibers, thus preventing central axons from sprouting into the capsule [155]. For this reason, the capsule has been termed the dead zone [136]. In contrast, we found the presence of small diameter unmyelinated fibers scattered throughout the second layer of the capsule, starting a few weeks post-implantation. These results suggest that the fibrotic network and sustained foreign body reaction triggered by the implant do not prevent regenerative sprouting of peripheral nerve axons. These axons may arise from two mechanisms. First, these thin axons may represent ongoing attempts of damaged axons to regenerate through the capsule. Second, this local sprouting may result from the continuing micro-motion of the tethered implant, which may trigger a recurrent cycle of inflammatory reaction and regenerative sprouting.

We detected an increased microvascular density and the presence of potentially pro-regenerative macrophages that have both been linked to regeneration in the peripheral nervous system [156, 157, 158, 159, 160, 161]. These biological responses led to an increase in impedance of the electrodes and in threshold charges during the first month post-implantation in all the tested rats. These pathophysiological reactions may be linked to the mechanical insult due to the insertion of the implant, to the foreign body response, the repeated delivery of current, or a mixture of all these mechanisms. To estimate the role of charge delivery, we conducted anatomical evaluations in a group of rats that never received electrical stimulation through the implant. This group of rats exhibited identical biological responses compared to rats that received stimulation, suggesting that electrical stimulation is not a major contributor in the development of the foreign body reaction. Consequently, we propose that the foreign body reaction was primarily linked to the insertion-associated trauma together with the mechanical and chemical mismatch between the implant and the nerve.

Many strategies may mitigate the mechanical impact of the implant insertion. First, computational modelling may help identifying optimal conditions for surgical insertion of the implants. Second, the geometry of the implant plays a significant role in defining the amount of damage during insertion. Here, we have exploited computational modelling of tissue deformation to various geometries of the entering implant tip [162] to design implants that minimize penetration damage. The limited damage observed a few hours after implantation confirmed that minimal mechanical damage resulted from the insertion. Shape memory alloys that change properties with temperature may provide an alternative material to design implants minimizing penetration damage [163]. Third, various strategies are explored to reduce the chemical and mechanical mismatches between tissue and implant, which both play a significant role in triggering foreign body reaction responses [164]. Chemically, surface modification of substrate materials [137, 165] and organic materials [166] may aid reducing the inflammation and granulomatous reaction, respectively. Mechanically, previous studies showed that reducing the mechanical mismatch between the neural structures and the implants minimize foreign body reaction. For example, soft spinal implants that matched the mechanical properties of the targeted tissue showed remarkable bio-integration in the central nervous system [167].

2.5.3 Potential for long-term clinical applications

The limited understanding of the dynamic interactions between neural tissue and implant functionality has hindered the dissemination of penetrating peripheral nerve implants in clinical applications. Despite the diversity of intraneural implants with various levels of selectivity, these implants have only been used for research studies in humans. Here, we conducted a comprehensive characterization of polyimide-based implants to quantify the potential of these electrodes for clinical applications. Based on our results in rats, we anticipate that this type of implants has the potential to remain functional for extended periods of time in humans. Indeed, the size mismatch between the implant and the targeted nerve is substantially larger in rats compared to humans. Consequently, the impact of motion and tethering forces are substantially larger in rats compared to humans, adding challenges for the resistance of the electrodes, wires, and connectors, which are often among the reasons for the loss of functional channels over the time of implantation. Moreover, rats exhibit more pronounced inflammatory responses and fibrotic reactions compared to humans [168].

The present results cannot be directly extrapolated to the nerve environment of humans. Yet, the milder foreign body reaction and lower impedance of intraneural electrodes reported in larger animal models and humans suggest that the electrode stability observed in rats over 6 months could translate into implants that remain functional and selective for periods ranging from years to decades in humans [135]. Moreover, we show that the removal of the implant from the nerve in the chronic stage did not cause detectable alteration of fine motor control capacities in our rats. Indeed, anatomical examination revealed that the removal of implant did not damage the neural tissue beyond an expected but non-impairing scar formation. The possibility to remove and exchange non-functional implants is critical for clinical settings. The present results open realistic perspectives for long-term clinical applications, including motor prostheses to alleviate motor deficits of the upper and lower limbs as well as sensory prostheses to restore lost sensation.

2.6 Conclusion

We characterized the electrical and functional properties of polyimide-based intraneural implants and their bio-integration in the peripheral nerve environment over extended durations in rodents. These parallel assessments provided a comprehensive and integrated understanding of the interplay between the properties of the implant and the biological responses to the chronic implantation. This knowledge is essential to refine and validate implants for long-term human applications. We showed that despite the unavoidable foreign body reaction, the electrodes remained functional and selective for the entire duration of the experiments, supporting high-precision control over ankle movements. Our results provide a comprehensive assessment of polyimide-based intraneural electrode functionality, stability, and bio-integration and open a realistic pathway to refine and disseminate such implants in clinical applications in humans.

General conclusion

In the work presented in this chapter, I provide an ensemble of neurophysiological and histological data that show, for the first time, the relationship between the stimulation properties of actively-used intraneural implants and their bio-integration within the host-tissue. I demonstrate that intraneural peripheral nerve stimulation can provide high-fidelity control of selective ankle kinematics after months of implantation. I show that the developing capsule does not hinder functionality, and may actually confer additional mechanical stability within the nerve. Those results underline the stability of such implants in the long term in spite of the strenuous experimental model combining multiple intramuscular EMG electrodes and an intraneural implant in healthy and freely moving rats over six months. This work was extremely important to demonstrate the possibility of long-term functionality and provides a solid backbone for the work carried out during my thesis but also for future work related to intraneural thin-film stimulating electrodes.

3 Combining peripheral nerve and spinal cord stimulation in a hybrid neuroprosthesis

Severe spinal cord injury interrupts the flow of information between the brain and the limbs, thereby causing paralysis of the affected body parts. Electrical epidural stimulation (EES) of the spinal cord reactivates the spinal cord below the lesion and is capable of generating locomotor activity. In humans the controllability of the produced movements may however be limited by difficulties in selectively recruiting and modulating distal muscle activation. In the first part of this thesis (chapter 2), I showed that intraneural peripheral nerve stimulation (PNS) selectively recruits distal muscles and permits high-fidelity control of their respective activation in real-time. However, this high specificity is a bottleneck to generate multi-joint, coordinated movements and control the involved muscles simultaneously. In this context, I propose that PNS and EES are complementary strategies and can be combined into a single and refined neuroprosthetic system. I developed and characterized a hybrid PNS-EES paradigm targeting the sciatic nerves and the spinal cord concomitantly in rat models of severe spinal cord injury. The hybrid PNS-EES strategy enabled highly controllable refinements of locomotion pattern in rodents during treadmill and overground locomotion. These developments had important implications for functional restoration in a humans. Indeed, the hybrid PNS-EES paradigm similarly permitted refined locomotion in a pilot experiment with an individual with spinal cord injury.

The content of the chapter is adapted from the manuscript **Wurth** et al., "Hybrid peripheral-spinal neuromodulation paradigm for refined movement restoration after paralysis" in preparation.

Personal contributions: Responsible for the project. Conceived the study (animal) and designed the experiments (animal sand human), performed animal-related procedures and experiments, acquired and analyzed the data, processed the tissue and performed the stainings, acquired and analyzed the images obtained from histology, prepared the figures, wrote the manuscript. The real-time control of PNS delivery during EES-mediated locomotion was implemented in C++ by J Gandar, the second author of the work.

Hybrid peripheral-spinal neuromodulation paradigm for refined movement restoration after paralysis

S Wurth[1,2], J Gandar[2], M Capogrosso[1,3], A Cutrone[4], N Pavlova[2,5], P Shkorbatova[2], E D'Anna[1], Q Barraud[2], S Raspopovic[1,4], F Wagner[2], K Minassian[2], S Micera[1,4*], G Courtine[2*]

[1] Bertarelli Foundation Chair in Translational Neuroengineering, Center for Neuroprosthetics and Institute of Bioengineering, École Polytechnique Fédérale de Lausanne (EPFL), Lausanne, Switzerland

[2] International Paraplegic Foundation Chair in Spinal Cord Repair, Center for Neuroprosthetics and Brain Mind Institute, École Polytechnique Fédérale de Lausanne (EPFL), Lausanne, Switzerland

[3] Department of Medicine and Physiology, Fribourg University, Fribourg, Switzerland

[4] The Biorobotics Institute, Scuola Superiore Sant'Anna, Pisa, Italy

[5] Pavlov Institute of Physiology, St Petersbourg, Russia

[*] Equal contribution as senior authors

3.1 Abstract

Neuromodulation of the lumbar spinal cord enabled extensor and flexor activity in muscles of paralyzed legs after spinal cord injury (SCI), both in animal models and humans. However, EES-mediated neuromodulation is not selective enough to modulate the distal musculature independently and efficiently, impeding a refined movement execution. Peripheral nerve stimulation selectively activates passing axons, which allowed precise control over agonist and antagonist muscles of the ankle in animal models. These results suggest that combined electrical stimulation of both spinal cord and peripheral nerves may provide a global and local control over leg movements, respectively. To evaluate this complementarity, we developed a hybrid peripheral-spinal neuroprosthetic system that electrically stimulated the spinal cord epidurally and both sciatic nerves intraneurally in rat models of leg paralysis. Real-time control of peripheral nerve stimulation within the hybrid peripheral-spinal stimulation paradigm allowed the selective and graded tuning of distal leg movements, permitting high controllability of leg movements during locomotion in rats. Preliminary results in humans suggest similar synergies between spinal cord and peripheral nerve stimulation, enabling refined locomotion mediated by peripheral control over distal muscle activation. Our findings define a novel approach to restoring dexterous movements after paralysis through a personalized and comprehensive electrical stimulation paradigm.

3.2 Introduction

Severe SCI interrupts communication between supraspinal control centres and spinal circuits associated with distal nerves and muscles, thereby causing paresis or paralysis of the affected body parts. Despite the disrupted connections, the spinal circuits and the distal neuromuscular system below the lesion remain largely intact [13]. The voluntary control of movement however is lost, severely impeding the mobility and independence of the afflicted.

Restorative neurology targets the residual, yet altered neural system to enhance recovery from injury [169]. One form, termed Functional Electrical Stimulation (FES), uses the persisting capacity of the peripheral nerves to conduct electricity and recruit muscles. FES can induce a direct muscle contraction by stimulating the nerve terminals on the motor endplate of the target muscle [55], or indirectly, via a multi-joint spinal reflex response that is triggered by stimulation of the nerve afferents [56, 57]. In people with incomplete SCI, the control over the distal musculature is often the most severely affected and FES can be utilized to facilitate foot clearance at the onset of the swing phase. Examples of commercially available systems are Fepa [170] or WalkAid [171]. Individuals suffering from severe SCI however lack sufficient trunk stability and knee and hip extension to benefit from such a local intervention. To address these issues, multi-site FES systems using transcutaneous stimulation [172, 62, 63, 64] or implanted electrodes [66] have been developed and target multiple muscles at once. Those systems can generate standing and short-distance ambulation under high energy expenditure using crutches or a walker for stability. Their setup however is relatively cumbersome, requires extremely high power consumption, the generated movements are slow, abrupt, and unnatural, and the systems suffers from the poor muscle quality of SCI individuals. Accordingly, their use is rather found in a clinical environment for exercising, where they provide a variety of secondary benefits other than mobility [71, 72].

An alternative approach of restorative neurology for the recovery of lower limb function consists in targeting the spinal networks involved in locomotion instead of the peripheral nerves or muscles. Electrical stimulation of the spinal cord recruits motorneurons transsynaptically, which consists in a more natural activation of motor neurons when compared to FES. Experimental studies in animal models have shown the possibility of recovering locomotor-like activity by recruiting these networks pharmacologically [173, 174, 175, 176], electrically [177, 178, 179, 180, 181, 182] or by means of or in combination with afferent feedback induced in the legs by a moving treadmill belt on which the animal was positioned [183, 184]. These experiments have endorsed the role of afferent sensory feedback in the control of coordinated locomotor activity and have promoted the idea that after SCI it was possible to raise the excitability of the spinal networks artificially to enable the sensory feedback to retake this role of regulator and re-establish locomotor output. For instance, epidural electrical stimulation (EES) of the lumbosacral spinal cord restored adaptive and weight bearing locomotion in severely paralyzed rats [33, 34, 35, 36, 32].

Increasing evidence from human studies shows that EES can similarly reactivate the lumbar motor circuits and modulate muscle activity after severe SCI [19, 185, 186, 37, 44, 38, 187]. Furthermore, EES applied during manually assisted treadmill stepping in complete spinal cord injured persons increased the excitability of the lumbar spinal networks and enhanced stepping-like muscle activity [37, 39, 40]. In spite of these encouraging results, it was not possible to actually generate stepping, indicating a clear translational gap between rodent experimentation and clinical studies [41, 42, 43]. Among others, anatomical (scale) and neurophysiological differences between rodents and humans will weigh on the translatability of EES paradigms [41, 46]. For instance, the natural firing rate of rodent afferent fibers is about four to five times higher than the one of humans ([47, 48, 49] and [50, 51, 52] respectively). This difference could heavily impact the interaction between EES and the naturally evoked muscle spindle feedback circuits during locomotion. Finally, in the referred animal studies, the spinal cord excitability was electrochemically enhanced with serotonin agonists, which is known to enhance the responsiveness to stimulation. In humans however, the administration of such neuromodulators is not approved. Those reasons may in part explain the lower success of the applied electrical stimulation when compared to the animal studies. Furthermore, human locomotion and human motor control are immensely more elaborate and skilled when compared to rodents. The human lower limb "dexterity" complements multi-joint movements (motor primitives) with precise, local control such as foot rotation or ankle dorsi-flexion. However, data from human studies seem to suggest that such specificity, for instance through selective recruitment of the tibilais anterior (TA) muscle, could be difficult to achieve with epidural spinal cord stimulation [40, 44, 38], among others because distal agonist and antagonist muscles seem to be partially innervated by the same spinal segments [45]. Consequently, EES paradigms for functional restoration of locomotion could be limited in humans by a lower selectivity in distal muscle activation.

I argue that in the context of restorative neurology, targeting the spinal cord and the peripheral nerves concomitantly is complementary and highly beneficial for providing both a global activation of locomotor networks and a peripheral refinement for increased functionality through selective activation of distal musculature. EES allows for a natural recruitment of synergistic muscle groups, leading to naturally coordinated movements through transynaptic activation of motorneurons, thereby retaining the natural recruitment order of fibers and avoiding to cause rapid fatigue. On the other hand, we have recently shown that intra-neural polyimide based multi-channel implants provide good functional selectivity, integrate well within the host tissue, and have chronically stable electrical properties. Using these electrodes, selective and high-fidelity control over agonist and antagonist muscles of the ankle could be achieved. Those findings suggest that combined electrical stimulation of both spinal cord and peripheral nerves may provide a comprehensive approach to restoring control over leg movements. Here, I developed a hybrid neuroprosthetic system that targeted the spinal cord with EES and the sciatic nerves with intra-neural PNS in rat models of leg paralysis. Real-time control of PNS allowed the selective and graded tuning of distal leg movements, which enabled refined locomotion in paralyzed rats. The combined stimulation strategy allowed them to sustain over-ground locomotion and to climb a staircase. Preliminary results in humans suggested similar synergies between spinal cord stimulation and PNS. These findings open promising perspectives for the development of hybrid neuroprosthetic systems in which EES acts as a general approach for paralysis, while being complemented by PNS to address patient-specific remaining deficits to restore refined, functional movements after SCI, and potentially other neurological disorders.

3.3 Materials and methods

3.3.1 Acute electrophysiology for functional mapping of PNS and EES

Animal model. To assess the complementarity of PNS and EES induced muscle recruitment, we performed terminal electrophysiology on four rats. Animals were anesthetized using urethane (1 g/kg, i.p., Sigma-Aldrich). Intramuscular bipolar electrodes were implanted in the following muscles (proximal to distal) of the right leg: gluteus medius (GLU), vastus lateralis (VL), iliopsoas (IL), semitendinosis (ST), gastrocnemius medialis (GM), tibialis anterioris (TA), extensor digitorum longus (EDL), flexor hallucis longus (FHL). Recording electrodes were fabricated as described previously (section 2.3.2). We implanted an epidural stimulating wire electrode on spinal level S1. Stimulating electrodes were similarly created by making a notch (1mm) in the insulation of Teflon-coated stainless steel wires (AS632, Cooner wire). A partial laminectomy was performed around T8 vertebra to expose the spinal cord. The wire electrode was then inserted below the vertebrae and secured at the mid-line overlying spinal level S1 by suturing the wire to the dura. A ground electrode was created by removing 1 cm of insulation at the distal extremity of another wire from the same plug, which was subcutaneously placed over the right shoulder. At last, we inserted an intraneural polyimide-based multichannel electrode into the right sciatic nerve (cf. section 2.3.2 for a detailed description of the implantation).

Data collection. We assessed the selectivity in muscle recruitment obtained by peripheral and spinal electrical stimulation respectively. For this, a custom-made stimulation protocol (Matlab, The MathWorks Inc, MA) prompted a stimulator unit (IZ2H, Tucker Davis Technologies, FL) to deliver biphasic cathodic-first current pulses (0.5 Hz) of increasing current intensities through the electrode being tested. EMG signals (24.414 kHz) were amplified (x1000), filtered (10 – 2000 Hz band-pass), and acquired into the TDT RZ2 system (Tucker Davis Technologies, FL) for offline analysis. We hypothesized that intraneural peripheral implants retain the capacity to selectively modulate distal muscle activation during epidural stimulation. To test this, we chose two selective channels from the intraneural implants that recruited ankle flexors and ankle extensors respectively. We then re-performed muscle recruitment curves with those channels while simultaneously sending pulses at constant intensity through the spinal epidural electrode.

Quantification. We measured the peak to peak value of each muscle's compound muscle action potential (CMAP) obtained by stimulating with peripheral and spinal electrodes respectively. For each muscle, we then compared the amount of normalized activation obtained with 50% of the maximal charge delivered through. For distal flexor (TA, EDL) and extensor (GM, FHL) muscles, data points obtained by stimulating through peroneal and tibial electrodes respectively were retained.

3.3.2 Chronic animal model and surgical procedures

A total of thirteen female Lewis rats (LEW-ORIj, Charles River Laboratories, France) with initial body weight of 200 g participated in the chronic experiments. The time-line of the different experimental paradigms and involved animal groups is graphically summarized in Fig. 3.1.

First surgery: EMG electrodes, EES electrodes, and SCI. To record chronic muscle activity, we implanted EMG wires electrodes into left and right GM and TA muscles. The electrodes were prepared as described previously (section 2.3.2). We implanted an epidural stimulating wire electrode on spinal levels L2 and S1. Stimulating electrodes were similarly created as described for the acute implantation (section 3.3.1). A ground electrode was created by removing 1 cm of insulation at the distal extremity of another wire. All wires from EMG electrodes and EES electrodes were routed to the same amphenol connector that was secured on the skull of the animal using dental cement. All animals received a severe spinal cord injury injury (complete transection n=4, severe contusion n=9) at a mid-thoracic level (T8). A dorsal mid-line skin incision was made from T5 to L2 and the muscles covering the dorsal vertebral column from T6 to T13 were removed. A partial laminectomy was performed from T7 to T9 in which the spinous processes and the dorsal and lateral aspects of the vertebral column were removed to expose the spinal cord. The dura was opened along the mid-line of the spinal cord. For contusive injuries, the animal wa then fitted in the Infinite Horizons Impactor (Precision Systems Instruments LCC) with special clamps attached to vertebrae T6 and T10. The spinal cord was then impacted by a metal probe (250 kDyn force) with a standard rat tip (2.5 mm diameter). For complete transections, the spinal cord was cut at the same level and discontinuity was verified by passing the surgical tool from below.

Second surgery: Bilateral intra-neural electrode implantation in left and right sciatic nerve. In a second surgery about four to five weeks after the first one, animals were bilaterally implanted with intra-neural polyimide-based multichannel electrodes into the right and left sciatic nerve (Fig. 3.2). For each

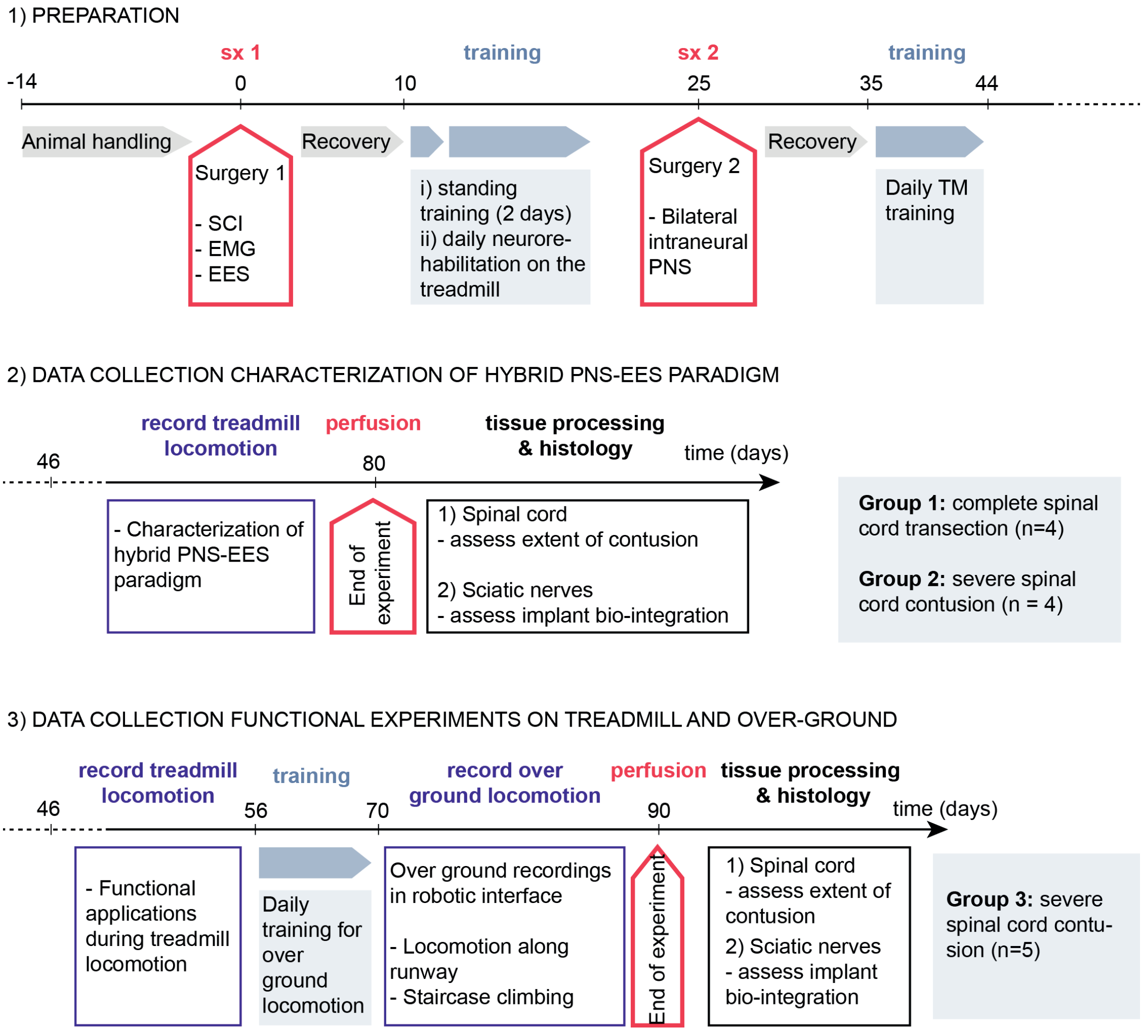
1) PREPARATION
sx 1
training
sx 2
training
-14
0
10
25
35
44
Animal handling
Surgery 1
- SCI
- EMG
- EES
Recovery
i) standing training (2 days)
ii) daily neurorehabilitation on the treadmill
Surgery 2
- Bilateral intraneural PNS
Recovery
Daily TM training
2) DATA COLLECTION CHARACTERIZATION OF HYBRID PNS-EES PARADIGM
record treadmill locomotion
perfusion
tissue processing & histology
46
80
time (days)
- Characterization of hybrid PNS-EES paradigm
End of experiment
1) Spinal cord
- assess extent of contusion
2) Sciatic nerves
- assess implant bio-integration
Group 1: complete spinal cord transection (n=4)
Group 2: severe spinal cord contusion (n = 4)
3) DATA COLLECTION FUNCTIONAL EXPERIMENTS ON TREADMILL AND OVER-GROUND
record treadmill locomotion
training
record over ground locomotion
perfusion
tissue processing & histology
46
56
70
90
time (days)
- Functional applications during treadmill locomotion
Daily training for over ground locomotion
Over ground recordings in robotic interface
- Locomotion along runway
- Staircase climbing
End of experiment
1) Spinal cord
- assess extent of contusion
2) Sciatic nerves
- assess implant bio-integration
Group 3: severe spinal cord contusion (n=5)

Figure 3.1 – Experimental time-line for the development and assessment of the hybrid peripheral-spinal neuromodulation paradigm in chronic rat model of SCI. All animals underwent the same preparation phase during the first six weeks (top row). Two groups of animals participated in the experiments for the characterization of the hybrid PNS-EES neuromodulation paradigm (n=4 with complete transection and n=4 with severe contusion respectively of the mid-thoracic spinal cord). A third group of contused animals (n=5) participated in the experiments on functional applications of the experimental paradigm.

leg, a longitudinal skin incision was made at the level of the mid-thigh. The sciatic nerve was carefully exposed and free from adhering tissues. Next, an approximatively 2 cm long incision was made over the lower lumbar spine. The backplug structure containing the single connector (NPD-18-DD-GS, Omnetics Connector Corp, MN) to which both implants were connected towards opposing directions using copper Cooner wires (CZ1187, Cooner Wire Corp. CA) was positioned onto this opening and fixed to the lower back muscles by sutures through four small holes on its core. To protect the implants during implantation, we inserted them into plastic tunnel guides that permitted manipulation without touching the active part. For each side, this construct was then passed from the back under the skin and muscles towards the sciatic nerve. We then removed the tunnel distally and inserted the guiding needle into the sciatic nerve above the bifurcation level separating peroneal from tibial fascicle. The extra-neural part was then sutured to the epineurium and the wires positioned in a stress-releasing loop under the skin to allow for leg movements without pulling on the implant.

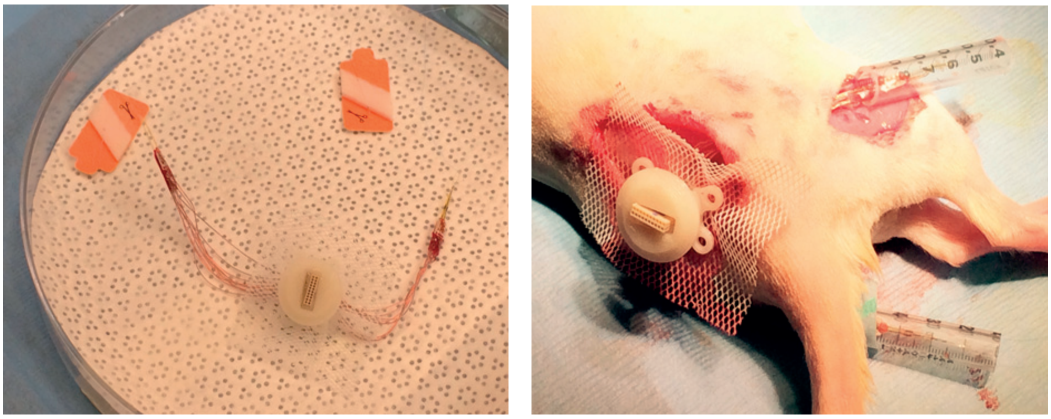

(a) Bilateral implant construct

(b) Implantation using tunnel guides for electrode protection

Figure 3.2 – Bilateral implantation of intraneural electrodes in sciatic nerves. (a) Construct routing two SELINE electrodes [109] to a common connector in a 3D printed pedestal. (b) Use of tunnel guides to protect implants during surgery.

All surgical procedures related to the chronic experimental model were performed under sterile conditions and general anesthesia (Isoflurane (1-3 %) in oxygen-enriched air). The animals were placed on heating pads to prevent hypothermia during the surgery. Analgesia (Buprenorphine (temgesic), ESSEX Chemie AG, 0.01-0.05 mg per kg, subcutaneous, twice per day) and antibiotics (Baytril 2.5%, Bayer Health Care AG, 5–10mg per kg, subcutaneous, once per day) were administered during 5 days post-surgery. Animals were housed on a 12h light-dark cycle with food and water ad libitum. Animal care, including manual bladder voiding, was performed twice per day throughout the injury period. Post-surgery, animals were housed individually but received daily social time with the other animals five times per week. All animal procedures were authorized by the Veterinarian office of the Canton of Geneva, Switzerland.

3.3.3 Neurorehabilitation procedure after SCI

Animals were trained in bipedal locomotion on a treadmill in sessions of twenty to thirty minutes five days a week. The detailed procedure for the neurorehabilitation was previously described [35]. Daily locomotion training started 10 days after the first surgery. Wearing custom made Velcro-fitted jackets, the animals were attached to the backplate of a body weight support (BWS) system that was connected to a motorized treadmill. To promote the excitation of the spinal cord below the lesion, we systemically administered the 5-HT2A receptor agonist quipazine (0.2–0.3 mg per kg, intraperitoneal) and the 5-HT1A,7 receptor agonist 8-OHDPAT (0.05–0.3 mg per kg, subcutaneous) [188]. We delivered monopolar electrical stimulation (0.2 ms, 100 - 300 μA) through L2 and S1 electrodes at 40 Hz. All animals were trained during two to three weeks until able to sustain 20 minutes of locomotion supporting at least 60 % of their own body weight. Treadmill speed was at 11 cm/s.

3.3.4 Multi-system recording platform

We recorded locomotion on the treadmill and over-ground to assess the impact of hybrid PNS-EES on gait patterns. During all recording sessions, 3D joint kinematics of the left and right hind-limbs were recorded using the high speed motion capture system Vicon (Vicon Motion Systems Ltd., UK) combining two high-definition and twelve infrared cameras. Small reflective markers were positioned on the following left and right hind-limb joints: iliac (crest), greater trochanter (hip), lateral condyle (knee), lateral malleolus (ankle), and metatarsophalangeal (MTP), building a 10 marker model of bilateral hind-limb joint kinematics. The kinematic data (200 Hz), EMG signals (2 kHz), and ground reaction forces via a force plate (2 kHz, HE6X6, AMTI, MA) were simultaneously recorded into the Vicon system.

3.3.5 Control architecture for phasic PNS based on monitoring of gait kinematics

Real-time environment. We aimed at delivering PNS at precise timings based on real-time feedback from gait kinematics. To this end, we implemented a PNS controller within a multi-threaded C++ code (Visual Studio 2012, Microsoft) running on a quad-core Microsoft Windows 7 computer. The basis of this platform has been previously described [132]. Briefly, gait patterns were monitored with the Vicon motion capture system that records 3D kinematic positions in real-time for each joint at a frequency of 200 Hz. These data were imported into the C++ environment in real time via Ethernet using the DataStream SDK software, where they were processed and filtered (adaptive least mean squares filters) for the generation of the triggering logic. Based on this triggering logic, PNS was delivered via an RZ2 processing unit connected to an IZ2H Stimulus Isolator (both Tucker-Davis Technologies, USA). An illustration of the system is presented in Fig. 3.3.

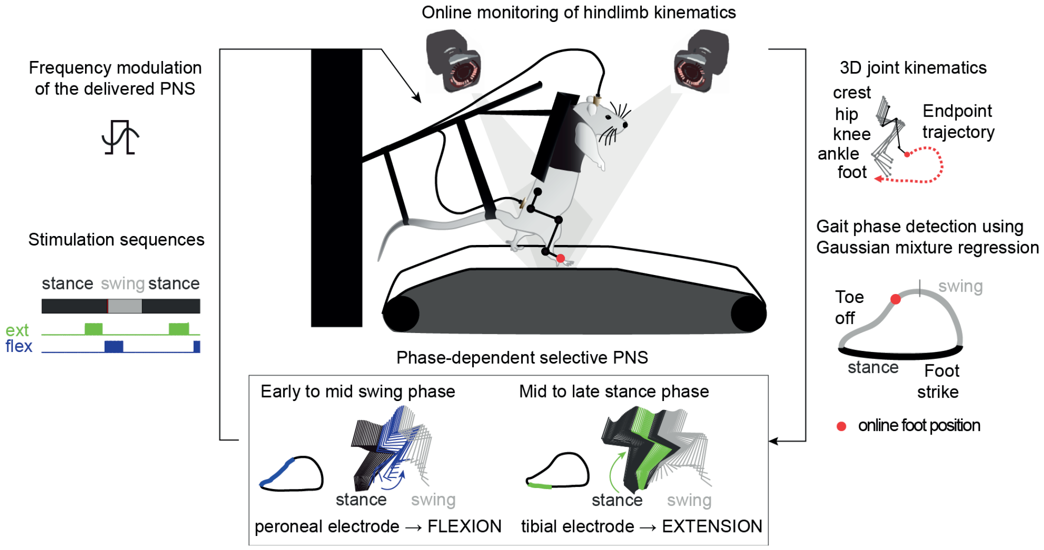
Online monitoring of hindlimb kinematics
Frequency modulation of the delivered PNS
Stimulation sequences
stance
swing
stance
ext
flex
3D joint kinematics
crest
hip
knee
ankle
foot
Endpoint trajectory
Gait phase detection using Gaussian mixture regression
Toe off
swing
stance
Foot strike
online foot position
Phase-dependent selective PNS
Early to mid swing phase
stance
swing
peroneal electrode → FLEXION
Mid to late stance phase
stance
swing
tibial electrode → EXTENSION

Figure 3.3 – Experimental setup for the characterization of the hybrid PNS-EES paradigm. Bilateral hind-limb joint kinematics are read in real-time through the 3D infrared motion capture system Vicon. The current phase of the gait is predicted in real time using Gaussian mixture models, based on which selective PNS for extension or flexion is delivered at varying frequencies.

Ensuring detection robustness. Since PNS was based on precise gait events defined by leg kinematics, we needed to ensure continuous and flawless detection of the concerned markers, which is challenging in a behavioural animal experiment environment. This was achieved through the development of a custom algorithm for the online extrapolation of missing markers through triangulation. Based on the 10-marker model for bilateral hind-limb joint kinematics (see section 3.3.4), correct labelling of each marker with respect to the appropriate joint landmark was continuously verified online [36].

Gaussian mixture model to provide model of foot trajectory during locomotion. We used Gaussian mixture models to provide a model of the rodent's gait, according to which stimulation could be delivered. The model was built offline using kinematic data from baseline recordings during treadmill locomotion (60 steps/animal, n=5 animals). A total of eight features were selected that represented best the phase φ of the gait cycle, namely velocity and position components of the MTP marker (foot) in the sagittal plane. These parameters were normalized to gait cycle duration. A K-means clustering method was used to split this 8-dimensional baseline data-set into nine clusters. The mean of each cluster defined the center of a Gaussian. The variance of each Gaussian was determined via the distance between the center and each of the elements of the cluster. Gaussians were then sorted and linked together as function of the mean path trajectory of all step cycles, yielding a generalized model of the foot trajectory throughout a gait cycle [189]. The phase of the gait cycle was then defined as φ ranging monotonically from 0 to 100 %. By definition, $\varphi = 100\%$ (end of one gait cycle), equals $\varphi = 0\%$ (the beginning of the next gait cycle). To avoid discontinuity of the gait phase when jumping from 100% to 0% (and thus prevent resulting edge effects in the triggering logic at the beginning or at the end of a gait cycle), we further split the phase into two cyclic parameters, namely $cos(\varphi)$ and $sin(\varphi)$. The procedure is graphically summarized in Fig. 3.4, only three parameters out of eight are shown for the sake of clarity of the figure.

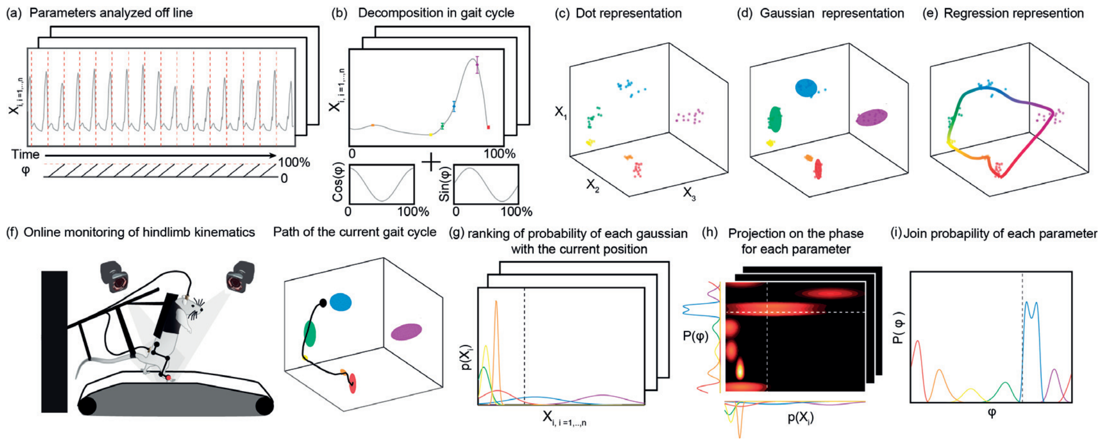
(a) Parameters analyzed off line
$X_{i, i=1,...,n}$
Time
φ
100%
0
(b) Decomposition in gait cycle
$X_{i, i=1,...,n}$
0
100%
Cos(φ)
Sin(φ)
0
100%
0
100%
(c) Dot representation
X_1
X_2
X_3
(d) Gaussian representation
(e) Regression represention
(f) Online monitoring of hindlimb kinematics
Path of the current gait cycle
(g) ranking of probability of each gaussian with the current position
$p(X_i)$
$X_{i, i=1,...,n}$
(h) Projection on the phase for each parameter
P(φ)
$p(X_i)$
(i)Join probapility of each parameter
P(φ)
φ

Figure 3.4 – Gaussian Mixture Model for the prediction of foot trajectories in real time. This example illustrates the concept using 3 parameters (8 were used). GMM creation to model foot trajectory for a given experimental paradigm follows the following steps: a) off-line extraction of kinematic parameters, b) normalization of parameters, decomposition into gait cycle, and computation of the phase, c) data clustering (K-means), d) computation of Gaussian around each mean, e) connection of Gaussians according to the path of the foot trajectory. Determination of gait phase in real time based on kinematics. f) Real-time recording of kinematics allows to represent the current path according to current parameters value, g) distance computation between current parameters values and each Gaussian and determination of most likely Gaussian to represent the current phase of the gait cycle, h) extraction of the most likely phase for each parameter, and i) combination of each individual probability into the final phase estimation.

Gaussian mixture regression to predict foot position in real time. During recording, Y and Z position and velocity coordinates of the foot marker were fed in real time into the Gaussian Mixture model as eight dimensional vector. For each time step, probabilities for the most likely Gaussian were computed for each dimension, based on distance between the current values of each dimension and each of the Gaussians defining the gait cycle. The final estimation of the current phase was computed as conditional probability knowing the individual probabilities of the most likely Gaussians for each dimension (Bayes theorem) and predicted the current phase of the gait cycle of the rat.

Stimulation logic for the phasic delivery of selective PNS. Bilateral PNS was delivered based on the phase of the gait cycle of each leg. The control logic could trigger the start of individual electrodes simultaneously. PNS duration was kept constant to minimize the effect of detection errors to the onset of stimulation only as opposed to detecting and triggering the end of stimulation as well. As such, the activation timing of each electrode was triggered when the computed phase φ crossed a user-defined threshold between (0 and 100). These thresholds (timings) for flexion and extension were first roughly determined based on EMG activation of ankle flexor and extensor muscles in offline recordings, and then optimized manually in a calibration trial for each rat.

3.3.6 Characterization of hybrid PNS-EES neuromodulation paradigm during treadmill locomotion

To understand the impact of hybrid peripheral-spinal neuromodulation on gait, we systematically characterized the combination of PNS and EES in paralyzed rats. Two groups of animals participated in this experimental paradigm (n=4 with complete transection of the spinal cord and n=4 with severe contusion of the spinal cord). For this, we first electrochemically enabled treadmill locomotion in paralyzed animals (cf. section 3.3.3), which served as baseline condition for the characterization experiments, referred to as "EES only". This baseline condition was recorded for every rat in every session. We had previously shown that the effects of selective intraneural PNS on lower leg kinematics were linearly adjustable by varying the frequency of stimulation in anesthetized animals for both ankle flexion and extension [190]. To verify this during locomotion, we characterized the effect of adding selective PNS with varying frequencies to the electrochemically enabled gait pattern on the treadmill. Intraneural PNS for extension and flexion were triggered at mid stance phase and at the onset of the swing phase respectively (cf. section 3.3.5). Ten steps in each condition (EES only, and hybrid PNS-EES with PNS at 30 Hz, 40 Hz, 50 Hz, 60 Hz, 70 Hz, and 80 Hz respectively) were recorded as described in section 3.3.4 and stored for offline analysis. During each experimental paradigm, we recorded the 3D coordinates of bilateral hind-limb joint markers. These data were used to compute a total of 110 parameters characterizing gait, kinematics, and ground reaction forces (Appendix A.1). We then used principal component analysis (PCA) to capture the set of parameters that best discriminated the gait patterns obtained in the different conditions. Factor loading on the first principal component (PC1) permitted to extract the kinematic variables most affected in response to the different stimulation conditions [33, 188].

3.3.7 Functional impact of hybrid PNS-EES neuromodulation during treadmill and over-ground locomotion

We evaluated the functional benefits of the hybrid peripheral-spinal neuromodulation paradigm during locomotion in a third group of animals (n=5) who had also received a severe spinal cord contusion at mid-thoracic level. In a first application, we used the hybrid PNS-EES paradigm to reduce foot dragging in real time during treadmill locomotion. A foot dragging event was defined by a combination of the velocity components of the MTP marker in the sagittal plane (YZ directions). We compared the amount of foot drag for each step between EES only and the hybrid PNS-EES conditions. We further assessed the efficiency of the hybrid PNS-EES to reduce dragging when it was detected and measured the amount of time stimulation was active in ten consecutive steps, comparing the strategy of stimulation when drag was detected with a stimulation paradigm employed during the characterization experiments (stimulation at every step). In a second application, we used PNS to selectively and bilaterally reinforce extension at the end of a training session on the treadmill. We hypothesized that collapse due to exhaustion could be remedied by selectively activating ankle extension at the end of each stance phase, thereby providing additional assistance to push the legs off the ground.

Over-ground locomotion was permitted with the aid of a robotic neurorehabilitation framework developed by our group [191, 192]. Briefly, this robotic interface provides adjustable trunk support in the three Cartesian directions as well as in rotation around the vertical axis. Rats are attached with their back to the trunk support plate in a bipedal posture. To provide additional stability in the horizontal plane, we restricted the movement of the robot to the sagittal plane (no sidewards movements). Movement was only possible when animals were advancing (no forward force was applied to help the animals advance). To start stepping, the animals needed to initiate a forward movement and then continue to push step by step, as opposed to the treadmill locomotion during which the running belt is responsible for the sensory feedback initiating locomotion. Animals were trained in this experimental paradigm for a minimum of ten days. We then compared locomotion performance between baseline (EES only) and hybrid PNS-EES stimulation paradigm by measuring walking speed in addition to step height and foot drag on the runway. Finally, we put stairs on the runway and compared the performance of the rodents (pass, tumble against, or fail the stairs) under both conditions (EES only vs hybrid PNS-EES).

3.3.8 Tissue processing and histology procedures

At the end of the experiment, animals were transcardially perfused with Ringer's solution containing 100'000 IU-L heparin followed by paraformaldehyde (PFA) 4%. The spinal cord and sciatic nerves were carefully dissected and post-fixated in the same fixative solution overnight.

Quantification of spinal cord injury. Spinal cords were carefully dissected and visually inspected to identify the lesion through an accumulation of connective tissue. After postfixation, the spinal cords were transferred to phosphate-buffered sucrose 30% for cryoprotection. After two days, the spinal cord segments were embedded in optimal cutting temperature compound (Tissue-Tek®, Sakura, Finetek, USA) for cutting at the cryostat. Serial coronal (contused spinal cords) or longitudinal (transected spinal cords) sections of 40 µm thickness were cut along the entire segment and mounted onto gelatin-coated glass slides. Sections were immunohistochemically labeled against glial fibrillary acid protein (GFAP, 1:1000, Dako Z0334, USA) to reveal reactive astrocytic activity in the tissue spared by the lesion. Immunoreactions were visualized with an appropriate secondary antibody labeled with Alexa fluor 488. Sections were mounted using anti–fade fluorescent mounting medium before being cover-slipped for microscopy. All slices were imaged at 20x magnification using a slide scanner (Olympus VS-120, Olympus Corp., EU). The percent of spared tissue at the lesion epicenter was calculated as the ratio between the remaining tissue at the lesion epicenter and the estimated cross-section of the spinal cord without lesion at the same level. The former was determined by measuring the area of remaining tissue on two representative slices stained by GFAP. The latter was determined by selecting two representative slices rostral and caudal to the lesion epicenter respectively and calculating their average cross-sectional area, approximating the estimated cross-sectional area at the spinal level of the lesion before the contusion injury. The results from assessing the amount of spared tissue in the lesion epicenter are presented in Appendix 2 (A.2).

Quantification of intraneural implant bio-integration. The nerves were processed for embedding in paraffin blocks and then transversally sectioned on a microtome (Hyrax M25, Microm, DE) at 4 µm thickness. Three tissue sections in a ribbon of ten were selected and mounted 3 by 3 onto coated glass slides (Superfrost Ultra Plus, Thermo Fisher Scientific, MA), yielding tissue slices of approximatively every 40 µm between glass slides. Mounted tissue samples were dried overnight at 37°C and then stored at +4°C until use. We selected slices at the level of the implantation to assess the tissue reaction to the implant that was implanted for 8 weeks and actively used on a daily basis. Consecutive slices were stained with Hematoxylin & Eosin and Sirius Red respectively using the automatic Tissue-Tek Prisma & Coverslipper HQ^{plus} machine (Sakura, NE). In addition, we immunohistochemically labelled sections against macrophage and monocyte marker CD68 (anti protein CD68 1:400 Serotec) to quantify inflammation. Briefly, slides were dewaxed and underwent antigen retrieval, followed by 1h blocking of non specific sites in bovine serum albumin (BSA 1% diluted in PBS 0.1M). Selected sections were then incubated overnight in primary antibody solution at 4°C. After washes in PBS, sections were incubated for 1h in secondary antibody solution (Alex fluor 488, Life Technologies, 1:400). Slides for fluorescence microscopy were mounted with a DAPI-containing medium (Vectashield, Vector Laboratories) and cover-slipped for microscopy.

All images of nerve sections were acquired at 20x magnification (optical and fluorescence, Olympus slide scanner VS120-L100, Olympus Corp., EU). We measured the cross sectional area of the nerve fascicles, the capsule around the implant, and the layer of foreign body giant cells manually out on H&E or SR sections using open source software Fiji for the area measurements (ImageJ, NIH, MD). Inflammation was quantified as described in chapter 2, section 2.3.11.

3.3.9 Pilot study investigating hybrid PNS-EES neuromodulation in an individual with SCI

Context. Our group runs a clinical feasibility study investigating the potential of EES in individuals with sensory and motor incomplete SCI classified as C or D according to the ASIA impairment scale (Table 1.1) in collaboration with the Centre Hospitalier Universitaire Vaudois (CHUV) in Lausanne and Balgrist Hospital in Zurich. In this study, electrical stimulation of the spinal cord is delivered through 16 contacts of an electrode array (Specify 5-6-5 surgical lead ™, Medtronic, USA) that is positioned epidurally over lumbar spinal cord segments. The stimulation strategy aims to mimic the spatio-temporal dynamics of motor-neuron activation in the lumbosacral spinal cord, stimulating spinal circuits underlying flexor and extensor movements or synergies (via different contacts on the array) at appropriate time-points during the gait cycle (swing vs. stance) [36]. Kinematics are monitored in real-time using the Vicon system and serve as triggering logic for these spatio-temporal stimulation profiles.

In the framework of this study, we had the possibility of testing the potential of the hybrid PNS-EES stimulation paradigm in a patient (patient A) participating in the clinical trial (Fig. 3.5 (a)). Patient A is a 28-year old man, who had severe paralysis of the lower limbs, especially the left one, due to a gymnastic accident. He was diagnosed with a spinal cord injury at the C7 cervical level and was evaluated as ASIA D with motor scores of 0 on his left leg at the time of his enrolment in the clinical study (Fig. 3.5 (b)). He was implanted with an epidural multi-electrode array over spinal segments of L2 to S1 (Fig. 3.5 (a), CT scan). He participated in rehabilitation sessions four times a week for a total of 80 sessions and was supported during locomotion with a multi-directional gravity-assist robotic assistive framework that provided adjustable forces in multiple directions for optimized trunk support [193]. Despite spatio-temporal stimulation patterns, EES was not able to selectively recruit the distal ankle muscles and and appropriately facilitate ankle dorsi-flexion during the swing phase. In this pilot study, I aimed to enhance the swing phase of the left leg during EES-mediated locomotion by applying the hybrid PNS-EES stimulation paradigm using transcutaneous PNS (Fig. 3.5 (a)).

Experimental setup. PNS was applied using surface stimulation through self-adhesive hydrogel stimulation electrodes attached to the skin. Stimulation was delivered using a commercially available CE marked

FES device (RehaStim stimulator, Hasomed, DE). We positioned two surface electrodes on his lateral lower leg (Fig. 3.5) to stimulate the peroneal nerve for elicitation of a flexion reflex. For this, we placed the cathode at the fibular head and the anode about 2cm more distal and anterior to the cathode (Fig. 3.5) and delivered rectangular, bi-phasic and charge balanced pulses with 0.5 msec pulse width [194]. Throughout the entire session amplitude, pulse width, and frequency were kept constant unless specified otherwise. The pulse train duration was 500 msec, and its start was locked to the onset of the EES-stimulation profile for flexion on the left leg.

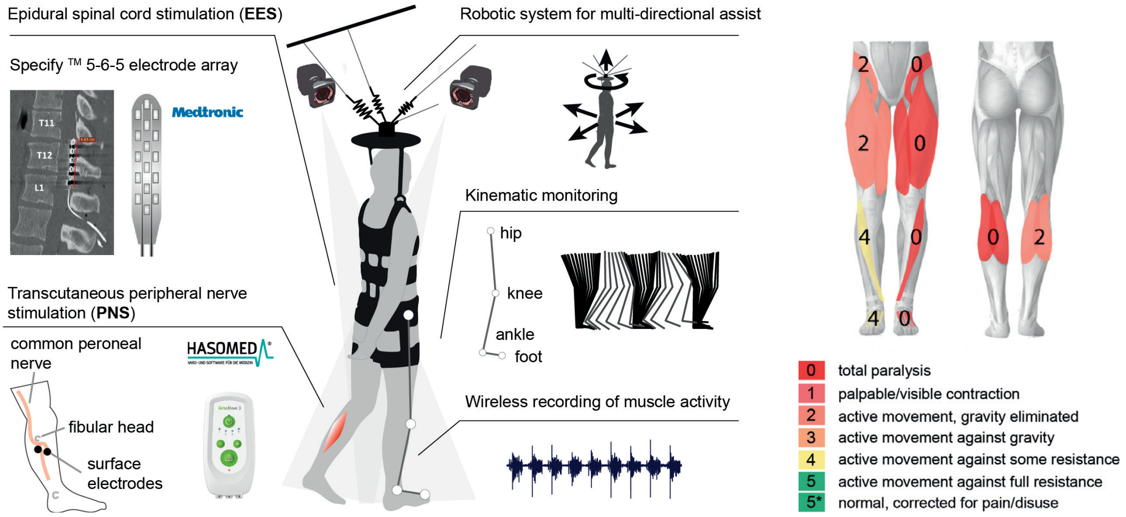
Epidural spinal cord stimulation (**EES**)
Specify ™ 5-6-5 electrode array
T11
T12
L1
Medtronic
Robotic system for multi-directional assist
Kinematic monitoring
hip
knee
ankle
foot
Transcutaneous peripheral nerve stimulation (**PNS**)
common peroneal nerve
HASOMED
fibular head
surface electrodes
Wireless recording of muscle activity
2
0
2
0
4
0
4
0
0
2
0 total paralysis
1 palpable/visible contraction
2 active movement, gravity eliminated
3 active movement against gravity
4 active movement against some resistance
5 active movement against full resistance
5* normal, corrected for pain/disuse

(a) Experimental setup **(b)** Motor score of patient A

Figure 3.5 – Experimental setup for hybrid PNS-EES paradigm in human SCI subject. (a) Hybrid PNS-EES with electrical stimulation of epidural spinal cord (top left) and the peroneal nerve (bottom left) via 5-6-5 Specify™electrode array over spinal segments L2-S1 and adhesive surface electrodes over the common peroneal nerve respectively. Right: Robotic system provides multi-directional assistance during locomotion. Lower limb kinematics and muscle activity are recorded to measure performance. (b) Leg motor scores of patient A at the time of his enrolment into the study.

Control architecture. In order to precisely control the timing of the delivered stimulation pulses and to synchronize PNS with the EES neuromodulation and the different phases of gait, we developed a real-time control over the RehaStim stimulator. The control was performed by a single-board computer (RaspberryPi), running a custom, multi-threaded C++ software. The communication between the single-board computer and the RehaStim was ensured via USB using a virtual serial interface (FTDI). The custom software triggered each stimulation pulse individually, thus imposing the overall stimulation frequency and allowing precise temporal control. PNS stimulation was synchronized with the EES stimulation protocol promoting flexion of the left leg, at the initiation of the swing phase, which was detected in real time on the main computer using the kinematic information provided by the Vicon software. The single-board computer was connected to the main computer wirelessly over Bluetooth. This link was used to send triggers from the main computer to the single-board computer, in order to turn stimulation ON and OFF at appropriate moments during the gait cycle. A dedicated thread read symbols from the virtual COM port established over Bluetooth, and triggered the stimulation accordingly. The dedicated thread structure allowed minimal delays by ensuring that the software was always ready to receive ON or OFF commands, even while stimulation was ongoing.

Experimental paradigm. In this pilot experiment, we assessed the direct functional benefits of the hybrid peripheral-spinal neuromodulation paradigm on locomotion. We tested walking under the conditions

EES only, PNS only, and hybrid PNS-EES while recording bilateral leg kinematics from hip, knee, ankle, and foot joints, as well as EMG activity from left and right tibialis anterior, peroneus longus, vastus lateralis and semitendinosus. EMG signals from distal muscles (peroneus longus, tibilis anterior) could not be analyzed because of signal corruption by stimulus artifacts. Ten steps in each condition were recorded. The assistive forces of the multi-directional gravity assistance were adjusted for optimal support during EES only (normal rehabilitation situation for the subject), and were then kept constant between conditions.

3.3.10 Statistical analysis

All data is presented as mean +- standard error of the mean (sem) unless otherwise specified. Group differences (> than 2 groups, at least 5 animals/group) were assessed using matched observations ANOVA with Bonferroni's post-hoc test to evaluate pairwise differences ad hoc. Comparisons between two groups only (at least 5 data point) were assessed using paired t-tests. Between group differences for single subject data (10 steps/condition) were assessed using unpaired observations ANOVA with Bonferroni's post-hoc test to evaluate pairwise differences ad hoc. Statistical significance was considered at $p < 0.05$.

3.4 Results

We developed a hybrid spinal-peripheral neuromodulation paradigm that we characterized and validated in a rat model of severe SCI. To this end, we first verified the complementarity of PNS and EES on muscle recruitment in acute electrophysiology experiments. Then, we conducted chronic experiments, for which we implanted stimulating electrodes on the epidural spinal cord and bilaterally into the sciatic nerves of severely paralyzed rats. Here, we characterized the effect of the hybrid neuromodulation by varying PNS frequency and investigated the impact of the different conditions on locomotion patterns. We then used the optimal hybrid neuromodulation to provide selective control over leg kinematics when assistance was needed. The bio-integration of the intraneural implants is in line with our previous results on thin-film intraneural electrodes (Chapter 2). Results from a pilot experiment with a human spinal cord injured individual enrolled in a clinical feasibility study conducted by our group suggest that similar synergies between EES and PNS can provide additional control over leg movements and increase functional outcome in humans.

3.4.1 PNS elicits selective sensory-motor responses

The analysis of motor evoked potentials elicited by intraneural PNS confirmed the ability to selectively recruit fibers related to flexor vs. extensor muscles and revealed that the evoked responses recorded in the EMG signals were mostly mixed, having neither a pure motor nor a pure sensory origin. This discrimination was based on i) the shape and width of the evoked potential and ii) the latency of the evoked CMAP in each muscle. For instance, the CMAP of ankle extensor GM muscle had a latency of 1.439 +- 0.184 (mean +- std) when evoked by PNS, while the latency was 2.536 +- 0.166 when evoked by EES (mean +- standard deviation, n = 4 animals). Fig. 3.6 illustrates the difference in latency obtained in GM CMAP for PNS (light grey) vs. EES (dark grey) stimulation in one representative animal. A pure sensory response through mono-synaptic excitation of motor fibers via Ia afferents would have a latency that was at least 3.5 msec [181, 30].

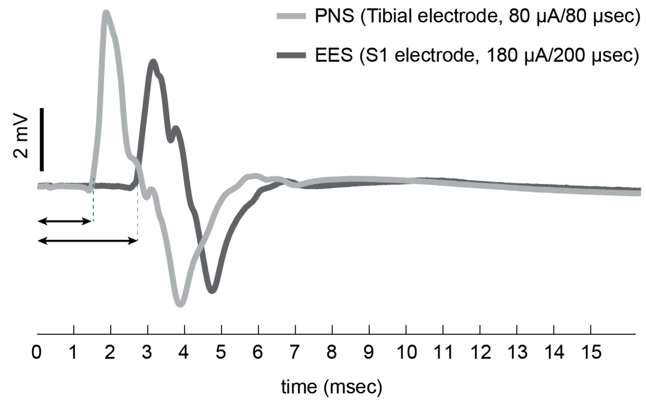

Figure 3.6 – Gastrocnemius Medialis compound muscle action potential (GM CMAP) obtained by PNS and EES exhibit different latencies.

The occurrence of PNS-induced mixed responses was confirmed when delivering pulse trains at 40 Hz (as opposed to single pulse stimulation when carrying out muscle recruitment curves). In anesthetized experiments, we had observed the generation of both local movements restricted to the ankle joint and leg movements affecting multiple joints (unpublished data obtained during experiments performed in the framework of assessing chronic functionality of intraneural stimulating electrodes, [190] and chapter 2). A direct, selective recruitment of motor fibers relating to ankle flexor and extensor muscles had resulted in precise ankle flexion and extension respectively (Fig. 3.7 top). Concomitant recruitment of afferent fibers was ascertained by observing evoked extension and flexion reflex responses acting at several joints (Fig. 3.7 bottom). Indeed, afferent fibers activate not only homonymous motor neurons but branch onto heteronymous but synergistic motorneurons, thereby being capable of activating specific muscles at different joints [195]. Despite the position of the rat on the edge of a small table preventing the observation of hip flexion, reflex responses show an enlarged range of motion both in extension and flexion trials (Fig. 3.8). The range of motion (ROM) refers to the amplitude of angular excursion during the trial.

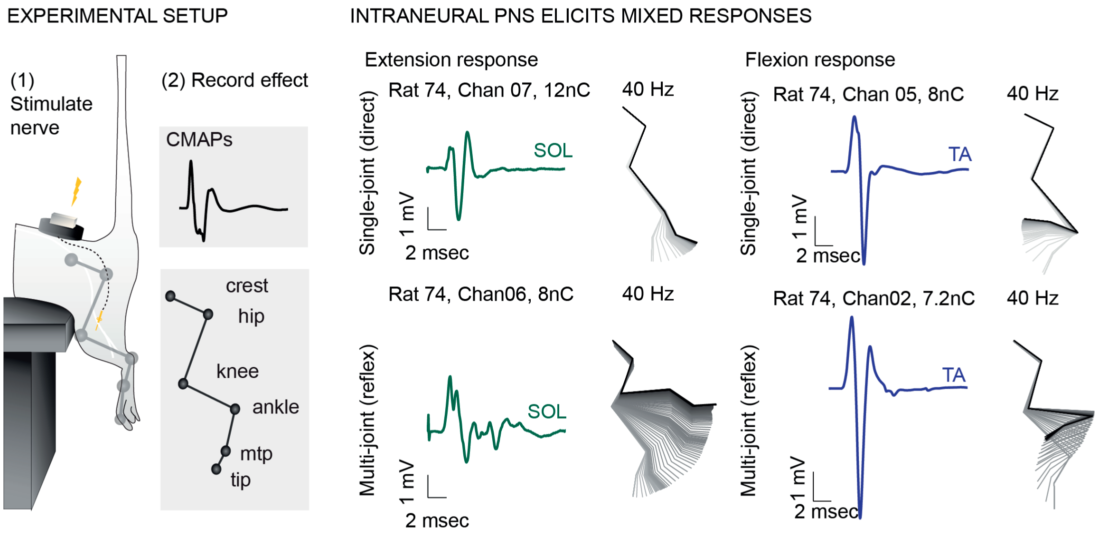

Figure 3.7 – PNS evokes mixed sensory-motor responses, leading to single-joint (top row) and multi-joint (bottom row) movements. For each case (flexion and extension, resulting in direct or reflex responses), the CMAP in SOL muscle (for extension) and TA muscle (for flexion) is shown as obtained by a single pulse with the indicated channel and charge.

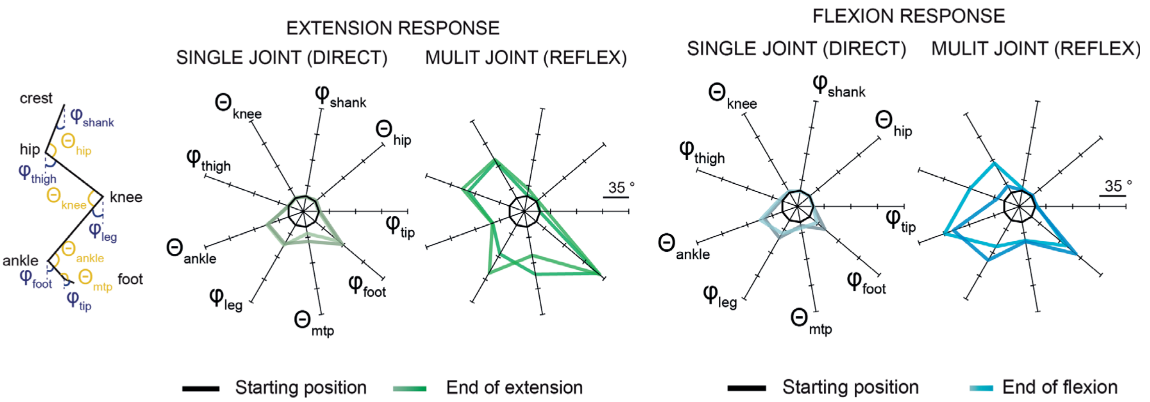

(a) Amplitude of PNS-evoked extensor responses

(b) Amplitude of PNS-evoked flexor responses

Figure 3.8 – Range of motion obtained by direct and reflex responses during extension and flexion. Reflex responses increase leg range of motion, direct responses provide more localized effect. Data are normalized to resting position (black circle) for each case. (n=2)

3.4.2 Complementary peripheral and spinal muscle recruitment

To demonstrate the complementary recruitment of leg muscles by peripheral and spinal electrical stimulation (PNS and EES respectively), we implanted flexor and extensor muscles acting on proximal and distal joints of the leg, and recorded EMG activity in each of those muscles upon peripheral and spinal stimulation respectively. Fig. 3.9 A illustrates the recruitment obtained by intraneural PNS (targeting either the peroneal or the tibial branch for selective activation of respectively flexor or extensor muscles), by EES at spinal level S1, and by conjointly delivering EES at S1 and PNS with either of the tibial or peroneal channels of the intraneural electrodes (residing in peroneal and tibial fascicles respectively).

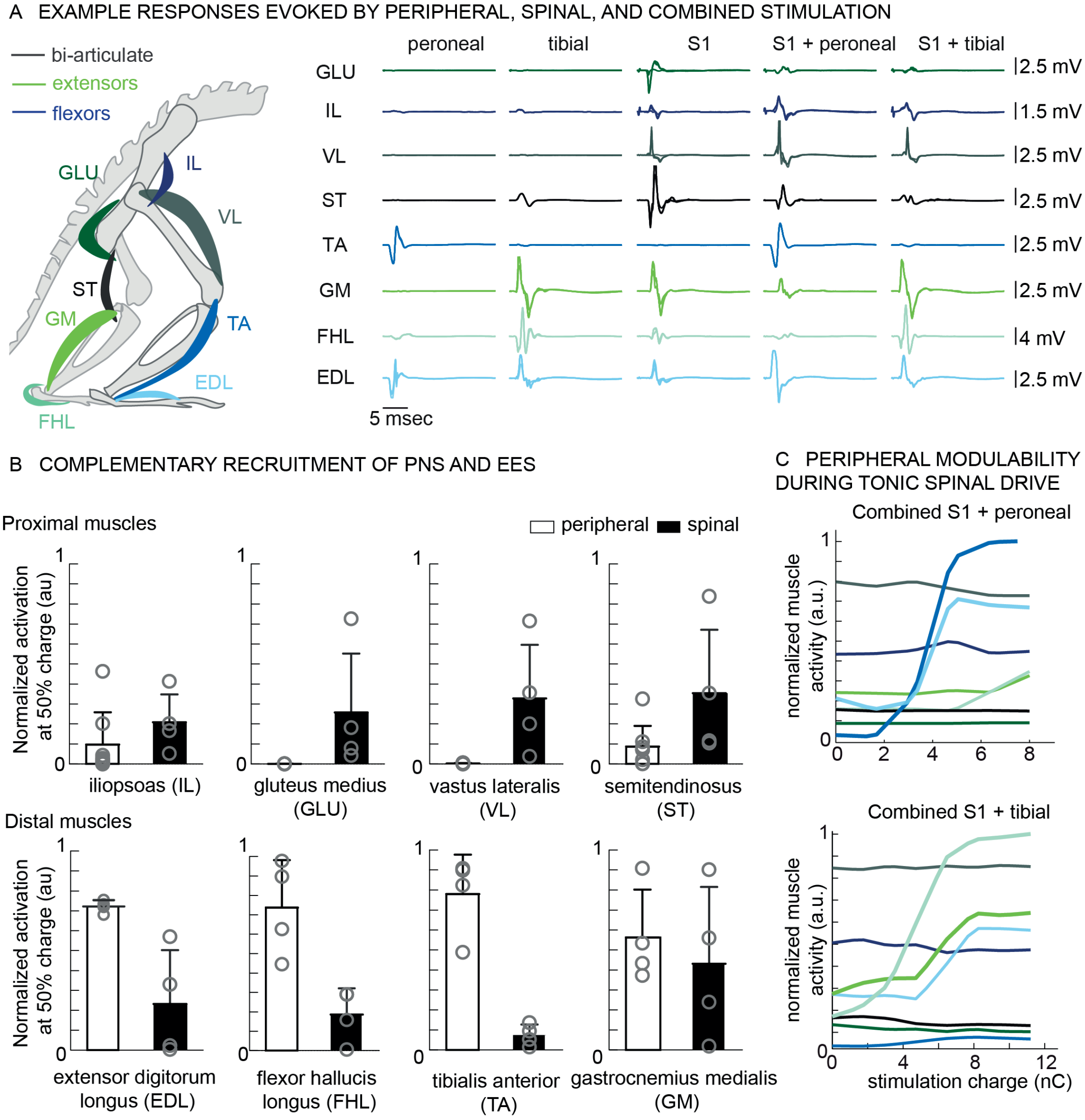

Figure 3.9 – (A) Sketch of rat hind-limbs illustrates the muscles that were implanted for this experiment in the left leg (distributed over the two legs for clarity of the figure). Peripheral, spinal, and combined evoked CMAPs from one representative animal. (B) Quantification of muscle recruitment by peripheral (white) and spinal (black) stimulation (n=4). (C) PNS allows to selectively modulate distal muscle activation during tonic epidural stimulation at S1 (same representative rat as in A).

Typically, at 50% of charge injection producing maximal activity in the target muscles, single pulse PNS did not induce much activity in any of the proximal muscles (IL, GLU, VL, ST), while selectively recruiting distal extensor and flexor muscles with tibial and peroneal channels respectively (GM, EDL, TA, FHL). Spinal stimulation always recruited proximal muscles and sometimes also activated distal muscles at 50% of maximal charge injection. Simultaneous delivery of peripheral and spinal stimulation allowed to recruit both distal and proximal muscles (Fig. 3.9 B). We confirmed that PNS retained its ability to selectively modulate distal muscle recruitment by performing recruitment curves stimulating conjointly the spinal cord at constant charge while increasing the delivered stimulus intensity via PNS (Fig. 3.9 C).

3.4.3 Characterization of hybrid PNS-EES neuromodulation paradigm

We hypothesized that the specificity of PNS, combined with the capacity of remaining exploitable (allowing modulation) during EES, would considerably increase functionality during neurorehabilitation after severe SCI. To test this hypothesis, we developed a hybrid PNS-EES neuromodulation paradigm and assessed its impact on locomotor performance in severely paralyzed rats during partial body-weight-supported treadmill locomotion enabled by electrochemical neuromodulation (here-after referred to as EES). We have previously shown that amplitude modulation of PNS can result in co-contraction of agonist and antagonist muscles, while PNS frequency achieved high-fidelity closed-loop control of evoked traction force (Chapter 2, section 2.4.2). Consequently, we characterized the impact of PNS frequency for flexion and extension on gait patterns obtained with the hybrid PNS-EES paradigm, and compared the performances to EES-enabled locomotion.

Initially four animals with complete spinal cord transection and four animals with severe spinal contusion injury should have participated in the characterization experiment. However, two animals with complete transection were excluded from all experiments when we realized that bilateral intraneural electrodes had been pulled from the nerve (no stimulation effect or stimulation artifact during stimulation, verified post-mortem). Of the remaining animals, we had selectivity for ankle flexion in five animals (two transected and three contused animals) and selectivity in ankle extension in five animals (one transected and four contused animals) at three weeks after implantation when experiments started. The data from both injury types is presented together as the modulation of leg kinematics was not affected by the injury type. For clarity, the data from transected animals is highlighted in bright color. Contused animals had a mean of 20.79 +- 26.69 % spared tissue at the lesion epicenter (Appendix A.2, Group 1).

Impact of PNS frequency evoking flexion responses during hybrid PNS-EES

In flexion trials, increments in PNS frequency permitted a gradual adjustments of gait patterns across animals (n=5). These gradual effects were obtained for responses localized at the ankle joint as well as for more global responses affecting multiple joints (Fig. 3.10 (a) and (b) respectively). Depending on the locomotion pattern of each animal in the EES only condition, it was not always clear from kinematics whether a reflex response or a direct response was elicited during hybrid PNS-EES mediated locomotion. Nevertheless, from EMG signals in the TA muscles, we could infer whether a direct or reflex response had been elicited, as direct ankle flexion induced increased activity in the TA muscle (Fig. 3.10 (a)), which was not necessarily the case during a reflex activation (Fig. 3.10 (b)), which had more pronounced flexion at hip and knee joints rather than the ankle. However, we did not record proximal EMG activity. In both cases, the signature obtained by the reconstruction of recorded joint kinematics and the foot trajectories in the sagittal plane illustrate the progressive changes obtained by direct and reflex responses (Fig. 3.10 (a) and Fig. 3.10 (b), top rows). The reflex response appeared to be modulated to a lesser extent (bigger difference between EES only (baseline) vs. all hybrid PNS-EES conditions than within hybrid PNS-EES conditions in reflex responses 3.10 (b)).

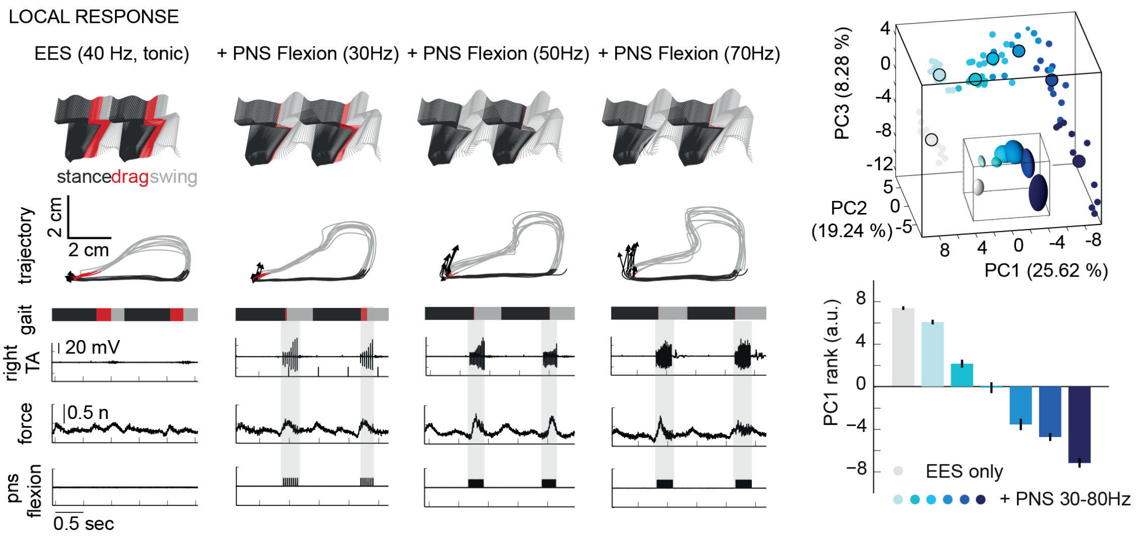

(a) Local response

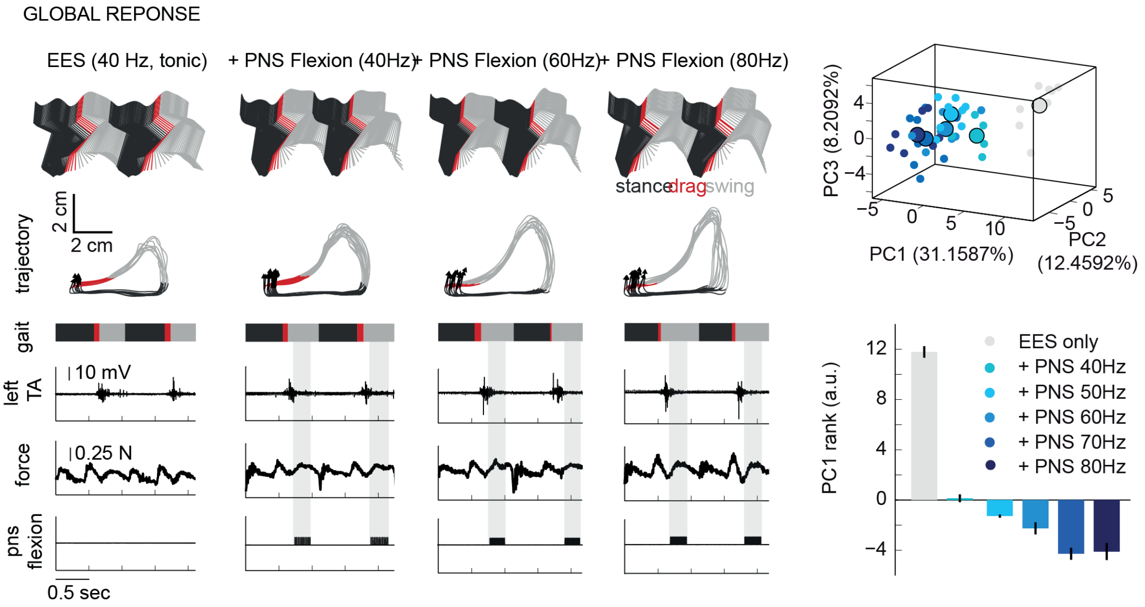

(b) Reflex response

Figure 3.10 – Characterization of hybrid PNS-EES paradigm with direct and reflex flexion responses. (a) Direct response (animal with complete spinal cord transection). (b) Reflex response (animal with severe spinal cord contusion). For (a) and (b): Left, from top to bottom row: unilateral hind-limb kinematics during two representative steps, trajectory of MTP marker over 10 steps, TA EMG signal, ground reaction forces, PNS signal. Right, top: PCA applied over 110 gait variables from 10 successive gait cycles during each condition (EES only vs hybrid PNS-EES with PNS frequency ranging from 30 to 80 Hz with a 10 Hz increment; grey to dark blue). Right, bottom: Score of each condition (mean +- sem) along the axis of PC1.

For each animal, the linearity of the responses with respect to increases in PNS frequency were well captured by projecting the data onto the axis defined by the first principal component (Fig. 3.11, left, normalized to baseline EES only, n=5). We obtained a mean R^2 of 0.8642 +- 0.0564 (mean +- standard deviation) when fitting a line to the data of each animal. Across animals, factor loading on PC1 revealed that the foot elevation angle and ankle joint angle were robustly modulated as function of PNS frequency during flexion trials (Fig. 3.11 middle and right respectively). The differences between group medians were significant (matched observation ANOVA, $p < 0.0001$). We used Bonferroni's multiple comparison ad-hoc test to perform pairwise comparisons between groups (Fig. 3.11).

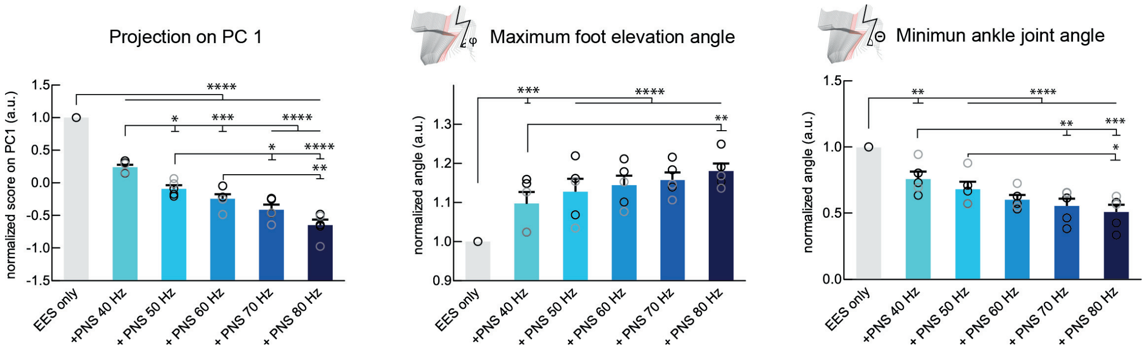

Figure 3.11 – Hybrid PNS-EES paradigm gradually adjusts distal kinematics (n=5). Left: Projections onto axis defined by PC1 after PCA. Middle: Foot elevation angle. Right: Ankle joint angle. Data presented as mean + sem as well as individual data points per animal (each data point represents the mean value of this variable over 10 consecutive steps). * $p<0.05$, ** $p<0.01$, *** $p<0.001$, **** $p<0.0001$ for pairwise comparisons using Bonferroni's ad hoc test.

Impact of PNS frequency evoking extension responses during hybrid PNS-EES

We similarly characterized the impact of hybrid PNS-EES neuromodulation using PNS evoking extensor movements during the last third of the stance phase. For each animal, we observed gradual effects of PNS frequency on specific variables defining gait patterns. Fig. 3.12 shows how leg kinematics and foot trajectories were gradually modulated as PNS frequency increased.

We captured the trend for gradual adjustments with PNS frequency across animals (n=5) in the projections of the data from each animal onto their respective PC1 (Fig. 3.13). The linearity of the data was confirmed by linear regression (mean R^2 across animals 0.8074 +- 0.099). Group medians were significantly different ($p < 0.001$) and Bonferroni's post-hoc multiple comparison's test was used to assess pairwise differences between all conditions (Fig. 3.13).

Despite the linearity obtained as function of the PNS frequency and thus, the controllability of PNS enhancing extension (Fig. 3.13), the affected variables differed from animal to animal as extensions that were elicited produced different effects (for instance ankle extension, distal toe plantar flexion or foot inversion). In some animals we observed an increased step-height on the stimulated leg that was modulated with PNS frequency, while in other animals the frequency modulated foot velocity, stepping path, or foot elevation angle. Representative kinematic variables affected for each animal are shown in Appendix A.3.

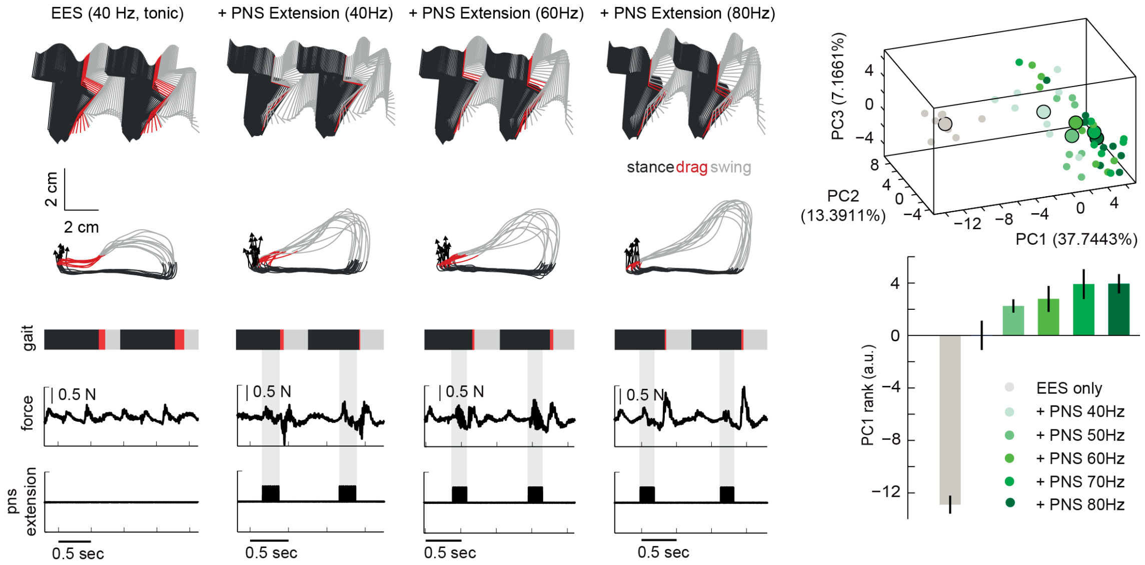

Figure 3.12 – Characterization of hybrid PNS-EES paradigm with extension responses. Left, from top to bottom row: unilateral hind-limb kinematics during two representative steps, trajectory of MTP marker over 10 steps, ground reaction forces, PNS signal. Right, top: PCA applied over 110 related gait variables from 10 successive gait cycles in each condition (EES only vs hybrid PNS-EES with PNS frequency ranging from 40 to 80 Hz (10 Hz increment); grey to dark green). Right, bottom: Score of each condition along the axis of PC1. Data presented as mean +- sem over 10 consecutive steps.

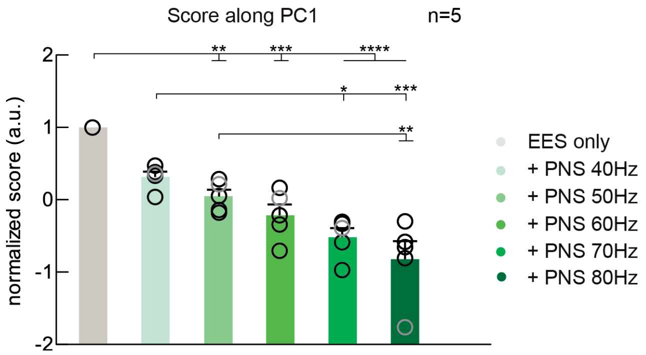

Figure 3.13 – Hybrid PNS-EES paradigm adjusts kinematics through enhanced extension. Differences are captured by projecting the data from each animal per condition (mean over 10 consecutive steps) onto their respective PC1 axis. * $p<0.05$, ** $p<0.01$, *** $p<0.001$, **** $p<0.0001$, Bonferroni's multiple comparison test. n=5. Light grey circles indicate completely transected, black severely contused animals.

3.4.4 Refined locomotion during treadmill and over-ground stepping using the hybrid PNS-EES neuroprosthesis

We used the hybrid PNS-EES paradigm to address specific gait features with the aim of increasing functionality. The second group of severely contused animals participated in these functional experiments (mean of 14.6 +- 4.46 % spared tissue at the lesion epicenter (Appendix A.2, Group 2)) and were trained for treadmill and over-ground locomotion (n=5). We leveraged the capacity to locally adjust leg kinematics to refine locomotor patterns by reducing foot dragging, to surpass obstacles by increasing step height, or to provide bilateral assistance during the stance phase to sustain locomotion and avoid collapse.

Refined locomotion through reduced foot dragging

The control over ankle and foot kinematics using PNS eliciting flexion had the potential to refine locomotion by reducing foot dragging at the onset of the swing phase. To assess this functionality, we built a control policy that controlled the delivery of PNS for flexion based on the detection of foot dragging in real time (Fig. 3.14 top). The experiment was performed during treadmill locomotion and PNS was delivered at a frequency of 60 Hz to all animals.

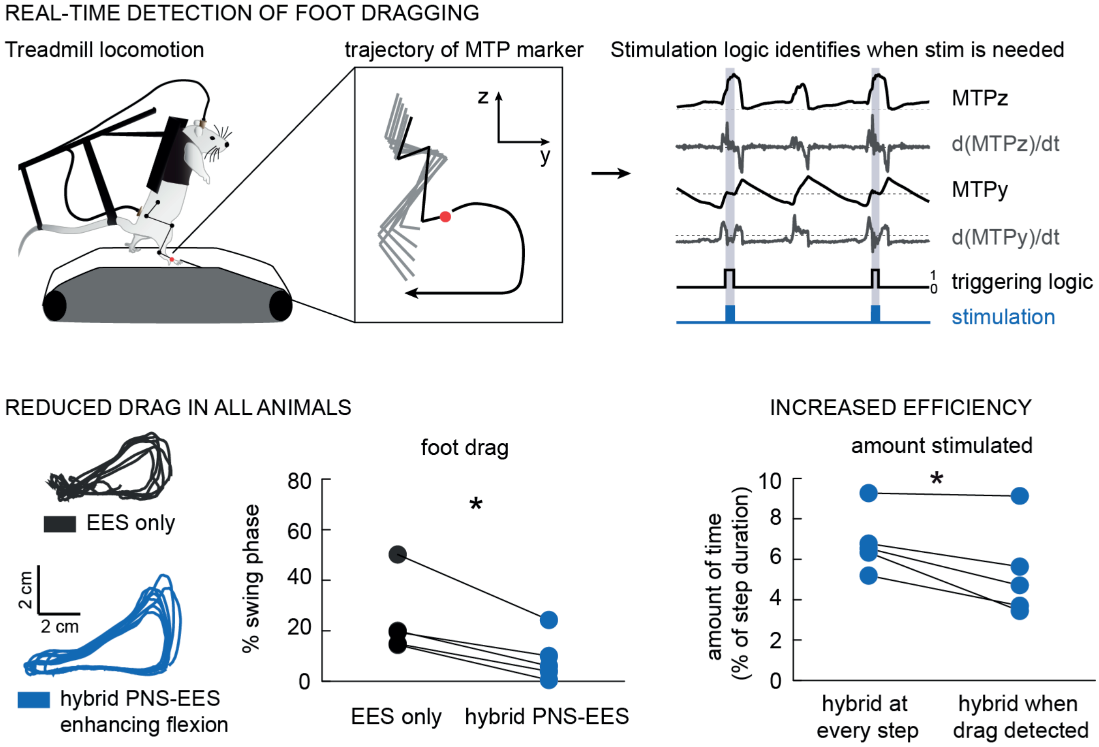

Figure 3.14 – Hybrid PNS-EES paradigm reduces foot dragging in real-time. Top: Control policies were based on the position and velocity components of the MTP marker in Y and Z directions. Bottom: Example of foot trajectories during EES only vs. hybrid PNS-EES stimulation paradigm. The stimulation strategy significantly reduced dragging in all animals and required significantly less stimulation time than stimulating at every step. * $p<0.05$, paired t-test.

This strategy significantly reduced dragging across animals ($p < 0.05$, paired t-test). Furthermore, it proved to be a significantly more ecological stimulation strategy when compared to stimulating at every step ($n = 5$, $p < 0.05$ (paired t-test) across animals), despite the fact that in one animal the amount of stimulation was not reduced because this animal was dragging at every step and thus needed assistance at every step.

Assisting locomotion over-ground

To illustrate that refined locomotion also benefits over-ground locomotion, we positioned the animals in a robotic interface that accompanied them during bipedal over-ground walking while providing assistance in the the vertical direction for body weight support. In this paradigm, hybrid PNS-EES stimulation enhancing flexion enabled an increased step height and walking speed, while reducing foot drag ($n = 3$ animals, Fig. 3.15, top). We then leveraged the increased functionality and used the hybrid PNS-EES neuroprosthetic system to facilitate surpassing obstacles. For this, we triggered PNS eliciting flexion when the target foot was within a distance of one to two cm from a stair (Fig. 3.15, bottom). We quantified the rate of successful, tumbling and failing steps in the EES only vs. the hybrid PNS-EES condition. The hybrid PNS-EES paradigm enabled higher success rate across animals.

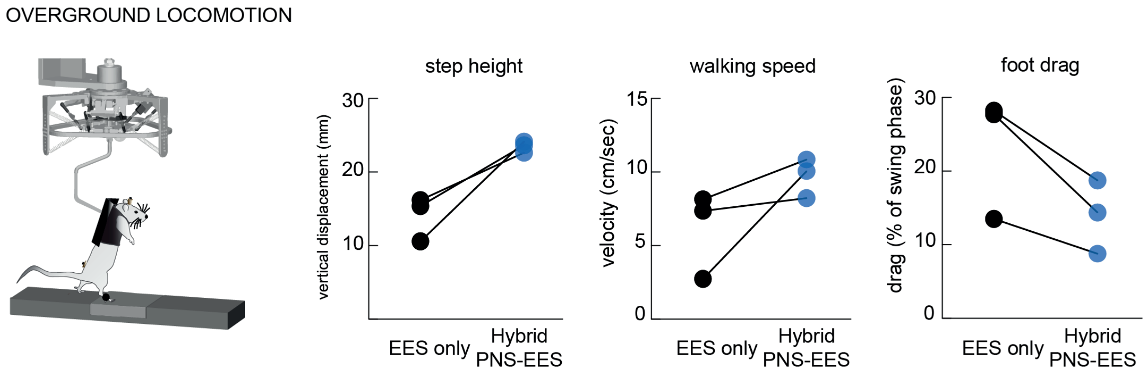

(a) Over-ground locomotion

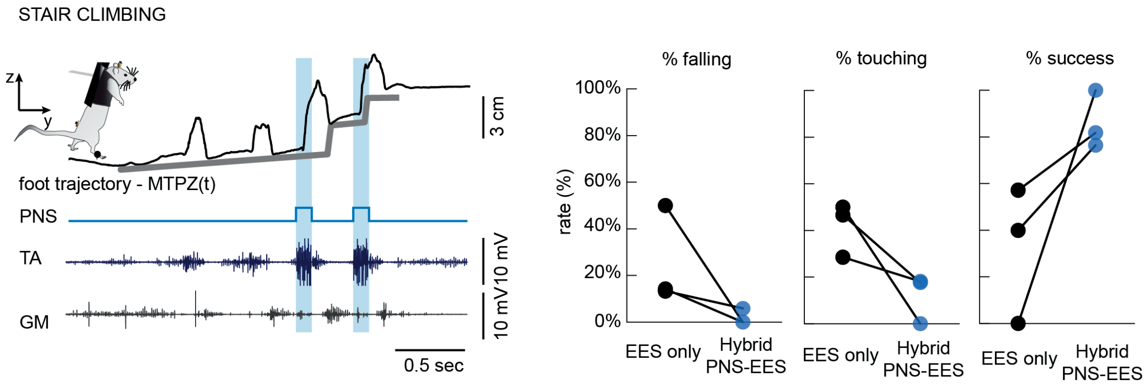

(b) Stair climbing

Figure 3.15 – Hybrid PNS-EES paradigm enhances function over-ground. (a) Increased step height and walking speed and decreased foot dragging during locomotion over-ground through the hybrid PNS-EES paradigm (n=3). (b) Example trial of hybrid PNS-EES mediating stair climbing. Reduced falling and tumbling rate and increased success-rate with the hybrid PNS-EES when compared to EES only (n=3).

Sustaining locomotion to avoid collapse

To illustrate how enhanced extension could assist sustaining locomotion, we pursued a treadmill training session until an animal was close to collapsing (45 minutes). We then used the hybrid PNS-EES paradigm to provide assistance during the end of the stance phase by facilitating bilateral extension to push the feet from the ground.

The reconstructed kinematics illustrate how consistent and clean stepping patterns could be recovered immediately (Fig. 3.16 (a)). When the hybrid PNS-EES paradigm was switched off, the animal was not able to sustain its body weight anymore and collapsed after a few steps. During hybrid PNS-EES, the foot trajectories were consistent (Fig. 3.16 (b) top) and permitted higher steps without dragging (Fig. 3.16 (b) bottom).

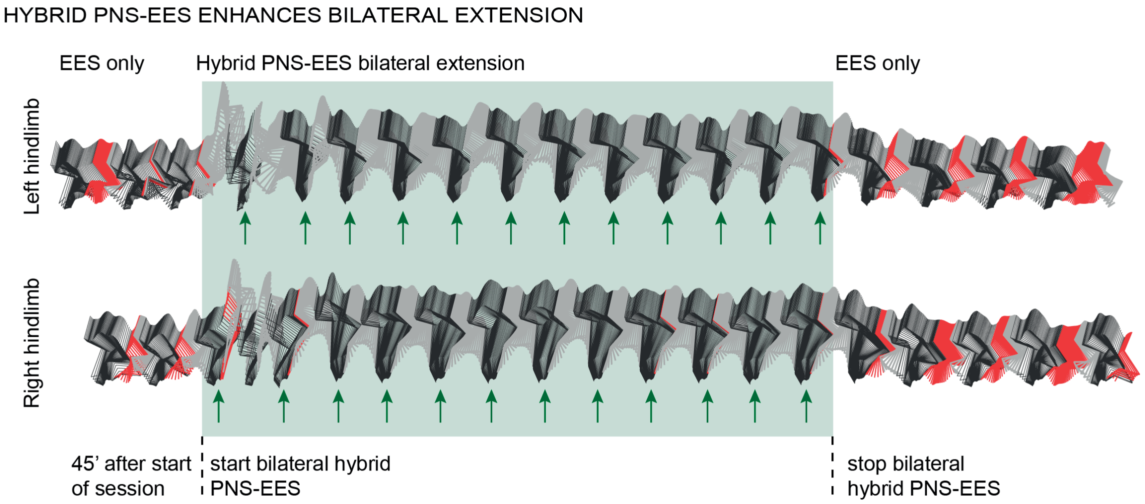

(a) Stick diagram of left and right hind limbs illustrate collapse avoidance through hybrid PNS-EES

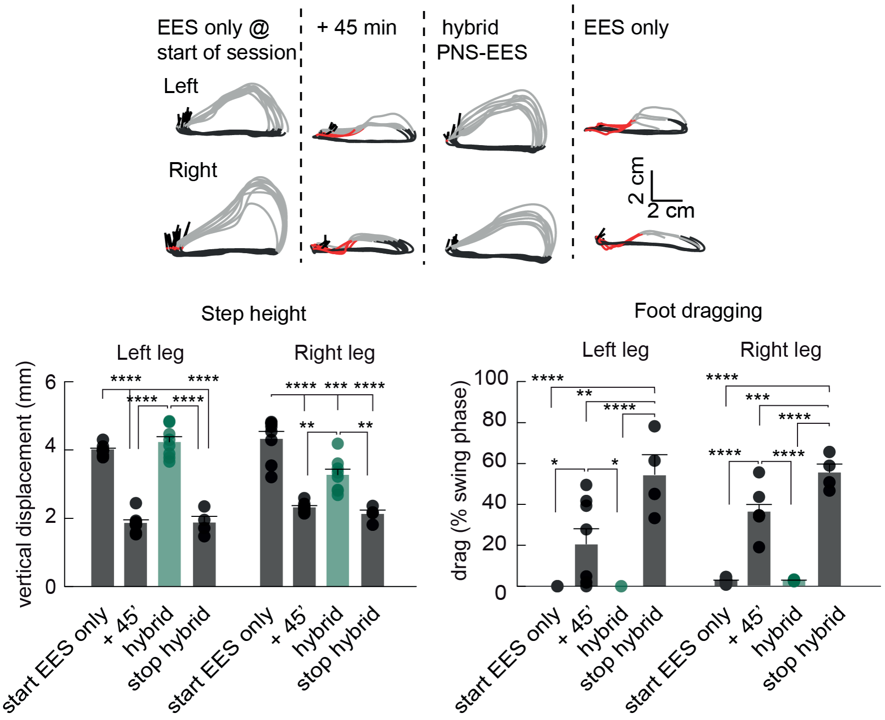

(b) Foot trajectories, step height, and dragging

Figure 3.16 – Hybrid PNS-EES enhancing bilateral extension maintains locomotion performance and avoids collapsing. (a) Reconstructed left (top) and right (bottom) hind-limb kinematics. (b) Hybrid PNS-EES permits increased step height and reduced dragging (ANOVA, followed by pairwise comparisons using Bonferroni's post-hoc test. *p<0.05,**p<0.01,***p<0.001,****p<0.0001).

3.4.5 Bio-integration of stimulating intraneural implants

To assess bio-integration we stained nerve sections from the contused animals that had participated in the chronic experiments with Hematoxylin & Eosin, Sirius Red, and immunohistochemically labelled against macrophage marker CD68. Albeit different experimental paradigms, and histology procedures performed at different time-points, we present this quantification alongside the data we had obtained in chapter 2 to provide a reference for interpretation.

Implant encapsulation On Sirius Red and Hematoxylin & Eosin stained sections, we observed a layer of multi-nucleated giant cells tightly adhering to the implant within the nerve (Fig. 3.17 top and inset, yellow, multi-nucelated layer around implant).

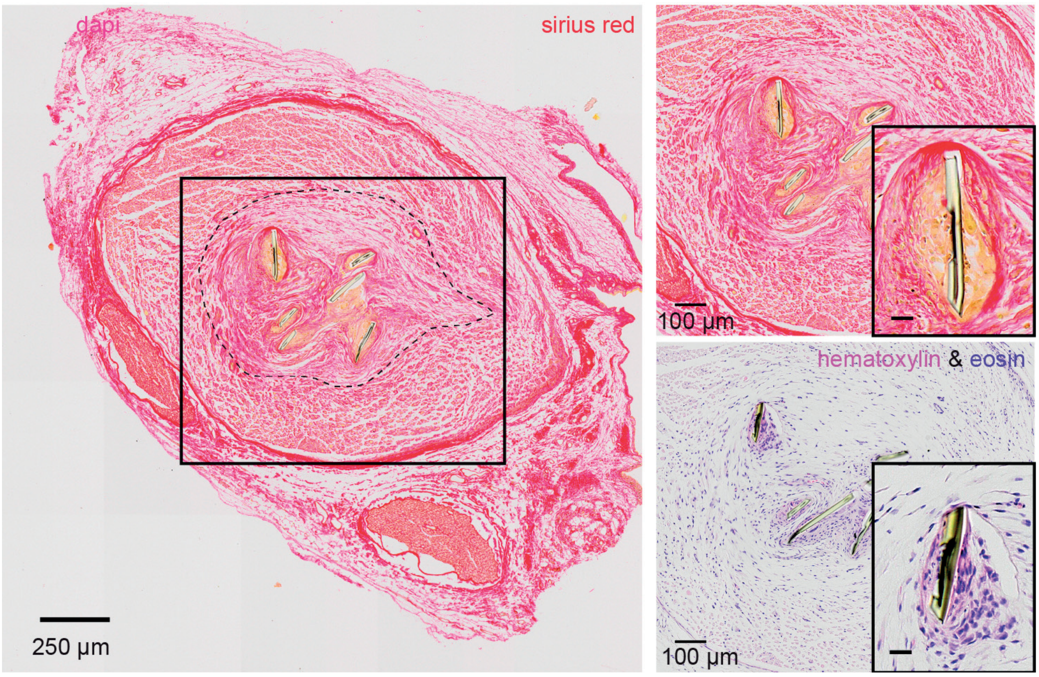

(a) Cross-section of implanted nerve stained with Sirius Red and Hematoxylin & Eosin (inset).

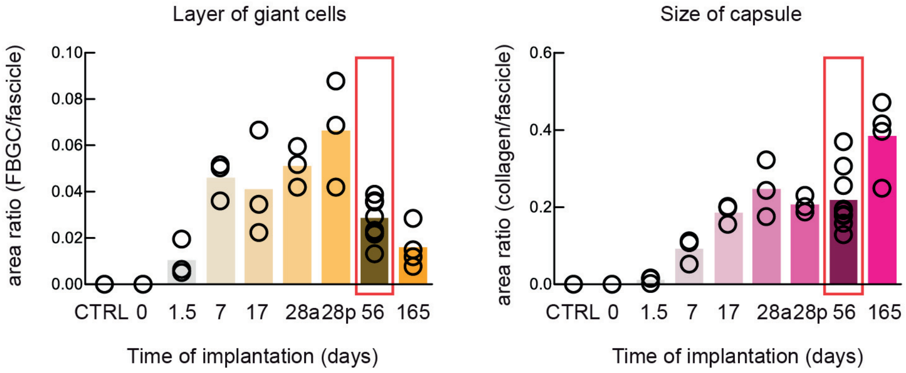

(b) Quantification of layer of giant cells and capsule size.

Figure 3.17 – Bio-integration of stimulating intraneural implants. (a) Implanted sciatic nerve cross-section stained with Sirius Red with the tibial fascicle containing the implant. Dashed line marks capsule. Inset shows layer of epitheliod giant cells adhering to the polyimide (yellow cytoplasmic structure). Inset from Hematoxylin & Eosin from adjacent section visualizes accumulation of cell nuclei. Scale bar on small insets is 25 µm. (b) Quantification of the extent of the layer of multi-nucleated giant cells (left) and the capsule (right) that formed around the implant. Red square indicates data from this study.

Around the implant and this layer, we observed an enlarged capsule (Fig. 3.17, indicated by black dotted line) that had a different aspect than adjacent tissue populated by fibers, mainly through longitudinally arranged fibrils (presumably collagen) and high amounts of cell nuclei. We measured the extent of the layer as well as the extent of the capsule and compared it to the results we had obtained in our previous study (Chapter 2). Two months post implantation (56 days) the layer of multi-nucleated giant cells was considerably reduced when compared to a month earlier (28 days). The size of the capsule around the implant had an average size similar to the one at one month post-implantation (Fig. 3.17 bottom).

Inflammatory response We measured the inflammatory response to daily and intensely used intraneural stimulating implants on nerve cross-sections immunohistochemically labelled against macrophage marker CD68 (Fig. 3.18 (a)).

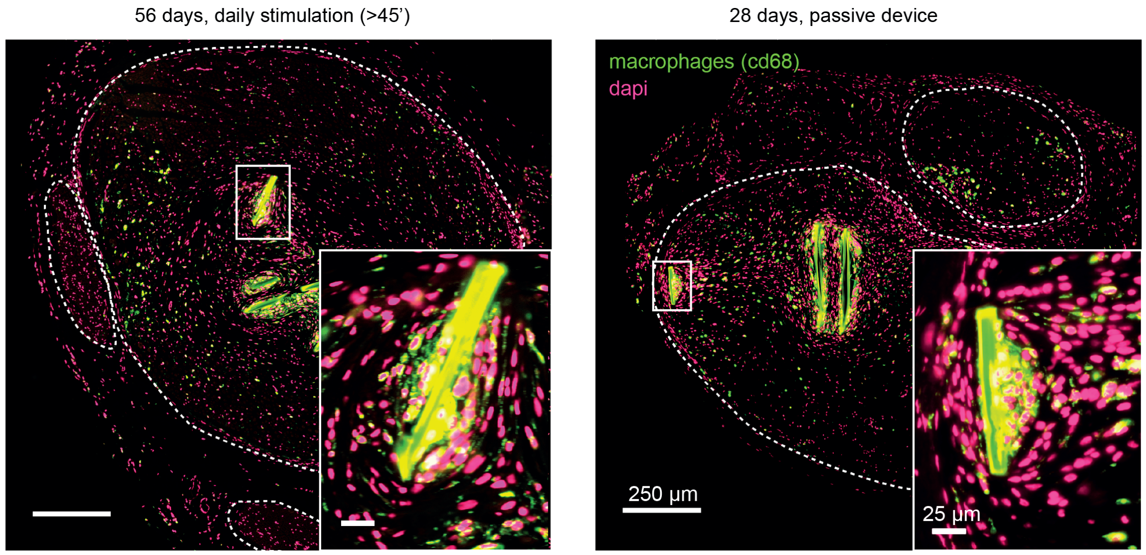

(a) Presence of inflammation at 56 days post implantation, daily used implant (left) and at 28 days post implantation, passive implant (right)

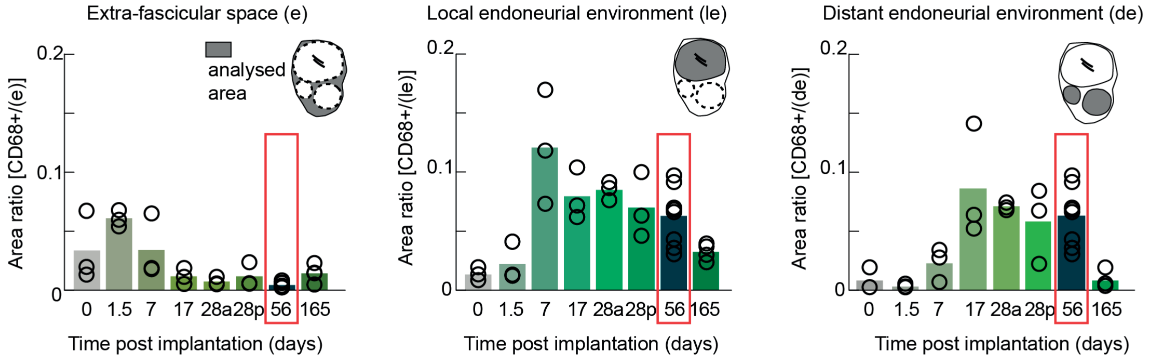

(b) Quantification of inflammatory response in nerve compartments of interest

Figure 3.18 – Inflammatory response to stimulating intraneural implants. (a) Left: Section from nerve implanted with an actively used electrode during 56 days. Right: For comparison, section from nerve implanted with a passive electrode during 28 days (unpublished image from the group P28p in Chapter 2). (b) Quantification of the presence of stained tissue in different nerve compartments. Red square indicates data from this study.

The inflammation was quantified in three nerve compartments of interest, namely the extra-fascicular space, the local endoneurial environment (fascicle in which the implant is visible on section used for quantification), and the distant endoneurial environment (other fascicles) (Fig. 3.18, bottom). At 56 days post-implantation of actively used implants, we found very little presence of inflammation in the extra-fascicular space as well as in the distant endoneurial environment. The presence of macrophages in the local endoneurial environment was substantially higher. Marked presence of CD68 positive tissue was found in close contact with the implant, locally coinciding with cell nuclei (revealed with dapi). This accumulation of CD68 positive tissue and cell nuclei confirm the cluster of multi-nucleated giant cells observed on sections stained with Sirius Red (yellow layer). For comparison, Fig. 3.18 (a) shows a nerve section of a completely passive implant that was implanted for one month and equally labelled with CD68 and dapi (unpublished image, data belonging to group P28p (passive) of the study presented in Chapter 2). Both the accumulation of cell nuclei around the implant and the macrophages dispersed through the fascicle resembled the response to actively used electrodes implanted during two months (Fig 3.18, top left).

3.4.6 Hybrid peripheral-spinal neuroprosthesis refines gait in individual with SCI

We assessed the direct functional benefits of the hybrid peripheral-spinal neuromodulation in a human SCI ASIA-C subject. To facilitate the left swing phase during locomotion, we positioned two surface electrodes on his the lateral lower leg. A spinal reflex (hip, knee, and ankle flexion) was obtained by a pulse train with pulses of 36 mA (six times threshold) and 0.5 msec pulse width at 100 Hz.

Hybrid PNS-EES refined locomotion on the treadmill

On the treadmill, the subject had 40% of body weight support in the vertical direction and 4 kg were applied in the forward direction for optimal locomotion. He was wearing ankle sneakers to provide ankle stability. One representative step in each condition is illustrated by the sequences of snapshots extracted from video recordings (Fig. 3.19).

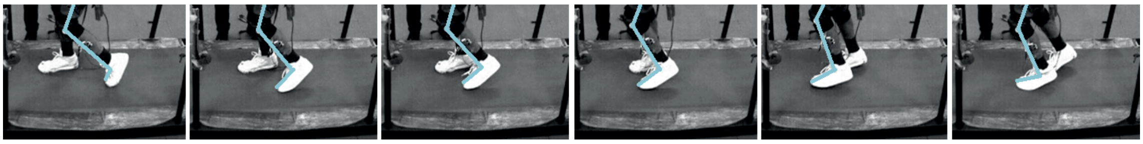

(a) Sequence of snapshots during one step with PNS only

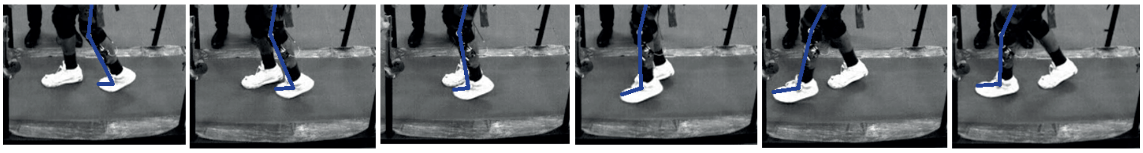

(b) Sequence of snapshots during one step with EES only

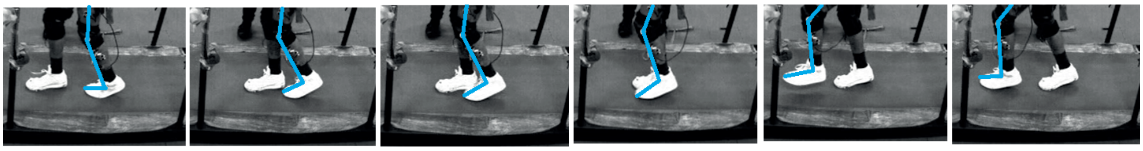

(c) Sequence of snapshots during one step with hybrid PNS-EES

Figure 3.19 – Snapshots extracted from video recordings showing a sequence of leg movements during (a) PNS only, (b) EES only, and (c) hybrid PNS-EES.

Using PNS only, the subject was not able to sustain locomotion and had to provide additional support with his arms on the side-racks of the treadmill. During the EES only condition, the subject touched the left side bar during the onset of the left swing phase. During the hybrid PNS-EES condition, the subject walked freely without holding the side-racks.

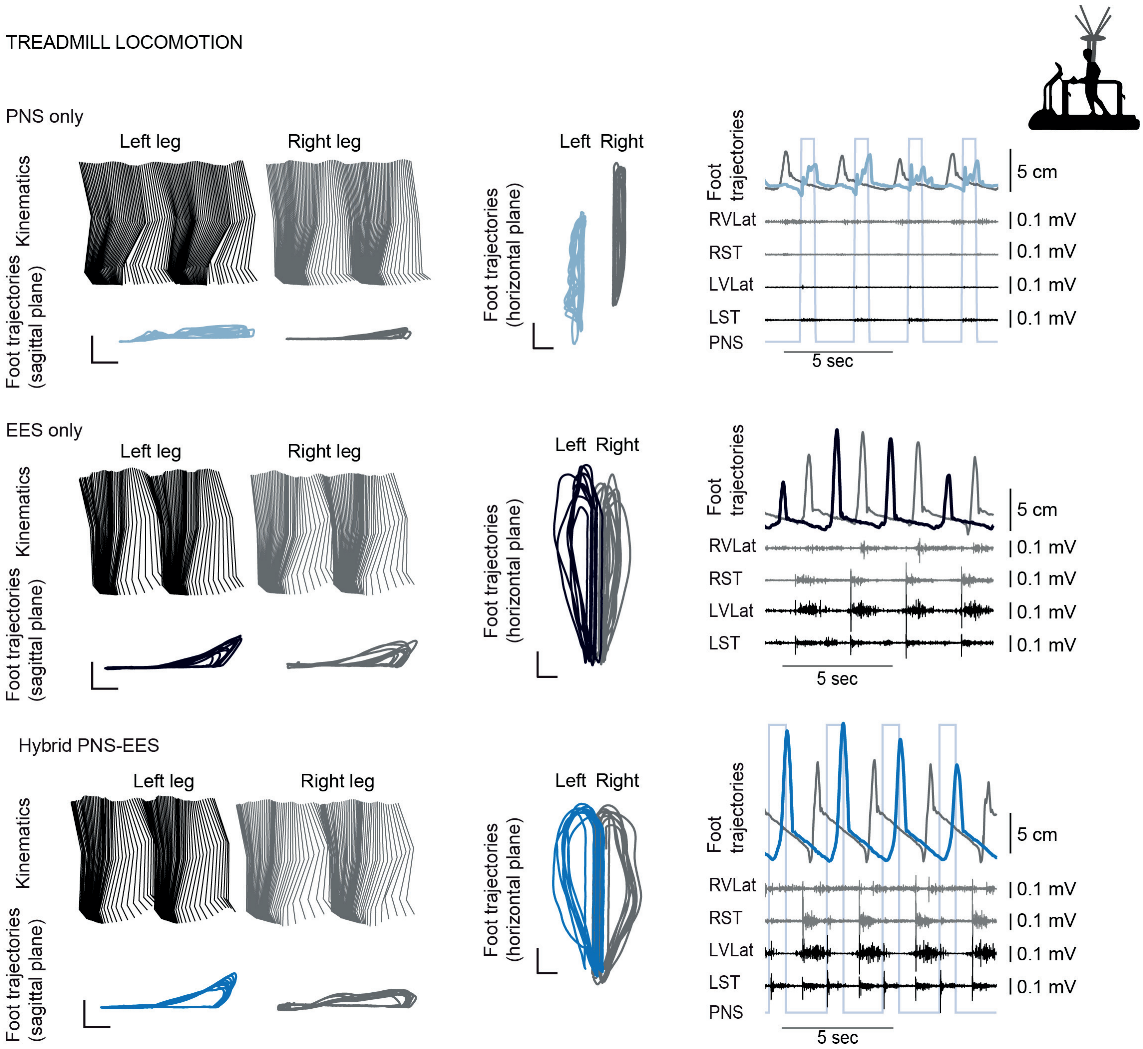

Figure 3.20 – Gait pattern of human subject under conditions PNS only (top row, light blue), EES only (middle row, dark blue), and hybrid PNS-EES (bottom row, flash blue). All scale bars represent 10 cm, unless otherwise specified on the figure. Shaded grey areas overlaid to the foot trajectories of left and right legs (right) represent the time during which PNS was delivered.

In spite of those differences in using additional support, the reconstruction of leg kinematics and foot trajectories clearly differentiated the three conditions (Fig. 3.20). The hybrid PNS-EES strategy restored symmetrical, consistent leg movements at high stepping amplitudes. This was verified by measuring proximal muscle activity (distal muscle signals were completely corrupted by the PNS stimulation artifact) as well as joint and limb angles, and by computing step height and foot drag as means to evaluate the gait (Fig. 3.21). In particular, muscle activity in left and right vastus lateralis (knee extensor) and semitendinosus (knee flexor and hip extensor) was lowest in the PNS condition and highest in the hybrid PNS-EES condition ($p<0.0001$, ANOVA and Bonferroni's post hoc test, (Fig. 3.21, left).

We observed similar trends in left (top row) and right (bottom row) joint and limb angles (Fig. 3.21, middle).

More precisely, on the left leg, PNS only strongly modulated the ankle joint angle through the induced flexion (light blue trace, Fig. 3.21, "Left ankle joint angle"). At the same time it caused a strong outward rotation during the swing phase (negative deflection in bright blue trace, Fig. 3.21, "Left foot rotation angle"). EES only did not modulate the left ankle joint angle (relatively flat dark blue trace in Fig. 3.21, "Left ankle joint angle") and caused an inward rotation of the left foot during lift-off (upwards excursion in the dark blue trace in Fig. 3.21, "Left foot rotation angle"). The hybrid PNS-EES paradigm (flash blue traces) modulated the left ankle joint angle as well as the foot rotation but to a more moderate (less exaggerated) extent, and without offset, when compared to the PNS only condition (light blue).

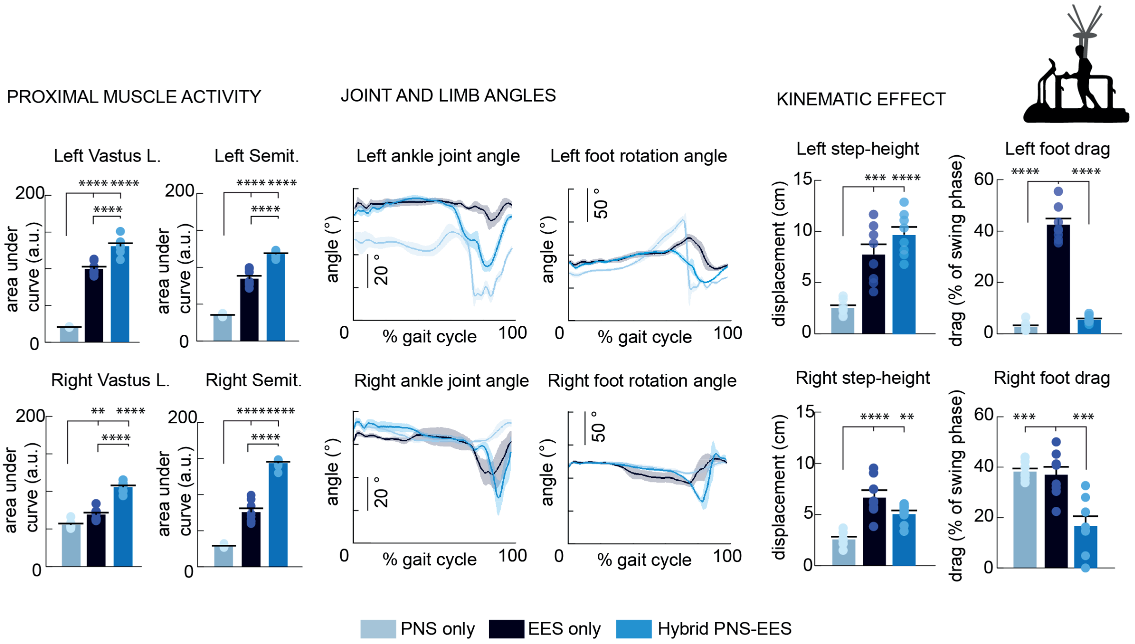

Figure 3.21 – Hybrid PNS-EES refines locomotion in human SCI subject on the treadmill. PNS was applied on the left leg. Left: EMG activity in Left (top) and right (bottom) vastus lateralis and semitensinosus muscles. Middle: Left (top) and right (bottom) ankle joint and foot elevation angles. Right: Step height and foot dragging measure benefits obtained with the hybrid PNS-EES stimulation paradigm. Right: Evolution of ankle joint angle and foot rotation angle during gait cycle shows refined angular excursions through PNS. Points represent data for individual steps (n=10 per condition). Bars are mean +- sem across the 10 steps for each condition. ** p<0.01, *** p<0.001, ****p<0.0001, Bonferroni's post-hoc test for pairwise comparisons between all groups.

As anticipated, on the right leg (bottom row), PNS only (light blue traces) produced very minimal modulation in ankle joint and foot rotation angles as the stimulation was delivered on the left leg. Similarly to muscle activity in the right leg, the hybrid PNS-EES also seemed to enhance right ankle flexion when compared to EES only (flash blue trace, Fig. 3.21, "Left ankle joint angle") , and similarly caused a right foot rotation in the opposite direction than during EES only (flash blue trace, Fig. 3.21, "Left foot rotation angle"). The functional impact of those modulations was measured by computing step height and foot dragging in both legs (Fig. 3.21, right). We found that on both legs, the PNS only condition generated the lowest step height while there was no significant difference between the step heights in the EES vs. the hybrid PNS-EES condition. Foot dragging on the left (stimulated leg) was significantly higher in the EES-only condition when compared to PNS only and hybrid PNS-EES. On the right (non-stimulated) leg, there was a significantly smaller amount of foot dragging in the hybrid PNS-EES condition than in the EES only or in the PNS only condition. These results show the striking impact on the targeted leg and demonstrate the advantage of combining PNS and EES into a common stimulation strategy, leveraging the benefits of both EES and PNS (here shown by increased step height and reduced foot dragging).

Hybrid PNS-EES refined locomotion over-ground

During over-ground locomotion between parallel bars, the subject had 10 % of body weight support in the vertical direction and no force was applied in forward or backward direction. The subject was wearing normal sports shoes that did not provide any stability to the ankle. In this very challenging condition, he kept his hands on the bars during every condition, both for stabilization and for compensation.

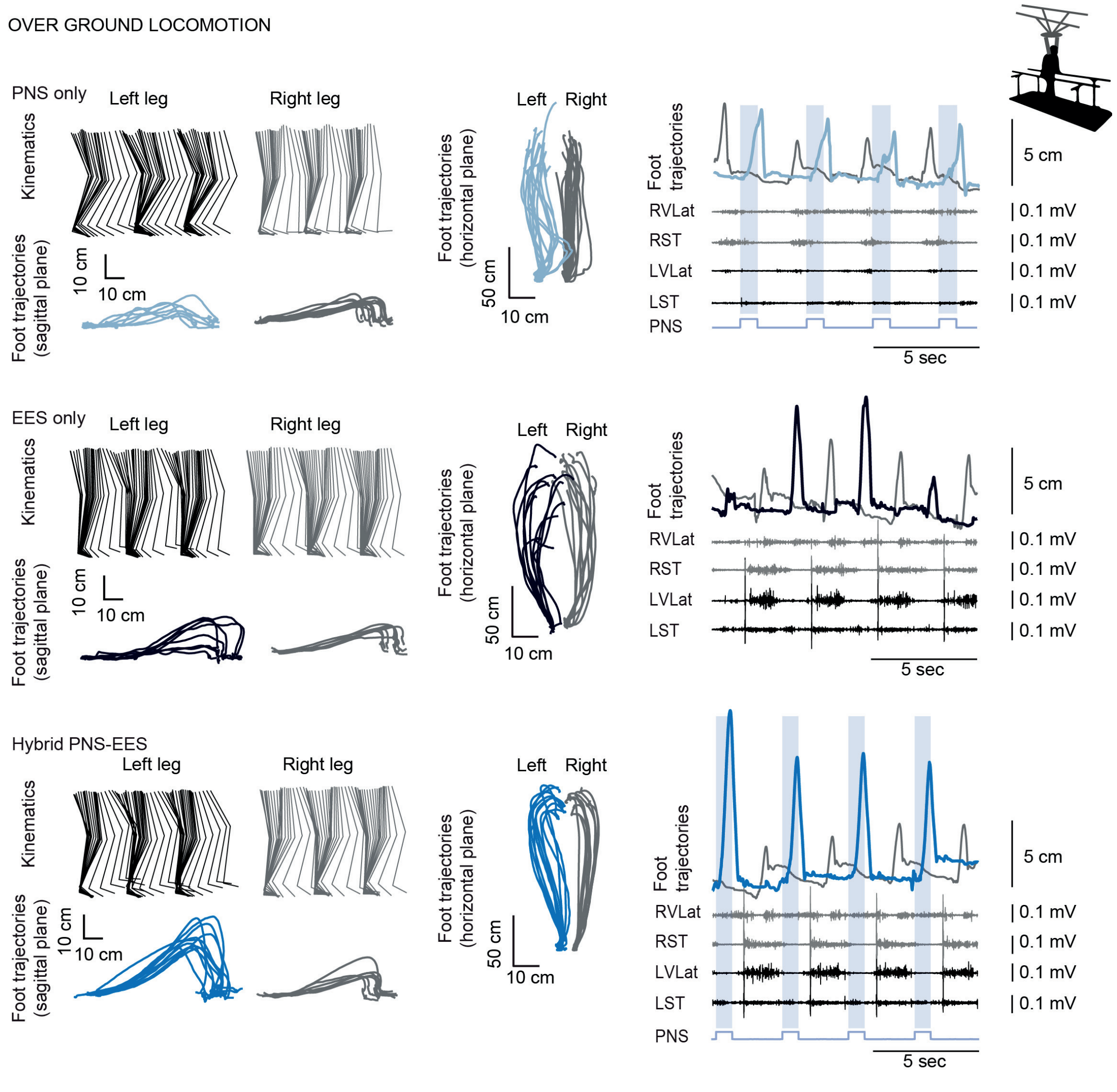

Figure 3.22 – Gait pattern of human subject under conditions PNS only (top row, light blue), EES only (middle row, dark blue), and hybrid PNS-EES (bottom row, flash blue). Shaded grey areas overlaid to the foot trajectories of left and right legs during 10 steps represent the time during which PNS was delivered.

This constraint biased muscle activation (less load) and foot drag (no drag in either condition due to uplifting of the body with the arms). Nevertheless, clear differences were observed from the measured foot trajectories between the three conditions on the left (stimulated) leg (Fig. 3.22). The right (non stimulated) leg seemed unaffected.

More precisely, we observed modulation of the left ankle joint angle during conditions PNS only and hybrid PNS-EES, but not during EES only (Fig. 3.23, left). Similarly as in on the treadmill, hybrid PNS-EES prevented the inward foot rotation that was visible during EES only at lift-off. On the right side, during the PNS only condition, the ankle joint angle was even modulated to a lesser extent than during both conditions containing EES, but as before, this was expected since no stimulation occurred at all on the right leg during the PNS only. Foot rotation was not affected on the right side. Functionally, this translated into an significantly increased step height during the hybrid PNS-EES condition on the left leg (Fig. 3.23, right).

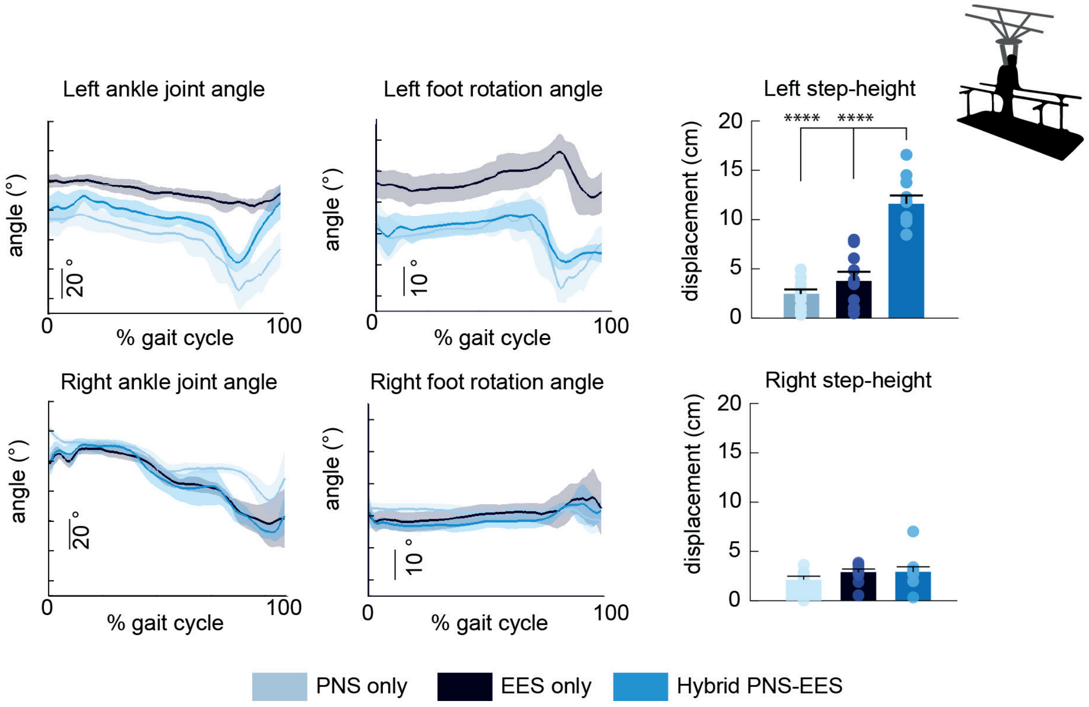

Figure 3.23 – Hybrid PNS-EES refines locomotion in human SCI subject during over-ground stepping. Left: Evolution of ankle joint angle and foot rotation angle during gait cycle shows refined angular excursions through PNS. Right: Step height measures benefits obtained with the hybrid PNS-EES stimulation paradigm. Points represent data for individual steps (n=10 per condition). Bars represent mean +- sem across the 10 steps for each condition. ****$p<0.0001$, Bonferroni's post-hoc test for pairwise comparisons between all groups.

3.5 Discussion

Several studies have reviewed and compared electrical stimulation strategies targeting the peripheral neuromuscular system vs. the spinal cord in the framework of restorative neurology after paralysis [196, 197, 198, 10]. The complementarity of the two strategies however has not been inferred. Here, we developed and characterized a hybrid neuromodulation paradigm that electrically stimulated the spinal cord and the peripheral nerves after severe SCI in rats. We demonstrated complementary muscle recruitment with the hybrid PNS-EES stimulation paradigm that permitted highly controllable refinement of locomotion patterns. We confirmed the hybrid PNS-EES mediated increased functionality in a pilot experiment with a human spinal cord injured subject using surface PNS and showed similar improvements in leg movements during locomotion. We critically discuss our findings with respect to functional impact, neurophysiological considerations, and importance for clinical applications.

3.5.1 Direct and reflex responses evoked by intraneural PNS

We observed the generation of selective single-joint movements as well as multi-joint reflex movements when stimulating the sciatic nerve intra-neurally, both during light sedation at rest (Dorbene, Graeub, DE, 0.0025 - 0.005 ml/kg, animals remained responsive to noise and touch but didn't move) as well as during electrochemically enabled locomotion, putting the spinal cord into a highly alert state. The intraneural implant was inserted 3 to 5 mm above the separation of peroneal and tibial fascicles. At this level, only fibers relating to the distal ankle and foot muscles remain, while fibers innervating more proximal muscles branched off [199]. The generation of knee and hip flexion during the reflex response can thus have two possible origins. One possibility could be that intraneural PNS elicits the flexor withdrawal reflex, a multi-joint response already described by Sherrington in 1910 [18]. Flexor withdrawal reflexes can be generated by noxious stimuli that are carried to the spinal cord via Aδ or C-type fibers carrying both information about pain. Both C-type fibers and Aδ fibers have small diameters (< 3 µm), Aδ fibers are thinly myelinated while C-type fibers carry no myelin. In light of these considerations, the electrical excitation of these fibers via intraneural stimulation would require large amounts of current that would i) very certainly recruit a vast amount of motor and other sensory fibers along, and ii) be painful. We did not observe reactions to pain in our animals, neither in the lightly sedated state, nor during locomotion. In the experiments under light sedation, albeit light and leaving animals responsive, the sedation used could have impacted their sensation. In paralyzed animals, the SCI should have prevented the conscious sensation of such a pain. Consequently, even though unlikely to electrically recruit pain fibers intra-neurally, we cannot completely exclude the nociceptive withdrawal reflex being the origin. An alternative explanation could be that the evoked reflex activates heteronymous but close synergist muscles [195, 200, 201, 202, 203]. These reflexes are mediated by group Ia proprioceptive afferents, which are much more likely to be excited electrically than Aδ or C-type fibers. Albeit different conduction velocities, the small size of the rat model makes a differentiation between response latencies unlikely. While the exact determination of the origin of those reflex responses was out of the scope of the present work, its investigation would provide valuable information for understanding precisely the interaction between peripheral and spinal electrical stimulation.

3.5.2 PNS permits selective and controllable activation of distal muscles during locomotion

A number of studies have demonstrated the selectivity of intraneural PNS to provide control over specific muscle activation in anesthetized animal models [204, 101, 122, 143, 205, 190]. Here, we show the controllability of selective movements (extension and flexion) across response types (direct or reflex) during EES-mediated locomotion of otherwise paralyzed rats. Extension- and flexion-mediated gradual adjustments in hind-limb kinematics were obtained through the modulation of stimulation frequency when stimulating the sciatic nerve through active sites located in the tibial and peroneal branches respectively. Both extension and flexion enhanced the leg movements enabled through EES. While the impact of flexion and its modulation by frequency were consistent across animals, extension affected different gait characteristics in each animal because the induced movements varied to a larger extent than in flexion and could not be captured by unique gait features such as step height or ankle joint angle. The tibial fascicle (extensor muscles) of the sciatic nerve is populated by fibers from more muscles than the peroneal fascicle (flexor muscles) and the ratio of their respective diameter is about 2:1 [199]. The exact position of the active sites of the intra-fascicular implant inside the tibial fascicle is thus of higher importance than in the peroneal fascicle to target a given muscle. We did not control the exact position of active sites inside the fascicles in this study and would anticipate difficulties in trying to achieve this precision in vivo, since the exact location of all fiber species (relating to different muscles) cannot be known with certainty before interacting electrically with the nerve. Functional mapping, using for instance microneurography needles, could potentially identify the target fibers. However, even if the intraneural electrode could be positioned to have an active site nearby, the developing capsule around the implant may push the target fibers away. Nevertheless, ankle extension could be generated across animals. In spite of the variability in the obtained movements, the linearity of the kinematic changes in response to extension frequency modulation were captured across animals (Fig. 3.13), demonstrating the controllability of intraneural PNS. In several experimental paradigms, we were able to show the functional benefits during locomotion that were obtained using PNS in combination with EES, either enhancing flexion or extension movements.

3.5.3 Synergistic interactions between PNS and EES

The combination of PNS and EES did not disrupt gait patterns or cause destabilization. On the contrary, locomotion patterns appeared more consistent using the hybrid PNS-EES paradigm, both in the rat and in the human experiments (for instance Figs. 3.12, 3.14, 3.20, and 3.22). This suggests that the effect of PNS was not only tolerated by the spinal system generating locomotion but got integrated into those networks. PNS induced single or multi-joint movements mediated by enhanced muscle contractions. In response to muscle contraction induced by PNS, the corresponding afferent fibers sent information about changes in muscle stretch and elongation back into the spinal networks. Simultaneously, EES recruited those proprioceptive afferents among many others at their entry into the spinal cord (dorsal roots) [29]. The integration of both types of information produced a coordinated and refined movement. Similarly, during PNS-evoked reflex responses, afferent information was sent into the spinal networks that in turn generated a reflex response, in accordance with the motor output generated via EES. While we do not know the precise nature of the afferent information that we induced, nor the exact mechanisms by which the spinal locomotor networks deal with this additional information on top of the general excitation provided by EES, it appeared that the well-timed and functionally appropriate PNS seemed to refine synergistic movements rather than impede them. Studies investigating the effect of flexor or extensor afferent stimulation timing on swing and stance phases during MLR-evoked fictive locomotion in cats have shown that stimulation of ankle flexor afferents during the stance phase of locomotion produced a resetting of the gait cycle, while the same stimulation during swing phase could enhance ankle flexor activity but did not alter the gait cycle [203, 206, 207]. Similarly, stimulation of ankle extensor afferents during stance phase produced an enhanced extensor activity, while stimulation during the swing phase terminated ongoing flexor activity [207, 208]. Our results are in line with these findings, even though we did not investigate whether inappropriately timed or functionally opposed PNS would permit to reproduce the results obtained during fictive locomotion.

3.5.4 Towards clinical applications

One of the major limitations of FES consists in a rapid generation of muscle fatigue. While we did not directly measure muscle fatigue at this stage, the hybrid PNS-EES paradigm has a very high potential to address this bottle neck. First, EES naturally recruits the muscles via Ia afferents, thus providing a strong and fatigue resistant backbone generating the locomotion [29]. Second, intraneural PNS permits the neutralization of the recruitment order of fibers with different diameters [89, 87, 90, 91] and could thus potentially induce less fatigue than FES. Third, if used phasically (instead of tonically), and with the aim of refining a movement rather than to produce it integrally, PNS would rather compensate for early signs of weaknesses through a complementary recruitment of muscle fibers instead of creating additional fatigue.

Our group has recently shown that employing spatio-temporal stimulation profiles through an electrode array (instead of two wire electrodes) with the aim of targeting functional hot-spots (leg flexion vs. extension) in a timely appropriate manner (swing vs. stance phase of each leg), increased functionality could be obtained in rats [36] and non-human primates [209] after severe and partial spinal cord injury respectively. In the present study, we characterized the effect of a hybrid PNS-EES strategy on locomotion in rodents using tonic 40 Hz EES applied over the mid-line of L2 and S1 spinal. We aimed at explicitly investigating the effect of PNS on EES-enabled gait patterns that did not need to be optimal. Projecting to human individuals with severe spinal cord injury, it is likely that locomotion patterns will not be as optimal as the ones obtained in severely paralyzed rats using such strategies [36]. Among others, EES will hardly achieve selective and individual control over the most distal muscles or joints, which are key to return dexterous control of movement after paralysis.

Large differences exist between rodents and humans, for instance rodents do not naturally walk bipedally and their limbs have limited functionality compared to humans. Despite this simpler model of locomotion, we were able to gradually adjust gait patterns through modulation of stimulation frequency targeting functionally distinct branches of the sciatic nerve of the rat. In the rat model, we used an intraneural implant to provide selectivity between ankle extensor and flexor muscles using a single interface. Implanted neuroprostheses require good bio-integration within the host tissue to allow for a successful translation into the clinics. We have previously investigated the bio-integration of active (stimulating) polyimide-based intraneural implants over extended durations in freely moving animals (Chapter 2). However, the duration of stimulation in that experiment did not necessarily reflect daily functional use (minutes to hours per day at high frequency) and consequently could not necessarily inform on the bio-integration of implants that are used daily at high stimulation frequency. It was hence of utmost importance to assess the encapsulation and inflammatory reaction of the current implants under the daily stimulating conditions. We show that the bio-integration of these implants seems to be in line with bio-integration of sporadically-used intraneural implants (Figs. 3.17 and 3.18), which is extremely encouraging for their translation towards use in clinical applications.

In the human pilot experiment, we tested the hybrid PNS-EES stimulation paradigm using surface electrodes for PNS and were able to reproduce results obtained in rats. For instance, ankle joint angle and step height were similarly affected using the hybrid PNS-EES stimulation paradigm when compared to EES. Furthermore, the induced reflex did not destabilize the subject during EES-mediated walking on the treadmill, but rather acted synergistically with EES and positively impacted the contralateral side, even though this needs to be confirmed with further subjects. Whether implanted or not, the functional benefits of combining spinal and peripheral electrical stimulation are extremely encouraging. EES is the elementary unit addressing paralysis and is complemented by PNS to address patient-specific remaining deficits and reduce imprecision to restore refined, functional movements after SCI. This work promotes a novel approach to returning functional movement after paralysis and has the potential to address other neuromotor disorders in which global and local control over movements could be beneficial.

General conclusion

Through the work presented in this chapter of my thesis, I propose a novel approach for restoring refined function to paralyzed limbs by leveraging the inherent advantages of both spinal cord stimulation and peripheral nerve stimulation into a single and refined neuroprosthetic system. I developed and comprehensively characterized the effect of the hybrid neuroprosthesis on gait patterns during treadmill locomotion in rat models of severe spinal cord injury. I confirmed the controllability of PNS obtained in anesthetized animals (cf. chapter 2) by demonstrating gradual adjustments in leg kinematics during EES-mediated locomotion. Similar results in a human pilot experiment suggest that the hybrid peripheral spinal stimulation paradigm is translatable and could have importance for functional restoration after paralysis. My findings demonstrate the feasibility and the potential of hybrid peripheral-spinal stimulation paradigms and could represent a paradigm shift towards personalizing motor-neuroprosthetic interventions. The hybrid approach is an unprecedented comprehensiveness in neuromodulation through the exploitation of the complementary properties of the peripheral and the central nervous systems. I advocate that this approach could significantly impact movement restoration after paralysis for lower limbs but also for upper limbs, where restoring the dexterity of the hand will require even more precision and selectivity.

4 Perspectives on functional restoration for lower and upper limb movements

The work presented in this thesis provides a solid basis for the deployment of hybrid peripheral-spinal neurprosthetic interventions for functional restoration after paralyzing injury. While epidural spinal arrays have been implanted in human patients since the 1960s [15], intraneural peripheral nerve interfaces have not yet surpassed the clinical investigation stage. I believe that the ensemble of data presented in thesis will inform the community about the stability and long-term usability of intraneural implants and raise the awareness about the potential of stimulating the peripheral nervous system to selectively refine movements in an efficient yet simple way. In this last chapter, I first discuss a few opportunities that could further ameliorate the developed hybrid neuroprosthesis in terms of bio-integration, closed-loop control of PNS, and personalization of the strategy (section 4.1). I end by projecting the results of my thesis onto functional restoration after upper limb paralysis.

4.1 Opportunities for refinement of the lower limb hybrid PNS-EES neuroprosthesis

Implantable neurotechnology and bio-integration

I have shown that thin-film polyimide-based intraneural implants integrate well within the nerve and that they remain functional over extended periods of time in spite of a developing tissue response that encapsulated the implant (Chapter 2). While increased stimulation activity did not exacerbate this response (Chapters 2 and 3), there is still room for improvement in terms of reducing the extent of the capsule as well as the the triggered inflammation.

Two main factors contribute to this observed response beyond the fact that any implantation or surgical intervention is accompanied by an inflammatory response as part of the normal physiological response to this intervention. First, the insertion associated injury traumatizes the nerve, even though we did not observe severed blood vessels inside the fascicles immediately after insertion. The trauma may be reduced by smart designs of the tip of the device that initiates the insertion [162] or by further miniaturization of the device, but can most probably not be avoided completely with penetrating intraneural implants. Second, there is a large mechanical mismatch between the implant and its surrounding tissue, which is further exacerbated by the tethering and related micro-motion during movement and thus continuously induces inflammatory responses [210, 211, 212].

Soft intraneural interfaces. Several strategies may mitigate the mechanical mismatch between tissue and intraneural implants [164, 213]. Polyimide (the substrate of the implants that were used in this work) is a relatively stiff substrate and does not easily conform to the movements and changes in elongation of the nerve during movement. A softer implant would induce less damage as the effect of micro-motion will be less insulting to the nerve. For instance, PDMS (polydimethylsiloxane), a soft silicone rubber used in implant technology, shown improved bio-integration and reduced mechanical impact on spinal tissue when implanted epidurally in rats [167]. However, PDMS-based implants have a larger footprint than implants based on thin-film technology that is likely to exceed the dimensions for intrafascicular implants. On the other hand, very thin and soft substrates cannot penetrate soft neural tissue or may be damaged during insertion into nerves. Such implants may be inserted with the aid of stiff insertion vectors that are subsequently removed from the tissue (for instance as in [214]). Alternatively, mechanically-adaptive materials could be used that are stiff during insertion but then change their properties when in contact with physiological conditions [215, 216]. Soft at five minutes post-implantation, those implants demonstrated a substantially reduced neuroinflammatory response when implanted intracortically in rats. These concepts have traditionally been developed for interfaces with the central nervous system. To date, such techniques have not been investigated to interface the peripheral nervous system intraneurally.

Anti-inflammatory and antioxidant coatings. A possibly complementary strategy could be to introduce an antioxidant or anti-inflammatory coatings onto the intraneural implant. For instance, cerium oxide nanoparticles (nanoceria) form a powerful antioxidant nanomaterial with great potential in biomedicine and tissue engineering fields through a self-regenerating capability as reactive oxygen species scavengers [217, 218]. Reactive oxygen species are signalling molecules that playing a key role in the progression of inflammatory responses. Their accumulation during inflammation can lead to oxidative stress, damaging cells and disrupting neural function. Nanoceria was shown to have a neuroprotective effect in models of Alzheimer's disease [219] and ischemia [220] and could have a beneficial impact on inflammation when coating the implant. Likewise, anti-inflammatory coatings of neural probes have elicited a reduced inflammatory response when compared to un-coated implants [221]. For instance, dexametasone, an anti-inflammatory corticosteroid, reduced reactive astrocytes and microglia in vitro [222] and in vivo [223, 214]. Also this type of research has historically concentrated on interfaces with the brain, but could certainly benefit peripheral nerve interfaces in similar ways.

Closed-loop control strategies for PNS in hybrid PNS-EES neuromodulation

Typical FES based neuroprostheses are based on either open loop or finite state controls and use movements of non-affected body areas, residual EMG activity recorded from wrist or forearm muscles or manual switches as input signals to the control structure [224]. However, acceptance rate among users has been hampered by the poorly intuitive nature of such control strategies and low marginal benefits in light of a complex and cumbersome setups. In the combined PNS-EES paradigm presented in this thesis, EES generates natural movements that are refined by PNS, but the refinement should come when needed and can therefore not be triggered by the user if a seamless and intuitive control is desired.

In the work presented in this thesis, the delivery of PNS was locked to events detected during gait cycles on the basis of kinematic information recorded through a motion capture system (Vicon ltd), while EES was tonically delivered without feedback loop. This may suit well for research and even clinical environments, but it can hardly comply with daily life. Recently, our group has shown how closed-loop control of EES alleviated gait deficits in rhesus macaques by decoding neural signals from leg motor cortex into toe off and foot strike events [209]. Additional signals can be used to control the onset of PNS [225], which in the paradigm presented in this thesis work should be based on a assist if needed strategy. Depending on the application, inertial measurement units or accelerometers could be fitted to the shoes of patients to inform about the phase of the gait (swing vs. stance) [226, 227, 228]. Likewise, those signals could potentially be used to inform about ankle joint angle excursions if ankle sneakers would be used (three sensing points necessary) and detect the need for assistance in real time.

Alternatively, and to avoid some of the disadvantages associated with external sensors [229], muscle or nerve activity can inform about the state of activation of target muscles in real time and trigger PNS based on user-specific thresholds to complement the activation up to the required level. For EMG activity sensing, this could be implemented as wearable surface EMG over distal muscles (for instance in knee-high socks). More robust, yet more invasive, similar control signal could be derived from neural recordings [230, 231], or even from the dorsal roots, providing sensory-only information about the state of muscle activation [232, 233, 234, 235]. Independent of the control signal, the idea would be to match the current activity to the natural and healthy activation of muscles or joint movements during movement.

Personalizing neuroprosthetics in clinical settings

Personalized neuroprosthetics strategies may become a breakthrough in restoring function to paralyzed individuals. One of the key advantages in the proposed hybrid PNS-EES paradigm is the high degree of modularity that it presents, being thus prone to individualized approaches for restoring function after paralysis.

In the hybrid peripheral-spinal neuroprosthetic system, through the multiple contacts in the epidural array, a myriad possibilities are given to set parameters, combine contacts, and assign anode or cathode among others to optimize the electrode configuration for each specific patient. Based on the discrepancies between desired and EES-enabled muscle activation, PNS is used additionally in a tailored manner to complement EES induced muscle activation based on patient-specific remaining deficits. This strategy is inscribed in a trend that is observed in the field of neuroprosthetics, namely the concept of mapping patient-specific circuitopathies and their potential for recovery to distinct combinations of neuroprosthetic technologies and individualized neurorehabilitation programs [236].

In chapter 3, I presented results from a pilot experiment that we performed with a human individual with spinal cord injury. Albeit preliminary, we will reproduce those experiments to address patient-specific remaining deficits with PNS in other patients enrolled in the study. The hybrid peripheral-spinal neuroprosthesis may have an important impact on functional restoration after paralysis through the capacity of addressing comprehensively patient-specific impairments.

4.2 Hybrid PNS-EES neuroprosthesis for functional restoration of upper limb movements after paralysis

Manipulation is crucial for all activities of daily living, permitting all interactions of human beings with the environment around them. Even if prehension is very complex because of the demanding requirements that must be satisfied during grasp, it appears straightforward. The restoration of manipulation is of paramount important for people who lost it for spinal cord injury [3, 4]. Recent developments in research groups around the world show the stake that is at hold.

Electrical stimulation of the cervical spinal cord has the potential to reanimate paralyzed forelimbs and restore motor function after neurological damage. For instance, spinal cord stimulation at the cervical segments generated motor responses in multiple forelimb muscles in rats [237] and in non-human primates [238, 239, 240] and has permitted to facilitate movements of paralyzed limbs in animal models [241, 242, 243, 244] and in a recent study in human subjects [245]. Taken together, it appears that different responses can be elicited, some of which may be useful to generate movement or improve its execution. It remains however unclear to what extent the evoked responses are reproducible and data suggests that the selectivity in distal muscle recruitment (wrist or digits) was insufficient to project to restoring dexterous and usable movements of the hand and so to restore multiple degrees of freedom [238, 237, 241]. Difficulties to identify a clear somatotopic organization of forelimb movements in the cervical spinal cord point out the hurdles that remain to be overcome before developing a real therapeutic application in this field. In spite of sub-optimal selectivity, the same experimental results highlight the potential of harnessing spinal circuits below the lesion to facilitate movement after spinal cord injury.

Functional neuromuscular electrical stimulation (FES) has been used for decades to restore movement after neurological disorders and has been integrated into various neuroprosthetic systems aiming at restoring grasping after paralyzing spinal cord injury or stroke [246, 247, 10]. FES devices have been developed by using surface (i.e., the HandMaster developed by NESS ltd, Israel [248] and the Bionic Glove developed by Neuromotion, Edmonton, Canada [249, 250]) or epimysial electrical stimulation (i.e., the FreeHand system developed at Case Western Reserve University, Cleveland, US, [251, 247]). The control over such a system has been implemented via the use of residual movements or residual EMG activity to trigger pre-programmed stimulation patterns causing the paralyzed muscles to contract into one or two basic types of grasp [224]. As for FES applied on the lower limbs, current surface stimulation systems are limited by requiring high currents to activate muscles, potentially creating skin problems and discomfort to the user. Their usability is further restricted by fast generation of muscle fatigue through unnatural recruitment order of muscle fibers. Using implanted muscle electrodes, researchers have restored wrist flexion and extension [252, 253] as well as grasping and holding a small ball after transient paralysis of hand muscles in non-human primates [254]. Implantable FES devices for upper limb movement restoration have been tested and validated in clinical studies on human individuals with cervical SCI [247, 255, 256, 257]. Some of these studies demonstrate the achievement of restoring one grasp type or a wrist motion with intramuscular stimulation, but the feasibility of up-scaling the system to higher number of muscles to restore functional grasping of different modalities remains to be determined. Furthermore, the generation of muscle fatigue remains an issue. For instance, in [256] a mobile arm support is required to assist weight support against gravity because intramuscular FES does not generate enough torque in single muscles and in coordination between muscles to reanimate a completely paralyzed arm. Similar to developments in the field of lower limb paralysis and FES, research groups have been targeting branches of the peripheral nervous system as an upstream alternative to muscular FES. For instance, cuff electrodes have been implemented in neuroprostheses aiming at restoring hand function after paralysis [77, 258, 259]. Unfortunately none of those systems is in wide clinical use due to limited functional benefits, necessity for surgical procedures and complicated external equipment that do not encourage daily use [260]. In fact, epineural electrodes, even though minimally invasive, may yield insufficient selectivity as they provide access only to superficial axons of the nerve. Addressing this issue, Ledbetter et al. have implanted penetrating microelectrode arrays in the median, ulnar, and radial nerves of anaesthetized non-human primates and were able to elicit two different grasp types [261]. Despite this proof of concept, to date no intraneural stimulation-based FES neuroprosthesis has been implemented in clinical applications.

The restoration of the full dexterity of a healthy and functional human hand is far from being achieved. There is need for the development of stimulation paradigms that restore functional and controllable grasping movements in contrast to simple predetermined grasps. The generated movements need to be strong and should stem from the coordinated activation of functional muscle groups, matching the natural generation of motor output. In addition to this basic building block, a selective access to agonist and antagonist muscles is required to comprehensively actuate the distal hand with high precision and the appropriate amount of force.

In light of these considerations and following from the developments presented in this thesis work, I argue that targeting the spinal cord and the peripheral nerves concomitantly will provide substantially increased functional restoration after paralysis of the upper limbs. Arm and hand movements are extremely complex. Their execution needs coordinated action at multiple joints to provide sufficient torque to permit usability. At the same time precise recruitment of distal muscles is required to refine the movement execution and return dexterity. While the former may be generated by cervical spinal cord stimulation, the latter could be achieved by intraneural stimulation of the ulnar, median and radial nerves.

To investigate the feasibility of recruiting distal hand muscles selectively with chronic intraneural implants in the upper limb nerves, we started a study in collaboration with Prof. Eric Rouiller at the University of Fribourg (CH) to address these points in a non-human primate model of upper limb paralysis (Swiss National Science Foundation Grant NeuGrasp [205321_170032]). The aim of the study is to verify intraneural recruitment properties in terms of selectivity and stability and to assess the precision and usability of the movements that can be generated. Preliminary data obtained in a pilot experiment (muscle recruitment curves following similar protocols as described in section 2.3.3 during a terminal experiment on a female macaca fascicularis) suggest that selectivity over wrist flexor and extensor muscles as well as digit and thumb flexion and extension can be achieved (Fig. 4.1).

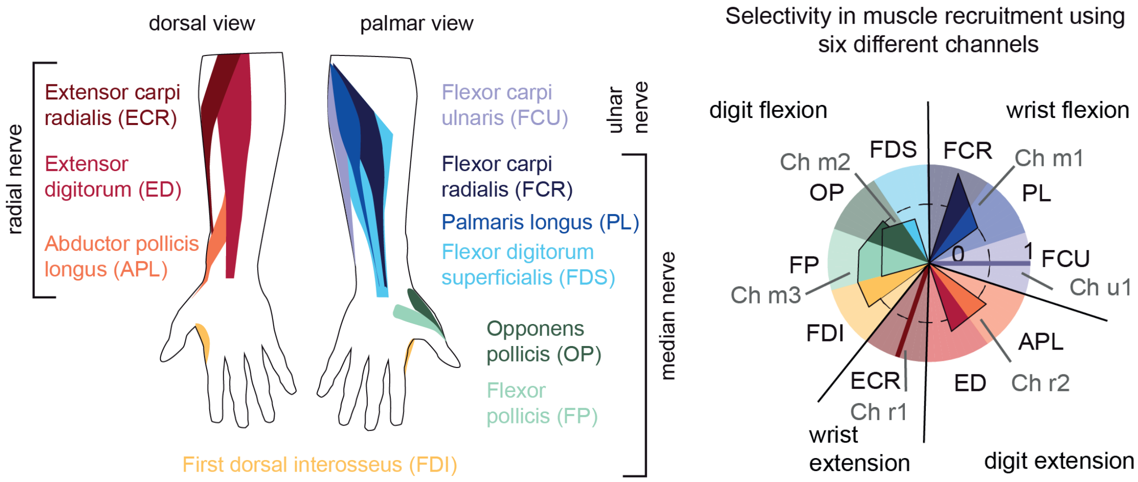

(a) Wrist and hand flexor and extensor muscles implanted for terminal experiment on a macaca fascicularis and their innervation by radial, median, and ulnar nerves

(b) Summary of preliminary results: selectivity in muscle recruitment obtained via stimulation of radial, median, and ulnar nerves.

Figure 4.1 – Muscle recruitment obtained by median, ulnar, and radial intraneural stimulation. (a) Muscles of interest implanted in macaca fascicularis arm and hand. (b) Summary of preliminary results in terms of selectivity in muscle recruitment using 1 contact in the ulnar nerve (Ch u1), 2 contacts in the radial nerve (Ch r1 and Ch r2) and 3 contacts in the median nerve (Ch m1, Ch m2, Ch m3).

Although extremely preliminary, those encouraging results suggest that selective recruitment of distal hand muscles is possible using intraneural implants. We will now work towards i) reproducing those results and ii) assessing the controllability of the obtained muscle activation in prospect of chronic implantation in models of upper limb paralysis.

5 General conclusion

This thesis provides a vast body of evidence about the stability and long-term usability of intraneural implants and demonstrates their potential for stimulating the peripheral nervous system with highly controllable output to complement and refine movement execution after paralysis.

Current strategies to restore functions to paralyzed limbs have separately investigated electrical stimulation of the spinal cord or of the distal peripheral nerves and muscles. While spinal cord stimulation as a treatment option for paralysis is still at an investigational stage in clinical research, it appears that translation from pre-clinical research in animal models is not straightforward [41, 42, 43]. Indeed, data from the first human studies applying electrical stimulation over the lumbosacral spinal cord suggested that while locomotor activity was enabled or even enhanced, it was not possible to generate actual stepping (as opposed to studies in animal models) [37, 39, 40]. Additionally, data suggested that the selectivity in distal muscle recruitment was low [40, 44, 38]. Precise control over distal musculature is however necessary to permit functional and usable locomotion. In turn, functional electrical stimulation of the distal neuromuscular system is widely accepted in clinical applications but is limited in applications through of a relatively modest performance associated with high metabolic cost [262, 263].

In this thesis, I advocate that targeting the distal neuromuscular system is necessary but not sufficient to permit refined movement restoration after paralysis and that combining it with spinal cord stimulation will permit a personalized approach to paralysis with improved functional restoration.

I argue that intraneural multi-channel thin-film implants are excellent candidates for interfacing the peripheral nerves, however their long-term stability and usability was not established due to a lack of pre-clinical evidence about long-term functionality, stability, and bio-integration. To bridge this gap, I present an ensemble of anatomical and electrophysiologicial data informing about the chronic functionality and bio-integration of actively used intraneural implants. My findings demonstrate that high selectivity, permitting high-fidelity control of muscle recruitment in real time, is conserved during months after implantation in spite of the development of a capsule around the implant as part of the tissue response to the implant. I confirmed the stability and usability of the implants in chronic animal models of paralysis and demonstrate that removal of the implants does not alter leg motor control. The data presented in this thesis is very important for permitting the translation of intraneural implants to clinical applications, not only for their stability in terms of bio-integration and stimulation properties, but also for the functionality they provide.

In the second part of my thesis, I exploited those properties in the framework of paralysis after spinal cord injury to precisely refine key movement characteristics and improve functional restoration when combined with spinal cord stimulation paradigms. I developed and validated a hybrid peripheral-spinal neuroprosthetic system that concomitantly stimulated the epidural lumbosacral spinal cord and the sciatic nerves intraneurally in severely paralyzed rats. I show that selective recruitment of distal agonist and antagonist muscles by peripheral nerve stimulation permits graded adjustments in leg movements that increase functionality and refine gait patterns. In a pilot study with a human individual with a spinal cord injury, I similarly used the hybrid peripheral-spinal neuroprosthesis to refine key leg movements that restored walking symmetry, prevented foot dragging, and thus improved locomotion. Albeit using surface electrodes, this proof of principle suggests that a comprehensive approach can bring important functional benefits.

The hybrid peripheral-spinal approach could thus have an important impact on functional restoration for lower limbs, but may similarly benefit upper limb functional restoration. Quadriplegic patients suffer immensely from the inability of using their arms and hands, but restoring useful function and dexterity is an arduous challenge. I believe that a hybrid peripheral-spinal approach could be key to attempt the restoration of usable upper limb function after paralysis. Spinal cord stimulation exploits the capabilities of the spinal circuits to enable the generation of motor synergies involving coordinated groups of muscles, thus providing the building block for the movement of the arm and hand. Peripheral nerve stimulation of ulnar, median, and radial nerves enable selective access to distal hand muscles, allowing graded control over their activation. Using this hybrid approach, it may thus be possible to restore a higher level of function and dexterity to the hand after paralysis. In a first step in this direction, we started a study in collaboration with the University of Fribourg to investigate the recruitment properties of intraneural thin-film electrodes in upper limb peripheral nerves in non-human primates. Preliminary data suggests that selective activation of wrist, thumb, and digit flexor and extensor muscles is possible using intraneural implants. Albeit exploratory, these results underline the usability of peripheral nerve stimulation and its potential for restoring refined movements after paralysis.

To conclude, the work presented in this thesis provides a solid basis for the deployment of intraneural peripheral nerve implants and demonstrates their potential for functional restoration after paralyzing injury. The following hybrid peripheral-spinal stimulation paradigm reveals how the complementarity of both strategies could effectively improve functional outcomes for paralyzed lower and upper limbs.

A Appendix

A.1 Kinematic and kinetic variables characterizing gait

Number	Description
I	**Temporal features of the gait cycle**
1	Cycle duration
2	Cycle velocity during stride
3	Stance duration (sec)
4	Relative stance duration (%)
5	Swing duration
II	**Related to limb endpoint (metatarsal phalange) trajectory**
6	Double stance
7	Stride length
8	Step length
9	Path length of endpoint marker
10	Maximum backward position of endpoint marker
11	Maximum forward position of endpoint marker
12	Normalized step height
13	Maximum endpoint marker velocity during swing
14	Relative timing of maximum velocity during swing
15	Endpoint marker acceleration at swing onset
16	Average endpoint marker velocity
17	Orientation of the endpoint marker velocity vector at swing onset
18	Drag duration (sec)
19	Relative drag duration (%)
III	**Stability**
i)	*Base of support*
20	Lateral displacement during swing
21	Stance width
ii)	*Trunk and pelvic position and oscillations*
22	Maximum hip sagittal position
23	Minimum hip sagittal position
24	Amplitude of sagittal hip oscillations
25	Variability of vertical hip movement
26	Variability of sagittal hip movement

27	Variability of the 3D hip oscillations
28	Amplitude of virtual center of mass (COM) in the forward direction
29	Amplitude of virtual COM in the medio-lateral direction
30	Amplitude of virtual COM in the vertical direction
31	Path length of virtual COM in 3D
IV	**Joint angles and segmental oscillations**
i)	*Elevation angles*
32	Minimum crest elevation angle
33	Minimum shank elevation angle
34	Minimum thigh elevation angle
35	Minimum foot elevation angle
36	Minimum limb axis angle in sagittal plane
37	Maximum crest elevation angle
38	Maximum shank elevation angle
39	Maximum thigh elevation angle
40	Maximum foot elevation angle
41	Maximum limb axis angle in sagittal plane
42	Amplitude of crest oscillations
43	Amplitude of shank oscillations
44	Amplitude of thigh oscillations
45	Amplitude of foot oscillations
46	Amplitude of whole limb oscillations in sagittal plane
ii)	*Joint angles*
47	Minimum hip joint angle
48	Minimum knee joint angle
49	Minimum ankle joint angle
50	Maximum hip joint angle
51	Maximum knee joint angle
52	Maximum ankle joint angle
53	Amplitude hip joint angle
54	Amplitude knee joint angle
55	Amplitude ankle joint angle
iii)	*Whole limb medio-lateral oscillations*
56	Minimum limb abduction angle
57	Maximum limb abduction angle
58	Amplitude limb abduction angle
iv)	*Foot rotation in coronal plane*
59	Foot abduction angle
60	Foot adduction angle
61	Amplitude foot rotation
V	**Velocity**
62	Minimum whole limb oscillation velocity
63	Minimum hip joint angle velocity
64	Minimum knee joint angle velocity
65	Minimum ankle joint angle velocity
66	Maximum whole limb oscillation velocity
67	Maximum hip joint angle velocity
68	Maximum knee joint angle velocity
69	Maximum ankle joint angle velocity
70	Amplitude whole limb oscillation velocity
71	Amplitude hip joint angle velocity

72	Amplitude knee joint angle velocity
73	Amplitude ankle joint angle velocity
VI	**Inter-segmental coordination**
74	Degree of linear coupling between joint oscillations
75	Temporal coupling between crest and shank oscillations
76	Temporal coupling between shank and thigh oscillations
77	Temporal coupling between thigh and foot oscillations
78	Correlation between crest and tight oscillations
79	Correlation between tight and thigh oscillations
80	Correlation between thigh and foot oscillations
81	Correlation between hip and knee oscillations
82	Correlation between knee and ankle oscillations
83	Correlation between ankle and MTP oscillations
84	Temporal lag between backward positions of crest and shank oscillations
85	Temporal lag between forward positions of crest and shank oscillations
86	Temporal lag between backward positions of shank and thigh oscillations
87	Temporal lag between forward positions of the shank and thigh oscillations
88	Temporal lag between backward positions of thigh and foot oscillations
89	Temporal lag between forward positions of thigh and foot oscillations
90	Phase of the crest elevation angle at maximal amplitude obtained by FFT
91	Maximal amplitude of the crest elevation angle obtained by FFT
92	Phase of the shank elevation angle at maximal amplitude obtained by FFT
93	Maximal amplitude of the shank elevation angle obtained by FFT
94	Phase of the thigh elevation angle at maximal amplitude obtained by FFT
95	Maximal amplitude of the thigh elevation angle obtained by FFT
96	Phase of the foot elevation angle at maximal amplitude obtained by FFT
97	Maximal amplitude of the foot elevation angle obtained by FFT
98	Lag of the cross correlation function between crest and shank elevation angle
99	Lag of the cross correlation function between shank and thigh elevation angles
100	Lag of the cross correlation function between thigh and foot elevation angles
101	Lag of the cross correlation function between hip and knee angles
102	Lag of the cross correlation function between knee and ankle angles
103	Lag of the cross correlation function between ankle and foot angles
104	Lag of cross-correlation function between right and left limb axis angle
VII	**Kinetics**
105	Mean medio-lateral forces
106	Mean antero-posterior forces
107	Mean vertical forces
108	Medio-lateral forces during single stance
109	Antero-posterior forces during single stance
110	Vertical forces during single stance

A.2 Quantification of spared tissue in lesion epicenter after severe SC contusion

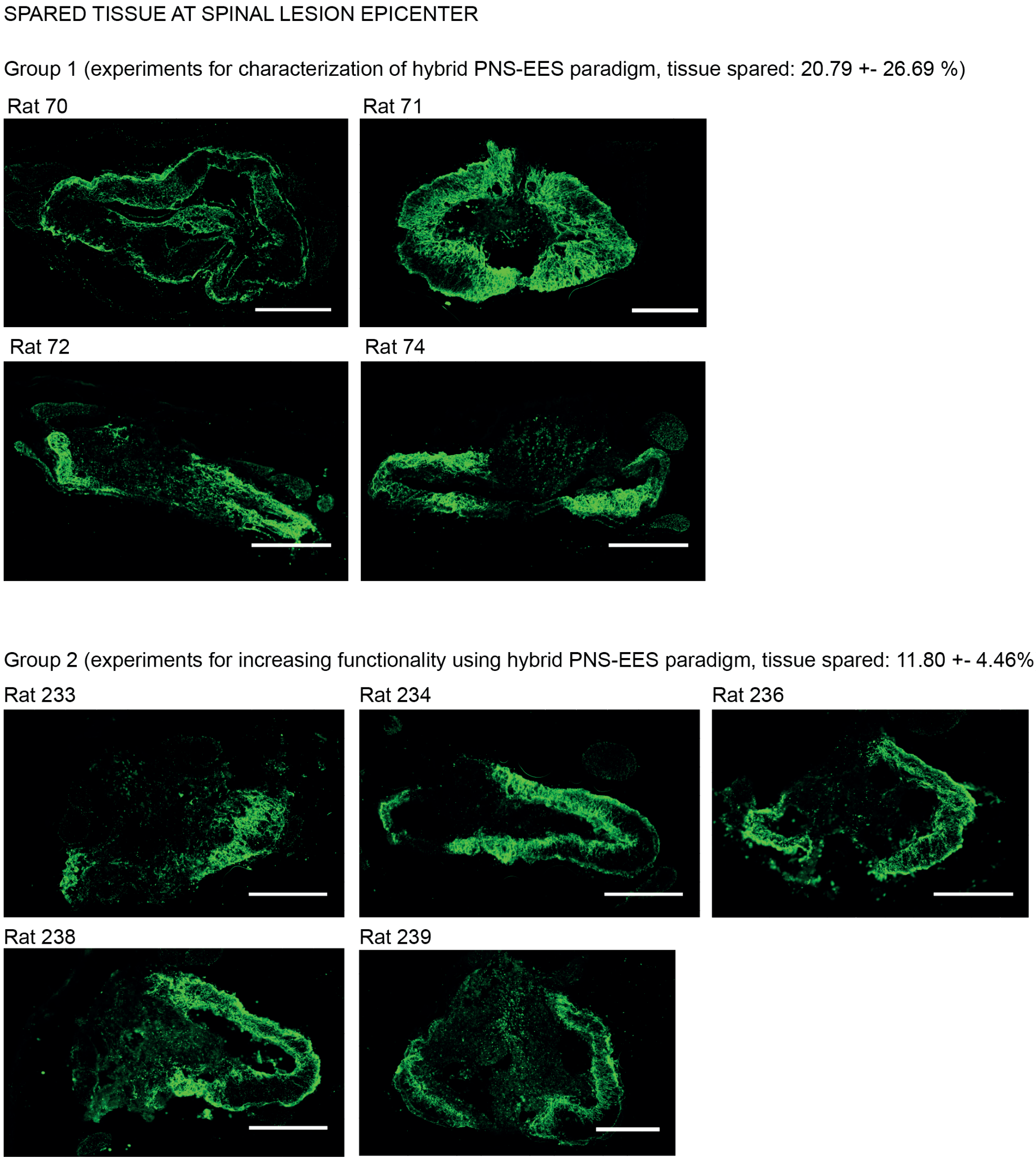
SPARED TISSUE AT SPINAL LESION EPICENTER
Group 1 (experiments for characterization of hybrid PNS-EES paradigm, tissue spared: 20.79 +- 26.69 %)
Rat 70
Rat 71
Rat 72
Rat 74
Group 2 (experiments for increasing functionality using hybrid PNS-EES paradigm, tissue spared: 11.80 +- 4.46%)
Rat 233
Rat 234
Rat 236
Rat 238
Rat 239

Figure A.1 – Lesion epicenter across contused animals. GFAP (Glial Fibrillary Acid Protein) reveals spared (living) tissue. Scale bar on all images is 500 μm

A.3 Effect of frequency modulation of enhanced extension in hybrid PNS-EES

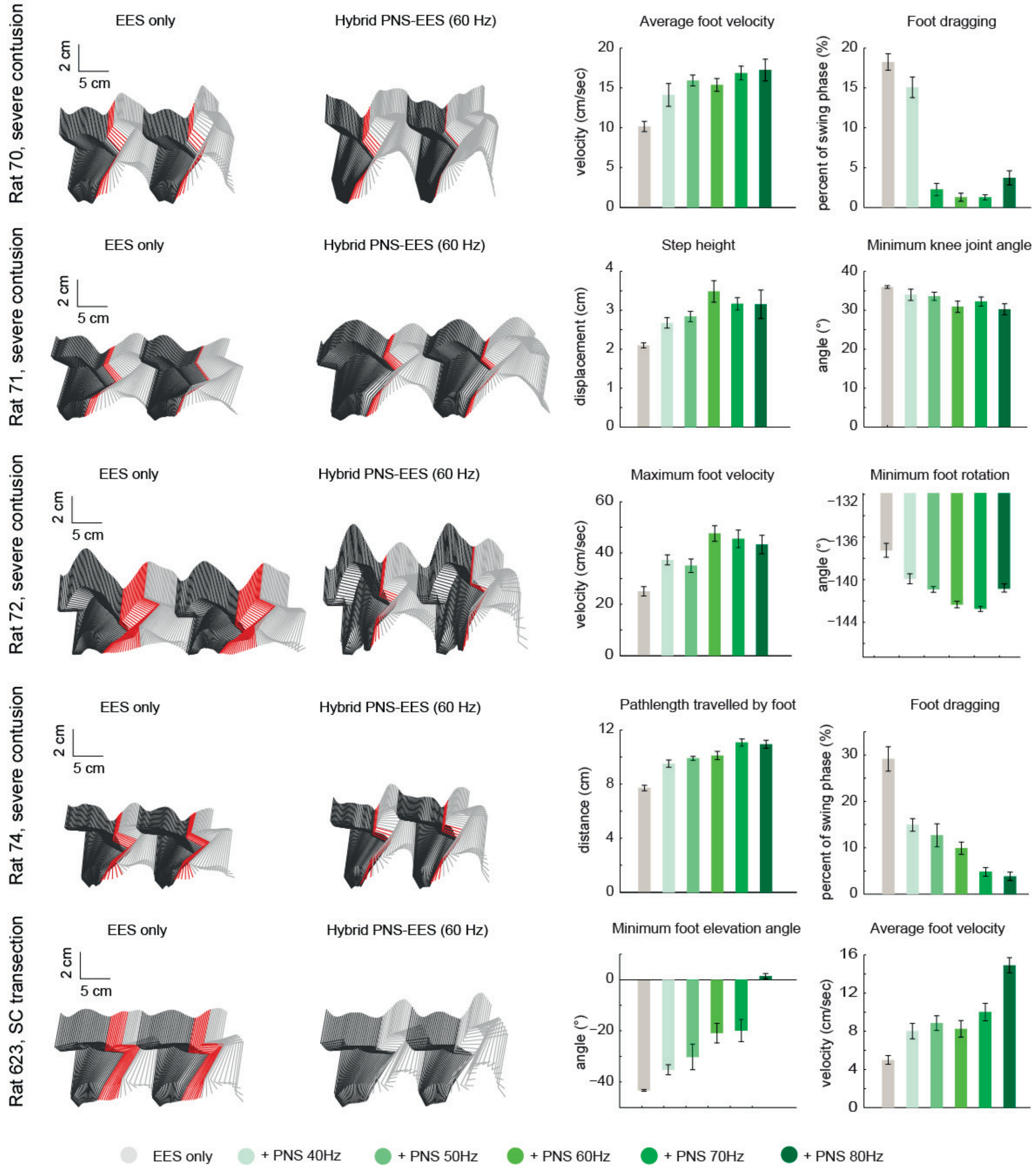

Figure A.2 – Enhanced extension affects different gait characteristics in different animals. From top to bottom, animals 70, 71, 72, 74 (contused spinal cord), and 623 (complete spinal cord transection).

Bibliography

[1] Colin Mathers. *The global burden of disease: 2004 update*. World Health Organization, 2008.

[2] Christopher and Dana Reeve Foundation. Stats about paralysis. Website, 2013. URL https://www.christopherreeve.org/living-with-paralysis/stats-about-paralysis.

[3] Kim D Anderson. Targeting recovery: priorities of the spinal cord-injured population. *Journal of Neurotrauma*, 21(10):1371–1383, 2004.

[4] Govert J Snoek, Maarten J IJzerman, Hermie J Hermens, Douglas Maxwell, and Fin Biering-Sorensen. Survey of the needs of patients with spinal cord injury: impact and priority for improvement in hand function in tetraplegics. *Spinal Cord*, 42(9):526, 2004.

[5] Ismael Seáñez-González and Ferdinando A Mussa-Ivaldi. Cursor control by Kalman filter with a non-invasive body–machine interface. *Journal of Neural Engineering*, 11(5):056026, 2014.

[6] Camilla Pierella, Farnaz Abdollahi, Ali Farshchiansadegh, Jessica Pedersen, Elias B Thorp, Ferdinando A Mussa-Ivaldi, and Maura Casadio. Remapping residual coordination for controlling assistive devices and recovering motor functions. *Neuropsychologia*, 79:364–376, 2015.

[7] Jonathan R Wolpaw. Brain-computer interfaces. *Handbook of Clinical Neurology*, 110:67–74, 2013.

[8] Maura Casadio, Rajiv Ranganathan, and Ferdinando A Mussa-Ivaldi. The body-machine interface: a new perspective on an old theme. *Journal of Motor behavior*, 44(6):419–433, 2012.

[9] Jennifer L Collinger, Michael L Boninger, Tim M Bruns, Kenneth Curley, Wei Wang, and Douglas J Weber. Functional priorities, assistive technology, and brain-computer interfaces after spinal cord injury. *Journal of Rehabilitation Research and Development*, 50(2):145, 2013.

[10] P Hunter Peckham and Kevin L Kilgore. Challenges and opportunities in restoring function after paralysis. *IEEE Transactions on Biomedical Engineering*, 60(3):602–609, 2013.

[11] Armour, Brian S and Courtney-Long, Elizabeth A and Fox, Michael H and Fredine, Heidi and Cahill, Anthony. Prevalence and Causes of Paralysis – United States, 2013. *American Journal of Public Health*, 106(10):1855–1857, 2016.

[12] Frederick M Maynard, Michael B Bracken, GJFD Creasey, John F Ditunno, William H Donovan, Thomas B Ducker, Susan L Garber, Ralph J Marino, Samuel L Stover, Charles H Tator, et al. International standards for neurological and functional classification of spinal cord injury. *Spinal Cord*, 35 (5):266–274, 1997.

[13] LS Illis. Central nervous system regeneration does not occur. *Spinal Cord*, 50(4):259, 2012.

[14] Milan R Dimitrijevic, Byron A Kakulas, W Barry McKay, and Gerta Vrbova. *Restorative neurology of spinal cord injury*. Oxford University Press, 2012.

[15] C Norman Shealy, J Thomas Mortimer, and James B Reswick. Electrical inhibition of pain by stimulation of the dorsal columns: preliminary clinical report. *Anesthesia & Analgesia*, 46(4):489–491, 1967.

[16] AW Cook and SP Weinstein. Chronic dorsal column stimulation in multiple sclerosis. Preliminary report. *New York State Journal of Medicine*, 73(24):2868–2872, 1973.

[17] Joseph M Waltz, Leslie O Reynolds, and Manuel Riklan. Multi-lead spinal cord stimulation for control of motor disorders. *Stereotactic and Functional Neurosurgery*, 44(4):244–257, 1981.

[18] Charles Scott Sherrington. Flexion-reflex of the limb, crossed extension-reflex, and reflex stepping and standing. *The Journal of Physiology*, 40(1-2):28–121, 1910.

[19] Milan R Dimitrijevic, Yuri Gerasimenko, and Michaela M Pinter. Evidence for a spinal central pattern generator in humans. *Annals of the New York Academy of Sciences*, 860(1):360–376, 1998.

[20] Jacques Duysens and Henry WAA Van de Crommert. Neural control of locomotion; Part 1: The central pattern generator from cats to humans. *Gait & posture*, 7(2):131–141, 1998.

[21] Ole Kiehn. Decoding the organization of spinal circuits that control locomotion. *Nature Reviews Neuroscience*, 17(4):224, 2016.

[22] S Grillner and P Zangger. On the central generation of locomotion in the low spinal cat. *Experimental Brain Research*, 34(2):241–261, 1979.

[23] Volker Dietz. Human neuronal control of automatic functional movements: interaction between central programs and afferent input. *Physiological Reviews*, 72(1):33–69, 1992.

[24] Arthur Prochazka, Valeriya Gritsenko, and Sergiy Yakovenko. Sensory control of locomotion: reflexes versus higher-level control. *Sensorimotor Control of Movement and Posture*, pages 357–367, 2002.

[25] Volker Dietz, Roland Müller, and Gery Colombo. Locomotor activity in spinal man: significance of afferent input from joint and load receptors. *Brain*, 125(12):2626–2634, 2002.

[26] KG Pearson. Role of sensory feedback in the control of stance duration in walking cats. *Brain Research Reviews*, 57(1):222–227, 2008.

[27] Sergey N Markin, Alexander N Klishko, Natalia A Shevtsova, Michel A Lemay, Boris I Prilutsky, and Ilya A Rybak. Afferent control of locomotor CPG: insights from a simple neuromechanical model. *Annals of the New York Academy of Sciences*, 1198(1):21–34, 2010.

[28] Frank Rattay, Kirkor Minassian, and MR Dimitrijevic. Epidural electrical stimulation of posterior structures of the human lumbosacral cord: 2. quantitative analysis by computer modeling. *Spinal Cord*, 38(8):473, 2000.

[29] Marco Capogrosso, Nikolaus Wenger, Stanisa Raspopovic, Pavel Musienko, Janine Beauparlant, Lorenzo Bassi Luciani, Grégoire Courtine, and Silvestro Micera. A computational model for epidural electrical stimulation of spinal sensorimotor circuits. *Journal of Neuroscience*, 33(49):19326–19340, 2013.

[30] Yury P Gerasimenko, Igor A Lavrov, Gregoire Courtine, Ronaldo M Ichiyama, Christine J Dy, Hui Zhong, Roland R Roy, and V Reggie Edgerton. Spinal cord reflexes induced by epidural spinal cord stimulation in normal awake rats. *Journal of Neuroscience Methods*, 157(2):253–263, 2006.

[31] Karen Minassian, W Barry McKay, Heinrich Binder, and Ursula S Hofstoetter. Targeting lumbar spinal neural circuitry by epidural stimulation to restore motor function after spinal cord injury. *Neurotherapeutics*, 13(2):284–294, 2016.

[32] Eduardo Martin Moraud, Marco Capogrosso, Emanuele Formento, Nikolaus Wenger, Jack DiGiovanna, Grégoire Courtine, and Silvestro Micera. Mechanisms underlying the neuromodulation of spinal circuits for correcting gait and balance deficits after spinal cord injury. *Neuron*, 89(4):814–828, 2016.

[33] Grégoire Courtine, Yury Gerasimenko, Rubia Van Den Brand, Aileen Yew, Pavel Musienko, Hui Zhong, Bingbing Song, Yan Ao, Ronaldo M Ichiyama, Igor Lavrov, et al. Transformation of nonfunctional spinal circuits into functional states after the loss of brain input. *Nature Neuroscience*, 12(10): 1333–1342, 2009.

[34] Rubia van den Brand, Janine Heutschi, Quentin Barraud, Jack DiGiovanna, Kay Bartholdi, Michèle Huerlimann, Lucia Friedli, Isabel Vollenweider, Eduardo Martin Moraud, Simone Duis, et al. Restoring voluntary control of locomotion after paralyzing spinal cord injury. *Science*, 336(6085):1182–1185, 2012.

[35] Nikolaus Wenger, Eduardo Martin Moraud, Stanisa Raspopovic, Marco Bonizzato, Jack DiGiovanna, Pavel Musienko, Manfred Morari, Silvestro Micera, and Grégoire Courtine. Closed-loop neuromodulation of spinal sensorimotor circuits controls refined locomotion after complete spinal cord injury. *Science Translational Medicine*, 6:255, 2014.

[36] Nikolaus Wenger, Eduardo Martin Moraud, Jerome Gandar, Pavel Musienko, Marco Capogrosso, Laetitia Baud, Camille G Le Goff, Quentin Barraud, Natalia Pavlova, Nadia Dominici, et al. Spatiotemporal neuromodulation therapies engaging muscle synergies improve motor control after spinal cord injury. *Nature Medicine*, 22(2):138, 2016.

[37] Karen Minassian, Ilse Persy, Frank Rattay, Michaela M Pinter, Helmut Kern, and Milan R Dimitrijevic. Human lumbar cord circuitries can be activated by extrinsic tonic input to generate locomotor-like activity. *Human Movement Science*, 26(2):275–295, 2007.

[38] Simon M Danner, Ursula S Hofstoetter, Brigitta Freundl, Heinrich Binder, Winfried Mayr, Frank Rattay, and Karen Minassian. Human spinal locomotor control is based on flexibly organized burst generators. *Brain*, 138(3):577–588, 2015.

[39] Susan Harkema, Yury Gerasimenko, Jonathan Hodes, Joel Burdick, Claudia Angeli, Yangsheng Chen, Christie Ferreira, Andrea Willhite, Enrico Rejc, Robert G Grossman, et al. Effect of epidural stimulation of the lumbosacral spinal cord on voluntary movement, standing, and assisted stepping after motor complete paraplegia: a case study. *The Lancet*, 377(9781):1938–1947, 2011.

[40] Claudia A Angeli, V Reggie Edgerton, Yury P Gerasimenko, and Susan J Harkema. Altering spinal cord excitability enables voluntary movements after chronic complete paralysis in humans. *Brain*, 137(5):1394–1409, 2014.

[41] Grégoire Courtine, Mary Bartlett Bunge, James W Fawcett, Robert G Grossman, Jon H Kaas, Roger Lemon, Irin Maier, John Martin, Randolph J Nudo, Almudena Ramon-Cueto, et al. Can experiments

in nonhuman primates expedite the translation of treatments for spinal cord injury in humans? *Nature Medicine*, 13(5):561–566, 2007.

[42] Volker Dietz and Martin E Schwab. From the rodent spinal cord injury model to human application: Promises and challenges. *Journal of Neurotrauma*, 34(9):1826–1830, 2017.

[43] Prithvi K Shah and Igor Lavrov. Spinal epidural stimulation strategies: Clinical implications of locomotor studies in spinal rats. *The Neuroscientist*, 0(0):1073858417699554, 2017.

[44] Dimitry G Sayenko, Claudia Angeli, Susan J Harkema, V Reggie Edgerton, and Yury P Gerasimenko. Neuromodulation of evoked muscle potentials induced by epidural spinal-cord stimulation in paralyzed individuals. *Journal of Neurophysiology*, 111(5):1088–1099, 2014.

[45] Clemens M Schirmer, Jay L Shils, Jeffrey E Arle, G Rees Cosgrove, Peter K Dempsey, Edward Tarlov, Stephan Kim, Christopher J Martin, Carl Feltz, Marina Moul, et al. Heuristic map of myotomal innervation in humans using direct intraoperative nerve root stimulation. *Journal of Neurosurgery: Spine*, 15(1):64–70, 2011.

[46] H Bart Van der Worp, David W Howells, Emily S Sena, Michelle J Porritt, Sarah Rewell, Victoria O'Collins, and Malcolm R Macleod. Can animal models of disease reliably inform human studies? *PLoS Medicine*, 7(3), 2010.

[47] Takashi Miwa, Yasuko Miwa, and Kenro Kanda. Dynamic and static sensitivities of muscle spindle primary endings in aged rats to ramp stretch. *Neuroscience Letters*, 201(2):179–182, 1995.

[48] Laurent De-Doncker, Florence Picquet, Julien Petit, and Maurice Falempin. Characterization of spindle afferents in rat soleus muscle using ramp-and-hold and sinusoidal stretches. *Journal of Neurophysiology*, 89(1):442–449, 2003.

[49] Valerie K Haftel, Edyta K Bichler, T Richard Nichols, Martin J Pinter, and Timothy C Cope. Movement reduces the dynamic response of muscle spindle afferents and motoneuron synaptic potentials in rat. *Journal of Neurophysiology*, 91(5):2164–2171, 2004.

[50] Benoni B Edin and Ab Vallbo. Dynamic response of human muscle spindle afferents to stretch. *Journal of Neurophysiology*, 63(6):1297–1306, 1990.

[51] Stephen E Grill and Mark Hallett. Velocity sensitivity of human muscle spindle afferents and slowly adapting type II cutaneous mechanoreceptors. *The Journal of Physiology*, 489(2):593–602, 1995.

[52] Paul J Cordo, Carmen Flores-Vieira, Sabine MP Verschueren, J Timothy Inglis, and Victor Gurfinkel. Position sensitivity of human muscle spindles: single afferent and population representations. *Journal of Neurophysiology*, 87(3):1186–1195, 2002.

[53] Jacob Kjell and Lars Olson. Rat models of spinal cord injury: from pathology to potential therapies. *Disease Models & Mechanisms*, 9(10):1125–1137, 2016.

[54] Charles Watson, George Paxinos, and Gulgun Kayalioglu. *The spinal cord: a Christopher and Dana Reeve Foundation text and atlas*. Academic press, 2009.

[55] Jan Holsheimer. Concepts and methods in neuromodulation and functional electrical stimulation: an introduction. *Neuromodulation*, 1(2):57–61, 1998.

[56] KH Lee and R Johnston. Electrically induced flexion reflex in gait training of hemiplegic patients: induction of the reflex. *Archives of Physical Medicine and Rehabilitation*, 57(1):311–314, 1976.

[57] A Kralj, T Bajd, R Turk, J Krajnik, and H Benko. Gait restoration in paraplegic patients: a feasibility demonstration using multichannel surface electrode FES. *Journal of Rehabilitation Research and Development*, 20(1):3–20, 1983.

[58] Dirk G Everaert, Richard B Stein, Gary M Abrams, Alexander W Dromerick, Gerard E Francisco, Brian J Hafner, Thy N Huskey, Michael C Munin, Karen J Nolan, and Conrad V Kufta. Effect of a foot-drop stimulator and ankle–foot orthosis on walking performance after stroke: a multicenter randomized controlled trial. *Neurorehabilitation and Neural Repair*, 27(7):579–591, 2013.

[59] Birgit Larsen and Andrei Patriciu. *ActiGait®: A Partly Implantable Drop-Foot Stimulator System*, pages 421–432. Wiley Online Library, 2013.

[60] Jane Burridge, Morten Haugland, Birgit Larsen, Ruth M Pickering, Niels Svaneborg, Helle K Iversen, P Brøgger Christensen, Jens Haase, Jannick Brennum, and Thomas Sinkjaer. Phase II trial to evaluate the ActiGait implanted drop-foot stimulator in established hemiplegia. *Journal of Rehabilitation Medicine*, 39(3):212–218, 2007.

[61] Imre Cikajlo, Zlatko Matjačić, Tadej Bajd, and Ryoko Futami. Sensory supported FES control in gait training of incomplete spinal cord injury persons. *Artificial Organs*, 29(6):459–461, 2005.

[62] D Graupe, Ross Davis, Hubert Kordylewski, and Kate H Kohn. Ambulation by traumatic T4-12 paraplegics using functional neuromuscular stimulation. *Critical Reviews in Neurosurgery*, 8(4): 221–231, 1998.

[63] Manfred Bijak, Winfried Mayr, Monika Rakos, Christian Hofer, Hermann Lanmüller, Dietmar Rafolt, Martin Reichel, Stefan Sauermann, Christoph Schmutterer, Ewald Unger, et al. The Vienna functional electrical stimulation system for restoration of walking functions in spastic paraplegia. *Artificial Organs*, 26(3):224–227, 2002.

[64] Manfred Bijak, Monika Rakos, Christian Hofer, Winfried Mayr, Maria Strohhofer, Doris Raschka, and Helmut Kern. Stimulation parameter optimization for FES supported standing up and walking in SCI patients. *Artificial Organs*, 29(3):220–223, 2005.

[65] Rudi Kobetic, Ronald J Triolo, and E Byron Marsolais. Muscle selection and walking performance of multichannel FES systems for ambulation in paraplegia. *IEEE Transactions on Rehabilitation Engineering*, 5(1):23–29, 1997.

[66] Rudi Kobetic, Ronald J Triolo, James P Uhlir, Carole Bieri, Michael Wibowo, Gordie Polando, E Byron Marsolais, JA Davis, Kathleen A Ferguson, and Mukut Sharma. Implanted functional electrical stimulation system for mobility in paraplegia: a follow-up case report. *IEEE Transactions on Rehabilitation Engineering*, 7(4):390–398, 1999.

[67] John Chae and Ronald Hart. Comparison of discomfort associated with surface and percutaneous intramuscular electrical stimulation for persons with chronic hemiplegia1. *American Journal of Physical Medicine & Rehabilitation*, 77(6):516–522, 1998.

[68] Philip W Ledger. Skin biological issues in electrically enhanced transdermal delivery. *Advanced Drug Delivery Reviews*, 9(2-3):289–307, 1992.

[69] Stuart A Binder-Macleod and Lynn Snyder-Mackler. Muscle fatigue: clinical implications for fatigue assessment and neuromuscular electrical stimulation. *Physical Therapy*, 73(12):902–910, 1993.

[70] Hunter Peckham and Peter Gorman. Functional electrical stimulation in the 21st century. *Topics in Spinal Cord Injury Rehabilitation*, 10(2):126–150, 2004.

[71] K John Klose, Patrick L Jacobs, James G Broton, Rosalind S Guest, Belinda M Needham-Shropshire, Nathan Lebwohl, Mark S Nash, and Barth A Green. Evaluation of a training program for persons with SCI paraplegia using the Parastep® 1 ambulation system: part 1. Ambulation performance and anthropometric measures. *Archives of Physical Medicine and Rehabilitation*, 78(8):789–793, 1997.

[72] Daniel Graupe, Humberto Cerrel-Bazo, Helmut Kern, and Ugo Carraro. Walking performance, medical outcomes and patient training in FES of innervated muscles for ambulation by thoracic-level complete paraplegics. *Neurological Research*, 30(2):123–130, 2008.

[73] Francisco J. Rodri, Dolores Ceballos, Martin Schu, Antoni Valero, Elena Valderrama, Thomas Stieglitz, and Xavier Navarro. Polyimide cuff electrodes for peripheral nerve stimulation. *Journal of Neuroscience Methods*, 98:105–118, 2000.

[74] G. E. Loeb and R. A. Peck. Cuff electrodes for chronic stimulation and recording of peripheral nerve activity. *Journal of Neuroscience Methods*, 64:95–103, 1996.

[75] Dustin J. Tyler and Dominique M. Durand. Functionally selective peripheral nerve stimulation with a flat interface nerve electrode. *IEEE Transactions on Neural Systems and Rehabilitation Engineering*, 10:294–303, 2002.

[76] Kevin Kilgore. *Implantable Neuroprostheses for Restoring Function*. Elsevier, 2015.

[77] William D. Memberg, Katharine H. Polasek, Ronald L. Hart, Anne M. Bryden, Kevin L. Kilgore, Gregory A. Nemunaitis, Harry A. Hoyen, Michael W. Keith, and Robert F. Kirsch. Implanted neuroprosthesis for restoring arm and hand function in people with high level tetraplegia. *Archives of Physical Medicine and Rehabilitation*, 95:1201–1211, 2014.

[78] John E Dowling. *Neurons and networks: an introduction to behavioral neuroscience*. Harvard University Press, 2001.

[79] Herbert S Gasser. The classification of nerve fibers. *The Ohio Journal of Science*, 41(3):145–159, 1941.

[80] Tatsuo Ushiki and Chizuka Ide. Three-dimensional organization of the collagen fibrils in the rat sciatic nerve as revealed by transmission-and scanning electron microscopy. *Cell and Tissue Research*, 260(1):175–184, 1990.

[81] Karen J Chandross. Nerve injury and inflammatory cytokines modulate gap junctions in the peripheral nervous system. *Glia*, 24(1):21–31, 1998.

[82] Donald R McNeal. Analysis of a model for excitation of myelinated nerve. *IEEE Transactions on Biomedical Engineering*, (4):329–337, 1976.

[83] Frank Rattay. Analysis of models for external stimulation of axons. *IEEE Transactions on Biomedical Engineering*, (10):974–977, 1986.

[84] Frank Rattay. Analysis of models for extracellular fiber stimulation. *IEEE Transactions on Biomedical Engineering*, 36(7):676–682, 1989.

[85] RA Gaunt, JA Hokanson, and DJ Weber. Microstimulation of primary afferent neurons in the l7 dorsal root ganglia using multielectrode arrays in anesthetized cats: thresholds and recruitment properties. *Journal of Neural Engineering*, 6(5):055009, 2009.

[86] Lee E Fisher, Christopher A Ayers, Mattia Ciollaro, Valérie Ventura, Douglas J Weber, and Robert A Gaunt. Chronic recruitment of primary afferent neurons by microstimulation in the feline dorsal root ganglia. *Journal of Neural Engineering*, 11(3):036007, 2014.

[87] Petrus H Veltink, Jan A van Alste, and HBK Boom. Multielectrode intrafascicular and extraneural stimulation. *Medical and Biological Engineering and Computing*, 27(1):19–24, 1989.

[88] Ken Yoshida and Ken Horch. Selective stimulation of peripheral nerve fibers using dual intrafascicular electrodes. *IEEE Transactions on Biomedical Engineering*, 40(5):492–494, 1993.

[89] Peter H Veltink, Jan A Van Alste, and Herman BK Boom. Simulation of intrafascicular and extraneural nerve stimulation. *IEEE Transactions on Biomedical Engineering*, 35(1):69–75, 1988.

[90] DJ Bourbeau, JA Hokanson, JE Rubin, and DJ Weber. A computational model for estimating recruitment of primary afferent fibers by intraneural stimulation in the dorsal root ganglia. *Journal of Neural Engineering*, 8(5):056009, 2011.

[91] Stanisa Raspopovic, Marco Capogrosso, Jordi Badia, Xavier Navarro, and Silvestro Micera. Experimental validation of a hybrid computational model for selective stimulation using transverse intrafascicular multichannel electrodes. *IEEE Transactions on Neural Systems and Rehabilitation Engineering*, 20(3):395–404, 2012.

[92] JB Hursh. Conduction velocity and diameter of nerve fibers. *American Journal of Physiology–Legacy Content*, 127(1):131–139, 1939.

[93] James B Ranck and Spencer L BeMent. The specific impedance of the dorsal columns of cat: an anisotropic medium. *Experimental Neurology*, 11(4):451–463, 1965.

[94] ANANDA Weerasuriya, ROBERT A Spangler, STANLEY I Rapoport, and RE Taylor. AC impedance of the perineurium of the frog sciatic nerve. *Biophysical Journal*, 46(2):167–174, 1984.

[95] Yanina Grinberg, Matthew A Schiefer, Dustin J Tyler, and Kenneth J Gustafson. Fascicular perineurium thickness, size, and position affect model predictions of neural excitation. *IEEE Transactions on Neural Systems and Rehabilitation Engineering*, 16(6):572–581, 2008.

[96] Xavier Navarro, Thilo B. Krueger, Natalia Lago, Silvestro Micera, Thomas Stieglitz, and Paolo Dario. A critical review of interfaces with the peripheral nervous system for the control of neuroprostheses and hybrid bionic systems. *Journal of the Peripheral Nervous System*, 10:229–258, 2005.

[97] Jaume Del Valle and Xavier Navarro. Interfaces with the peripheral nerve for the control of neuroprostheses. *International Review of Neurobiology*, 109:63–83, 2013.

[98] E. A. Tanagho, R. A. Schmidt, and B. R. Orvis. Neural stimulation for control of voiding dysfunction: a preliminary report in 22 patients with serious neuropathic voiding disorders. *The Journal of Urology*, 142:340–345, 1989.

[99] Markus Hohenfeller, Daniela Schultz-Lampel, Stefan Dahms, Klaus Matzel, and Joachim W. Thuroff. Bilateral chronic sacral neuromodulation for treatment for lower urinary tract dysfunction. *The Journal of Urology*, 160:821–824, 1998.

[100] Yi Jae Lee, Han-Jun Kim, Sun Hee Do, Ji Yoon Kang, and Soo Hyun Lee. Characterization of nerve-cuff electrode interface for biocompatible and chronic stimulating application. *Sensors and Actuators B: Chemical*, 237:924–934, 2016.

[101] Tim Boretius, Jordi Badia, Aran Pascual-Font, Martin Schuettler, Xavier Navarro, Ken Yoshida, and Thomas Stieglitz. A transverse intrafascicular multichannel electrode (TIME) to interface with the peripheral nerve. *Biosensors and Bioelectronics*, 26:62–69, 2010.

[102] Almut Branner, Richard B. Stein, and Richard A. Normann. Selective stimulation of cat sciatic nerve using an array of varying-length microelectrodes. *Journal of Neurophysiology*, 85:1585–1594, 2001.

[103] Almut Branner, Richard B. Stein, Eduardo Fernandez, Yoichiro Aoyagi, and Richard A. Normann. Long-term stimulation and recording with a penetrating microelectrode array in cat sciatic nerve. *IEEE Transactions on Biomedical Engineering*, 51:146–157, 2004.

[104] H. A. C. Wark, K. S. Mathews, R. A. Normann, and E. Fernandez. Behavioral and cellular consequences of high-electrode count Utah Arrays chronically implanted in rat sciatic nerve. *Journal of Neural Engineering*, 11:046027, 2014.

[105] TS Davis, HAC Wark, DT Hutchinson, DJ Warren, K O'Neill, T Scheinblum, GA Clark, RA Normann, and B Greger. Restoring motor control and sensory feedback in people with upper extremity amputations using arrays of 96 microelectrodes implanted in the median and ulnar nerves. *Journal of Neural Engineering*, 13(3):036001, 2016.

[106] Almut Branner and Richard Alan Normann. A multielectrode array for intrafascicular recording and stimulation in sciatic nerve of cats. *Brain research bulletin*, 51(4):293–306, 2000.

[107] MB Christensen, SM Pearce, NM Ledbetter, DJ Warren, GA Clark, and PA Tresco. The foreign body response to the utah slant electrode array in the cat sciatic nerve. *Acta Biomaterialia*, 10(11): 4650–4660, 2014.

[108] Jordi Badia, Tim Boretius, Arán Pascual-Font, Esther Udina, Thomas Stieglitz, and Xavier Navarro. Biocompatibility of chronically implanted transverse intrafascicular multichannel electrode (TIME) in the rat sciatic nerve. *IEEE Transactions on Biomedical Engineering*, 58:2324–2332, 2011.

[109] A Cutrone, J Del Valle, D Santos, J Badia, C Filippeschi, S Micera, X Navarro, and S Bossi. A three-dimensional self-opening intraneural peripheral interface (SELINE). *Journal of Neural Engineering*, 12(1):016016, 2015.

[110] Natalia Lago, Ken Yoshida, Klaus P. Koch, and Xavier Navarro. Assessment of biocompatibility of chronically implanted polyimide and platinum intrafascicular electrodes. *IEEE Transactions on Biomedical Engineering*, 54:281–290, 2007.

[111] Kim D Anderson. Consideration of user priorities when developing neural prosthetics. *Journal of Neural Engineering*, 6(5):055003, 2009.

[112] Silvestro Micera and Xavier Navarro. Bidirectional interfaces with the peripheral nervous system. *International Review of Neurobiology*, 86:23–38, 2009.

[113] W. T. Liberson, H. J. Holmquest, David Scot, and Margot Dow. Functional electrotherapy: stimulation of the peroneal nerve synchronized with the swing phase of the gait of hemiplegic patients. *Archives of Physical Medicine and Rehabilitation*, 42:101–105, 1961.

[114] P. Strojnik, R. Acimovic, E. Vavken, V. Simic, and U. Stanic. Treatment of drop foot using an implantable peroneal underknee stimulator. *Scandinavian Journal of Rehabilitation Medicine*, 19: 37–43, 1986.

[115] J. Holsheimer, G. Bultstra, A. J. Verloop, H. E. Van Der Aa, and H. J. Hermens. Implantable dual channel peroneal nerve stimulator. pages 42–44, 1993.

[116] Gerard M. Lyons, Thomas Sinkjær, Jane H. Burridge, and David J. Wilcox. A review of portable FES-based neural orthoses for the correction of drop foot. *IEEE Transactions on Neural Systems and Rehabilitation Engineering*, 10:260–279, 2002.

[117] Robert P. Wilder, Tyler C. Wind, Elizabeth V. Jones, Brenda E. Crider, and Richard F. Edlich. Functional electrical stimulation for a dropped foot. *Journal of long-term effects of medical implants*, 12:149–159, 2001.

[118] Katharine H. Polasek, Harry A. Hoyen, Michael W. Keith, and Dustin J. Tyler. Human nerve stimulation thresholds and selectivity using a multi-contact nerve cuff electrode. *IEEE Transactions on Neural Systems and Rehabilitation Engineering*, 15:76–82, 2007.

[119] Katharine H. Polasek, Harry A. Hoyen, Michael W. Keith, Robert F. Kirsch, and Dustin J. Tyler. Stimulation stability and selectivity of chronically implanted multicontact nerve cuff electrodes in the human upper extremity. *IEEE Transactions on Neural Systems and Rehabilitation Engineering*, 17: 428–437, 2009.

[120] Lee E. Fisher, Michael E. Miller, Stephanie N. Bailey, John A. Davis Jr, James S. Anderson, Lori R. Murray, Dustin J. Tyler, and Ronald J. Triolo. Standing after spinal cord injury with four-contact nerve-cuff electrodes for quadriceps stimulation. *IEEE Transactions on Neural Systems and Rehabilitation Engineering*, 16:473, 2008.

[121] Ken Yoshida, Ksenija Jovanovic, and Richard B. Stein. Intrafascicular electrodes for stimulation and recording from mudpuppy spinal roots. *Journal of Neuroscience Methods*, 96:47–55, 2000.

[122] Jordi Badia, Tim Boretius, David Andreu, Christine Azevedo-Coste, Thomas Stieglitz, and Xavier Navarro. Comparative analysis of transverse intrafascicular multichannel, longitudinal intrafascicular and multipolar cuff electrodes for the selective stimulation of nerve fascicles. *Journal of Neural Engineering*, 8:36–23, 2011.

[123] Stanisa Raspopovic, Marco Capogrosso, Francesco Maria Petrini, Marco Bonizzato, Jacopo Rigosa, Giovanni Di Pino, Jacopo Carpaneto, Marco Controzzi, Tim Boretius, and Eduardo Fernandez. Restoring natural sensory feedback in real-time bidirectional hand prostheses. *Science Translational Medicine*, 6:222, 2014.

[124] Christina Hassler, Tim Boretius, and Thomas Stieglitz. Polymers for neural implants. *Journal of Polymer Science Part B: Polymer Physics*, 49:18–33, 2011.

[125] Edwin M. Maynard, Craig T. Nordhausen, and Richard A. Normann. The Utah intracortical electrode array: a recording structure for potential brain-computer interfaces. *Electroencephalography and Clinical Neurophysiology*, 102:228–239, 1997.

[126] Richard A. Normann, Edwin M. Maynard, Patrick J. Rousche, and David J. Warren. A neural interface for a cortical vision prosthesis. *Vision research*, 39:2577–2587, 1999.

[127] Aritra Kundu, Kristian Rauhe Harreby, Ken Yoshida, Tim Boretius, Thomas Stieglitz, and Winnie Jensen. Stimulation selectivity of the “thin-film longitudinal intrafascicular electrode” (tfLIFE) and the “transverse intrafascicular multi-channel electrode” (TIME) in the large nerve animal model. *IEEE Transactions on Neural Systems and Rehabilitation Engineering*, 22:400–410, 2014.

[128] Jaume Del Valle, Natália de la Oliva, Matthias Müller, Thomas Stieglitz, and Xavier Navarro. Biocompatibility evaluation of parylene C and polyimide as substrates for peripheral nerve interfaces. In *2015 7th International IEEE/EMBS Conference on Neural Engineering (NER)*, pages 442–445. IEEE, 2015.

[129] Annarita Cutrone, Sivia Bossi, and Silvestro Micera. Development of a Self-Opening Neural Interface. *Journal of Medical Devices*, 7:020938, 2013.

[130] Claude Veraart, Warren M. Grill, and J. Thomas Mortimer. Selective control of muscle activation with a multipolar nerve cuff electrode. *IEEE Transactions on biomedical Engineering*, 40:640–653, 1993.

[131] Tim Boretius, Ken Yoshida, Jordi Badia, K Harreby, Aritra Kundu, Xavier Navarro, Winnie Jensen, and Thomas Stieglitz. A transverse intrafascicular multichannel electrode (TIME) to treat phantom limb pain – Towards human clinical trials. In *Biomedical Robotics and Biomechatronics (BioRob), 2012 4th IEEE RAS & EMBS International Conference on*, pages 282–287. IEEE, 2012.

[132] Eduardo Martin Moraud, Nikolaus Wenger, Jerome Gandar, Jack DiGiovanna, Pavel Musienko, Gregoire Courtine, and Silvestro Micera. A real-time platform for studying the modulatory capacity of epidural stimulation after spinal cord injury. pages 1449–1452. Ieee, 2013.

[133] David Marr and Ellen Hildreth. Theory of edge detection. *Proceedings of the Royal Society of London B: Biological Sciences*, 207(1167):187–217, 1980.

[134] David G Lowe. Distinctive image features from scale-invariant keypoints. *International Journal of Computer Vision*, 60(2):91–110, 2004.

[135] Pallav Sengupta. The laboratory rat: relating its age with human's. *International Journal of Preventive Medicine*, 4, 2013.

[136] Vadim S. Polikov, Patrick A. Tresco, and William M. Reichert. Response of brain tissue to chronically implanted neural electrodes. *Journal of Neuroscience Methods*, 148:1–18, 2005.

[137] Wei He and Ravi V. Bellamkonda. Nanoscale neuro-integrative coatings for neural implants. *Biomaterials*, 26:2983–2990, 2005.

[138] George C. McConnell, Howard D. Rees, Allan I. Levey, Claire-Anne Gutekunst, Robert E. Gross, and Ravi V. Bellamkonda. Implanted neural electrodes cause chronic, local inflammation that is correlated with local neurodegeneration. *Journal of Neural Engineering*, 6:056003, 2009.

[139] Warren M. Grill and J. Thomas Mortimer. Electrical properties of implant encapsulation tissue. *Annals of Biomedical Engineering*, 22:23–33, 1994.

[140] William F. Agnew, Douglas B. McCreery, Ted G. H. Yuen, and Leo A. Bullara. Histologic and physiologic evaluation of electrically stimulated peripheral nerve: considerations for the selection of parameters. *Annals of Biomedical Engineering*, 17:39–60, 1989.

[141] Daniel W. Tan, Matthew A. Schiefer, Michael W. Keith, James Robert Anderson, Joyce Tyler, and Dustin J. Tyler. A neural interface provides long-term stable natural touch perception. *Science Translational Medicine*, 6:257, 2014.

[142] Mitchell A. Frankel, Brett R. Dowden, V. John Mathews, Richard A. Normann, Gregory A. Clark, and Sanford G. Meek. Multiple-input single-output closed-loop isometric force control using asynchronous intrafascicular multi-electrode stimulation. *IEEE Transactions on Neural Systems and Rehabilitation Engineering*, 19:325–332, 2011.

[143] R. A. Normann, B. R. Dowden, M. A. Frankel, A. M. Wilder, S. D. Hiatt, N. M. Ledbetter, D. A. Warren, and Gregory A. Clark. Coordinated, multi-joint, fatigue-resistant feline stance produced with intrafascicular hind limb nerve stimulation. *Journal of Neural Engineering*, 9:026019, 2012.

[144] G. S. Dhillon, T. B. Krüger, J. S. Sandhu, and K. W. Horch. Effects of short-term training on sensory and motor function in severed nerves of long-term human amputees. *Journal of Neurophysiology*, 93:2625–2633, 2005.

[145] Warren M. Grill, Sharon E. Norman, and Ravi V. Bellamkonda. Implanted neural interfaces: biochallenges and engineered solutions. *Annual Review of Biomedical Engineering*, 11:1–24, 2009.

[146] G. Stoll, J. W. Griffin, C. Yan Li, and Bruce D. Trapp. Wallerian degeneration in the peripheral nervous system: participation of both Schwann cells and macrophages in myelin degradation. *Journal of Neurocytology*, 18:671–683, 1989.

[147] Andrew D. Gaudet, Phillip G. Popovich, and Matt S. Ramer. Wallerian degeneration: gaining perspective on inflammatory events after peripheral nerve injury. *Journal of Neuroinflammation*, 8:1, 2011.

[148] J. W. Fawcett and Roger J. Keynes. Peripheral nerve regeneration. *Annual Review of Neuroscience*, 13: 43–60, 1990.

[149] James M. Anderson, Analiz Rodriguez, and David T. Chang. Foreign body reaction to biomaterials. *Seminars in Immunology*, 20(2):86 – 100, 2008. Innate and Adaptive Immune Responses in Tissue Engineering.

[150] James M. Anderson. Biological responses to materials. *Annual Review of Materials Research*, 31: 81–110, 2001.

[151] Ravi V. Bellamkonda, S. Balakrishna Pai, and Philippe Renaud. Materials for neural interfaces. *Mrs Bulletin*, 37:557–561, 2012.

[152] H. Mei Liu, Lin Hsue Yang, and Yu Jen Yang. Schwann cell properties: 3. C-fos expression, bFGF production, phagocytosis and proliferation during Wallerian degeneration. *Journal of Neuropathology & Experimental Neurology*, 54:487–496, 1995.

[153] Jeffry F. Goodrum and Thomas W. Bouldin. The cell biology of myelin degeneration and regeneration in the peripheral nervous system. *Journal of Neuropathology & Experimental Neurology*, 55:943–953, 1996.

[154] P. L. Williams and S. U. S. A. N. M. Hall. Chronic Wallerian degeneration–an in vivo and ultrastructural study. *Journal of Anatomy*, 109:487, 1971.

[155] Jerry Silver and Jared H. Miller. Regeneration beyond the glial scar. *Nature Reviews Neuroscience*, 5: 146–156, 2004.

[156] Anne-Laure Cattin, Jemima J. Burden, Lucie Van Emmenis, Francesca E. Mackenzie, Julian J. A. Hoving, Noelia Garcia Calavia, Yanping Guo, Maeve McLaughlin, Laura H. Rosenberg, and Victor Quereda. Macrophage-induced blood vessels guide Schwann cell-mediated regeneration of peripheral nerves. *Cell*, 162:1127–1139, 2015.

[157] Nassir Mokarram, Alishah Merchant, Vivek Mukhatyar, Gaurangkumar Patel, and Ravi V. Bellamkonda. Effect of modulating macrophage phenotype on peripheral nerve repair. *Biomaterials*, 33:8793–8801, 2012.

[158] Elke Ydens, Anje Cauwels, Bob Asselbergh, Sofie Goethals, Lieve Peeraer, Guillaume Lornet, Leonardo Almeida-Souza, Jo A. Van Ginderachter, Vincent Timmerman, and Sophie Janssens. Acute injury in the peripheral nervous system triggers an alternative macrophage response. *Journal of Neuroinflammation*, 9(1):176, 2012.

[159] Peiwen Chen, Xianhua Piao, and Paolo Bonaldo. Role of macrophages in Wallerian degeneration and axonal regeneration after peripheral nerve injury. *Acta Neuropathologica*, 130:605–618, 2015.

[160] Jon P Niemi, Alicia DeFrancesco-Lisowitz, Jared M Cregg, Madeline Howarth, and Richard E Zigmond. Overexpression of the monocyte chemokine CCL2 in dorsal root ganglion neurons causes a conditioning-like increase in neurite outgrowth and does so via a STAT3 dependent mechanism. *Experimental Neurology*, 275(Part 1):25–37, 2016.

[161] Michael Gray, Winnie Palispis, Phillip G. Popovich, Nico van Rooijen, and Ranjan Gupta. Macrophage depletion alters the blood-nerve barrier without affecting Schwann cell function after neural injury. *Journal of Neuroscience Research*, 85:766–777, 2007.

[162] Annarita Cutrone, Pier Nicola Sergi, Silvia Bossi, and Silvestro Micera. Modelization of a self-opening peripheral neural interface: A feasibility study. *Medical Engineering & Physics*, 33:1254–1261, 2011.

[163] Jaronie Mohd Jani, Martin Leary, Aleksandar Subic, and Mark A. Gibson. A review of shape memory alloy research, applications and opportunities. *Materials & Design*, 56:1078–1113, 2014.

[164] Stéphanie P Lacour, Grégoire Courtine, and Jochen Guck. Materials and technologies for soft implantable neuroprostheses. *Nature Reviews Materials*, 1:16063, 2016.

[165] Nicholas A. Kotov, Jessica O. Winter, Isaac P. Clements, Edward Jan, Brian P. Timko, Stéphane Campidelli, Smita Pathak, Andrea Mazzatenta, Charles M. Lieber, and Maurizio Prato. Nanomaterials for neural interfaces. *Advanced Materials*, 21:3970–4004, 2009.

[166] Gregory H. Altman, Frank Diaz, Caroline Jakuba, Tara Calabro, Rebecca L. Horan, Jingsong Chen, Helen Lu, John Richmond, and David L. Kaplan. Silk-based biomaterials. *Biomaterials*, 24:401–416, 2003.

[167] Minev, Ivan R. and Musienko, Pavel and Hirsch, Arthur and Barraud, Quentin and Wenger, Nikolaus and Moraud, Eduardo Martin and Gandar, Jérôme and Capogrosso, Marco and Milekovic, Tomislav and Asboth, Léonie. Electronic dura mater for long-term multimodal neural interfaces. *Science*, 347: 159–163, 2015.

[168] M. Warnken, S. Haag, S. Matthiesen, U. R. Juergens, and K. Racke. Species differences in expression pattern of arginase isoenzymes and differential effects of arginase inhibition on collagen synthesis in human and rat pulmonary fibroblasts. *Naunyn-Schmiedeberg's Archives of Pharmacology*, 381: 297–304, 2010.

[169] John Carew Eccles and Milan R Dimitrijević. *Upper motor neuron functions and dysfunctions*, volume 1. S Karger Ag, 1985.

[170] L Vodovnik, A Kralj, U Stank, R Acimovic, and N Gros. Recent applications of functional electrical stimulation to stroke patients in Ljubljana. *Clinical Orthopaedics and Related Research*, 131:64–70, 1978.

[171] M Wieler, S Naaman, and RB Stein. WalkAid - An improved functional electrical stimulator for correcting foot-drop. In *Proceedings of the International Functional Electrical Stimulation Society*, pages 101–104, 1996.

[172] Daniel Graupe and Kate H Kohn. Functional neuromuscular stimulator for short-distance ambulation by certain thoracic-level spinal-cord-injured paraplegics. *Surgical Neurology*, 50(3):202–207, 1998.

[173] Sten Grillner. Ion channels and locomotion. *Science*, 278(5340):1087–1088, 1997.

[174] Connie Chau, Hugues Barbeau, and Serge Rossignol. Early locomotor training with clonidine in spinal cats. *Journal of Neurophysiology*, 79(1):392–409, 1998.

[175] M Antri, C Mouffle, D Orsal, and J-Y Barthe. 5-HT1A receptors are involved in short-and long-term processes responsible for 5-HT-induced locomotor function recovery in chronic spinal rat. *European Journal of Neuroscience*, 18(7):1963–1972, 2003.

[176] Eric S Landry, Nicolas P Lapointe, Claude Rouillard, Daniel Levesque, Peter B Hedlund, and Pierre A Guertin. Contribution of spinal 5-HT1A and 5-HT7 receptors to locomotor-like movement induced by 8-OH-DPAT in spinal cord-transected mice. *European Journal of Neuroscience*, 24(2):535–546, 2006.

[177] Emilio Bizzi, Matthew C Tresch, Philippe Saltiel, and Andrea d'Avella. New perspectives on spinal motor systems. *Nature Reviews Neuroscience*, 1(2):101, 2000.

[178] Vivian K Mushahwar, Deborah M Gillard, Michel JA Gauthier, and Arthur Prochazka. Intraspinal micro stimulation generates locomotor-like and feedback-controlled movements. *IEEE Transactions on Neural Systems and Rehabilitation Engineering*, 10(1):68–81, 2002.

[179] RM Ichiyama, Yu P Gerasimenko, H Zhong, RR Roy, and VR Edgerton. Hindlimb stepping movements in complete spinal rats induced by epidural spinal cord stimulation. *Neuroscience Letters*, 383(3): 339–344, 2005.

[180] Lisa Guevremont, Costantino G Renzi, Jonathan A Norton, Jan Kowalczewski, Rajiv Saigal, and Vivian K Mushahwar. Locomotor-related networks in the lumbosacral enlargement of the adult spinal cat: activation through intraspinal microstimulation. *IEEE Transactions on Neural Systems and Rehabilitation Engineering*, 14(3):266–272, 2006.

[181] Igor Lavrov, Grégoire Courtine, Christine J Dy, Rubia van den Brand, Andy J Fong, Yuri Gerasimenko, Hui Zhong, Roland R Roy, and V Reggie Edgerton. Facilitation of stepping with epidural stimulation in spinal rats: role of sensory input. *Journal of Neuroscience*, 28(31):7774–7780, 2008.

[182] Gregoire Courtine, Bingbing Song, Roland R Roy, Hui Zhong, Julia E Herrmann, Yan Ao, Jingwei Qi, V Reggie Edgerton, and Michael V Sofroniew. Recovery of supraspinal control of stepping via indirect propriospinal relay connections after spinal cord injury. *Nature Medicine*, 14(1):69, 2008.

[183] RD De Leon, JA Hodgson, RR Roy, and VR Edgerton. Full weight-bearing hindlimb standing following stand training in the adult spinal cat. *Journal of Neurophysiology*, 80(1):83–91, 1998.

[184] Hugues Leblond, Marion L'Espérance, Didier Orsal, and Serge Rossignol. Treadmill locomotion in the intact and spinal mouse. *Journal of Neuroscience*, 23(36):11411–11419, 2003.

[185] Yu Gerasimenko, O Daniel, J Regnaux, M Combeaud, and B Bussel. Mechanisms of locomotor activity generation under epidural spinal cord stimulation. *NATO Science Series, I: Life and Behavioural Sciences*, 326:164–171, 2001.

[186] Karen Minassian, Bernhard Jilge, Frank Rattay, MM Pinter, H Binder, Franz Gerstenbrand, and Milan R Dimitrijevic. Stepping-like movements in humans with complete spinal cord injury induced by epidural stimulation of the lumbar cord: electromyographic study of compound muscle action potentials. *Spinal Cord*, 42(7):401, 2004.

[187] Y. P. Gerasimenko, Z. McKinney, D. G. Sayenko, Parag Gad, R. M. Gorodnichev, W. Grundfest, V. Reggie Edgerton, and I. B. Kozlovskaya. Spinal and sensory neuromodulation of spinal neuronal networks in humans. *Human Physiology*, 43(5):492–500, Sep 2017. doi: 10.1134/S0362119717050061.

[188] Pavel Musienko, Rubia van den Brand, Olivia Märzendorfer, Roland R Roy, Yury Gerasimenko, V Reggie Edgerton, and Grégoire Courtine. Controlling specific locomotor behaviors through multidimensional monoaminergic modulation of spinal circuitries. *Journal of Neuroscience*, 31(25): 9264–9278, 2011.

[189] Sylvain Calinon, Florent Guenter, and Aude Billard. On learning, representing, and generalizing a task in a humanoid robot. *IEEE Transactions on Systems, Man, and Cybernetics, Part B (Cybernetics)*, 37(2):286–298, 2007.

[190] S Wurth, M Capogrosso, S Raspopovic, J Gandar, G Federici, N Kinany, A Cutrone, A Piersigilli, N Pavlova, R Guiet, et al. Long-term usability and bio-integration of polyimide-based intra-neural stimulating electrodes. *Biomaterials*, 122:114–129, 2017.

[191] Nadia Dominici, Urs Keller, Heike Vallery, Lucia Friedli, Rubia Van Den Brand, Michelle L Starkey, Pavel Musienko, Robert Riener, and Grégoire Courtine. Versatile robotic interface to evaluate, enable and train locomotion and balance after neuromotor disorders. *Nature Medicine*, 18(7):1142–1147, 2012.

[192] H Vallery, P Lutz, J Von Zitzewitz, G Rauter, M Fritschi, Christophe Everarts, Renaud Ronsse, A Curt, and M Bolliger. Multidirectional transparent support for overground gait training. In *Rehabilitation Robotics (ICORR), 2013 IEEE International Conference on*, pages 1–7. IEEE, 2013.

[193] Jean-Baptiste Mignardot, Camille G Le Goff, Rubia Van Den Brand, Marco Capogrosso, Nicolas Fumeaux, Heike Vallery, Selin Anil, Jessica Lanini, Isabelle Fodor, Grégoire Eberle, et al. A multidirectional gravity-assist algorithm that enhances locomotor control in patients with stroke or spinal cord injury. *Science Translational Medicine*, 9(399):eaah3621, 2017.

[194] Cindy S-Y Lin, Jane HL Chan, Emmanuel Pierrot-Deseilligny, and David Burke. Excitability of human muscle afferents studied using threshold tracking of the H reflex. *The journal of Physiology*, 545(2): 661–669, 2002.

[195] JC Eccles, Rosamond M Eccles, and A Lundberg. The convergence of monosynaptic excitatory afferents on to many different species of alpha motoneurones. *The Journal of Physiology*, 137(1): 22–50, 1957.

[196] Bernice Lau, Lisa Guevremont, and Vivian K Mushahwar. Strategies for generating prolonged functional standing using intramuscular stimulation or intraspinal microstimulation. *IEEE Transactions on Neural Systems and Rehabilitation Engineering*, 15(2):273–285, 2007.

[197] Vivian K Mushahwar, Patrick L Jacobs, Richard A Normann, Ronald J Triolo, and Naomi Kleitman. New functional electrical stimulation approaches to standing and walking. *Journal of Neural Engineering*, 4(3):S181, 2007.

[198] Karen Minassian, Ursula Hofstoetter, Keith Tansey, and Winfried Mayr. Neuromodulation of lower limb motor control in restorative neurology. *Clinical neurology and neurosurgery*, 114(5):489–497, 2012.

[199] Jordi Badia, Arán Pascual-Font, Meritxell Vivó, Esther Udina, and Xavier Navarro. Topographical distribution of motor fascicles in the sciatic-tibial nerve of the rat. *Muscle & Nerve*, 42(2):192–201, 2010.

[200] Steven G Nelson and Lorne M Mendell. Projection of single knee flexor ia fibers to homonymous and heteronymous motoneurons. *Journal of Neurophysiology*, 41(3):778–787, 1978.

[201] S Edgley, E Jankowska, and D McCrea. The heteronymous monosynaptic actions of triceps surae group Ia afferents on hip and knee extensor motoneurones in the cat. *Experimental Brain Research*, 61(2):443–446, 1986.

[202] David A McCrea. 4 Spinal Cord Circuitry and Motor Reflexes. *Exercise and Sport Sciences Reviews*, 14 (1):105–142, 1986.

[203] P Guertin, MJ Angel, MC Perreault, and DA McCrea. Ankle extensor group I afferents excite extensors throughout the hindlimb during fictive locomotion in the cat. *The Journal of Physiology*, 487(1): 197–209, 1995.

[204] Ken Yoshida and Ken Horch. Reduced fatigue in electrically stimulated muscle using dual channel intrafascicular electrodes with interleaved stimulation. *Annals of Biomedical Engineering*, 21(6): 709–714, 1993.

[205] Mitchell A Frankel, V John Mathews, Gregory A Clark, Richard A Normann, and Sanford G Meek. Control of Dynamic Limb Motion Using Fatigue-Resistant Asynchronous Intrafascicular Multi-Electrode Stimulation. *Frontiers in Neuroscience*, 10:414, 2016.

[206] MC Perreault, MJ Angel, P Guertin, and DA McCrea. Effects of stimulation of hindlimb flexor group II afferents during fictive locomotion in the cat. *The Journal of Physiology*, 487(1):211–220, 1995.

[207] David A McCrea. Spinal circuitry of sensorimotor control of locomotion. *The Journal of Physiology*, 533(1):41–50, 2001.

[208] Gordon W Hiebert, Patrick J Whelan, Arthur Prochazka, and Keir G Pearson. Contribution of hind limb flexor muscle afferents to the timing of phase transitions in the cat step cycle. *Journal of Neurophysiology*, 75(3):1126–1137, 1996.

[209] Marco Capogrosso, Tomislav Milekovic, David Borton, Fabien Wagner, Eduardo Martin Moraud, Jean-Baptiste Mignardot, Nicolas Buse, Jerome Gandar, Quentin Barraud, David Xing, et al. A brain–spinal interface alleviating gait deficits after spinal cord injury in primates. *Nature*, 539(7628):284, 2016.

[210] Pouria Moshayedi, Gilbert Ng, Jessica CF Kwok, Giles SH Yeo, Clare E Bryant, James W Fawcett, Kristian Franze, and Jochen Guck. The relationship between glial cell mechanosensitivity and foreign body reactions in the central nervous system. *Biomaterials*, 35(13):3919–3925, 2014.

[211] Kelsey A Potter, Mehdi Jorfi, Kyle T Householder, E Johan Foster, Christoph Weder, and Jeffrey R Capadona. Curcumin-releasing mechanically adaptive intracortical implants improve the proximal neuronal density and blood–brain barrier stability. *Acta Biomaterialia*, 10(5):2209–2222, 2014.

[212] James C Barrese, Naveen Rao, Kaivon Paroo, Corey Triebwasser, Carlos Vargas-Irwin, Lachlan Franquemont, and John P Donoghue. Failure mode analysis of silicon-based intracortical microelectrode arrays in non-human primates. *Journal of Neural Engineering*, 10(6):066014, 2013.

[213] Jonathan Rivnay, Huiliang Wang, Lief Fenno, Karl Deisseroth, and George G Malliaras. Next-generation probes, particles, and proteins for neural interfacing. *Science Advances*, 3(6):e1601649, 2017.

[214] C Boehler, C Kleber, N Martini, Y Xie, I Dryg, T Stieglitz, UG Hofmann, and M Asplund. Actively controlled release of dexamethasone from neural microelectrodes in a chronic in vivo study. *Biomaterials*, 129:176–187, 2017.

[215] Taylor Ware, Dustin Simon, David E Arreaga-Salas, Jonathan Reeder, Robert Rennaker, Edward W Keefer, and Walter Voit. Fabrication of responsive, softening neural interfaces. *Advanced Functional Materials*, 22(16):3470–3479, 2012.

[216] Jessica K Nguyen, Daniel J Park, John L Skousen, Allison E Hess-Dunning, Dustin J Tyler, Stuart J Rowan, Christoph Weder, and Jeffrey R Capadona. Mechanically-compliant intracortical implants reduce the neuroinflammatory response. *Journal of Neural Engineering*, 11(5):056014, 2014.

[217] Soumen Das, Janet M Dowding, Kathryn E Klump, James F McGinnis, William Self, and Sudipta Seal. Cerium oxide nanoparticles: applications and prospects in nanomedicine. *Nanomedicine*, 8 (9):1483–1508, 2013.

[218] Gianni Ciofani, Giada G Genchi, Ioannis Liakos, Valentina Cappello, Mauro Gemmi, Athanassia Athanassiou, Barbara Mazzolai, and Virgilio Mattoli. Effects of cerium oxide nanoparticles on pc12 neuronal-like cells: proliferation, differentiation, and dopamine secretion. *Pharmaceutical Research*, 30(8):2133–2145, 2013.

[219] AY Estevez and JS Erlichman. Cerium oxide nanoparticles for the treatment of neurological oxidative stress diseases. In *Oxidative Stress: Diagnostics, Prevention, and Therapy*, pages 255–288. ACS Publications, 2011.

[220] AY Estevez, S Pritchard, K Harper, JW Aston, A Lynch, JJ Lucky, JS Ludington, P Chatani, WP Mosenthal, JC Leiter, et al. Neuroprotective mechanisms of cerium oxide nanoparticles in a mouse hippocampal brain slice model of ischemia. *Free Radical Biology and Medicine*, 51(6):1155–1163, 2011.

[221] Yinghui Zhong and Ravi V Bellamkonda. Dexamethasone-coated neural probes elicit attenuated inflammatory response and neuronal loss compared to uncoated neural probes. *Brain Research*, 1148:15–27, 2007.

[222] Reecha Wadhwa, Carl F Lagenaur, and Xinyan Tracy Cui. Electrochemically controlled release of dexamethasone from conducting polymer polypyrrole coated electrode. *Journal of Controlled Release*, 110(3):531–541, 2006.

[223] Christian Boehler and Maria Asplund. A detailed insight into drug delivery from pedot based on analytical methods: Effects and side effects. *Journal of Biomedical Materials Research Part A*, 103(3): 1200–1207, 2015.

[224] Ronald L Hart, Kevin L Kilgore, and P Hunter Peckham. A comparison between control methods for implanted fes hand-grasp systems. *IEEE Transactions on Rehabilitation Engineering*, 6(2):208–218, 1998.

[225] Richard Williamson and Brian J Andrews. Sensor systems for lower limb functional electircal stimulation (fes) control. *Medical Engineering & Physics*, 22(5):313–325, 2000.

[226] Lisa Guevremont, Jonathan A Norton, and Vivian K Mushahwar. Physiologically based controller for generating overground locomotion using functional electrical stimulation. *Journal of Neurophysiology*, 97(3):2499–2510, 2007.

[227] Avril Mansfield and Gerard M Lyons. The use of accelerometry to detect heel contact events for use as a sensor in fes assisted walking. *Medical Engineering & Physics*, 25(10):879–885, 2003.

[228] KA Mazurek, BJ Holinski, DG Everaert, RB Stein, R Etienne-Cummings, and VK Mushahwar. Feed forward and feedback control for over-ground locomotion in anaesthetized cats. *Journal of Neural Engineering*, 9(2):026003, 2012.

[229] Barry J Upshaw and Thomas Sinkjær. Natural versus artificial sensors applied in peroneal nerve stimulation. *Artificial Organs*, 21(3):227–231, 1997.

[230] Morten Hansen, Morten K Haugland, and Thomas Sinkjær. Evaluating robustness of gait event detection based on machine learning and natural sensors. *IEEE Transactions on Neural Systems and Rehabilitation Engineering*, 12(1):81–88, 2004.

[231] Ken Yoshida and Ken Horch. Closed-loop control of ankle position using muscle afferent feedback with functional neuromuscular stimulation. *IEEE Transactions on Biomedical Engineering*, 43(2): 167–176, 1996.

[232] GE Loeb, MJ Bak, and J Duysens. Long-term unit recording from somatosensory neurons in the spinal ganglia of the freely walking cat. *Science*, 197(4309):1192–1194, 1977.

[233] Douglas J Weber, Richard B Stein, Dirk G Everaert, and Arthur Prochazka. Decoding sensory feedback from firing rates of afferent ensembles recorded in cat dorsal root ganglia in normal locomotion. *IEEE Transactions on Neural Systems and Rehabilitation Engineering*, 14(2):240–243, 2006.

[234] Tatsuya Umeda, Kazuhiko Seki, Masa-aki Sato, Yukio Nishimura, Mitsuo Kawato, and Tadashi Isa. Population coding of forelimb joint kinematics by peripheral afferents in monkeys. *PloS One*, 7(10): e47749, 2012.

[235] Tim M Bruns, Joost B Wagenaar, Matthew J Bauman, Robert A Gaunt, and Douglas J Weber. Real-time control of hind limb functional electrical stimulation using feedback from dorsal root ganglia recordings. *Journal of Neural Engineering*, 10(2):026020, 2013.

[236] David Borton, Silvestro Micera, José del R Millán, and Grégoire Courtine. Personalized neuroprosthetics. *Science Translational Medicine*, 5(210):210rv2–210rv2, 2013.

[237] Michael D Sunshine, Frances S Cho, Danielle R Lockwood, Amber S Fechko, Michael R Kasten, and Chet T Moritz. Cervical intraspinal microstimulation evokes robust forelimb movements before and after injury. *Journal of Neural Engineering*, 10(3):036001, 2013.

[238] Chet T Moritz, Timothy H Lucas, Steve I Perlmutter, and Eberhard E Fetz. Forelimb movements and muscle responses evoked by microstimulation of cervical spinal cord in sedated monkeys. *Journal of Neurophysiology*, 97(1):110–120, 2007.

[239] Jonas B Zimmermann, Kazuhiko Seki, and Andrew Jackson. Reanimating the arm and hand with intraspinal microstimulation. *Journal of Neural Engineering*, 8(5):054001, 2011.

[240] Abigail N Sharpe and Andrew Jackson. Upper-limb muscle responses to epidural, subdural and intraspinal stimulation of the cervical spinal cord. *Journal of Neural Engineering*, 11(1):016005, 2014.

[241] MR Kasten, MD Sunshine, ES Secrist, Philip J Horner, and CT Moritz. Therapeutic intraspinal microstimulation improves forelimb function after cervical contusion injury. *Journal of Neural Engineering*, 10(4):044001, 2013.

[242] Jonas B Zimmermann and Andrew Jackson. Closed-loop control of spinal cord stimulation to restore hand function after paralysis. *Frontiers in Neuroscience*, 8, 2014.

[243] Yukio Nishimura, Steve I Perlmutter, and Eberhard E Fetz. Restoration of upper limb movement via artificial corticospinal and musculospinal connections in a monkey with spinal cord injury. *Frontiers in Neural Circuits*, 7:57, 2013.

[244] Monzurul Alam, Guillermo Garcia-Alias, Benita Jin, Jonathan Keyes, Hui Zhong, Roland R Roy, Yury Gerasimenko, Daniel C Lu, and V Reggie Edgerton. Electrical neuromodulation of the cervical spinal cord facilitates forelimb skilled function recovery in spinal cord injured rats. *Experimental Neurology*, 291:141–150, 2017.

[245] Daniel C Lu, V Reggie Edgerton, Morteza Modaber, Nicholas AuYong, Erika Morikawa, Sharon Zdunowski, Melanie E Sarino, Majid Sarrafzadeh, Marc R Nuwer, Roland R Roy, et al. Engaging cervical spinal cord networks to reenable volitional control of hand function in tetraplegic patients. *Neurorehabilitation and Neural Repair*, 30(10):951–962, 2016.

[246] Milos R Popovic, Thierry Keller, IPI Papas, Volker Dietz, and Manfred Morari. Surface-stimulation technology for grasping and walking neuroprostheses. *IEEE Engineering in Medicine and Biology Magazine*, 20(1):82–93, 2001.

[247] P Hunter Peckham, Kevin L Kilgore, Michael W Keith, Anne M Bryden, Niloy Bhadra, and Fred W Montague. An advanced neuroprosthesis for restoration of hand and upper arm control using an implantable controller. *The Journal of Hand Surgery*, 27(2):265–276, 2002.

[248] GJ Snoek, Maarten Joost IJzerman, TS Stoffers, G Zilvold, et al. Use of the ness handmaster to restore handfunction in tetraplegia: clinical experiences in ten patients. *Spinal Cord*, 38(4):244, 2000.

[249] Arthur Prochazka, Michel Gauthier, Marguerite Wieler, and Zoltan Kenwell. The bionic glove: an electrical stimulator garment that provides controlled grasp and hand opening in quadriplegia. *Archives of Physical Medicine and Rehabilitation*, 78(6):608–614, 1997.

[250] Dejan Popović, Aleksandar Stojanović, Andjelka Pjanović, Slobodanka Radosavljević, Mirjana Popović, Stevan Jović, and Dragan Vulović. Clinical evaluation of the bionic glove. *Archives of Physical Medicine and Rehabilitation*, 80(3):299–304, 1999.

[251] P Taylor, J Esnouf, and J Hobby. The functional impact of the freehand system on tetraplegic hand function. clinical results. *Spinal Cord*, 40(11):560, 2002.

[252] Chet T Moritz, Steve I Perlmutter, and Eberhard E Fetz. Direct control of paralyzed muscles by cortical neurons. *Nature*, 456(7222):639, 2008.

[253] Eric A Pohlmeyer, Emily R Oby, Eric J Perreault, Sara A Solla, Kevin L Kilgore, Robert F Kirsch, and Lee E Miller. Toward the restoration of hand use to a paralyzed monkey: brain-controlled functional electrical stimulation of forearm muscles. *PloS One*, 4(6):e5924, 2009.

[254] Christian Ethier, Emily R Oby, MJ Bauman, and Lee E Miller. Restoration of grasp following paralysis through brain-controlled stimulation of muscles. *Nature*, 485(7398):368–371, 2012.

[255] P Hunter Peckham, Michael W Keith, Kevin L Kilgore, Julie H Grill, Kathy S Wuolle, Geoffrey B Thrope, Peter Gorman, John Hobby, MJ Mulcahey, Sara Carroll, et al. Efficacy of an implanted neuroprosthesis for restoring hand grasp in tetraplegia: a multicenter study. *Archives of Physical Medicine and Rehabilitation*, 82(10):1380–1388, 2001.

[256] A Bolu Ajiboye, Francis R Willett, Daniel R Young, William D Memberg, Brian A Murphy, Jonathan P Miller, Benjamin L Walter, Jennifer A Sweet, Harry A Hoyen, Michael W Keith, et al. Restoration of reaching and grasping movements through brain-controlled muscle stimulation in a person with tetraplegia: a proof-of-concept demonstration. *The Lancet*, 389(10081):1821–1830, 2017.

[257] David A Friedenberg, Michael A Schwemmer, Andrew J Landgraf, Nicholas V Annetta, Marcia A Bockbrader, Chad E Bouton, Mingming Zhang, Ali R Rezai, W Jerry Mysiw, Herbert S Bresler, et al. Neuroprosthetic-enabled control of graded arm muscle contraction in a paralyzed human. *Scientific Reports*, 7(7), 2017.

[258] KT Ragnarsson. Functional electrical stimulation after spinal cord injury: current use, therapeutic effects and future directions. *Spinal Cord*, 46(4):255, 2008.

[259] Natalie A Brill, Stephanie Naufel Naufel, Katharine H Polasek, Christian Ethier, Jennifer Cheesborough, Sonya Agnew, Lee E Miller, and Dustin J Tyler. Evaluation of high-density, multi-contact nerve cuffs for activation of grasp muscles in monkeys. *Journal of Neural Engineering*, 2017.

[260] Rósa Hugosdóttir, Skúli Þór Jónasson, Haraldur Sigþórsson, and Þórður Helgason. Feasibility study of a novel electrode concept for a neuroprosthesis for augmentation of impaired finger functions. *European Journal of Translational Myology*, 24(3):209–215, 2014.

[261] Noah M Ledbetter, Christian Ethier, Emily R Oby, Scott D Hiatt, Andrew M Wilder, Jason H Ko, Sonya P Agnew, Lee E Miller, and Gregory A Clark. Intrafascicular stimulation of monkey arm nerves evokes coordinated grasp and sensory responses. *Journal of Neurophysiology*, 109(2):580–590, 2013.

[262] Niloy Bhadra and P Hunter Peckham. Peripheral nerve stimulation for restoration of motor function. *Journal of Clinical Neurophysiology*, 14(5):378–393, 1997.

[263] Régine Brissot, Philippe Gallien, Marie-Pierre Le Bot, Anne Beaubras, Dominique Laisné, Jocelyne Beillot, and Josette Dassonville. Clinical experience with functional electrical stimulation-assisted gait with parastep in spinal cord–injured patients. *Spine*, 25(4):501–508, 2000.

Sophie WURTH

Date of birth: 30/07/1988
Nationality: Luxembourgish, Swiss Residence Permit B
Address: Av. Mon-Loisir, 4 1006 Lausanne, CH
Contact: sophie.wurth@epfl.ch, +41788410130

PROFESSIONAL EXPERIENCE

01/14 – 01/18	**PhD student at the Translational Neural Engineering Lab, EPFL (CH)** *PhD thesis supervisor: Prof. Silvestro Micera, Co-supervisor: Prof. Grégoire Courtine*
09/12 – 08/13	**Research scholar at Rehabilitation Institute of Chicago (RIC) & Northwestern University, Chicago (USA),** *Master thesis in Neural Engineering at the Center for Bionic Medicine, Supervisors: Prof. Todd Kuiken, Prof. Levi Hargrove*
03 - 05/2011	**Internship at the BioHealth Cluster of Luxinnovation EIG, Luxembourg (LUX)** *National agency for the promotion of Innovation and Research in sectors of economic interest (clusters)*
09/10 – 01/11	**Internship at Otto Bock Health Care GmbH, Duderstadt (DE)** *Multinational MedTech Company and world leader in orthopedic prostheses, based in Germany*

EDUCATION

08/15	**Summer school on Neurophysiology for Neural and Biomedical Engineers, Zermatt (CH)** *Topic: Reading the brain, Brian and spinal cord in action, Locomotion – neuroscience and robotics*
09/14	**Summer school on Neurorehabilitation (SSNR 2014), Baiona (E)** *Topic: Meeting clinical and patient needs and expectations*
01/14 - present	**PhD in Neuroscience, EPFL**
09/11 - 08/13	**Master of Science in Bioengineering at Swiss Federal Institute of Technology (EPFL), Lausanne (CH),** *Minor in Biomedical Technologies*
2007 – 2010	**Bachelor of Science in Life Sciences and Technologies at Swiss Federal Institute of Technology (EPFL), Lausanne (CH)**
2000 – 2007	**Baccalaureate, Lycée des Garçons du Luxembourg, Luxembourg (LUX)** *Section "Latin, Natural and Mathematical Sciences", Passed with distinction "Excellent"*

LANGUAGES

Native: *Luxembourgish*
Native fluent: *German*, *French*, and *English*
Intermediate level (B2): *Spanish*
Beginner level (A2): *Italian*

EXTRACURRICULAR EXPERIENCE

09/2017	**Organization of EPFL-ETH-Brown University Summer School on Translational Neuroscience and Neuroengineering** *6 day-program on main experimental tools and concepts in neurophysiology, 30 participants, 8 international plenary speakers, 4 symposium speakers*
09/2011	**Forum EPFL Association, Lausanne,** *Assistant Committee Member* *10-day Swiss recruiting platform with more than 150 companies on the EPFL campus*
2009 – 2011	**Challenge of EPFs Association, Lausanne,** *Committee Member (Animation)* *4-day ski- and snowboard contest between the 2 Swiss Federal Institutes of Technology (350 participants)*
2007 - 2010	**WorldMUN EPFL Association, Lausanne,** *Committee Member (Treasurer) 09/2008 - 09/2009*

Model of United Nations: Representation of different countries during simulated international debates

- Responsible for accounting and bookkeeping, Set up the annual budget
- Participation in Harvard WorldMUN in Puebla, Mexico (03/08) and Den Haag, Netherlands (04/09)

Others	Alpine and high altitude trekking, Dancing (since 1992 Jazz and Classic Ballet), Scouting (since 1994)

PUBLICATIONS & PATENTS

Journal publications

- E Martin, J Von Zitzewitz, J Miehlbradt, **S Wurth**, E Formento, J Di Giovanna, M Capogrosso, G Courtine, S Micera. “Closed-loop control of trunk posture improves locomotion through the regulation of leg proprioceptive feedback after spinal cord injury.” *Nature Scientific Reports, accepted for publication 12/2017*
- **S Wurth**, M Capogrosso, S Raspopovic, J Gandar, G Federici, N Kinany, A Cutrone, A Piersigilli, N Pavlova, R Guiet, G Taverni, J Rigosa, X Navarro, Q Barraud, G Courtine, S Micera. “Long-term usability and bio-integration of polyimide-based intra-neural stimulating electrodes.” *Biomaterials 122 (2017), 114-129*.
- J Florez, M Shah, E Martin, **S Wurth**, L Baud, J Von Zitzewitz, R Van den Brand, S Micera, G Courtine, and J Paik**.** “Rehabilitative Soft Exoskeleton for Rodents.” *IEEE Transactions on Neural Systems and Rehabilitation Engineering, 25.2 (2017), 107-118.*
- K Musick, J Rigosa, S Narasimhan, **S Wurth**, M Capogrosso, D Chew, J Fawcett, S Micera, and S Lacour**.** "Chronic multichannel neural recordings from soft regenerative microchannel electrodes during gait" *Nature Scientific Reports* 5 (2015): 143-63.
- **S Wurth**, and LJ Hargrove**.** "A real-time comparison between direct control, sequential pattern recognition control and simultaneous pattern recognition control using a Fitts' law style assessment procedure" *Journal of NeuroEngineering and Rehabilitation* 11.1 (2014): 91.

Conference publications and poster presentations

- M Badi***, S Wurth*,** M Kaeser, M Capogrosso, S Durand, W Raffoul, G Courtine, P Cvancara, T Stieglitz, E Rouiller, S Micera. Development of an intraneural peripheral stimulation paradigm for reversing hand paralysis in non-human primates. *Society for Neuroscience (SfN) 2017, 47th Annual Meeting.*
- **S Wurth,** J Gandar, M Capogrosso, A Cutrone, S Raspopovic, N Pavlova, P Shkorbatova, L Baud, E D’Anna, Q Barraud, K Minassian, F Wagner, S Micera, G Courtine. Hybrid peripheral-spinal neuromodulation therapies enable refined locomotion after paralysis by combining global and local control of leg movements. *Society for Neuroscience (SfN) 2017, 47th Annual Meeting.*
- **S Wurth,** M Capogrosso, S Raspopovic, J Gandar, A Cutrone, N Kinany, G Federici, Q Barraud, N Pavlova, G Courtine, S Micera. Stable and biocompatible intraneural electrodes alleviate locomotor deficits after spinal cord injury. *Society for Neuroscience (SfN) 2016, 46th Annual Meeting.*
- R Guiet, **S Wurth**, O Burri, S Micera, G Courtine, and A Seitz. “Blob diameter and ring thickness: application to measure axons and their myelin sheet.” European Light Microscopy Initiative (ELMI) 2016, *16th Annual Meeting.*
- **S Wurth**, M Capogrosso, S Raspopovic, J Gandar, Q Barraud, A Cutrone, J Rigosa, G Taverni, N Kinany, N Pavlova, G Courtine, and S Micera. **“**Chronic functionality and biocompatibility assessment of an intra-neural stimulating electrode in the rat sciatic nerve” *Society for Neuroscience (SfN) 2015, 45th Annual Meeting.*
- **S Wurth**, N Kinany, J Gandar, G Courtine, and S Micera**. “**Combined peripheral nerve and epidural spinal cord electrical stimulation for a refined locomotor rehabilitation in real time – A pilot study” *Neural Engineering (NER) 2015, 7th International IEEE/EMBS Conference on.*
- **S Wurth***, J Miehlbradt*, E Martin, J Von Zitzewitz, G Courtine, and S Micera. **“**Closed-loop control of dynamic trunk posture improves gait patterns during locomotor training after spinal cord injury” *Society for Neuroscience (SfN) 2014, 44th Annual Meeting.*
- **S Wurth** and LJ Hargrove**.** “A real time performance assessment of simultaneous pattern recognition myoelectric control for multifunctional upper limb prostheses.” Neural Engineering (*NER) 2013, 6th International IEEE/EMBS Conference on.*

Patents

European patent application No 17163191.4: ‘A Neurostimulation System for Central Nervous System (CNS) and Peripheral Nervous System (PNS). S Wurth, G Courtine, S Micera (application filed 03/2017).